REPORT NO. UMTA-MA-06-0041-80-1

LORAN-C RFI MEASURED IN LOS ANGELES, CALIFORNIA

W.R. Vincent
G. Sage

Systems Control, Inc. (Vt)
1801 Page Mill Road
Palo Alto, CA 94304

OCTOBER 1980

FINAL REPORT

Prepared for

U.S. DEPARTMENT OF TRANSPORTATION
URBAN MASS TRANSPORTATION ADMINISTRATION
Office of Technology Development and Deployment
Office of Bus and Paratransit Technology
Washington DC 20590

PREFACE

This report presents the results of tests conducted to determine the nature of Loran-C RFI in the Los Angeles area which would be encountered by vehicularly installed Loran-C navigation systems.

The tests were conducted by Systems Control, Inc. (SCI (Vt)) under subcontract to Gould Inc., Information Identification Division under Contract No. DOT-TSC-1237. The text was prepared by W.R. Vincent and G. Sage of SCI (Vt), while the summary was prepared by John Hovorka of the Transportation Systems Center and Fred Heathcock of Gould Inc. The work was sponsored by the Urban Mass Transportation Administration, Office of Bus and Paratransit.

METRIC CONVERSION FACTORS

Approximate Conversions to Metric Measures

Symbol	When You Know	Multiply by	To Find	Symbol
		LENGTH		
in	inches	2.5	centimeters	cm
ft	feet	30	centimeters	cm
yd	yards	0.9	meters	m
mi	miles	1.6	kilometers	km
		AREA		
in^2	square inches	6.5	square centimeters	cm^2
ft^2	square feet	0.09	square meters	m^2
yd^2	square yards	0.8	square meters	m^2
mi^2	square miles	2.6	square kilometers	km^2
	acres	0.4	hectares	ha
		MASS (weight)		
oz	ounces	28	grams	g
lb	pounds	0.45	kilograms	kg
	short tons (2000 lb)	0.9	tonnes	t
		VOLUME		
tsp	teaspoons	5	milliliters	ml
Tbsp	tablespoons	15	milliliters	ml
fl oz	fluid ounces	30	milliliters	ml
c	cups	0.24	liters	l
pt	pints	0.47	liters	l
qt	quarts	0.95	liters	l
gal	gallons	3.8	liters	l
ft^3	cubic feet	0.03	cubic meters	m^3
yd^3	cubic yards	0.76	cubic meters	m^3
		TEMPERATURE (exact)		
°F	Fahrenheit temperature	5/9 (after subtracting 32)	Celsius temperature	°C

Approximate Conversions from Metric Measures

Symbol	When You Know	Multiply by	To Find	Symbol
		LENGTH		
mm	millimeters	0.04	inches	in
cm	centimeters	0.4	inches	in
m	meters	3.3	feet	ft
m	meters	1.1	yards	yd
km	kilometers	0.6	miles	mi
		AREA		
cm^2	square centimeters	0.16	square inches	in^2
m^2	square meters	1.2	square yards	yd^2
km^2	square kilometers	0.4	square miles	mi^2
ha	hectares (10,000 m^2)	2.5	acres	
		MASS (weight)		
g	grams	0.035	ounces	oz
kg	kilograms	2.2	pounds	lb
t	tonnes (1000 kg)	1.1	short tons	
		VOLUME		
ml	milliliters	0.03	fluid ounces	fl oz
l	liters	2.1	pints	pt
l	liters	1.06	quarts	qt
l	liters	0.26	gallons	gal
m^3	cubic meters	35	cubic feet	ft^3
m^3	cubic meters	1.3	cubic yards	yd^3
		TEMPERATURE (exact)		
°C	Celsius temperature	9/5 (then add 32)	Fahrenheit temperature	°F

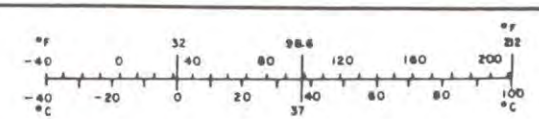

TABLE OF CONTENTS

TABLE OF CONTENTS (CONT.)

LIST OF ILLUSTRATIONS

LIST OF ILLUSTRATIONS (CONT.)

LIST OF ILLUSTRATIONS (CONT.)

LIST OF TABLES

SUMMARY

NOISE AND RFI MEASUREMENTS: BASIS FOR THE TESTS

The relatively poor Loran-C signals in the Los Angeles area indicated by a Teledyne Survey prompted an investigation and identification of the primary types of noise and RFI that a Loran-C receiver operating in the urban and suburban environment of Los Angeles would encounter. The literature provides excellent information which can be used to predict the natural atmospheric noise areas (1) but at that time very little (if any) information was available on the interference to be found in the urban environment. However, it was known that terrestrial Loran-C experiments in Tennessee were experiencing problems. Since the time corresponding to the SCI tests, a test program has been conducted in Tennessee for the U.S. Department of Transportation to determine the effects of high voltage TVA transmission lines (operating with and without supervisory carrier signals) on the performance of typical Loran-C receivers. The results of these tests have been published in a document (2) available to the public. The SCI Los Angeles test results correlate well with the quantitative measurements and conclusions of this late Tennessee work. The SCI data supplements and extends the Tennessee report by identifying other major types and sources of noise and interference which may be expected in the signal environment of urban and suburban Los Angeles. A detailed description of the SCI tests and results are presented in this report.

LOS ANGELES (SCI) MEASUREMENTS: SUMMARY

The measurements of man-made noise and RFI in the urban and suburban areas of Los Angeles provided considerable insight into the many types of noise sources and the spatial characteristics of some of these sources. The SCI measurements identified the following types of high-level man-made noise and interference as factors which may limit the performance of Loran-C receivers in urban and suburban areas:

(1) Impulsive Noise
(2) Power Line Carrier Communications
(3) Localized Continuous Wave Signals

(4) Low Level Signals

(5) Ignition Noise

(6) Conventional Power Line Noise.

Implusive Noise

Severe impulsive noise was found to exist in a number of locations. The spectral shapes of implusive noise were observed to vary from relatively flat (in which case the RF filter of measurement equipment established the observed spectral shape) to non-frequency-flat spectral shapes implying that frequency-selective properties are associated with the noise signal. The primary source of the radio noise was found to be impulses emanating from nearby electric utility lines. In some cases, the noise could be associated with a particular distribution line. In almost all cases, primary time intervals between impulses of 16.6 and 8.3 ms were observed in the data. These intervals can be associated with 60 and 12 Hz triggering rates. In some cases, the data can be related to three-phase sources with 16.6 and 8.3 ms intervals having slightly different phase relationships. This noise appears to be due to utility customers who employ high power solid state or gaseous switching devices for industrial process control (SCR). The transmission mechanisms between the actual source and the Loran-C antenna (which may be located several blocks or even miles away from the source) is not well understood. The near-field coupling mechanism between the Loran-C antenna and the power lines cause the noise levels to vary by large values over very short distances (tens of feet). In some cases, the amplitudes of the impulsive noise were observed to change as much as 50 dB over a distance as short as 100 feet. In these instances, the received Loran-C signal-to-noise ratios would change from a relatively high positive value to a high negative value (approximately -20 dB and greater) which would significantly degrade the performance of most Loran-C receivers.

Power Line Carrier (PLC) Communications

The second most serious type of interference observed was associated with radiation from electric utility transmission lines. Electric utilities employ

low frequency carriers for voice communication, analog telemetry, and digital data transmission. These signals are used for the supervision, control, and protection of power generation and transmission facilities. CW signals associated with this type of source were recorded by SCI and have also been observed at numerous locations and frequencies during and after the SCI measurements. It is believed that PLC's with frequency spacings as dense as every 1 kHz in the Loran-C and adjacent frequency spectrum (60-140 kHz) exist in Southern California. SCI documented relatively high level CW signals at approximately 80, 90, 100, and 108 kHz and relatively low level signals at about 103, 120, 130, 140, and 150 kHz. The impact of these CW signals on the performance of a Loran-C receiver is dependent upon the complex combination of a number of important factors:

(1) PLC transmission frequency
(2) PLC signal strength
(3) Available Loran-C signal strength
(4) Synchronous/Asynchronous properties of PLC
(5) Loran-C receiver design.

The received PLC signal strength is primarily a function of the proximity of the Loran-C antenna to the power lines, the PLC frequency relative to the receiver bandpass, and the power of the PLC transmitter. Electric utility companies are known to use PLC transmitter powers ranging between 1 and 100 watts. The SCI and Gould measurements noted CW signal levels sufficient to degrade the Loran-C receiver performance of two different commercial receivers at ranges from power lines form approximately 100 feet to several thousand feet.

Other Types of Interference

The SCI measurements also identified other types of noise and interference which affect the operation of Loran-C receivers to a lesser degree. Types of interference included in this category are localized CW signals, ignition noise, conventional power line noise and far-field CW signals. In general, these types are considered less serious because of one or more of the following factors:

(1) Infrequent occurrence

(2) Very localized nature

(3) Frequency can be notched out.

The SCI measurements observed locations where very localized CW signals at or near 100 kHz were present. Signal properties varied with location. At several street intersections there was observed a very localized CW signal within the Loran-C spectrum. This appeared to be associated with traffic control sensors. In at least two other cases, CW signals were observed in the Loran-C spectrum with frequency spacings of approximately 16 kHz. Here the constant separation and simultaneous rise and fall of all CW signals suggested that a single nearby source was involved. (TV horizontal sync pulses at 15.75 kHz have been observed to cause problems with marine Loran-C receivers on ships and boats in the past.) At a few locations, CW signals at or close to 100 kHz were recorded which were associated with unshielded overhead telephone lines. The only far-field signal observed by Gould or SCI over a wide area of the Los Angeles vicinity was from a Navy transmitter located in Northern California operating at approximately 120 kHz. The notches of the Loran-C receiver can be set to attenuate this particular signal.

1. INTRODUCTION

Radio noise and RFI at and near frequencies employed by Loran-C radio navigation systems were investigated in portions of Los Angeles, California. Emphasis was placed on the definition of the detailed time and frequency domain structure of noise and RFI which might degrade the reception of Loran-C signals in urban, suburban, and industrial areas of Los Angeles. Furthermore, the measurements were directed toward obtaining an understanding of the noise and RFI environment which would be encountered by vehicularly installed Loran-C navigation systems.

The measurements were made at and around the 100 kHz band of frequencies employed by Loran-C, and they were made from a mobile van. An attempt was made to duplicate the vehicular antenna installations employed by many Loran-C receiving systems and to achieve a signal detection sensitivity comparable to Loran-C receivers. The noise and RFI instrumentation was somewhat different than the instrumentation used for conventional measurements, and it is described in Section 2. While the instrumentation was capable of collecting data to provide comprehensive statistical descriptors of noise, this was not done. The measurements were primarily of a diagnostic nature where data were rapidly collected at a very large number of sites and during mobile operation. These data were employed to achieve an understanding of the detailed properties of noise and RFI at each site and while moving along streets and highways. The output format of the data, Polaroid photographs of calibrated 3-axis views of noise, RFI and Loran-C signals, was chosen to provide a simplified and rapid means of describing noise and RFI at each site and to permit the comparison of conditions from site to site. In addition, an attempt was made to gather data which would permit the comparison of actual noise and RFI conditions with the performance of Loran-C receivers installed in mobile vehicles.

The Phase I measurements described in this report were made during the period of December 18 through December 22, 1978, while the Phase II measurements were made during the period of January 22 through January 27, 1979.

2. INSTRUMENTATION

The instrumentation used to acquire data presented in this report is described in Figure 2-1. A standard 108 inch long whip antenna was employed to sense signals and noise. A low noise preamplifier was used to achieve a signal detection capability roughly equivalent to the RF sensitivity of a Loran-C receiver. An RF bandpass filter was employed in the preamplifier to prevent intermodulation product generation in the amplifier and subsequent stages from nearby radio stations and nearby radio broadband noise sources during the Phase I measurements. However, most of the data taken during Phase II were taken without the RF filter. A Hewlett-Packard Series 140 Spectrum Analyzer was employed as a scanning receiver to drive an EMTEL Model 7200B 3-Axis Display. The 3-axis display provided a moving real-time visual representation of signals and noise received by the scanning receiver.

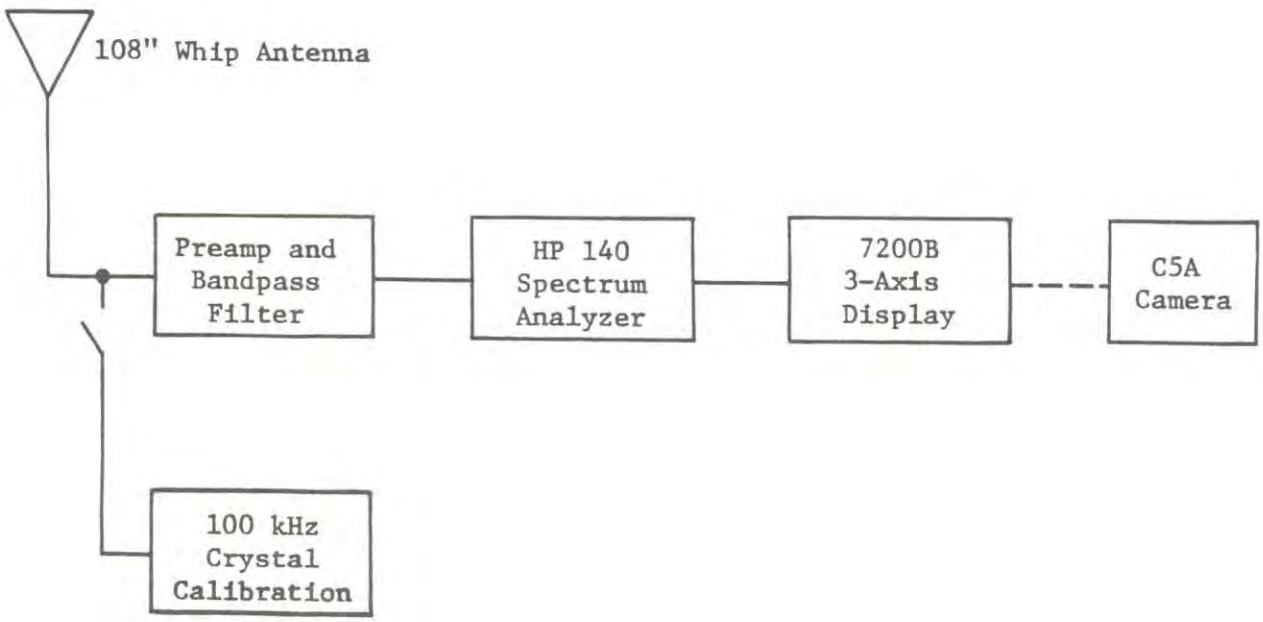

FIGURE 2-1. BLOCK DIAGRAM OF NOISE AND RFI MEASUREMENT SYSTEM

The instrumentation was installed in an Econoline van for mobility and convenience in noise and signal measurements. The van was driven along streets representative of conditions encountered by urban and suburban area vehicles and to some locations previously identified as problem areas for Loran-C reception. Both mobile and fixed location measurements were made as necessary to define a particular noise or signal situation.

To acquire data the spectrum analyzer was adjusted to scan across a block of frequencies centered at 100 kHz. As the spectrum analyzer scanned through a block of frequencies, its output was divided by the 3-axis display into 512 equally spaced data points. The received signal or noise amplitude at each data point was represented by an 8-bit digital word which provided an amplitude resolution at 256 levels for each data point. When a scan was completed, the 512 amplitude words were stored in memory and then presented as line 1 on the display CRT. When the second scan was completed, its data were stored in memory, line 1 on the CRT moved to line 2, and the new scan was shown on line 1. Subsequent scans moved the earlier lines step by step along the time axis until the entire memory was filled and a total of 60 scan lines were presented in the 3-axis view. When the memory was full, each new scan caused the oldest scan to be discarded. The resulting animated moving view of signals and noise provided a unique and easy-to-interpret visual picture of noise and signals in the blocks of frequencies under observation.

The 3-axis display system has a number of controls to assist the operator in interpreting the signals. Among these controls are a stop-action control to freeze any desired view for detailed observation, geometry controls to vary the viewing aspect, display mode controls to select any segment of the total view for detailed examination, and a threshold control to vary the background noise level.

The 3-axis views presented in this report were obtained by photographing the display in its stop-action mode. In interpreting the data, consideration must be given to situations where repetitive impulsive signals are observed by the repetitive scanning process. The relative repetition rates of impulsive signals and the scan rate of the receiver produce distinctive bands that slant across the CRT.

System calibration factors necessary to accurately scale the 3-axis views are as follows:

Preamplifier Gain	18 dB
Preamplifier Gain Without Filter (Phase II only)	15 dB
30 kHz IF Bandwidth Factor	0 dB
10 kHz IF Bandwidth Factor ..... (Apply to Loran-C and noise but not CW signals)	8 dB
3 kHz IF Bandwidth Factor ..... (Apply to Loran-C and noise but not to CW signals)	12 dB
1 kHz IF Bandwidth Factor ..... (Apply to Loran-C and noise but not to CW signals)	20 dB

The RF bandwidth of the preamplifier filter is shown in Figure 2-2. Appropriate gain versus frequency calibration factors for views which used the filter can be scaled from the filter bandwidth curve.

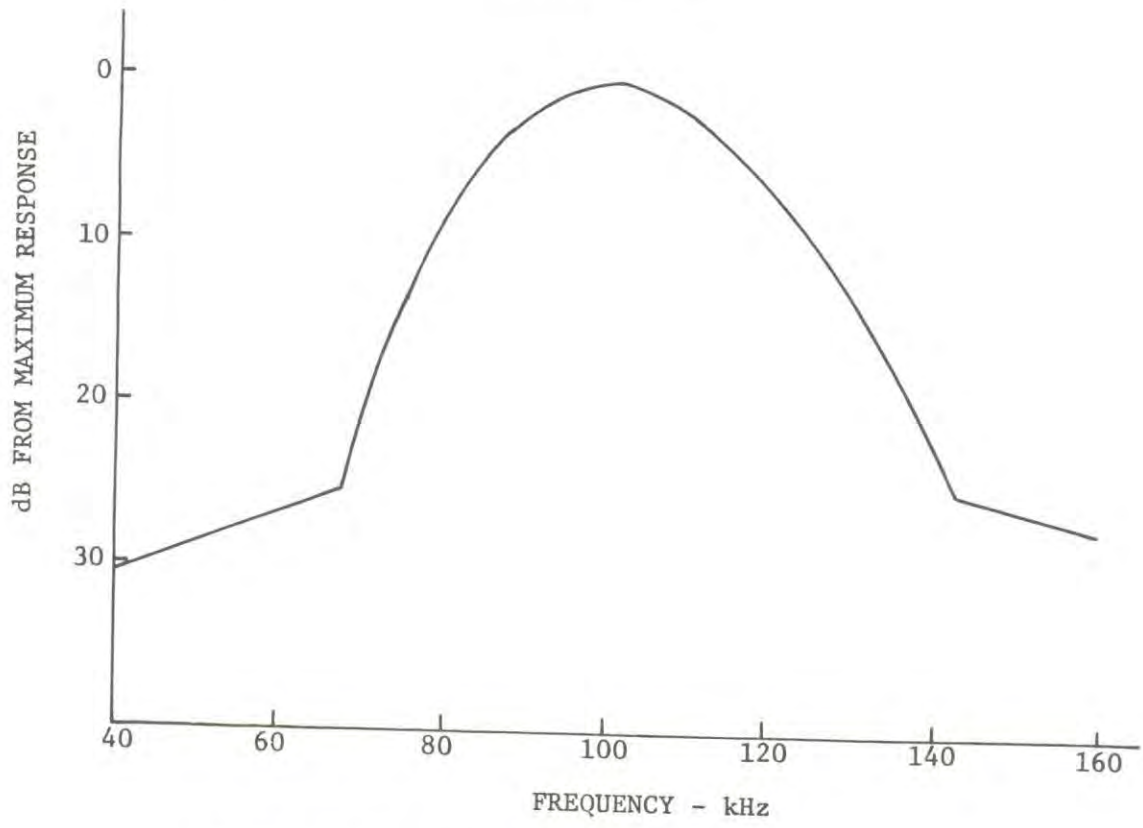

FIGURE 2-2. PREAMPLIFIER BANDPASS FILTER RESPONSE

To accurately scale the absolute amplitude of Loran-C, noise, and CW signals at the antenna output (or preamplifier input), the system calibration factors must be applied to the amplitude scale on each set of 3-axis views in this report. These system calibration factors can be applied as described in the following steps.

1. An 18 dB factor has been applied to all Phase I 3-axis display amplitude scales to account for preamplifier gain; for Phase II scales a 18 dB or 15 dB factor has been applied.

2. Use the appropriate IF bandwidth factor:

   a. If the IF bandwidth is 10 kHz, add 8 dB to each Loran-C or noise amplitude measurement.

   b. If the IF bandwidth is 3 kHz, add 12 dB to each Loran-C or noise amplitude measurement.

   c. If the IF bandwidth is 1 kHz, add 20 dB to each Loran-c or noise amplitude measurement.

3. If the preamplifier bandpass filter was used and if the measured noise, Loran-C, or CW signal amplitude is more than ± 10 kHz from 100 kHz, obtain an RF bandpass calibration factor from the filter characteristic curve and add this dB value to the measured amplitude.

The noise, Loran-C, or CW received signal levels obtained after taking the system calibration factors into account will describe the signal level available to a Loran-C receiver when connected to a mobile 108 inch whip antenna. These values can also be used to convert measured received power into field strength values by employing appropriate antenna conversion factors. Typical antenna conversion factors are available from a number of sources.

Each 3-axis view is identified by a two-line code where the top line gives (1) the date of measurement, (2) the local time of day of the measurement, and (3) the site location or site identification number. The second line gives a number of system-oriented parameters, where the various parameters are (1) the model of scanning receiver (always an HP 140 Spectrum Analyzer for the Phase I and II measurements), (2) the antenna (always a 108

inch whip), (3) the center frequency (F), (4) the frequency scan width (W), (5) the IF bandwidth, and (6) the scan time (ST). The last item for the Phase I measurements consists of two numbers necessary to establish an amplitude calibration for each view where the first number gives the RF attenuator setting for the HP 140, and the second number is the IF attenuator setting. For the Phase II measurements the last item consists of three numbers necessary to establish an amplitude calibration for each view where the first number gives the IF calibration factor for the HP 140, the second number gives the HP 140 RF attenuator setting, and the third number gives the RF preamplifier gain. When the letters NF follow the three amplitude calibration numbers, a broadband RF filter was employed and amplitude versus frequency calibration factors are not required. When the letters BPF appear, this indicates an RF bandpass filter was used and amplitude versus frequency factors from Figure 2-2 must be applied to the 3-axis view.

3. PRESENTATION OF SIGNIFICANT DATA

3.1 GENERAL APPROACH

Prior measurements of Loran-C receiver performance had been made in portions of Los Angeles by the technical staff of Gould Inc. These measurements identified certain streets, street intersections, and general areas where Loran-C receiver performance was marginal and at times inadequate. These locations were received from Gould personnel, and they served as the basis for selecting the locations of noise and RFI measurements described in this section.

In general, the measurement van was driven to an area identified by Gould Inc., and noise was examined as the van was slowly driven along a selected street. When unusual conditions were observed, a repeat run would be made, or the measurement van would be parked at a specific location for detailed fixed location measurements. Additional streets and areas were surveyed while proceeding to, between, and from sites. These additional measurements augmented data collected at the prescribed sites.

Very little technical data on the details of the noise and RFI were available prior to the measurements. Thus, some time was used to become familiar with the various kinds of noise and RFI encountered in Los Angeles. As the various sites were visited and the general properties of the noise and RFI were developed, consideration was given to important factors such as defining noise and RFI characteristics, spatial coverage, relationships to nearby physical objects, possible sources, and other items needed to describe the noise and RFI environment.

As the data were collected it became obvious that the noise and RFI could be placed into convenient categories, and these categories could be rated in terms of overall importance. Subsequent subsections of this report are organized in accordance with the various categories selected to describe conditions in Los Angeles. These subsections contain examples of the 3-axis display views to illustrate the results obtained. The text describes each set of 3-axis views and discusses the important features of each view.

3.2 BEST LORAN-C SIGNAL RECEPTION

Reference 3-Axis Views: 12/21/78, 1009 (Figure 3-1)
12/22/78, 1107 (Figure 3-2)

The 3-axis views taken on 12/21/78 at 1009 show the amplitude (upper view) and timing (lower view) of Loran-C signals received in Los Angeles during very low ambient noise and RFI states. The lower photograph shows four clustered slanting lines downward through the view, and a set of single slanting lines at a different angle. Each line of a group of four represents the eight sequential pulses of a particular station in the U.S. West Coast Chain where the first signal from the left is the Master (Fallon, Nevada); the second signal is W (George, Washington); the third signal is X (Middletown, California); and the fourth signal is Y (Searchlight, Nevada). The set of single slanting lines is Y (George, Washington) of the West Coast Canadian Chain, which has a slightly different time spacing between successive signals from a given station when compared to the U.S. West Coast Chain. The distinct visual signature in the 3-axis views caused by the slight timing difference allowed signals from either chain to be immediately identified.

The upper view shows the same data of the lower view with the display elevation control changed from full elevation to 0° elevation, amplitude compression removed, and the azimuth control adjusted to line up all 60 scans of data for the U.S. West Coast Chain. This view shows the amplitudes of each signal and provides a good estimate of the S/N for each signal. Signal amplitudes should be measured at the 100 kHz frequency region near the center of the x-axis since some signal reduction will occur at the left and right edges of the view due to less signal energy at 95 and 105 kHz.

A second related and similar view of Loran-C signals is shown in the views taken on 12/22/78 at 1107, where the receiver scan width is increased from 10 kHz to 50 kHz. The Loran-C signals are compressed toward the center of the frequency axis.

In these views the fourth pulse group of the U.S. West Coast Chain (Searchlight, Nevada) is the strongest at about -50 dBm when referenced to the scanning receiver input; the next strongest is the third pulse group (Middletown, California); the next is the first pulse group or the Master station (Fallon, Nevada); and the weakest is the second pulse group (George, Washington). A CW signal is shown at about 117 kHz at a level about 4 dB below the Master station signal and 18 dB below the strongest signal. Peak signal to average noise estimates of each signal are as follows:

Station	S/N
Y	+20 dB
X	+15 dB
M	+ 7 dB
W	+ 4 dB
CW	+ 3 dB

The two sets of views are typical of the best Loran-C signal reception found in Los Angeles, and they represent baseline cases for establishing optimum signal levels for performance estimates.

12/21/78, 1009, Grand & 54th St. (parked)
HP 140, Whip, F 100 kHz, W 10 kHz, IF 3 kHz, ST 500 ms, RF 0 dB, IF -20 dbm

FIGURE 3-1. 12/21/78, 1009.

12/22/78, 1107, 51st St. & Compton
HP 140, Whip, F 100 kHz, W 50 kHz, IF 3 kHz, ST 500 ms, RF 0 dB, IF -10 dbm

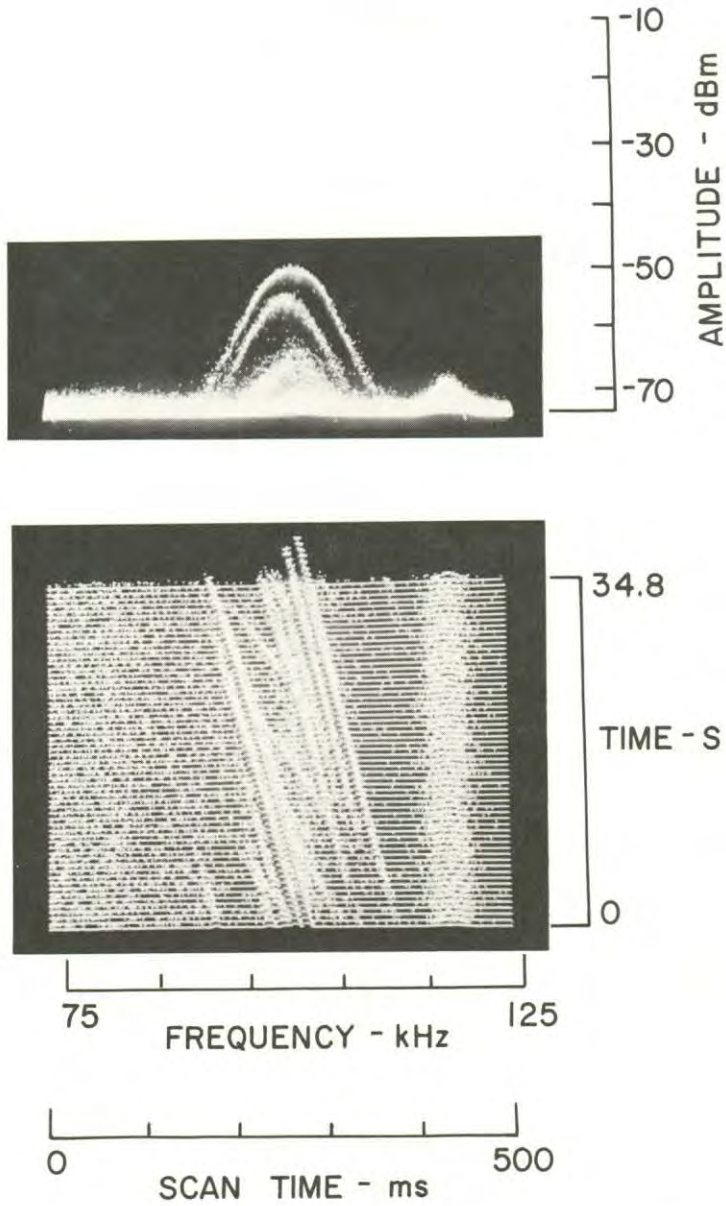

FIGURE 3-2. 12/22/78, 1107

3.3 SEVERE IMPULSIVE NOISE

Reference 3-Axis Views:
12/19/78, 1358 (Figure 3-3)
12/19/78, 1311 (Figure 3-4)
12/18/78, 1303 (Figure 3-5)
12/18/78, 1510 (Figure 3-6)
12/22/78, 1150 (Figure 3-7)
12/22/78, 1142 (Figure 3-8)
12/22/78, 1143 (Figure 3-9)

The above-listed views portray cases where severe impulsive noise was observed. The views have been selected to define the properties of the impulsive noise as well as to show examples of Loran-C signals immersed in the noise.

The 12/19/78, 1358 view (lower photograph) shows Loran signals which were free of noise in the upper portion of the view. As the measurement van moved along Compton St. toward 53rd St. (and approached an overhead electric distribution line along 53rd St. which connected to a line along Compton starting at 53rd St.), severe impulse was encountered. The noise abruptly increased in level at 53rd St. and reached a peak amplitude of 40 dBm (about 10 dB above the strongest Loran-C signal). The noise decreased in level about 10 dB as the measurement van moved along Compton, and the noise amplitude remained about equal to the strongest Loran-C signal along Compton for the remainder of the block.

The noise impulses are uniformly spaced at 8.3 ms intervals, which suggests that the noise source was a high power switching device operating on both the positive and negative portions of a 1Ø power line. The spectral shape of the noise was similar to the RF filter shape of the preamplifier filter, suggesting that the noise was essentially flat in amplitude over the frequency range shown.

The 12/19/78, 1311 view shows a similar but more complex impulsive noise found at 12th St. and Towne St. The data were taken with the measurement van parked. The upper view shows three distinct amplitude levels for the noise as well as the strongest Loran signal, Y, at about -50 dBm. The bottom view shows a very complex and variable set of spacings between successive impulses. However, all impulses were synchronized to the frequency of the power line. The close spacing and different spacings observed imply that multiple switching devices triggering at different switching points on the voltage cycle were fed by the distribution line. Close examination of the view shows that some slanting lines are distinct while others are less pronounced. The most distinct lines are spaced 8.3 ms apart and are shown as N_1 on the amplitude scale. N_2 and N_3 correspond to other less pronounced lines. 49 separate impulses can be identified across the 100 ms scan period at the threshold setting of -70 dBm used for the bottom view. Thus a Loran receiver operating at this site at this time would receive a separate distinct noise impulse at an average of about every 2 ms.

The 12/18/78, 1303 example shows another case of impulsive noise, along with a decrease in the strength of the Loran-C signals. As the measurement van moved along Hooper, modest noise was encountered just prior to 50th St. A brief and sharp decrease in the noise and the Loran signals occurred at 50th St. followed by slower variations of the noise and signal amplitude along Hooper. These variations were associated with various nearby structures and overhead cables. While the noise amplitude was not as large as shown in previous examples, the signal level decreases caused a poor signal-to-noise situation. The slanting lines of the noise impulses appeared to be spaced further apart than previous examples and their width was not as distinct.

Another examination of the noise at Hooper and 50th made on 12/18/78 at 1510 is shown with an expanded time scale. Multiple users with overlapping impulse times can be seen in the view. The primary noise impulses occurred at 8.3 ms spacings, and other impulses can be seen between the primary lines.

The 12/22/78, 1150 view was taken two blocks further along Hover at 52nd St. A more simplistic type of impulsive noise situation is shown where the impulses were evenly spaced at 16.6 ms intervals. This spacing suggests that a switching device was being fed by the nearby transmission line that operated on only the positive (or the negative) portion of the power line waveform. The pulse amplitude was equal to the strongest Loran-C signal or about -50 dBm.

The scanning receiver was changed from a frequency scanning mode of operation to a fixed frequency mode. The output sampling rate was increased by setting the analog signal scan time to 20 ms in the view at 12/22/78, 1142, and to 10 ms in the views at 12/22/78, 1143. These views show successive A-scope (amplitude-time) views of the individual pulses of a Loran group as well as 16 ms spaced noise impulses. In the top view of the 1142 data, 60 scan lines are shown. In the middle view eight scan lines of data from the upper view were expanded for a more detailed view of possible contamination of a Loran-C pulse group by a noise impulse. In the bottom view, the lower four lines of the middle view are further expanded for a detailed look at the noise spike coincidence with the sixth pulse of the group on line 2. The middle view shows a second coincidence on line 6 at the fifth pulse.

In the view at 1142, noise produced a Loran-like impulse at the start of the pulse group shown on line 3 of the lower view and line 8 of the upper view. The noise impulses provided a ninth pulse at the correct timing.

12/19/78, 1358, Compton at about 53rd St (traveling)
HP 140, Whip, F 100 kHz, W 50 kHz, IF 3 kHz, ST 500 ms, RF 0 dB, IF -10 dbm

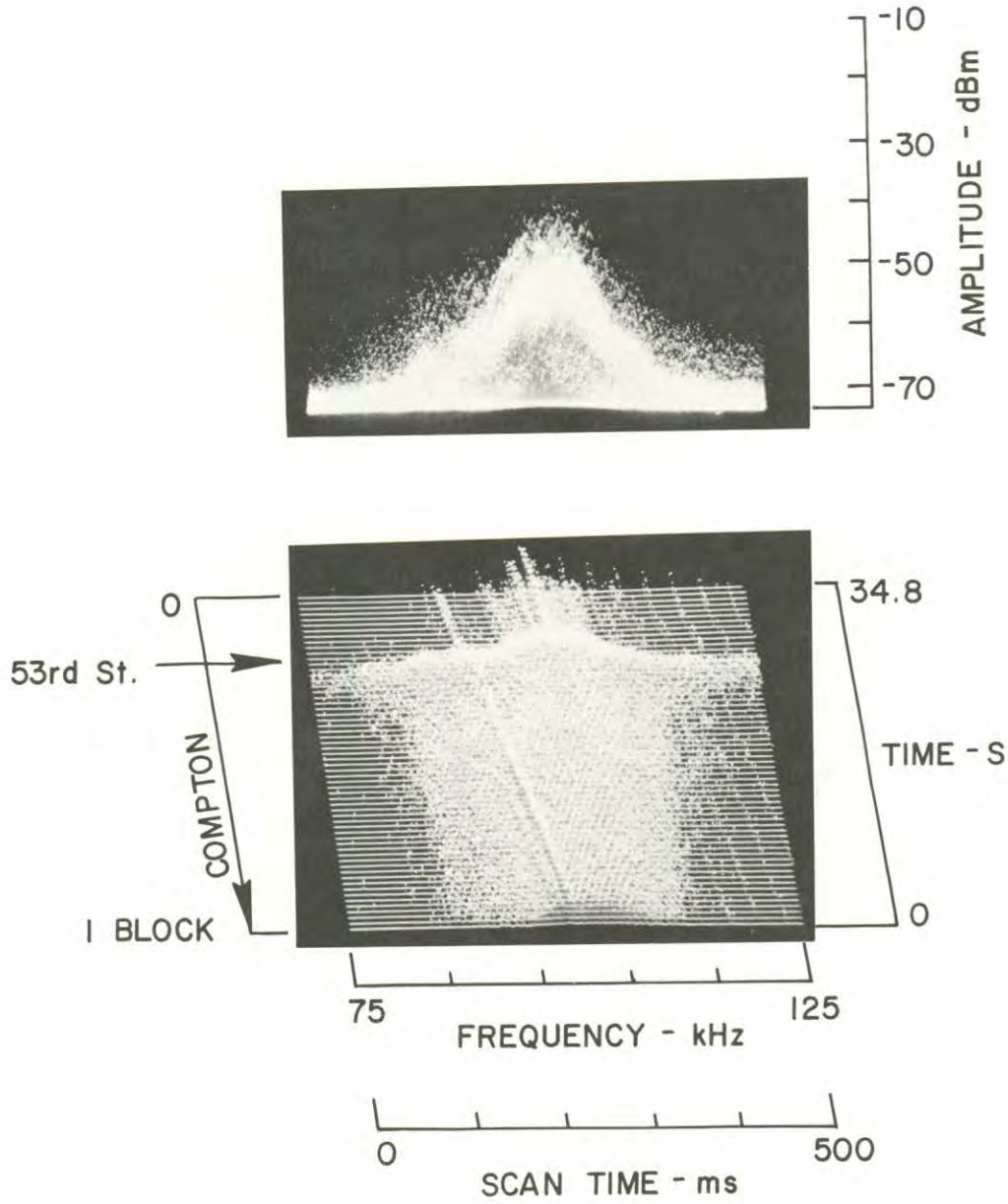

FIGURE 3-3. 12/19/78, 1358

12/19/78, 1311, 12th & Towne (Parked)
HP 140, Whip, F 100 kHz, W 50 kHz, IF 3 kHz, ST 100 ms, RF 0 dB, IF -10 dbm

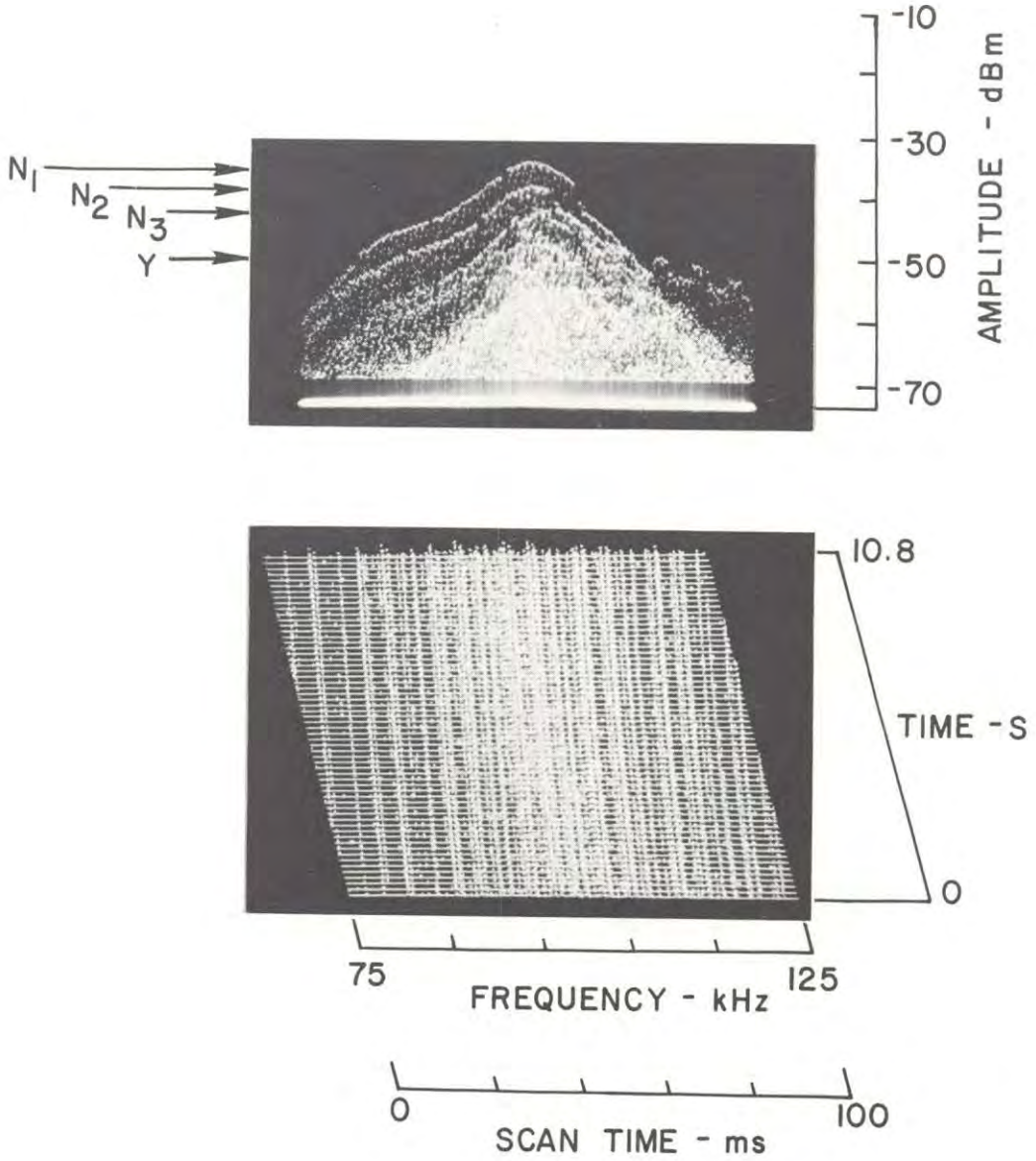

FIGURE 3-4. 12/19/78, 1311

12/18/78, 1303, Hooper & 50th (C16) Moving
HP 140, Whip, F 100 kHz, W 50 kHz, IF 10 kHz, ST 500 ms, RF 0 dB, IF -12 dbm

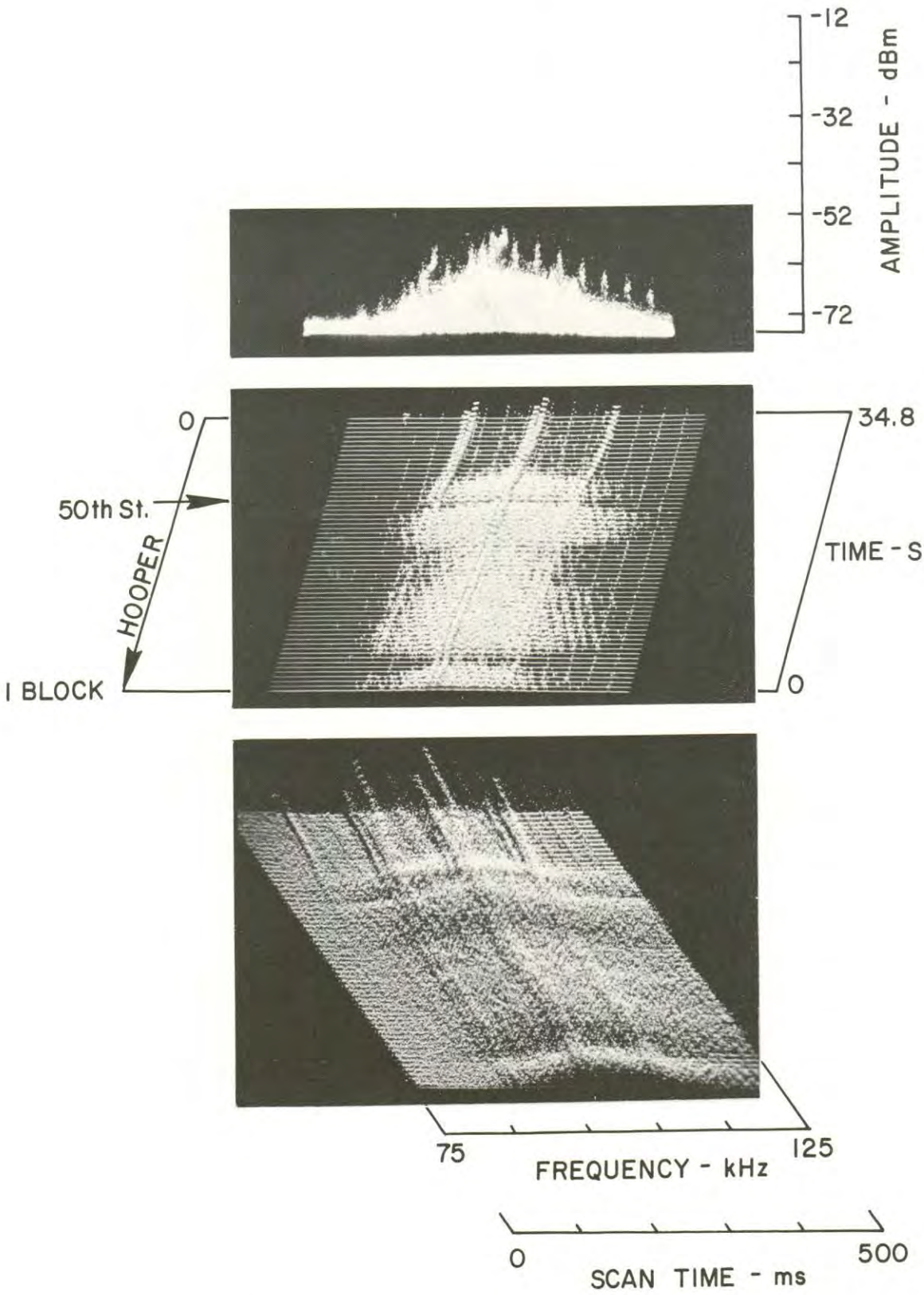

FICURE 3-5. 12/18/78, 1303

12/18/78, 1510, Hooper & 50th (C16) Parked
HP 140, Whip, F 100 kHz, W 20 kHz, IF 10 kHz, ST 100 ms, RF 0 dB, IF -12 dbm

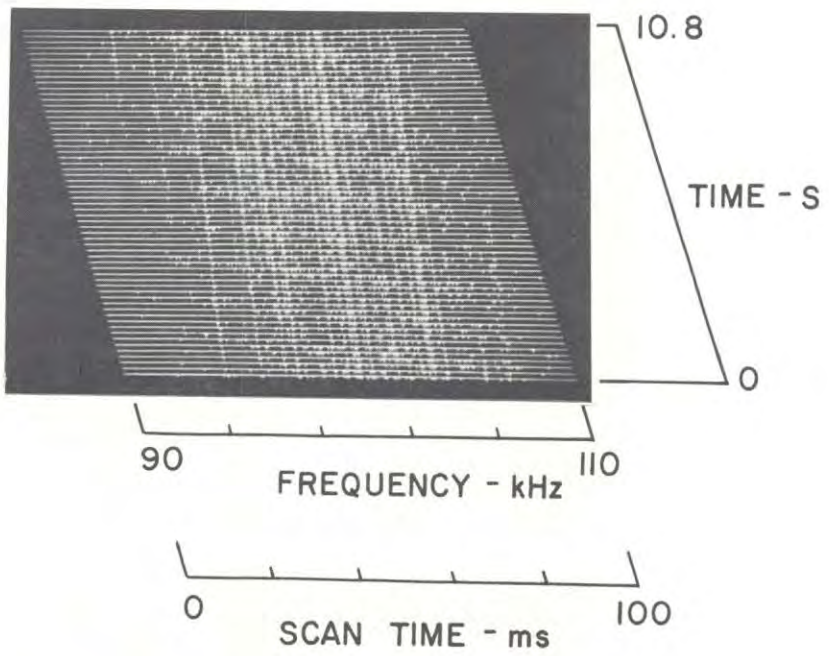

FIGURE 3-6. 12/18/78, 1510

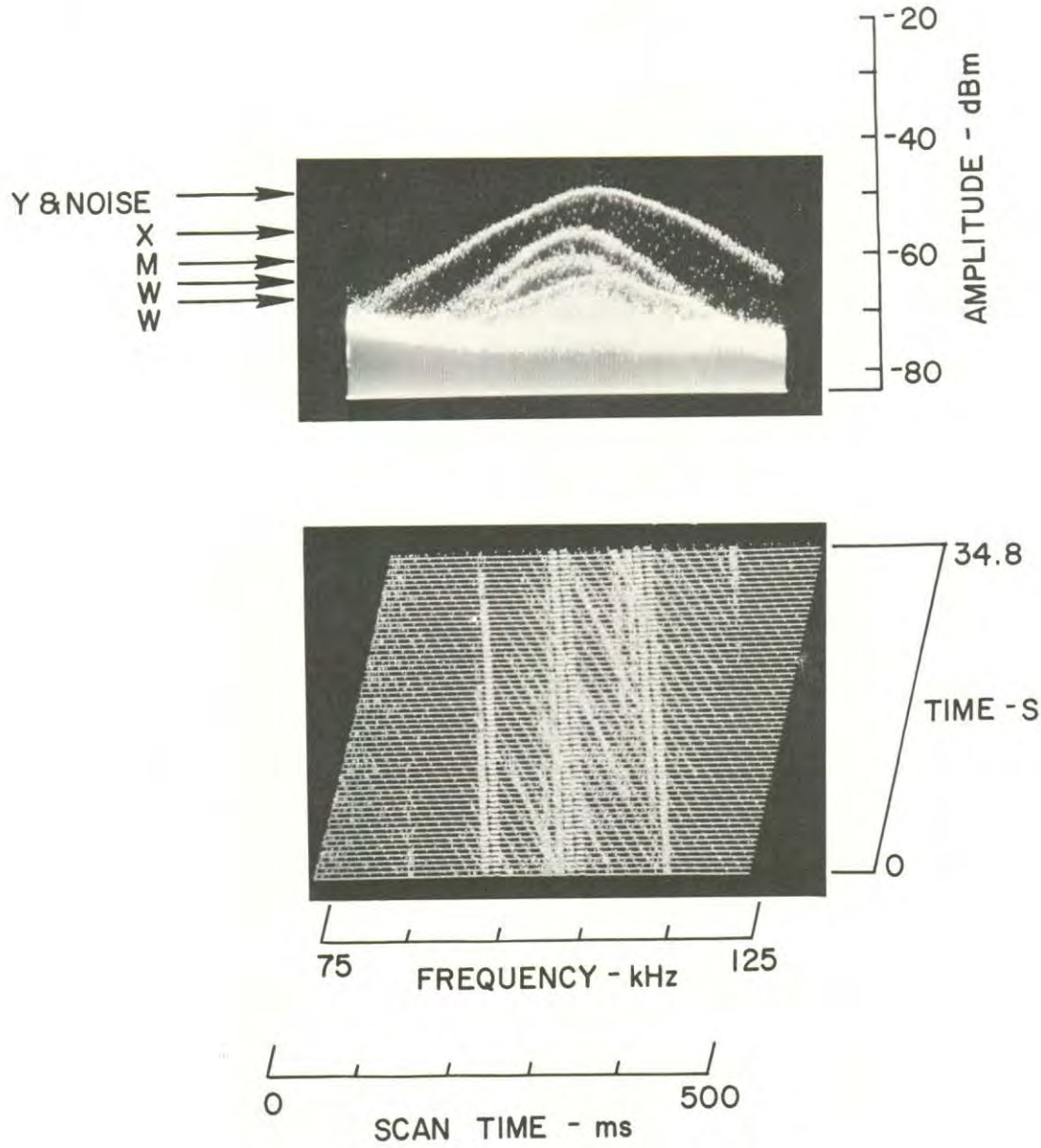

12/22/78, 1150, Hover & 52nd St.
HP 140, Whip, F 100 kHz, W 50 kHz, IF 10 kHz, ST 500 ms, RF 0 dB, IF -20 dbm

FIGURE 3-7. 12/22/78, 1150

12/22/78, 1142, Hover & 52nd St.
HP 140, Whip, F 100 kHz, W 0-TT, IF 10 kHz, ST 20 ms, RF 0 dB, IF -20 dbm

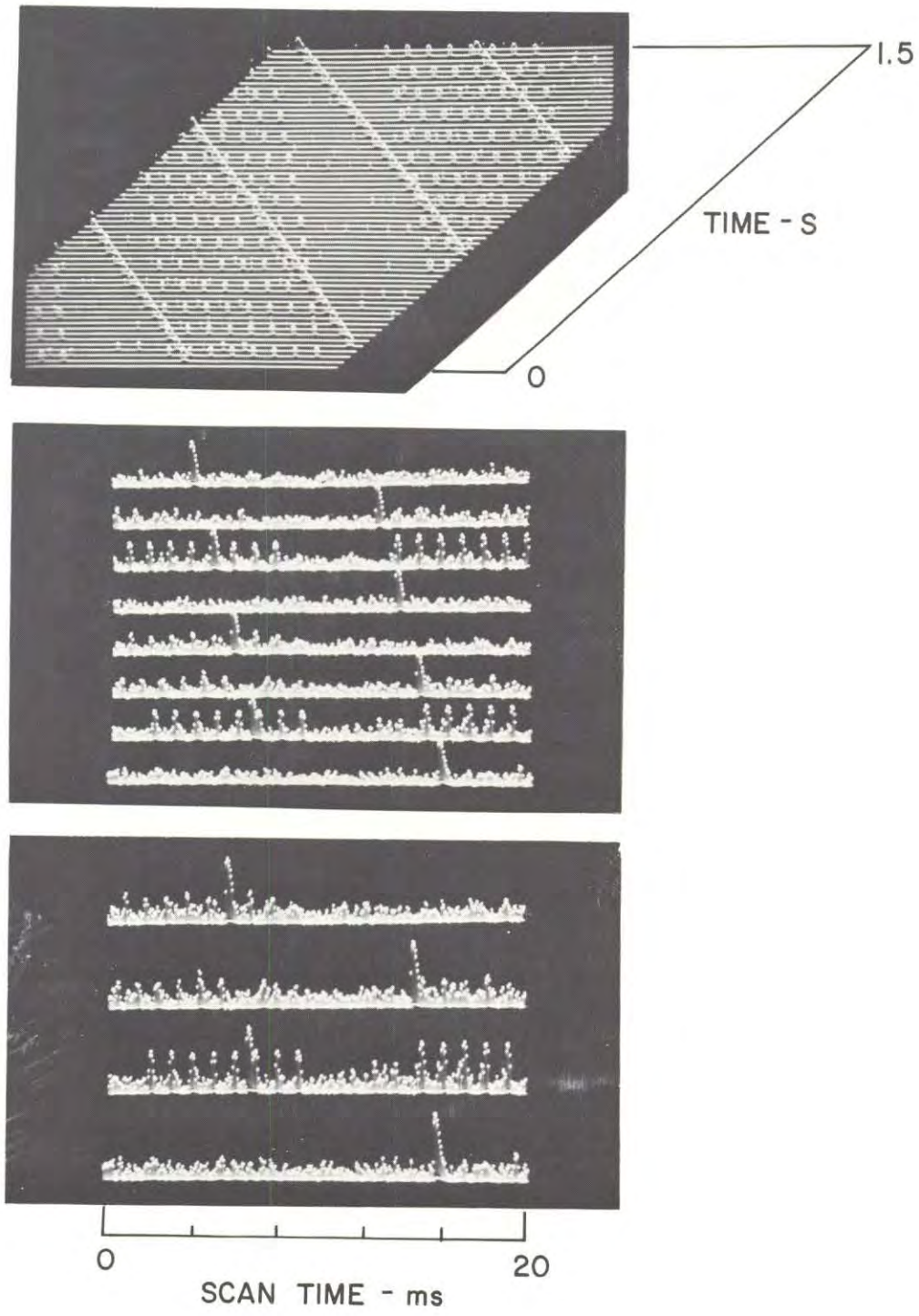

FIGURE 3-8. 12/22/78, 1142

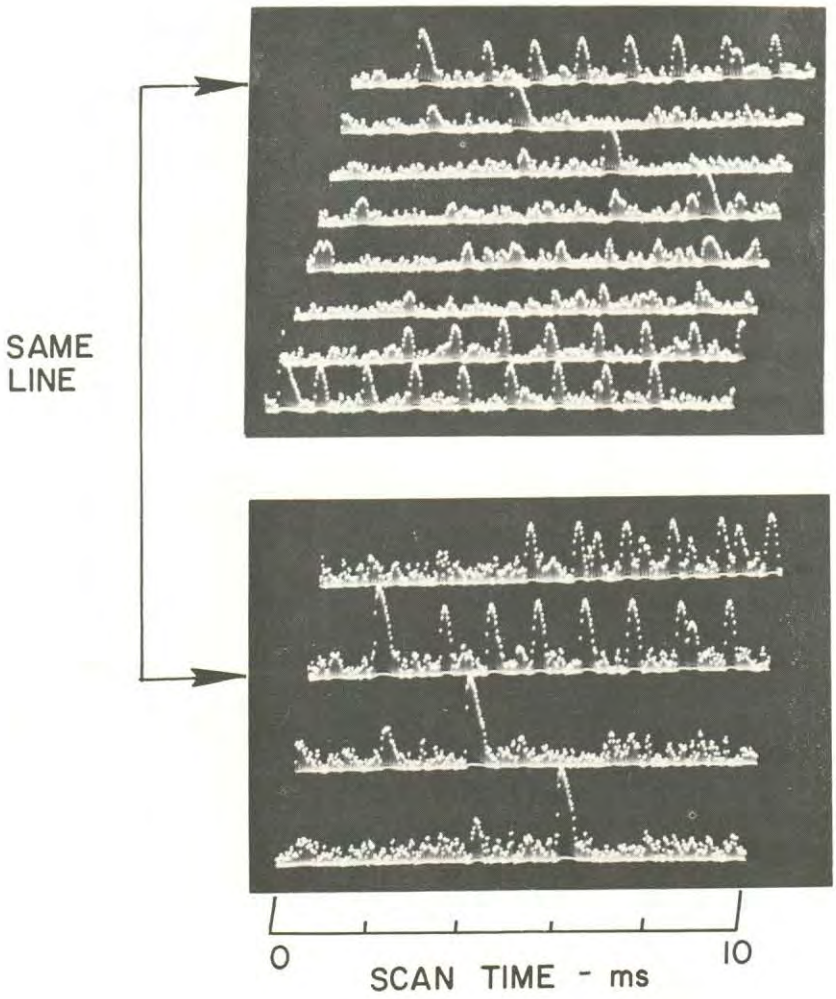

12/22/78, 1143, Hover & 52nd St.
HP 140, Whip, F 100 kHz, W 0-TT, IF 10 kHz, ST 10 ms, RF 0 dB, IF -20 dbm

FIGURE 3-9. 12/22/78, 1143

3.4 QUASI-RANDOM NOISE AND MIXED NOISE

Reference 3-Axis Views:	12/22/78, 1026	(Figure 3-10)
	12/22/78, 1045(a)	(Figure 3-11)
	12/22/78, 1045(b)	(Figure 3-12)
	12/22/78, 1045(c)	(Figure 3-13)
	12/22/78, 1019	(Figure 3-14)
	12/22/78, 1059(a)	(Figure 3-15)
	12/22/78, 1059(b)	(Figure 3-16)
	12/20/78, 1132	(Figure 3-17)
	12/21/78, 1033	(Figure 3-18)

The above-listed views portray cases of modest to severe quasi-random noise and quasi-random noise mixed with the impulsive noise described in Section 3.2. Again, the views show the general properties of the noise as well as examples of Loran-C signals immersed in the noise. The term quasi-random noise has been used to categorize situations where no distinct and major time or spectral domain properties existed in the noise. The scanning receiver and display controls were employed to search for any distinctive noise features without success.

The 12/22/78, 1026 data obtained at Compton and Slauson shows an example of noise lacking distinctive structure. Loran-C signals are more distinct at the lower frequencies, suggesting that the noise energy slowly increased with frequency. In the upper view two separate noise amplitude levels can be identified in the right portion of the amplitude view. A close examination of the lower view suggests that the stronger noise in that portion of the view was impulsive at a period of 16.6 ms. However, near the center of the frequency scale at 100 kHz, the impulsive noise and the random noise were at about equal amplitudes. Composite noise situations which were not uniform across the bandwidth of the Loran-C signal were noted at several locations.

Another view of the same noise is shown in the 12/22/78, 1045(a) data where the frequency axis was increased to cover a 50 kHz wide block of frequencies. The two distinct types of noise can also be identified in the two views. Also, a CW signal is shown at about 118 kHz. A time-time view of this situation is shown in the 1045(b) data. In the upper view the amplitude threshold control has been carefully adjusted to show peaks of the Loran-C pulses. The threshold control was lowered a few dB in the bottom view and the noise contamination was sufficiently severe that visual signal identification was extremely difficult. In the top view of the 1045(c) data, eight scan lines of data from 1045(b) were expanded. Pulse groups from station Y can be seen on lines 1 and 8. A pulse group from station X is on line 2. The bottom four lines of the upper view are further expanded in the bottom view. The noise severely distorted the Loran-C pulses and exceeded all Loran stations in amplitude except for Y signals which were received at a very low signal-to-noise margin.

Data at the same location at other times were taken which showed somewhat different noise properties. The views of 12/22/78, 1019, show a mixture of random noise and impulsive noise with a spacing of about 8 ms. The 12/22/78, 1059(a) data show a period when the impulsive noise increased in level and dominated the random noise. In the upper view the threshold control was adjusted to show Loran-C peak pulse amplitudes. The impulsive noise also exceeded this amplitude. In the bottom view the threshold control was lowered to include the random noise. The 1059(b) data show expanded time views. Eight lines are shown in the upper two views where the threshold control was set at zero. Loran-C signals from station Y, impulses, and random noise are shown. In the middle view, the threshold control was adjusted to the level of the top view of 1059(a). The first four lines are shown with further detail in the bottom view where considerable signal distortion is evident, as well as a coincidence between the eighth pulse and a noise impulse.

Another view of quasi-random noise is shown in the 12/20/78, 1132 data. Loran-C signal levels exceed the noise in the lower portion of the frequency range but are equal to the noise level in the upper frequencies. Noise contamination from the ignition system of a 110 volt gasoline generator is shown at a level about 5 dB above the Loran-C and noise signal.

A view of the onset of quasi-random noise as the instrumentation van approached a distribution line at Grand St. and 45th St. is shown in the data for 12/21/78, 1033. Prior to 45th St. Loran-C signals were received very well. Within a few feet of travel the noise peaks increased in level to roughly equal that of the Y signal.

12/22/78, 1026, Compton & Slauson
HP 140, Whip, F 100 kHz, W 20 kHz, IF 3 kHz, ST 500 ms, RF 0 dB, IF -10 dbm
Two insulator distribution lines along Compton from Slauson to 53rd St.
Noise similar along Compton

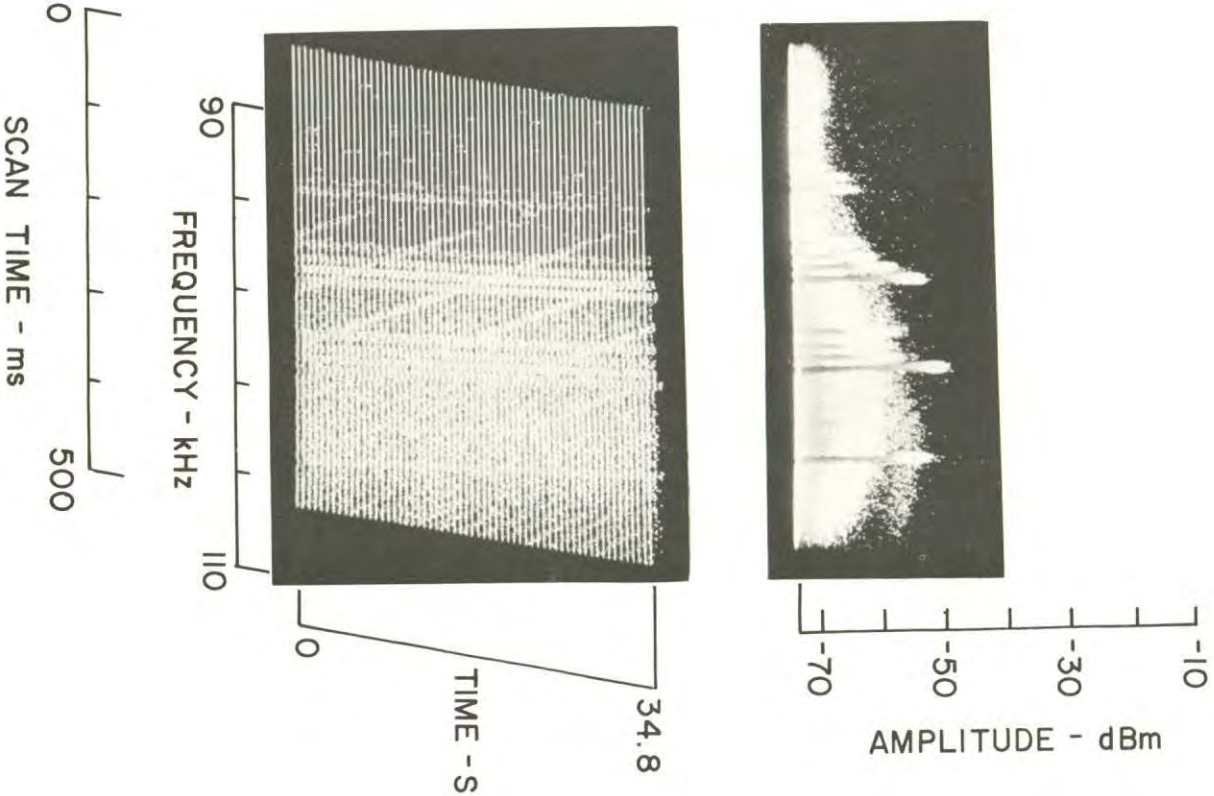

FIGURE 3-10. 12/22/78, 1026

12/22/78, 1045(a), Compton and Slauson
HP 140, Whip, F 100 kHz, W 50 kHz, IF 3 kHz, ST 500 ms, RF 0 dB, IF -10 dbm

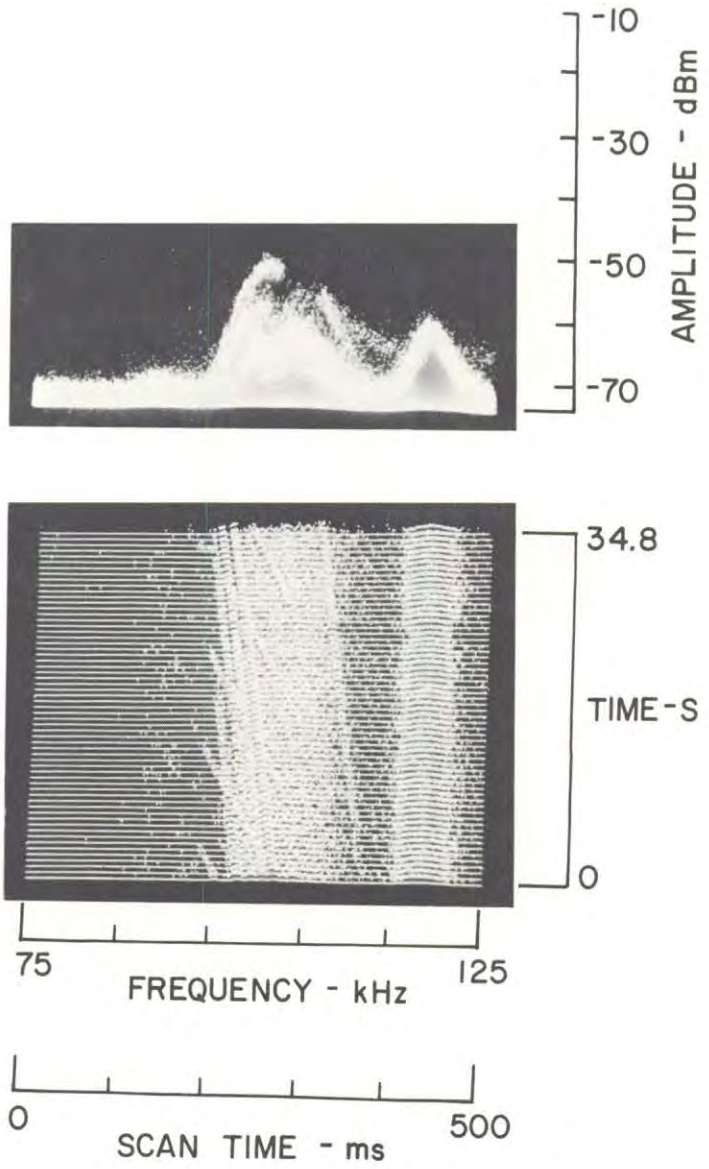

FIGURE 3-11. 12/22/78, 1045(a)

12/22/78, 1045(b), Compton and Slauson
HP 140, Whip, F 100 kHz, W 0-TT, IF 10 kHz, ST 10 ms, RF 0 dB, IF -10 dbm

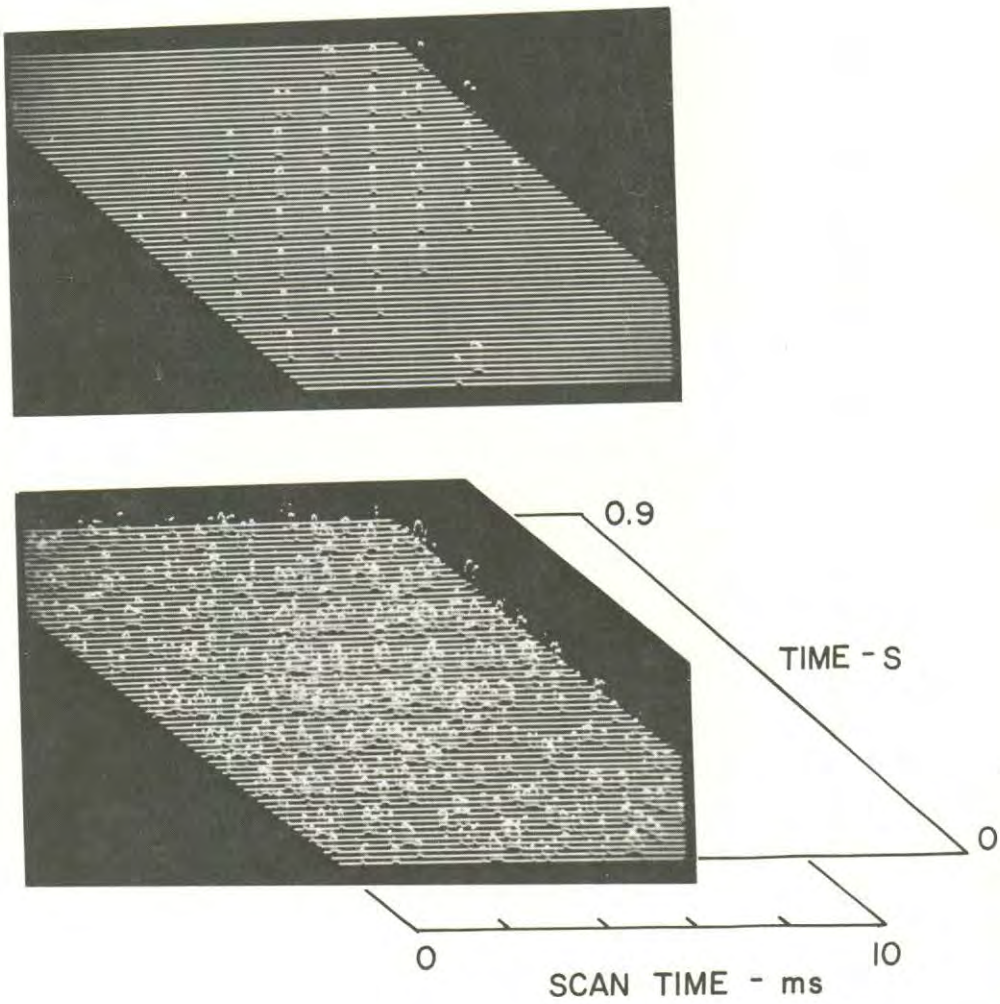

FIGURE 3-12. 12/22/78, 1045(b)

12/22/78, 1045(c), Compton and Slauson
HP 140, Whip, F 100 kHz, W 0-11, IF 10 kHz, ST 10 ms, RF 0 dB, IF -10 dbm

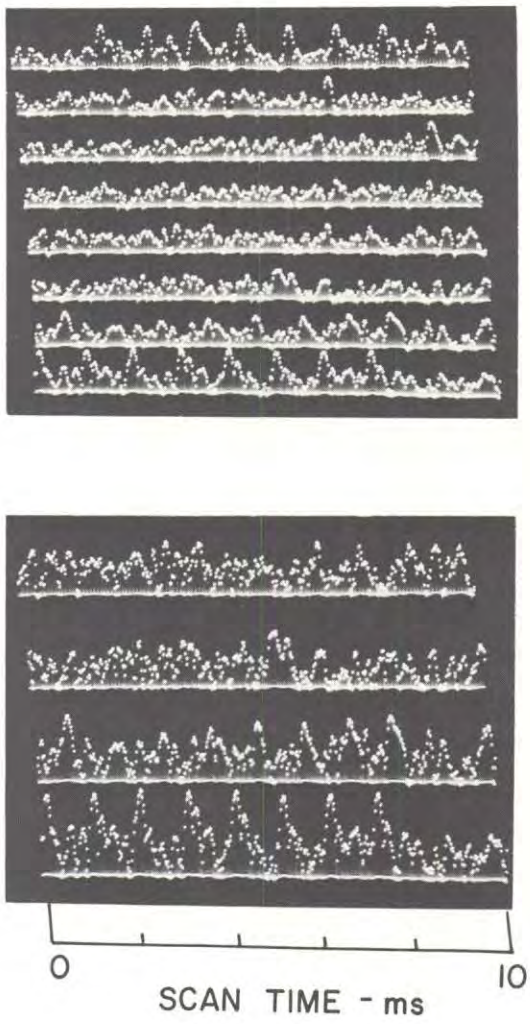

FIGURE 3-13. 12/22/78, 1045(c)

12/22/78, 1019, Compton & Slauson
HP 140, Whip, F 100 kHz, W 0-TT, IF 10 kHz, ST 20 ms, RF 0 dB, RF 0 dB, IF -10 dbm

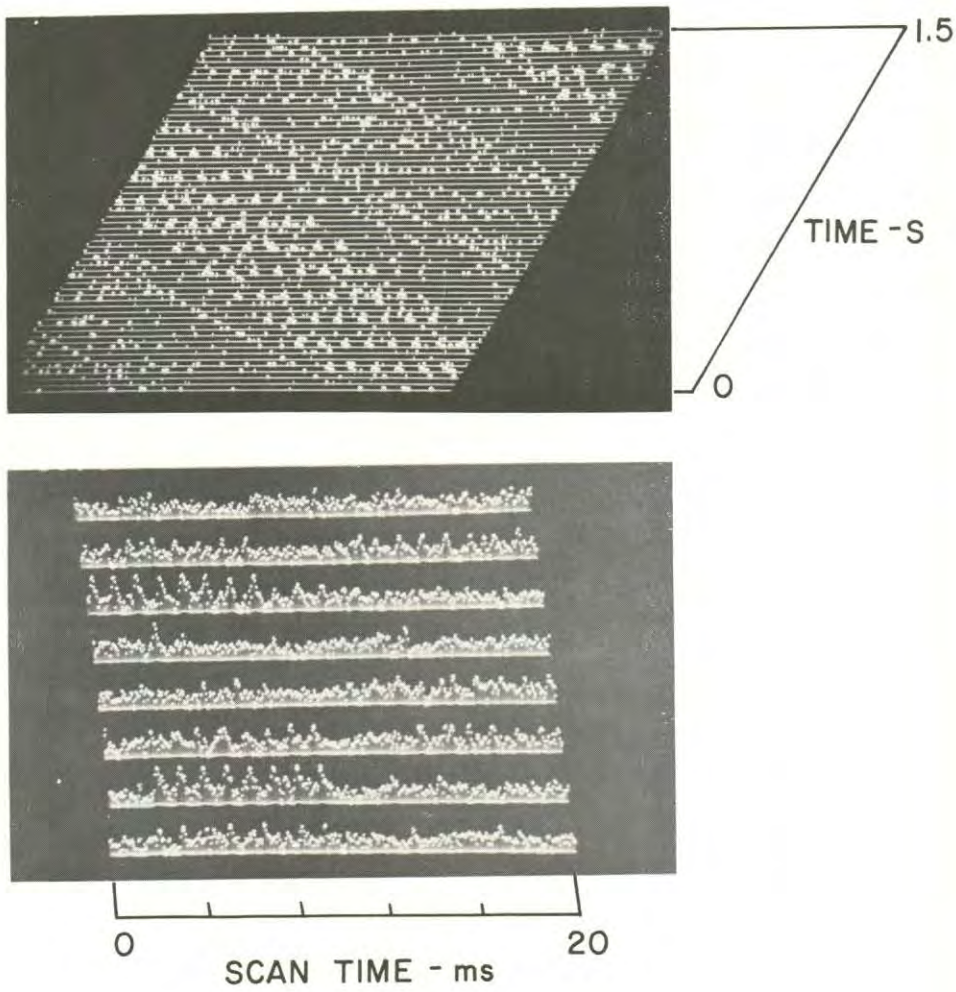

FIGURE 3-14. 12/22/78, 1019

12/22/78, 1059(a), Compton and Slauson
HP 140, Whip, F 100 kHz, W 0-TT, IF 10 kHz, ST 20 ms, RF 0 dB, IF -10 dbm

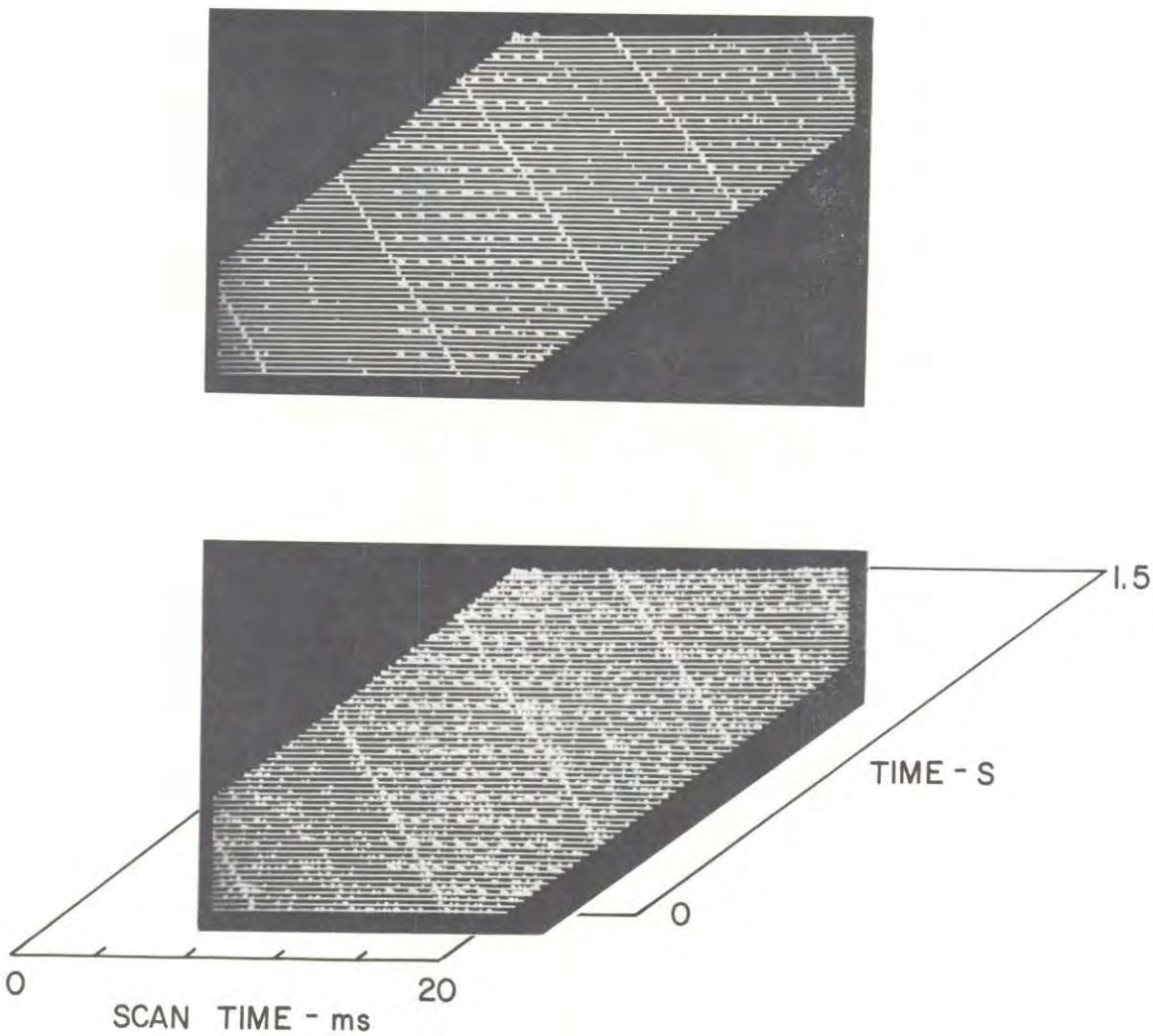

FIGURE 3-15. 12/22/78, 1059(a)

12/22/78, 1059(b), Compton and Slauson
HP 140, Thin, F 100 kHz, W 0-TT, IF 10 kHz, ST 20 ms, RF 0 dB, IF -10 dbm

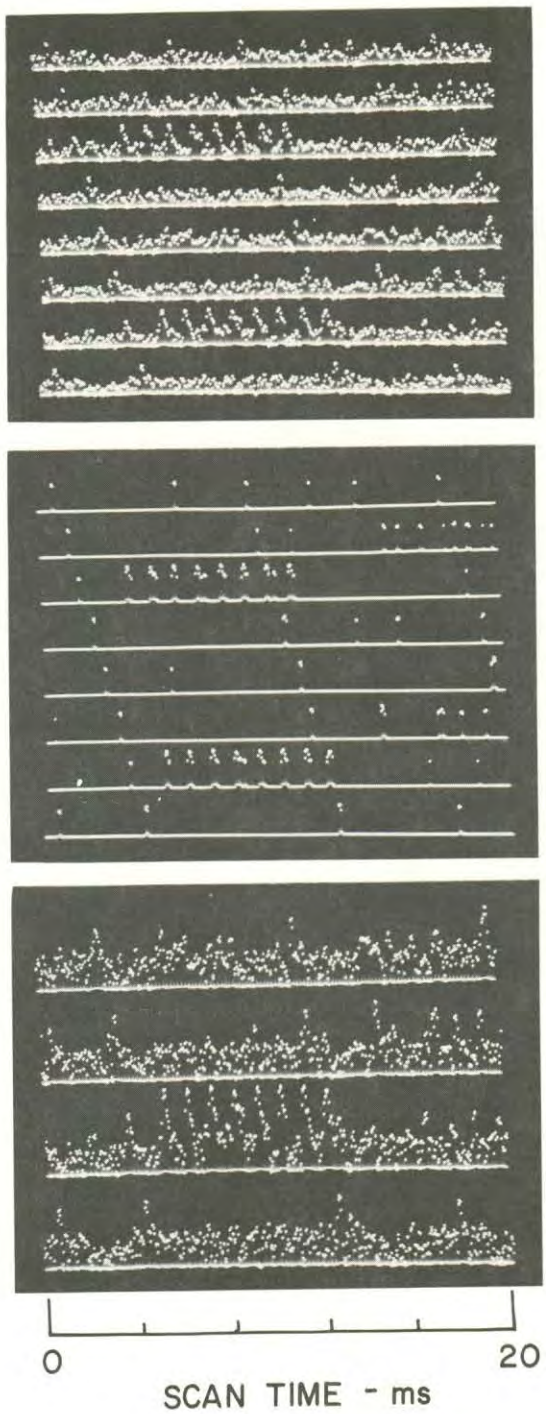

FIGURE 3-16. 12/22/78, 1059(b)

12/20/78, 1132, Exposition at Gramercy (parked)
HP 140, Whip, F 100 kHz, W 20 kHz, IF 3 kHz, ST 500 ms, RF 0 dB, IF -10 dbm
Noise along Exposition until about Arlington

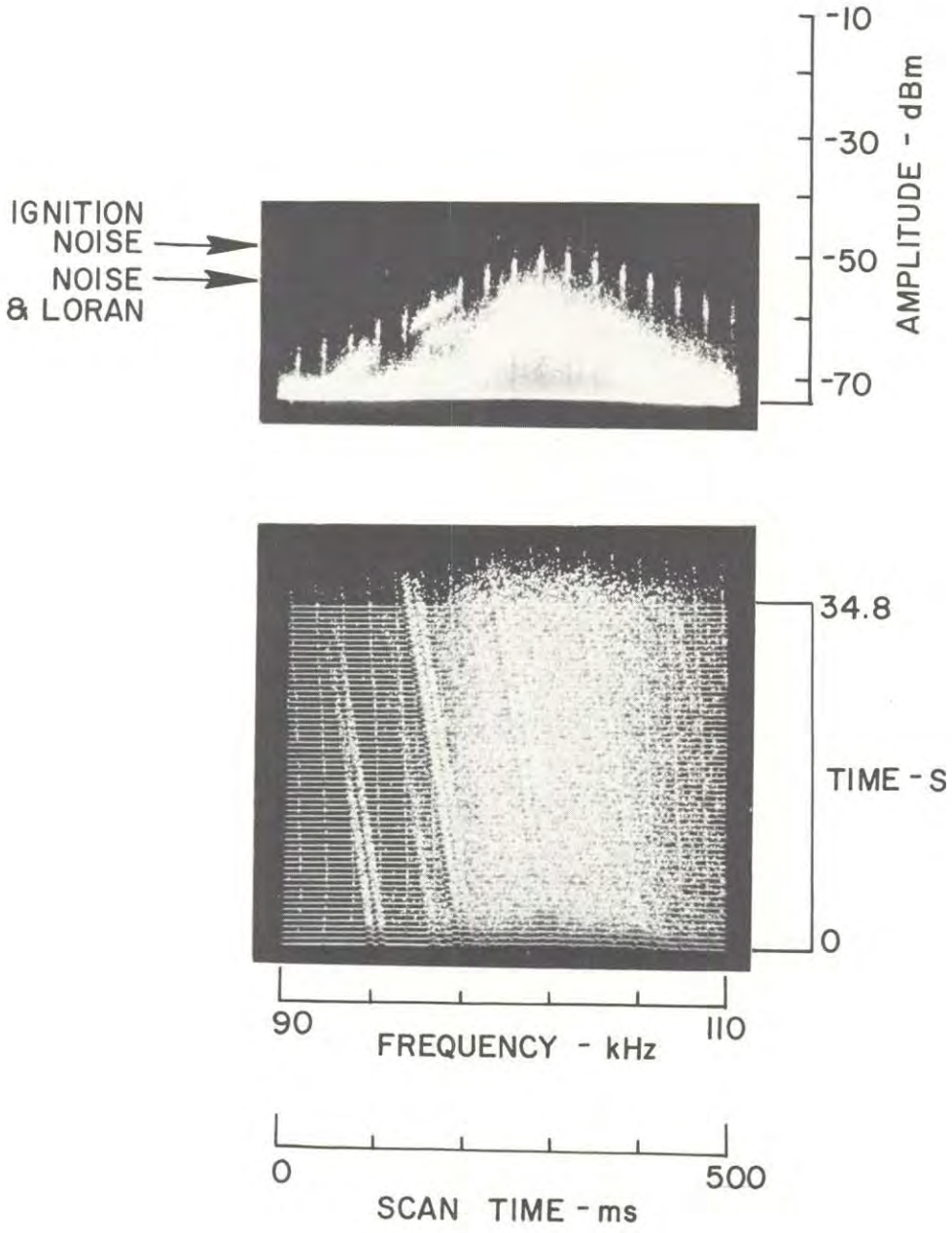

FIGURE 3-17. 12/20/78, 1132

12/21/78, 1033, Grand & 45th St. (moving)
HP 140, Whip, F 100 kHz, W 50 kHz, IF 3 kHz, ST 500 ms, RF 0 dB, IF -20 dbm

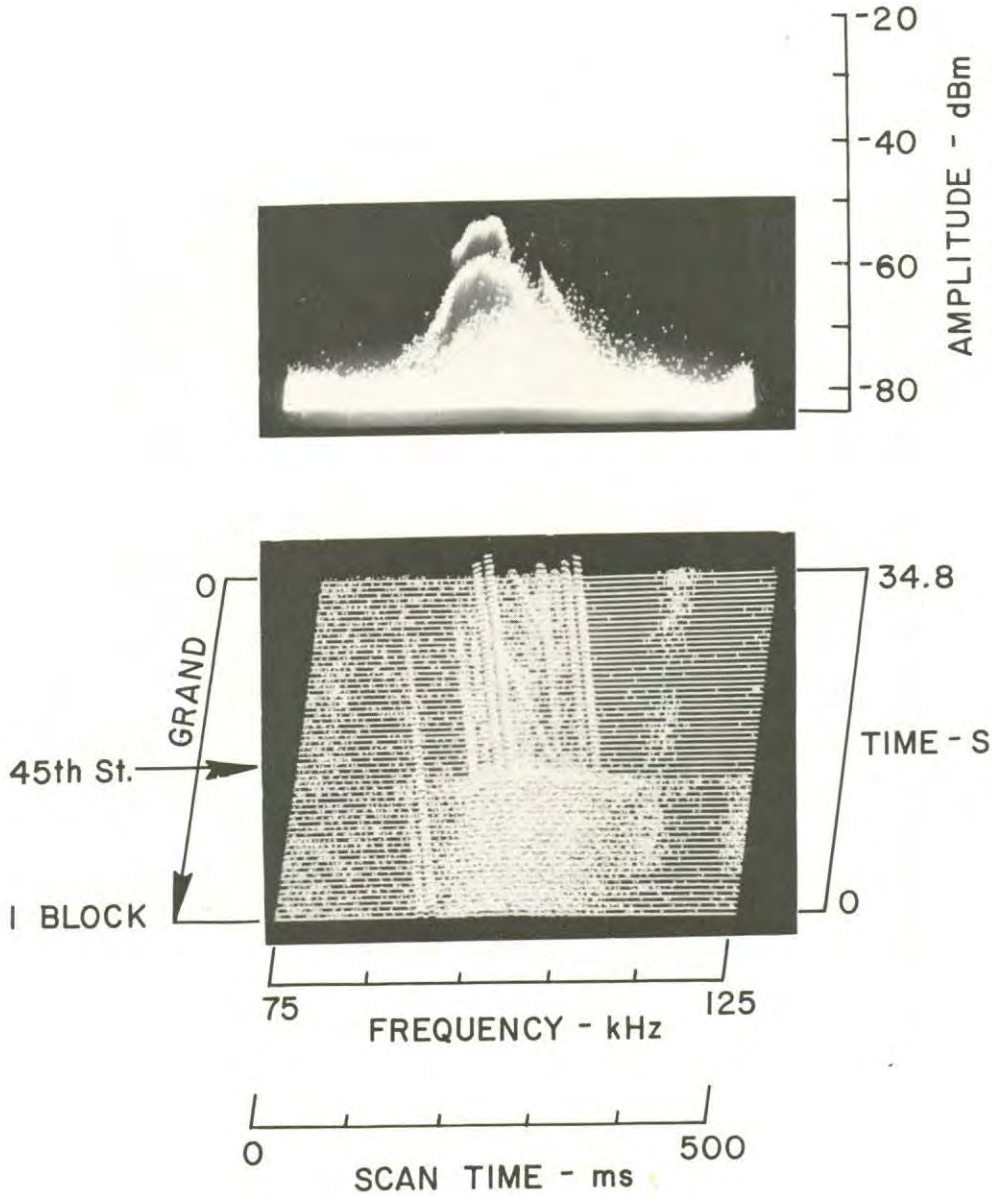

FIGURE 3-18. 12/21/78, 1033

3.5 STRONG LOCAL AREA NEAR FIELD SIGNALS

Reference 3-Axis Views: 12/21/78, 1130 (Figure 3-19)
12/20/78, 1407 (Figure 3-20)
12/19/78, 1543 (Figure 3-21)
12/21/78, 1135 (Figure 3-22)
12/20/78, 1400 (Figure 3-23)

The 12/21/78, 1130 data show a typical example of strong local area CW signals. These signals abruptly rise from below receiver noise levels to very strong signal levels in a few tens of feet. In the 1130 example four distinct CW signals appeared simultaneously at about 75, 92, 108, and 124 kHz and very rapidly increased in amplitude, and the 108 kHz signal rose to a level equal to the Loran Y signal. The four signals decreased in level and disappeared below the receiver threshold level as abruptly as the increase. The location of the signal source is obviously at Trinity and 22nd St. but the precise source was not firmly established. Inspection of the area did not reveal a specific box labeled "LF oscillator."

Another example is shown in the data taken at 12/20/78, 1407, where six separate and discrete frequency CW signals appeared in the 3-axis view and rose to a maximum in about 100 feet of travel along Halldale. The maximum signal appeared at the corner of Halldale and Vernon. The 77, 92, 109, and 123 kHz signals are very similar to those in the previous example at 12/21/78, 1130. A weak 100 kHz signal can be seen in the upper view directly under the maximum peak of the Loran-C Y signal. The 117 kHz signal amplitude did not vary in amplitude with the others, and it was observed at many other locations unassociated with the strong local area signals. The 117 kHz signal is believed to be an LF communications signal from a distant transmitter. The source of the local area signal was again not obvious.

A third example of local area CW signals is shown in the data for 12/19/78, 1543. Discrete frequencies of 93, 102, 108, 118, and 123 kHz were observed where the 93, 108, and 123 kHz signals were classified as local area. These signals were associated with overhead unshielded telephone wires; however, precise location equipment was not used to firmly verify this association. No other obvious sources were found in an inspection of the area.

Another somewhat different observation of the 92 and 108 kHz CW signals previously classified as of the local area type is shown in the data for 12/21/78, 1135. The signals abruptly appeared but remained in the 3-axis view for an entire block. The consistent and rapid fading of both signals suggest that they are from the same source and that the source is on 25th St. near Trinity. However, the radiation mechanism must involve wires along 25th St. Brief bursts of signal at 123 kHz can also be seen which coincide with amplitude peaks in the 92 and 108 kHz signals which further suggest that the source mechanism is similar to that of the previous examples.

Another example of local area CW signals is shown in the data at 12/20/78, 1400. Also shown in the view is noise typical of that emitted from power lines with electrical leakage along insulators. The local area signal at about 108 kHz and the power line noise were about equal in amplitude to the Loran-C Y signal, while the 92 kHz signal was about 10 dB below the Y signal amplitude.

12/21/78, 1130, Trinity at 22nd St. (moving slowly)
HP 140, Whip, F 100 kHz, W 50 kHz, IF 3 kHz, ST 500 ms, RF 0 dB, IF -20 dbm

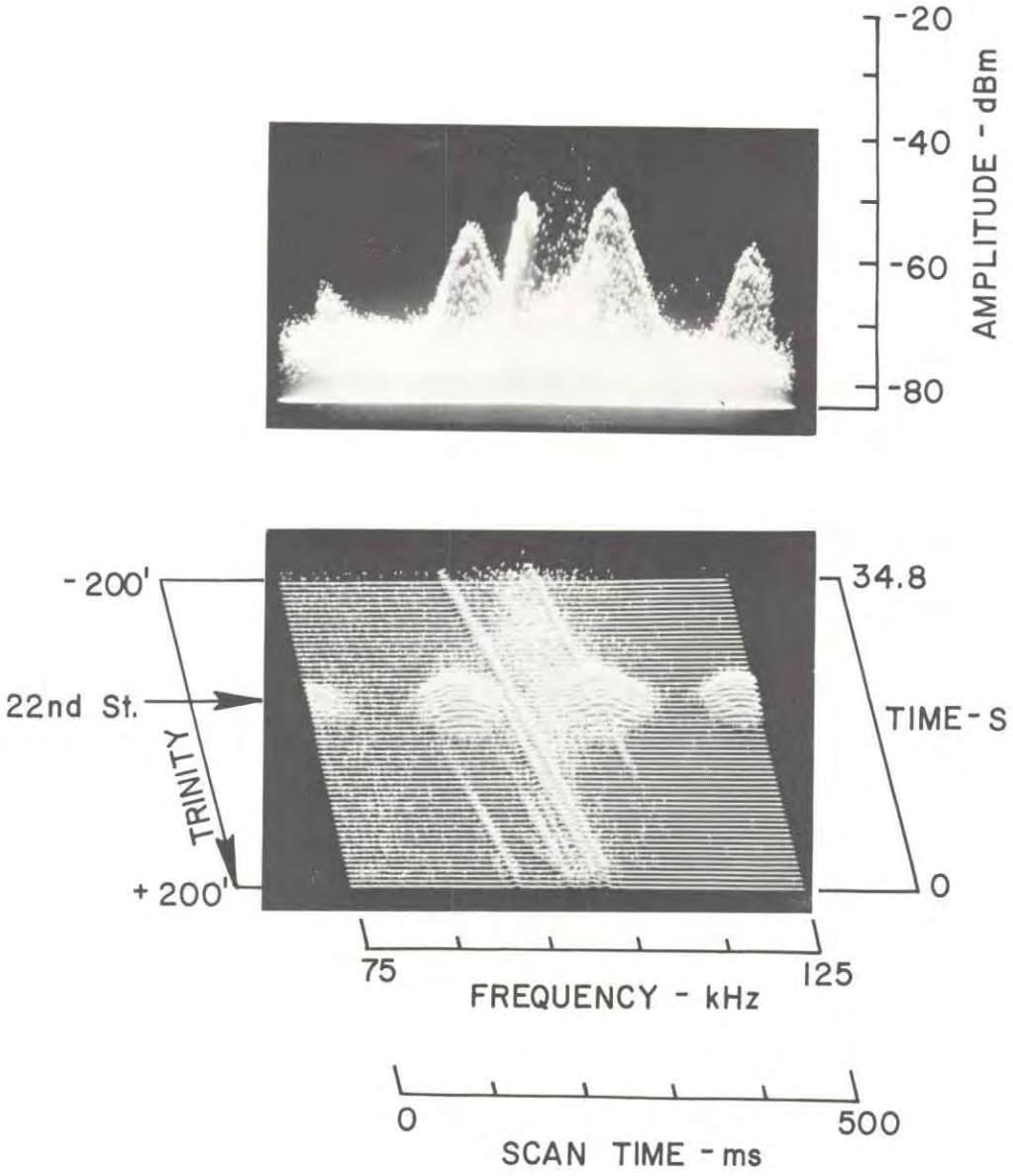

FIGURE 3-19. 12/21/78, 1130

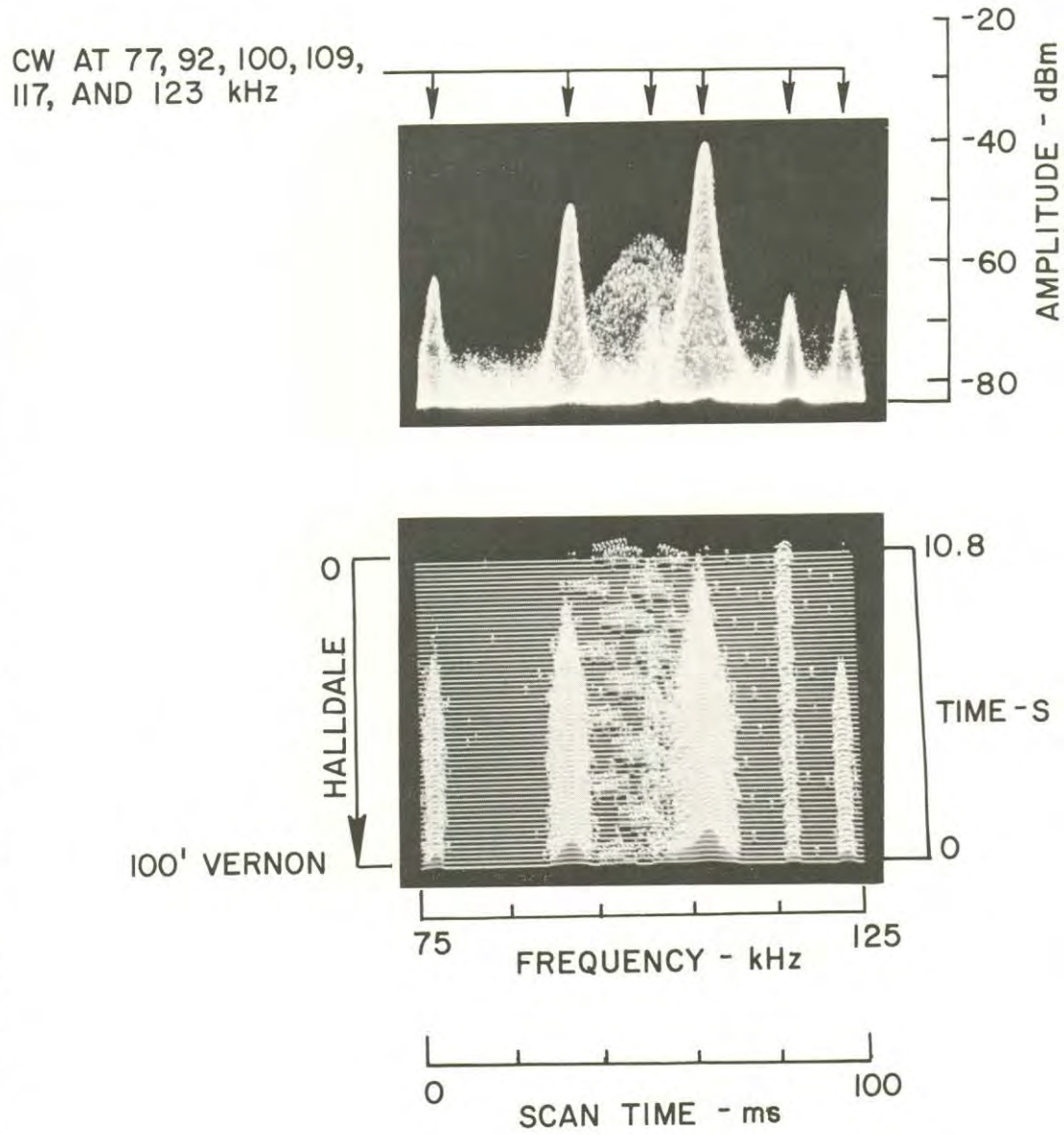

12/20/78, 1407, Halldale at Vernon (moving slowly)
HP 140, Thin, F 100 kHz, W 50 kHz, IF 1 kHz, ST 100 ms, RF 0 dB, IF -20 dbm

FIGURE 3-20. 12/20/78, 1407

12/19/78, 1543, 46th St. and turn left on McKinley
HP 140, F 100 kHz, W 50 kHz, IF 1 kHz, ST 100 ms, RF 0 dB, IF -38 dbm

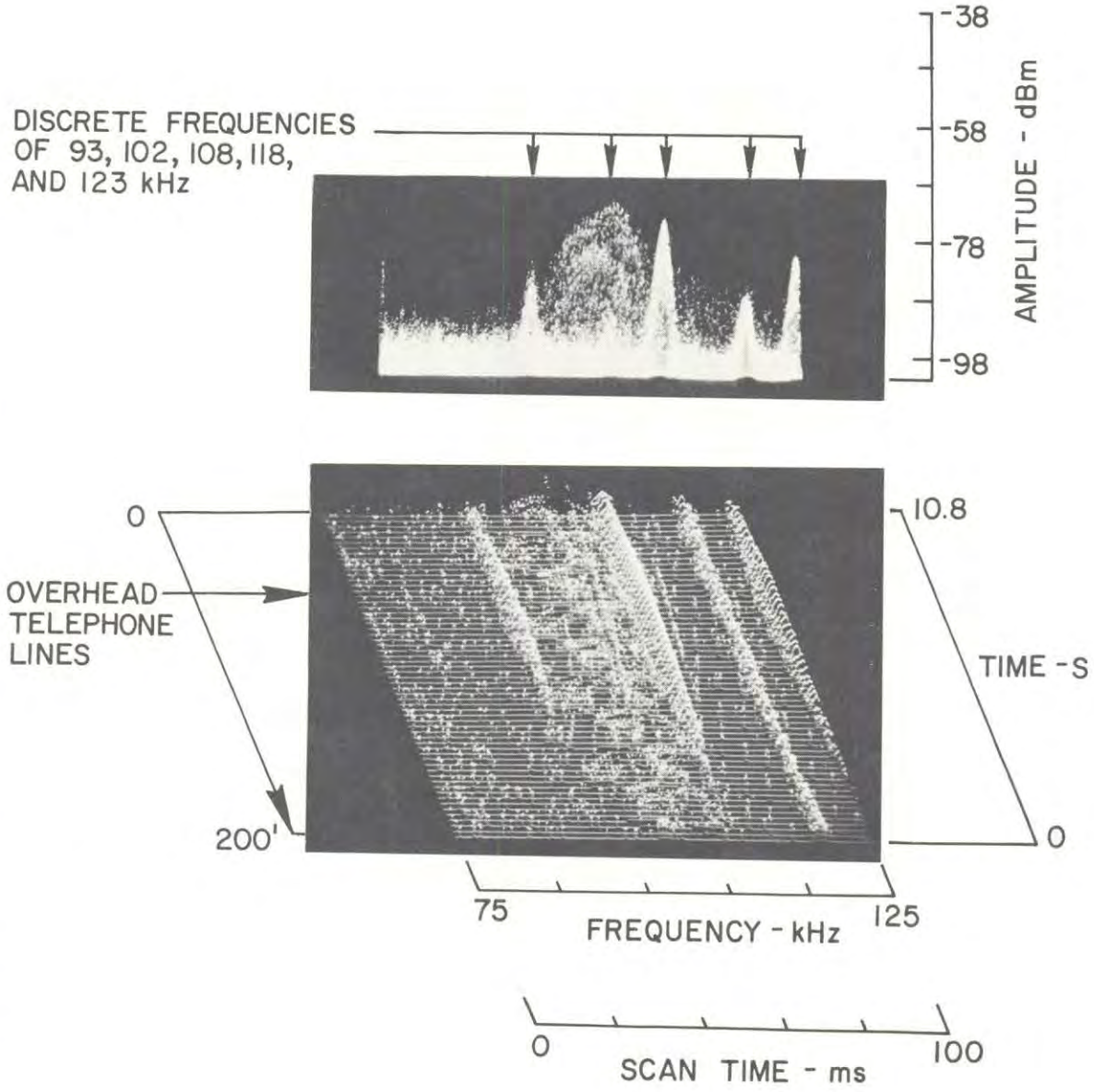

FIGURE 3-21. 12/19/78, 1543

12/21/78, 1135, 25th St. between Trinity and Maple
HP 140, Whip, F 100 kHz, W 50 kHz, IF 3 kHz, ST 500 ms, RF 0 dB, IF -20 dbm

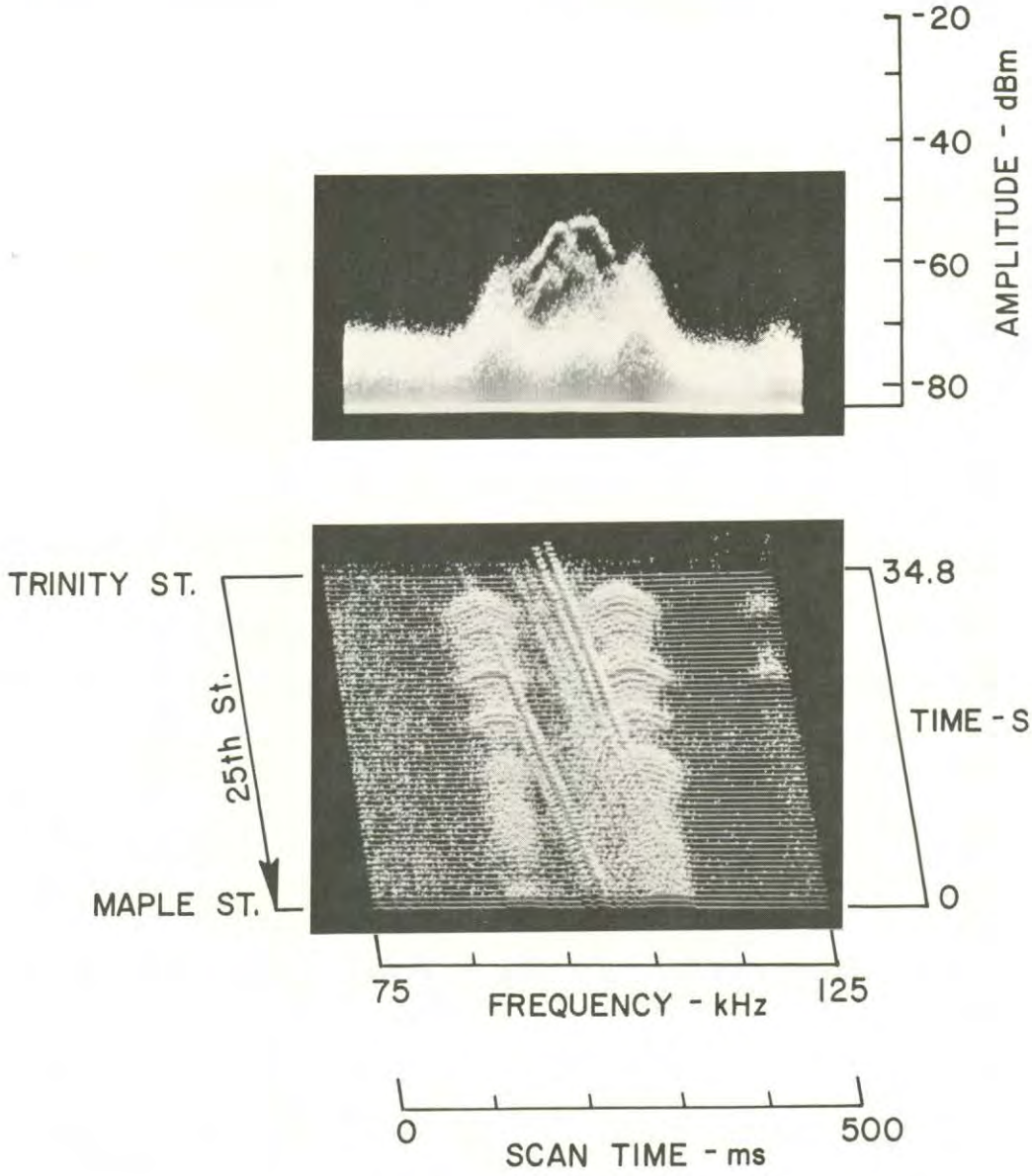

FIGURE 3-22. 12/21/78, 1135

12/20/78, 1400, Vernon & Dalton (moving)
HP 140, Whip, F 100 kHz, W 20 kHz, IF 3 kHz, ST 100 ms, RT 0 dB, IF -10 dbm

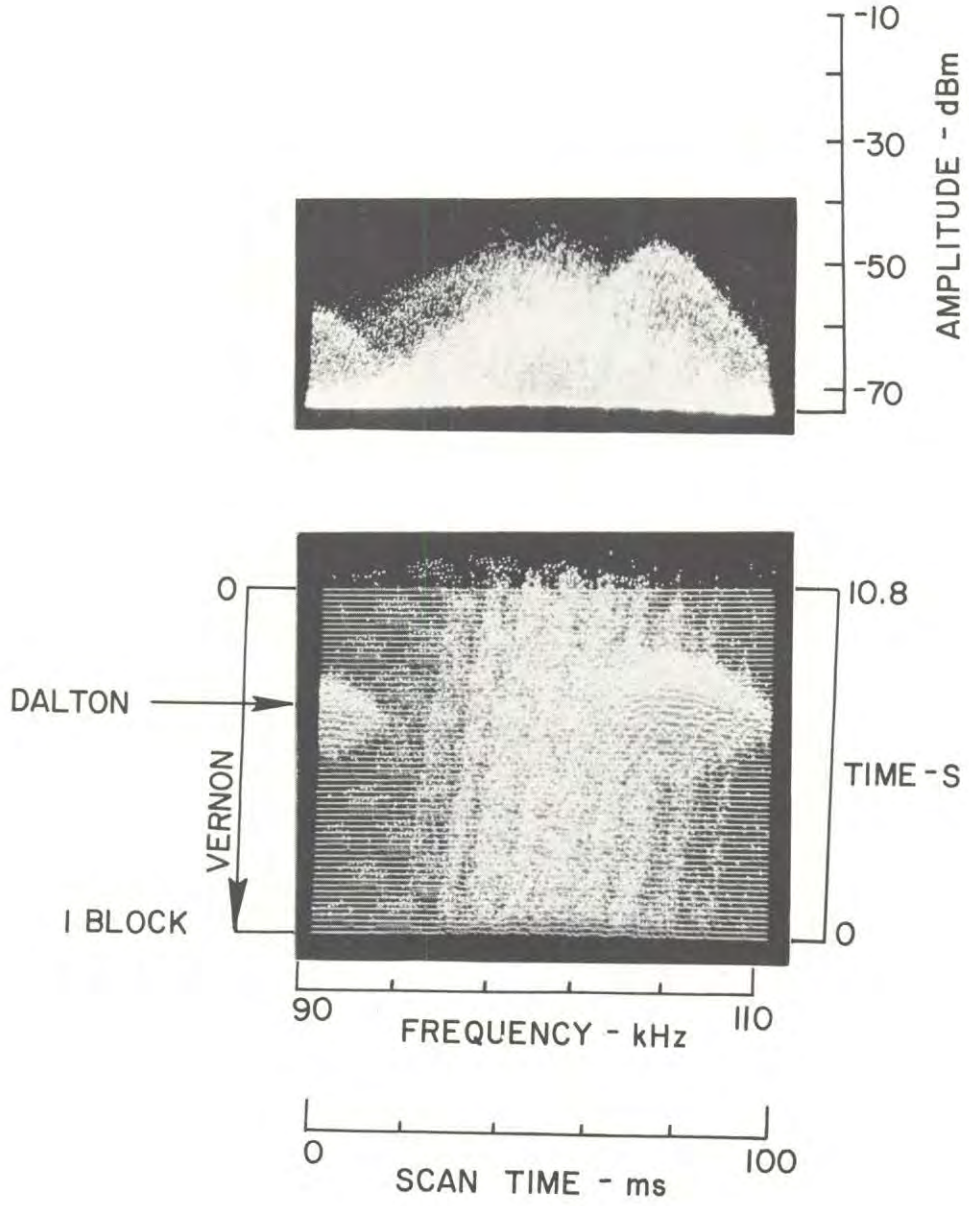

FIGURE 3-23. 12/20/78, 1400

3.6 WEAK LARGE AREA SIGNALS

Reference 3-Axis Views: 12/21/78, 0936 (Figure 3-24)
12/21/78, 1500 (Figure 3-25)

Weak CW signals were received at many of the measurement locations. These signals were detectable with the measurement system over large areas of Los Angeles. They also fell below the measurement sensitivity of the system in some areas. The 12/21/78, 0936 measurements show six low level CW carriers in the 50 to 150 kHz band during a morning system check-out at the Los Angeles Coliseum. Signals were found at about 100, 103, 120, 130, 140, and 150 kHz. The system sensitivity was improved for this measurement, compared to most other measurements described in this report, by employing a 0.3 kHz IF bandwidth.

Another measurement of low level CW signals was made on 12/21/78, 1500, which detected weak signals at about 88, 104, 116, and 120 kHz. A 100 kHz calibration signal is shown on the upper six lines of the 1500 3-axis view. The IF bandwidth used for this measurement was 1 kHz.

Similar weak CW signals could be detected at a large number of the measurement sites by merely adjusting the IF bandwidth of the scanning receiver to a very narrow value and employing the increased CW signal detection capability to search for such signals. Loran-C signals and noise were severely attenuated by the narrow IF bandwidth; thus, narrow IF bandwidths were not normally employed for most measurements.

12/21/78, 0936, Coliseum
HP 140, Whip, F 100 kHz, W 100 kHz, IF 0.3 kHz, ST 500 ms, RF 0 dB, IF -40 dbm
Search for weak CW signals

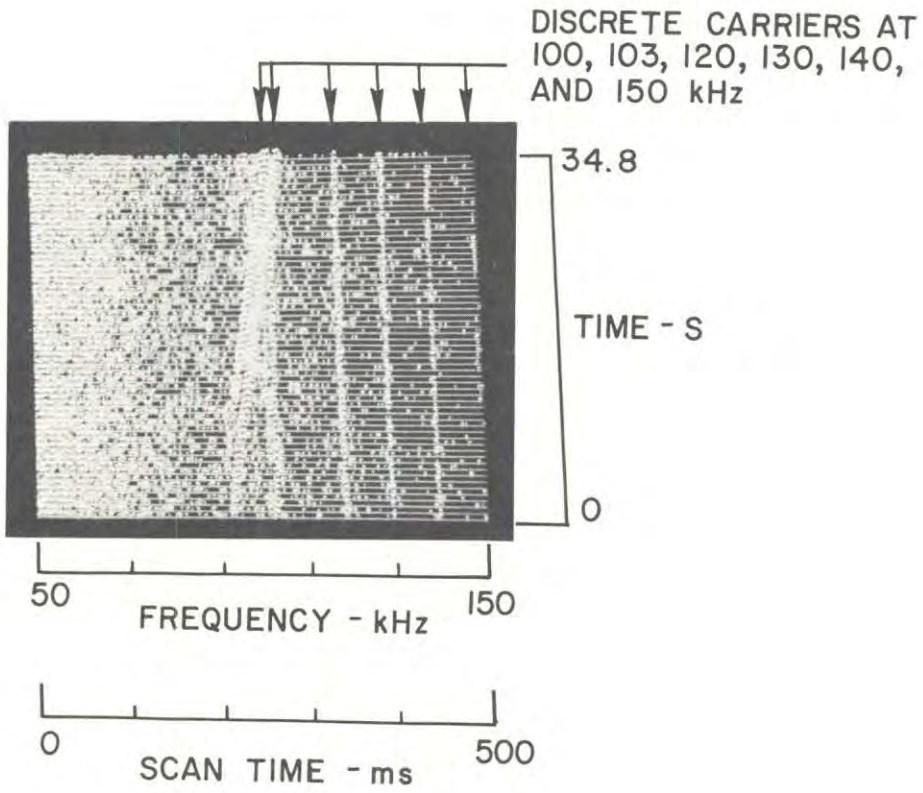

FIGURE 3-24. 12/21/78, 0936

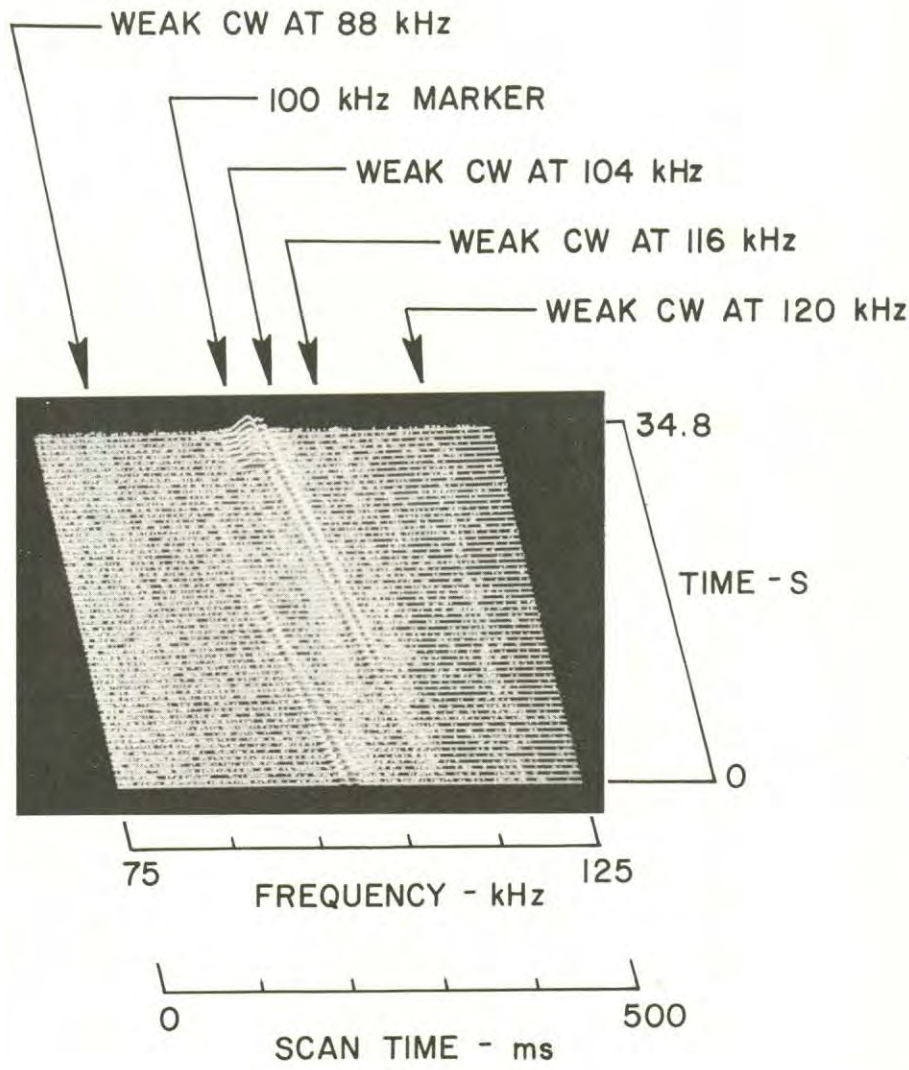

12/21/78, 1500, Broadway & Alpine
HP 140, Whip, F 100 kHz, W 50 kHz, IF 1 kHz, ST 500 ms, RF 0 dB, IF -20 dbm

FIGURE 3-25. 12/21/78, 1500

3.7 POWER TRANSMISSION LINE CARRIER COMMUNICATIONS

Reference 3-Axis Views: 12/21/78, 1356 (Figure 3-26)
12/21/78, 1420 (Figure 3-27)
12/21/78, 1520 (Figure 3-28)
12/21/78, 1525 (Figure 3-29)

The electric power utilities employ VLF and LF frequencies in carrier communications systems. Usually such systems are used on high voltage transmission lines for power switching and control purposes. Very few carrier systems are used on utility distribution systems, although occasionally a utility will conduct special measurements or technical tests using a particular distribution line. While no signals could be associated with power line carrier communications on Los Angeles electric utility distribution lines, a specific case was identified on a very high voltage transmission line as shown at 12/21/78, 1356. A discrete CW power carrier was identified at 100 kHz as the line was approached while driving on Artesia Freeway. A very sudden increase in signal level occurred when the measurement van passed directly under the transmission line where the 100 kHz signal was about +15 dB above the Loran Y signal. Very strong but infrequent noise impulses were also noted under the line which were about 25 dB above the Y signal.

A second measurement of the power carrier signal was made about four blocks from the transmission line as shown in the data at 12/21/78, 1420. The narrow bandwidth of the receiver IF suppressed the amplitude of the Loran-C and the impulsive signals in the view by about 10 dB which resulted in a Loran Y signal strength of about 5 dB above the 100 kHz CW power carrier signal. The impulsive noise shown in the view originated from a local distribution line and was about 5 dB above the Y signal amplitude. This mixture of power carrier and impulsive noise was found throughout the light industrial area in the vicinity of Victoria St. and Main St.

Another suspected case of power carrier RFI was investigated on a second high voltage transmission line. The data taken at 12/21/78, 1520, show the complex signals observed on North Spring as the measurement van passed over a complex set of rail lines and under a transmission line. A number of discrete CW signals were found which were too low in amplitude for power carrier on the transmission line. One signal at 96 kHz could have been a power carrier signal since it peaked in level directly under the transmission line. However, it also peaked directly over a number of railroad cables, lines, and facilities. Signals of lower levels at 86, 116, and 122 kHz also had maximum values directly under the transmission line and directly over the railroad facilities. A wideband ($\approx$ 10 kHz wide) signal at about 104 kHz was noted which was better defined by decreasing the scan time from 100 to 200 ms as shown in the data at 12/21/78, 1525. From these views the signal was determined to be FM modulated at a 200 Hz rate with a deviation of about 50. This unusual signal originated from some nearby source since it was not observed on either side of the North Spring railroad overpass.

While the signals in 12/21/78, 1520 and 12/21/78, 1525 are shown in the section on power transmission line carrier communications (Section 4.5), there is considerable doubt that most of the signals belong in this category. Additional measurements employing directional loopsticks will be required to establish the sources of each of the CW signals and of the broadband signal.

12/21/78, 1356, Artesia Freeway (north end)
HP 140, Whip, F 100 kHz, W 50 kHz, IF 3 kHz, ST 500 ms, RF 0 dB, IF -20 dbm

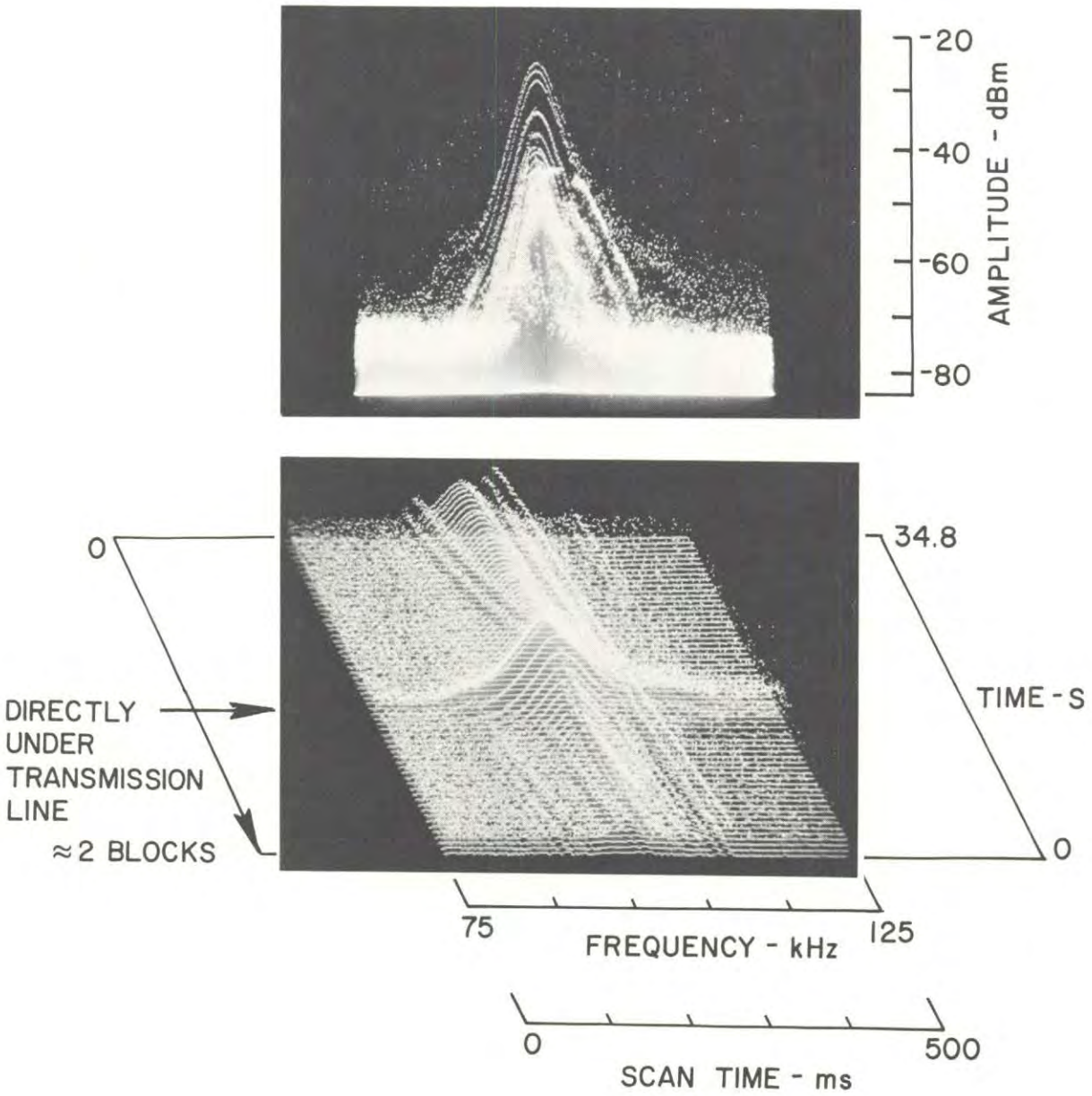

FIGURE 3-26. 12/21/78, 1356

12/21/78, 1420, Main & Lifford
HP 140, Whip, F 100 kHz, W 50 kHz, IF 1 kHz, ST 500 ms, RF 0 dB, IF -20 dbm

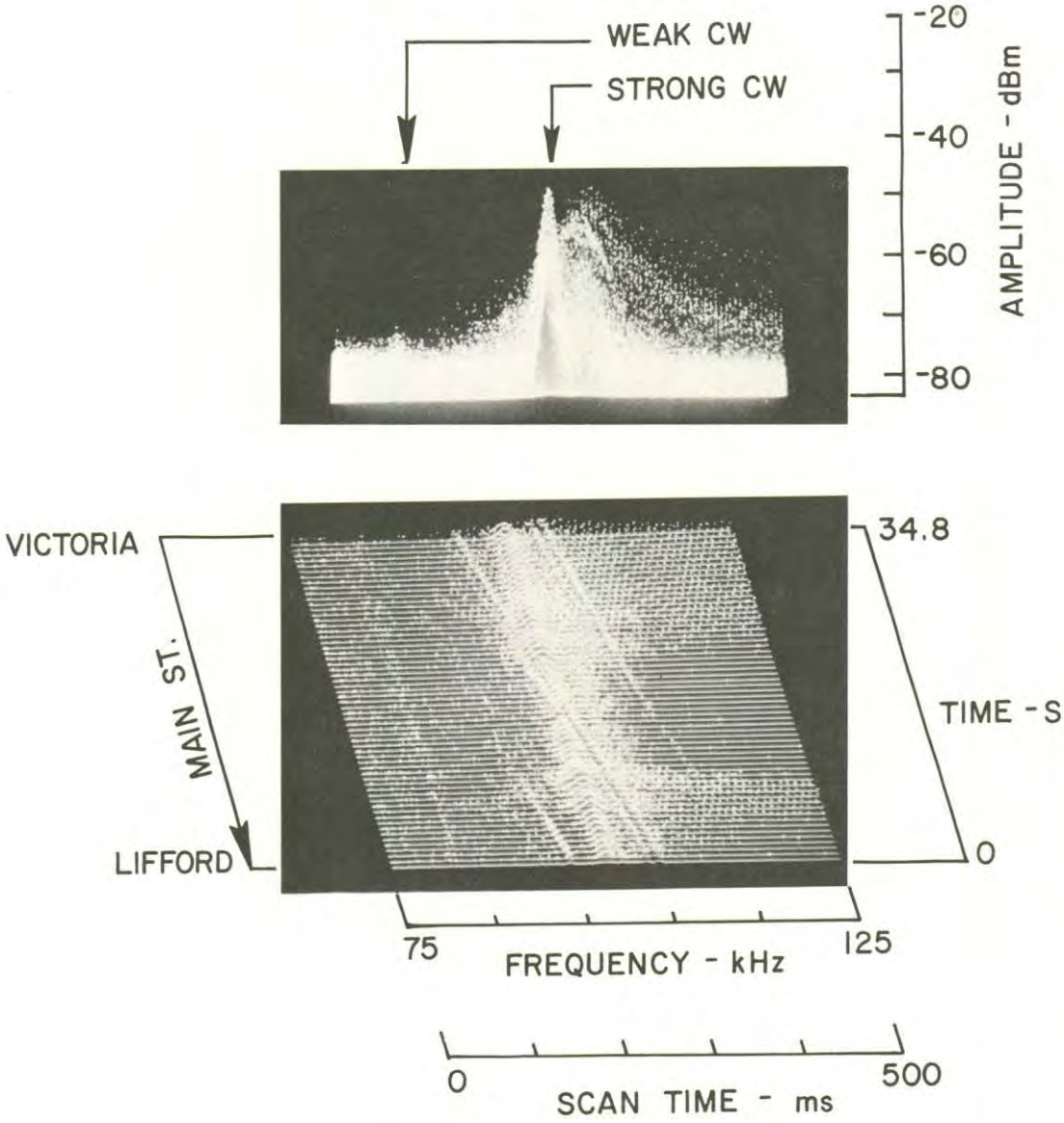

FIGURE 3-27. 12/21/78, 1420

12/21/78, 1520, N. Spring on Railroad overpass (between Aurora & 18th Ave.)
HP 140, Whip, F 100 kHz, W 50 kHz, IF 1 kHz, ST 100 ms, RF 0 dB, IF -20 dbm

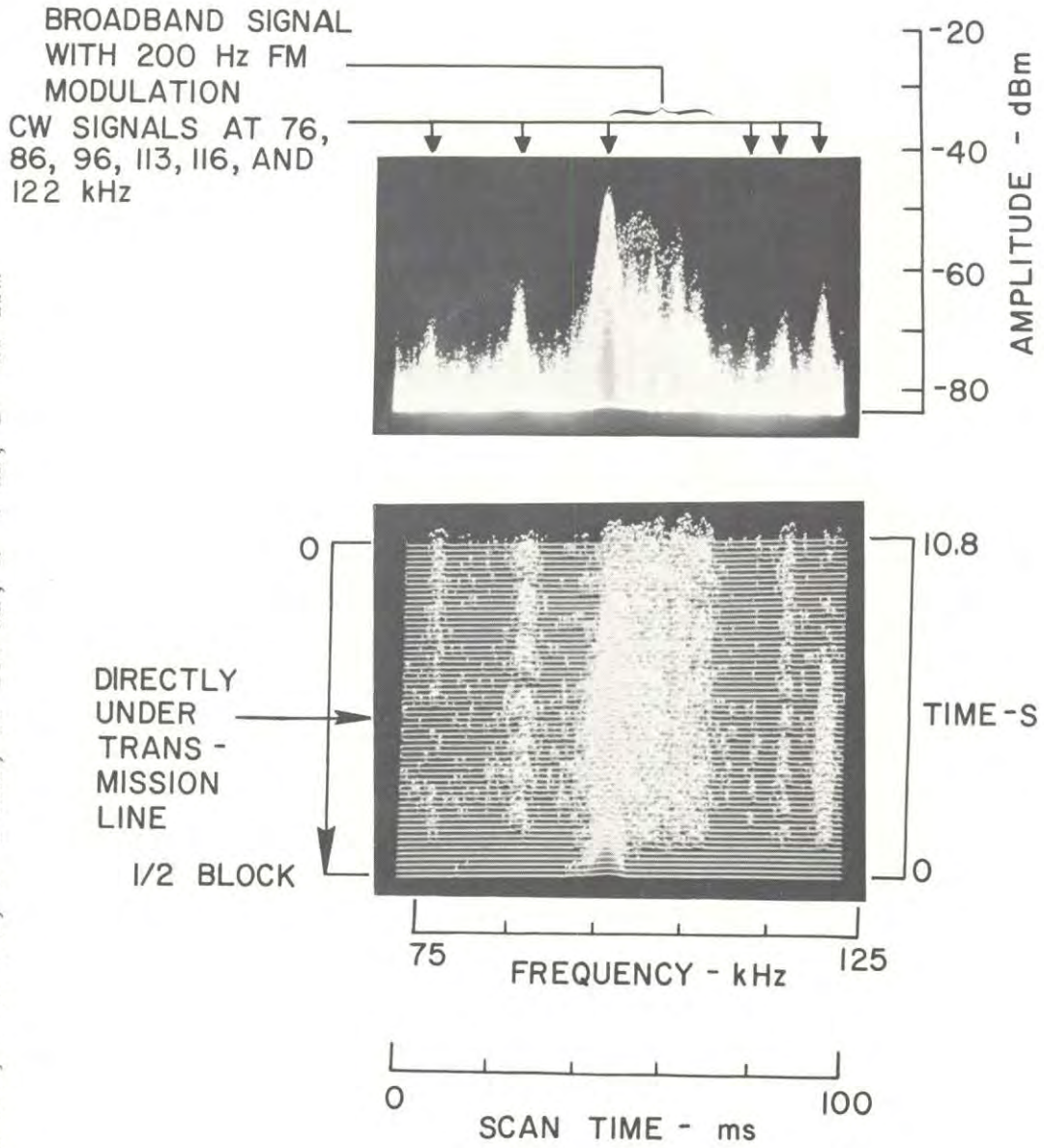

FIGURE 3-28. 12/21/78, 1520

12/21/78, 1525, N. Spring on Railroad overpass between Aurora & 18th Ave.
HP 140, Whip, F 100 kHz, V 50 kHz, IF 0.3 kHz, ST 200 ms, RF 0 dB, IF -20 dbm

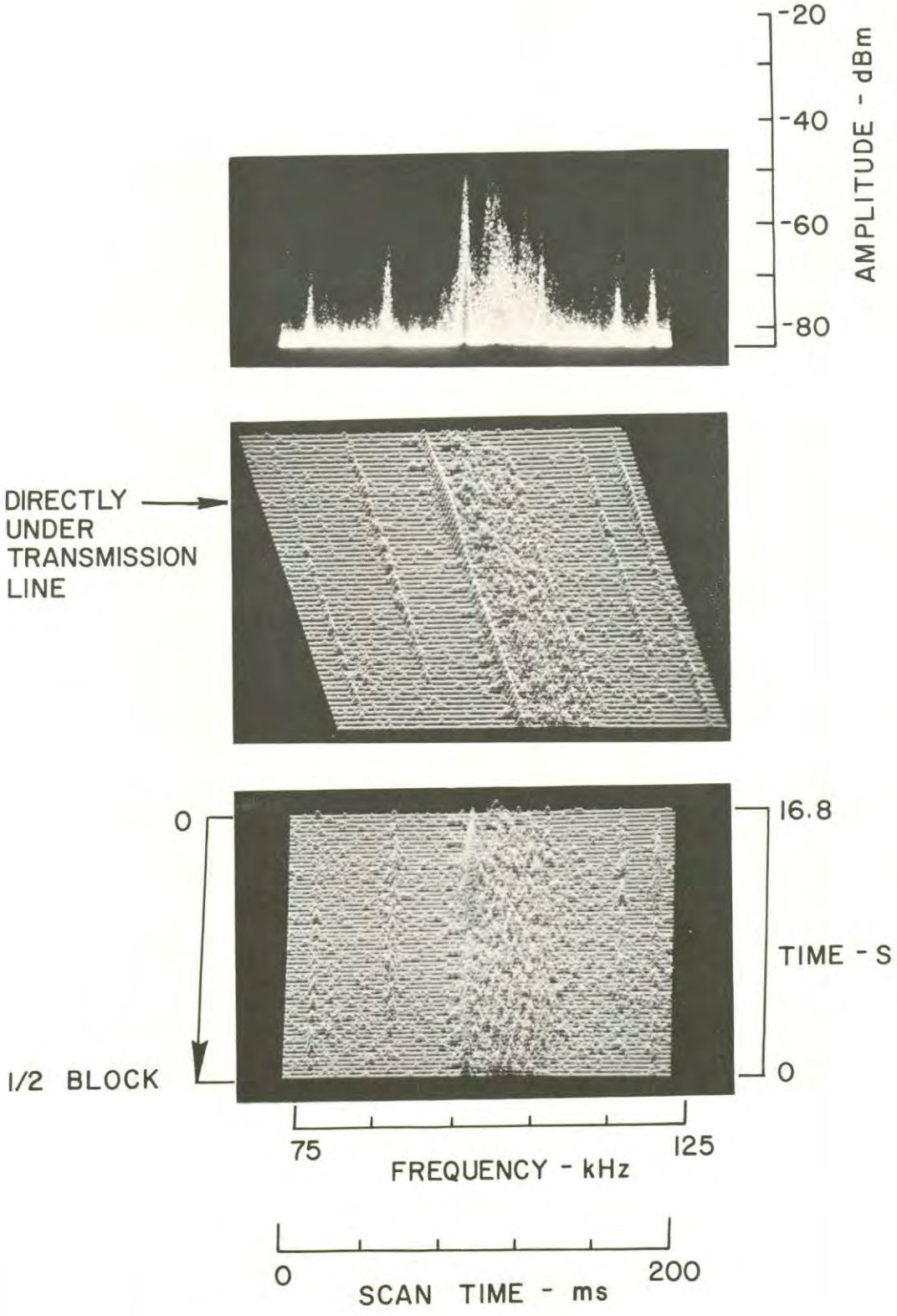

FIGURE 3-29. 12/21/78, 1525

3.8 FREEWAY RECEPTION

Reference 3-Axis Views: 12/19/78, 1611/1612 (Figure 3-30)
12/19/78, 1614/1622 (Figure 3-31)

Loran-C signal reception was briefly examined during travel between measurement sites. Generally, reception was quite good along open and elevated freeways. Occasional brief periods of noise would be encountered as the measurement van traveled by or under electric utility distribution lines containing impulsive noise. Signal fades were very noticeable as the measurement van traveled under an overpass or a large overhead highway sign. Two examples of signal fading associated with travel under an overpass are shown in the data at 12/19/78, 1611/1612. The bottom example shows a signal fade associated with an overhead highway sign which extended across the freeway.

The vertical lines shown in all views were ignition noise from the gasoline generator supplying power to the measurement system. This noise should be ignored since it was considered an unnecessary noise contaminent in some of the data.

12/19/78, 1611/1612, Harbor Freeway
HP 140, Whip, F 100 kHz, W 20 kHz, IF 3 kHz, ST 500 ms, RF 0 dB, LF -20 dbm

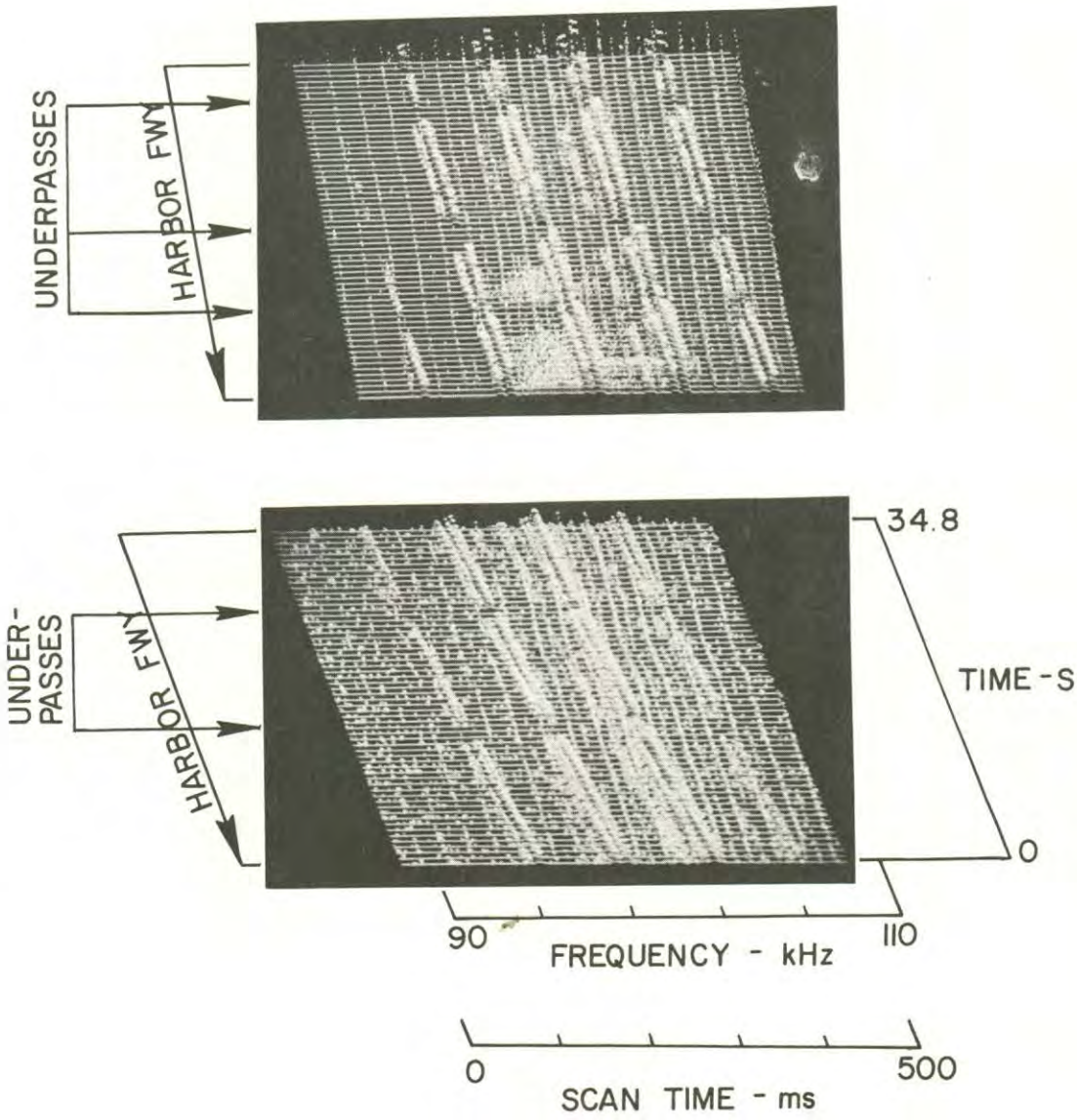

FIGURE 3-30. 12/19/78, 1611/1612

12/19/78, 1614/1622, Harbor Freeway
HP 140, Thin, F 100 kHz, W 20 kHz, IF 3 kHz, ST 500 ms, RF 0 dB, IF -20 dbm
Bottom view 50% comp

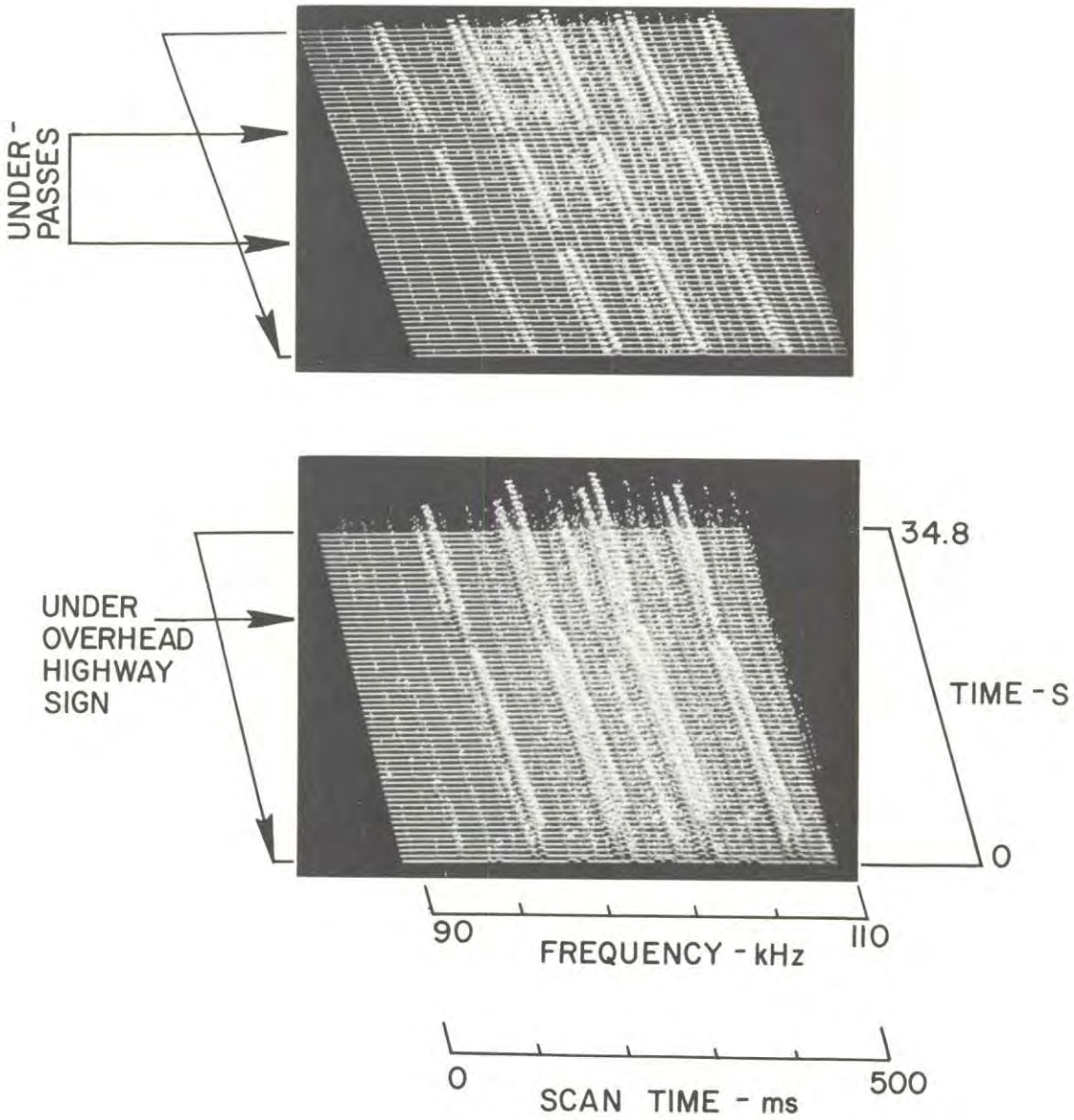

FIGURE 3-31. 12/19/78, 1614/1622

4. DISCUSSION

4.1 GENERAL COMMENTS

The identification of locations and streets where noise, RFI, or some other unusual condition existed was of significant assistance in getting noise and RFI measurements underway efficiently, and this eliminated the need to make a large scale area survey. Locations where Loran-C receiver performance degradation was experienced were critically examined, and subsequent direct comparisons of Loran-C receiver results with noise and RFI results appear to be meaningful and feasible. In general, the locations identified had noise, RFI, or combinations of both. The few locations where noise or RFI were lacking seemed to be due to the intermittent and time-changing aspects of noise rather than due to pertinent technical differences.

During the measurements modest changes in noise levels and noise characteristics were often noted. Occasionally very large changes were noted suggesting that a primary source of the noise was either turned on or off during a particular measurement. No particular patterns or particular times for noise changes were deduced from the measurements, but the site-to-site movements of the instrumentation did not provide a good means to observe time-varying changes.

4.2 NOISE FROM ELECTRIC UTILITY DISTRIBUTION LINES

The impulsive noise and the quasi-random noise (Sections 3.3 and 3.4) were always associated with overhead electric utility distribution lines. Generally the measurement van had to be close to a distribution line before the noise was of sufficient magnitude to be of concern. When the measurement van was more than about 200 feet from a distribution line, very little impulsive or quasi-random noise was found. Also, some distribution lines appeared to be entirely free of such noise. When noise was found to be emanating from a particular distribution line and the measurement van

followed the line along the street, the noise was noted for many blocks. If the line left the street or if the measurement van turned off the street, the noise would immediately disappear. Noise properties were generally consistent with distance when following a given distribution line.

The timing of impulsive noise was always associated with the 60 Hz line frequency. No unusual timing reference situations were found during the one week measurement period. Very simple impulse timing patterns were found where the impulses were associated with triggering on only one-half of the 60 Hz waveform (impulses spaced each 16.6 ms) and where the impulses were associated with triggering on both halves of the 60 Hz waveform (impulses spaced each 8.3 ms). More complex impulse periods were found which appeared to be associated with the triggering of 3Ø devices or by multiple devices triggering at different locations on the power line waveform. At one location the average impulse period was about 2 ms where all impulses were repetitive and synchronized with the power line frequency.

4.3 STRONG LOCAL AREA SIGNALS

The strong local area near field signals described in Section 3.5 were quite unexpected. Their frequent occurrence and large strengths made the signals very noticeable in the 3-axis views, and of course they produced significant interference to Loran-C signals at the specific locations where such signals were found. The very small and restricted areas where such signals were found imply that the sources were low in power, small in physical size, and near field signal intercept was involved. These signals were sometimes found at street corners where traffic control devices were evident. However, they were also found on other street corners where no traffic control devices existed, and they could not be found on many corners with obvious traffic control devices. Also, they were found in residential areas. No definite association could be made between these signals and local area objects even though the actual

source was at times probably less than 100 feet from the measurement van. A small hand-held loopstick with a diode detector and meter indicator would have solved the location and identification problems, but such a device was not available.

The source of many of the strong local area signals was the subject of considerable discussion and some frustration at not being able to identify an emitter obviously so close to the measurement van. Speculation about the source could not be avoided. Some of the probable sources were:

1. Traffic control devices
2. Ultrasonic burglar alarms
3. TV set radiation
4. Telephone line signals.

4.4 WEAK CW SIGNALS

Sections 3.5 and 3.6 described several weak CW signals which were present over large portions of the measurement area. The signal at 117 or 118 kHz was the most persistent, and it was present in about one-half of the data taken in Los Angeles. Its source is believed to be a distant communications transmitter. Other CW signals at 88, 100, 103, 120, 130, 140, and 150 kHz were detected at various times during the measurement period. The source of these signals was not investigated during the brief one week of the Los Angeles measurements. The measurement van was equipped with an LF direction finding capability, but this equipment was not employed during the measurement period because of a lack of time.

The weak 100 kHz signal might be far field radiation from the power carrier communications signal described in Section 3.7. This, of course, is again speculation. This can be easily verified by simple DF measurements, and coordinating with the utility involved to observe the 100 kHz signal during a brief carrier communications shut-down period.

4.5 POWER TRANSMISSION LINE CARRIER COMMUNICATIONS

One definite case of a power carrier communications signal on an electric utility high voltage power transmission line at or very close to 100 kHz was identified. The carrier communications signal rose to a level well above the strongest Loran-C signal when the measurement van was on the Artesia Freeway directly under the transmission line, and the signal was received at lower signal levels for a few blocks on either side of the line. In addition a few spikes of very high level noise were received when directly under the line. The CW signal at or near 100 kHz was also observed on other nearby streets which passed under the transmission line. However, the particular transmission line involved was not investigated at other locations nor was a map showing its routing available during the measurements. It is a reasonable assumption that the 100 kHz signal would be received at other streets and highways passing under the line.

The identification of a 100 kHz power carrier signal within an area where Loran-C had been considered for vehicular navigation purposes raises serious questions of compatibility between the two systems for a region along the length of the transmission line. This is an obvious case where frequency coordination efforts must be undertaken with the appropriate city, utility, and Federal government agencies and officers. However, immediate and rapid resolution of the issue appears to be unnecessary since the area affected is limited and does not involve major portions of Los Angeles of immediate concern for Loran-C.

A second case of signals somewhat like power carrier signals was identified near North Spring and 18th Avenue where a high voltage transmission line crossed North Spring. However, extensive railway and telephone communications facilities were also found in the same vicinity. The mobile instrumentation employed during the week's measurement period could not resolve the actual source of these signals. While they are listed under the power carrier section (Section 3.7), additional measurements with directional near field probes and measurements at other

locations under the transmission line will be required to identify their specific source.

4.6 SPATIAL CONSIDERATIONS

Most of the impulsive noise, quasi-random noise, and strong CW signal RFI were limited to a large number of very small geographic areas whose limits were surprisingly well defined. These areas were obviously associated with noise and RFI radiation mechanisms which were located very close to the noise or RFI maximum, and near field signal reception conditions were obviously involved in most of the noise and RFI situations. If an overhead transmission line containing impulsive current extended along a given street, then noise was found along that street. If the affected line was approached from a cross street, the noise level rapidly increased as the line was approached and rapidly decreased as the vehicle moved away from the line. Noise was no longer observed at distances of 100 feet to 200 feet from an affected line.

Similar near field signal reception conditions applied to the strong CW RFI. The strong signal areas were very small in physical size, and these areas were usually surrounded by larger areas of extremely low noise or noise of an entirely different type.

The very small physical areas containing high noise and RFI levels suggest that terrain maps of the noise and RFI must be made on an extremely fine scale in order to be meaningful in understanding the radio environment encountered by Loran-C receivers installed in vehicles. Cases were found where a street with high noise levels would be paralleled by another street one block away which was virtually free of noise. Gross terrain mapping techniques cannot realistically represent such situations.

Alternate noise and RFI mapping approaches must be considered to describe the Los Angeles area in sufficient detail to permit relating

actual noise to Loran-C receiver performance. Some approaches which might adequately describe the spatial aspects of noise and RFI are:

1. Measure and define noise along specific streets of interest and do not apply these results to other nearby streets.
2. Map the electric utility overhead distribution lines and then measure and rate each section of line with a noise value related to vehicular Loran-C receiver performance.

Any noise mapping scheme will be plagued by the time-changing characteristics of noise emanating from a particular distribution line. Noise on the line will vary as customers change their loads, add new loads, expand their operations, go out of business, move, etc. The electric utilities can change noise conditions on a given street by changing the configuration of their distribution network to accommodate normal demands for electric service. These aspects of noise and RFI suggest that today's noise map may not apply to tomorrow's vehicular Loran-C needs.

4.7 NOISE SOURCES AND POSSIBLE CONTROLS

The actual devices causing the impulsive noise are believed to be various high power switching devices employed by small, medium, and large size industry for electrical and industrial controls. These high power switching devices suddenly turn current on at some reference point on the power line voltage waveform. Very high currents, typically hundreds of amperes, flow at the switching time and the switching impulses propagate back into the local area distribution lines. Initial measurements of the impulse propagation back into distribution lines from specific identified sources have been made under other work tasks by Systems Control, Inc. The Los Angeles data are very similar to these prior results.

Actual devices causing the Los Angeles measured impulse noise were not tracked down and traced to specific industries or other sources. The mobile type of Los Angeles measurements described in this report were not sufficient to identify the actual sources. However, source identification measurements are feasible, and they can be accomplished with slightly different instrumentation arrangements. Many sources distributed among many electric utility customers are undoubtedly involved. While electric utility hardware, distribution lines, and devices seem to be the transporting mechanism of the impulses and their radiator, the electric utilities do not originate the noise.

Filtering at the source appears to be the most logical technical solution. However, it is not clear how one would establish technical specifications for filters for the offending devices, how one would implement a program to install expensive filters, or who would pay for the filters. A short term solution would be extremely difficult to achieve. A long term solution would require considerable coordination among industry, the manufacturers of the source equipments, public utilities, Loran-C interests, and the appropriate government agencies involved with radio spectrum management.

The high level CW signals found at many locations can be traced to their radiator with a small loopstick-detector-meter indicator type device. The identification of the radiating device will undoubtedly lead to the actual source device. Only after the source devices are identified can suitable control recommendations be formulated.

The weak CW signals can be traced to their sources by employing tuned loopstick antennas with preamplifiers in place of the 108 inch whip employed in the Los Angeles measurements. The tuned loopstick antennas can be rotated to identify the direction of arrival of each signal. Measurements at several separate locations will provide sufficient data to ascertain if the signals originate from sources outside Los Angeles or sources inside Los Angeles. If any of the sources are inside Los Angeles, then close-in measurements can be used to identify the specific radiator involved.

4.8 LORAN-C SIGNAL RECEPTION

Loran-C station Y of the U.S. West Coast Chain (Searchlight, Nevada) provided a very strong signal throughout most of Los Angeles. Exceptions were in downtown Los Angeles among nearby tall buildings and when the measurement vehicle was in a road underpass. Minor signal fades of Y were noted when the measurement van passed under overhead wires, signs, cables, and other structures. The Y signal was above power line associated noise levels except for a few unusual noise situations. However, the local area CW signals often approached the level of station Y for perhaps $\pm$ 50 feet along a street. Frequently these high strength areas were at street corners.

Station X (Middletown, California) provided a reasonable signal over most of the test area with the exception of downtown Los Angeles and underpasses. The signal was above noise levels throughout large portions of the test areas, but the signal-to-noise levels were considerably lower than for station Y.

The Loran Y Master station (Fallon, Nevada) signal was adequate for operation under ideal conditions where buildings, underpasses, or noise were not involved. However, most noise sources exceeded the Master signal level and at times exceeded the signal level by very large amounts. Master station signal level increases will be necessary to cope with the radio noise and RFI environment of Los Angeles. An increase in level of at least 10 dB is recommended.

5. PRESENTATION OF SIGNIFICANT DATA

5.1 GENERAL APPROACH

The first phase of a field measurement effort to investigate and ascertain the performance of Loran-C receivers installed in land vehicles was conducted in late 1978 in the Los Angeles area. These measurements identified certain streets, street intersections, and areas where unusual radio noise and RFI conditions existed. The noise and RFI at selected locations and along selected streets was examined in detail by Systems Control, Inc. (SCI) in December of 1978, and the noise and RFI conditions described in Sections 3 and 4 of this report.

The late 1978 measurements of Loran-C receiver performance in the Los Angeles area were continued into early 1979 at additional locations and areas not previously examined. During the week of January 22 through January 26, 1979, the SCI radio noise and RFI measurement van accompanied the Gould Inc. mobile Loran-C receiver measurement van to a number of sites selected by Gould Inc. personnel. The sites selected were typical of expected operational areas for municipal vehicles and other vehicles which might be equipped with Loran-C navigation systems at some future time. Loran-C receiver performance measurements were made at each selected site simultaneously with measurements of radio noise and RFI by SCI. The noise and RFI measurements are presented in this section.

In addition to measurements at predetermined sites, supplementary measurements of noise and RFI were made while traveling from site to site, at locations close to the fixed sites, and at additional locations of special interest. The results of these supplementary measurements are also presented in this section.

The noise and RFI measurements described in Sections 3 and 4 employed a bandpass filter in the matching network between the antenna and the preamplifier. The use of the filter required that a bandwidth calibration factor be applied to the amplitude of signals and noise below about 90 kHz and above about 110 kHz. The filter was used to ensure that strong CW signals and wideband noise would not saturate the preamplifier and cause unwanted intermodulation products to appear in the 3-axis views. The filter was successful in that intermodulation products were not encountered in the Phase I measurements. An alternate preamplifier with a wideband filter was constructed for the Phase II measurements. The preamplifier with the wideband filter was employed for most of the Phase II measurements, although some of the early measurements and some measurements in areas where high level, wideband power line noise was encountered were made with the Phase I narrowband unit. Data taken with the narrowband filter are clearly labeled.

5.2 FIXED SITE MEASUREMENTS

An extensive geographic survey of the greater Los Angeles area had been completed prior to the Phase II effort. From this survey a number of sites were selected for detailed measurements of Loran-C receiver performance and for radio noise and RFI measurements. The site identification numbers and site categories have been used in this section to simplify the task of comparing the results of the two measurements.

A three-letter code was used to identify the particular municipal areas selected for joint measurements. This code was followed by three additional numbers which identified the sites selected for measurements. The municipal area codes are given in Table 5-1. Table 5-2 provides a convenient summary of the measurement locations, site identification numbers, the general activity in the vicinity of each site, the heading of the measurement van along the street, and the presence or absence of nearby electric utility power lines.

TABLE 5-1. IDENTIFICATION NUMBERS FOR MUNICIPAL AREAS

Municipal Area	Identification #
El Segundo	104
Torrance	106
Southgate	107
Compton	108
Carson	109
Lincoln/Boyle HTs	110

TABLE 5-2. LORAN-C SITE SURVEY DATA

	SITE ID #	STREET INTERSECTION*	SITE CATEGORY**	MEAS. VAN HEADING	POWER LINES†
REGION 6 TORRANCE	106-001	Artesia/Van Ness	C	W	1
	106-002	178th/Falda	R	W	0
	106-003	182nd/Crenshaw	C	E	1
	106-004	190th/Prairie	I	E	2
	106-005	Fisk/Spreckels	R	S	0
	106-006	Redbeam/Towers	R	N	0
	106-007	Anza/Torrance	C	N	1
	106-008	Maricopa/Madrona	O	N	0
	106-009	Crenshaw/Dominguez	I	N	1
	106-010	Del Amo/Crenshaw	I	E	2
REGION 9 CARSON	109-011	182nd/Wall	R	S	0
	109-012	192nd/1800' west of Avalon	O	E	0
	109-013	Dominguez/Avalon	C	E	0
	109-014	Carson/Orrick	C	W	1
	109-015	Avalon/223rd	C	S	1
	109-016	Wilmington/Sepulveda	I	N	1
	109-017	Sepulveda/Alemeda	I	W	2
	109-018	Watson Center/Wilmington	I	E	0
	109-019	Tillman/Denwall	R	N	0
	109-020	Brenner/Annalee	R	W	0

* Intersection shows location of van as first street listed (i.e., 3rd/Vine = van on 3rd).

** Site category: C - commercial, R - residential, I - industrial, O - open.

† Power lines show number of lines present (one side or both sides of street): 1 - one side, 2 - both sides, underline of number - van directly under lines.

TABLE 5-2. LORAN-C SITE SURVEY DATA (CONTINUED)

	SITE ID #	STREET INTERSECTION*	SITE CATEGORY**	MEAS. VAN HEADING	POWER LINES†
REGION 8 COMPTON	108-021	Wilmington/Walnut	I	N	1
	108-022	Acacia/Carob	I	S	0
	108-023	Compton College Parking Lot (500' north of Artesia/west of Delta)	O	S	0
	108-024	Johnson/Alemeda	I	E	1
	108-025	Tichenor/Oleander	R	W	1
	108-026	Mayo/Myrrh	R	N	0
	108-027	N. Sloan/E. Palmer	R	S	1
	108-028	Rosecrans/Santa Fe	C	E	0
	108-029	Rosecrans/Matthisen	C	W	1
	108-030	Alondra/Wilmington	C	E	1
REGION 7 SOUTHGATE	107-031	Rayo/Firestone Pl.	I	S	1
	107-032	Firestone Blvd/Atlantic (on Dorothy 400' north)	C	W	1
	107-033	Dorothy/Firestone Blvd.	I	E	1
	107-034	Otis/Ardmore	I	N	2
	107-035	State/Firestone Blvd.	C	S	0
	107-036	Tweedy/State	C	E	0
	107-037	Sequoia/Mariposa	R	E	0
	107-038	San Gabriel/Tenaya	R	S	0
	107-039	Kauffman/Duane	R	N	0
	107-040	Parking lot northeast of Hildreth/Duane	O	W	0

* Intersection shows location of van as first street listed (i.e., 3rd/Vine = van on 3rd).

** Site category: C - commercial, R - residential, I - industrial, O - open.

† Power lines show number of lines present (one side or both sides of street): 1 - one side, 2 - both sides, underline of number - van directly under lines.

TABLE 5-2. LORAN-C SITE SURVEY DATA (CONTINUED)

	SITE ID #	STREET INTERSECTION*	SITE CATEGORY**	MEAS. VAN HEADING	POWER LINES†
REGION 10 LINCOLN/BOYLE HEIGHTS	110-041	Terrace Heights/Penrith	R	W	0
	110-042	4th/Soto	C	E	1
	110-043	Evergreen Cemetary at Evergreen/Michigan	O	N	0
	110-044	St. Louis/Michigan	R	S	1
	110-045	Murchison/Lancaster	C	N	1
	110-046	Soto/Multnomah	I	N	1
	110-047	Mission/N. Broadway	C	S	2
	110-048	Zonal/Griffin-Mission	I	W	1
	110-049	Gallardo/Mission (bottom of bridge)	I	S	0
	110-050	Kearney/Pennsylvania	R	E	1
REGION 4 EL SEGUNDO	104-051	Flournoy/36th	R	W	1
	104-052	Rosecrans/Highland	C	W	1
	104-053	Parking lot west of Grand/Vista Del Mar	O	E	0
	104-054	Mariposa/Loma Vista	R	E	1
	104-055	Whiting/Holly	R	N	0
	104-056	Eucalyptus/Grand	C	S	1

* Intersection shows location of van as first street listed (i.e., 3rd/Vine = van on 3rd).

** Site category: C - commercial, R - residential, I - industrial, O - open.

† Power lines show number of lines present (one side or both sides of street): 1 - one side, 2 - both sides, underline of number - van directly under lines.

Three special sites were selected for daily measurements of Loran-C receiver performance. These sites were the Los Angeles Coliseum, Broadway and Pico, and the Los Angeles Municipal Transportation Authority Building at 425 Main Street. Figures 5-1 and 5-2 show typical conditions at the Los Angeles Coliseum. Very little radio noise was encountered, but three CW signals of modest strength and two weak CW signals are shown in the 3-axis views taken on 1/24/79 and 1/26/79. The relative amplitudes of each of the received signals at the Coliseum with all calibration factors applied are:

Frequency	Approximate Level
80 kHz CW	-86 dBm
90 kHz CW	-80 dBm
100 kHz CW	-86 dBm
108 kHz CW	-105 dBm
119 kHz CW	-80 dBm
Loran M	-78 dBm
Loran W	< -93 dBm
Loran X	-73 dBm
Loran Y	-63 dBm

Figure 5-3 illustrates RFI conditions at Broadway and Pico. The 100 kHz CW signal increased in level substantially over that observed at the Coliseum site, while the 80 kHz and 90 kHz CW signals were much lower in level. Impulsive noise was not present. The relative amplitudes of each of the signals in the 3-axis view are:

Frequency	Approximate Level
80 kHz CW	-88 dBm
90 kHz CW	-90 dBm
100 kHz CW	-76 dBm
108 kHz CW	-92 dBm
119 kHz CW	-80 dBm
Loran M	< -93 dBm
Loran W	< -93 dBm
Loran X	-70 dBm
Loran Y	-63 dBm

1/24/79, 0730, Coliseum
HP 140, Whip, F 100 kHz, W 50 kHz, IF 3 kHz, ST 500 ms, A -20 dBm/0/+15 dB/NF

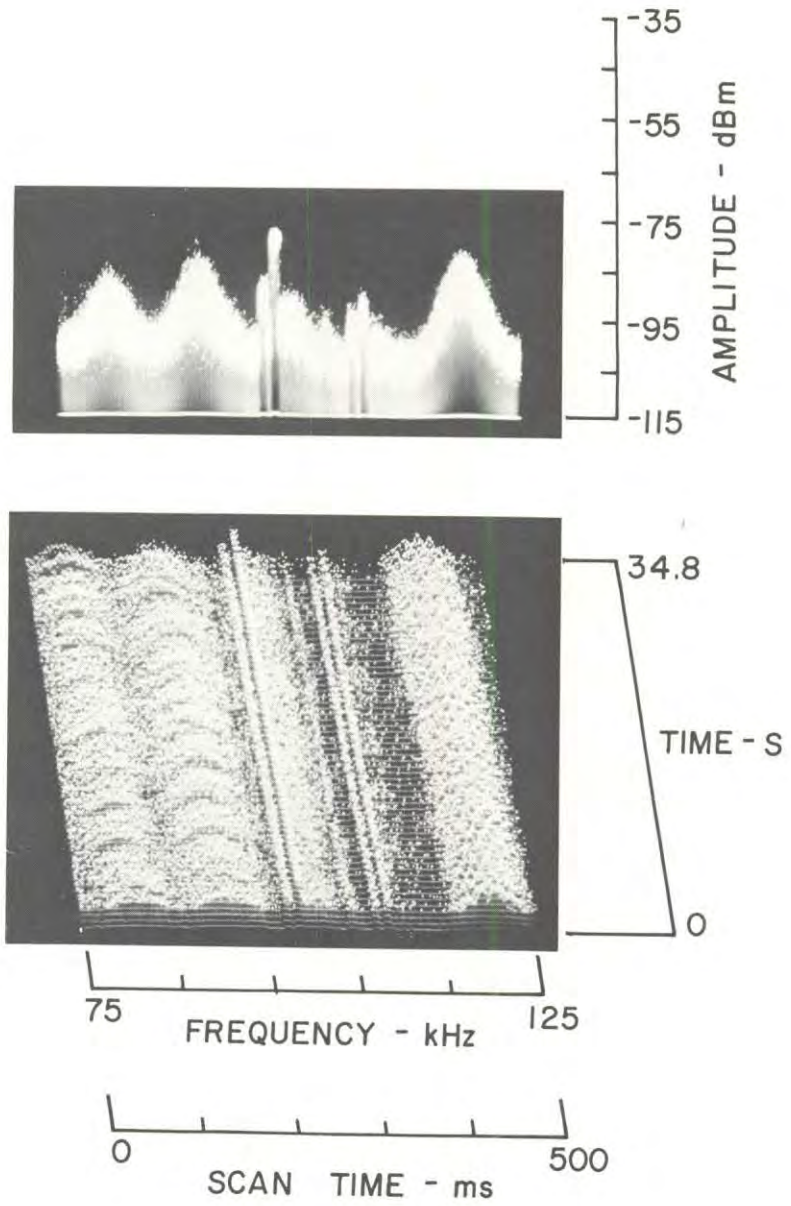

FIGURE 5-1. 3-AXIS VIEW, 1/24/79, 0730, COLISEUM

1/26/79, 0748, Coliseum
HP 140, Whip, F 100 kHz, W 50 kHz, IF 3 kHz, ST 500 ms, A -20 dBm/0/+15 dB/NF

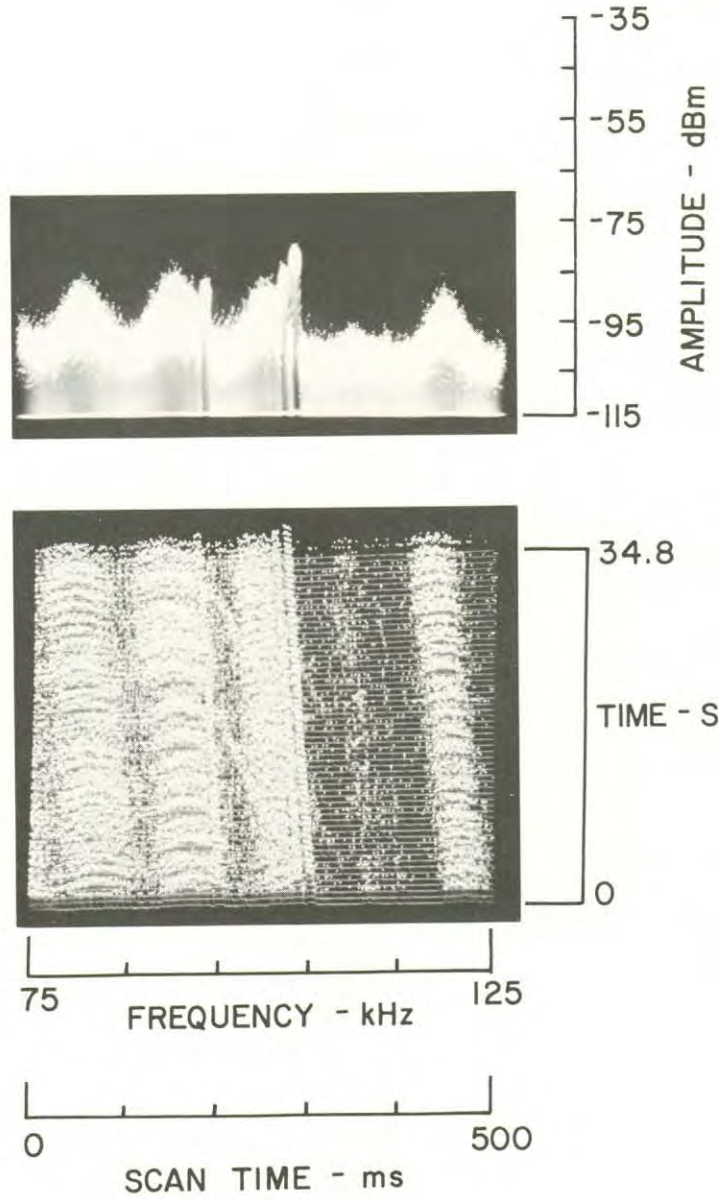

FIGURE 5-2. 3-AXIS VIEW, 1/26/79, 0748, COLISEUM

1/24/79, 0715, Broadway & Pico
HP 140, Whip, F 100 kHz, W 50 kHz, IF 3 kHz, ST 500 ms, A -20 dBm/0/+15 dB/NF

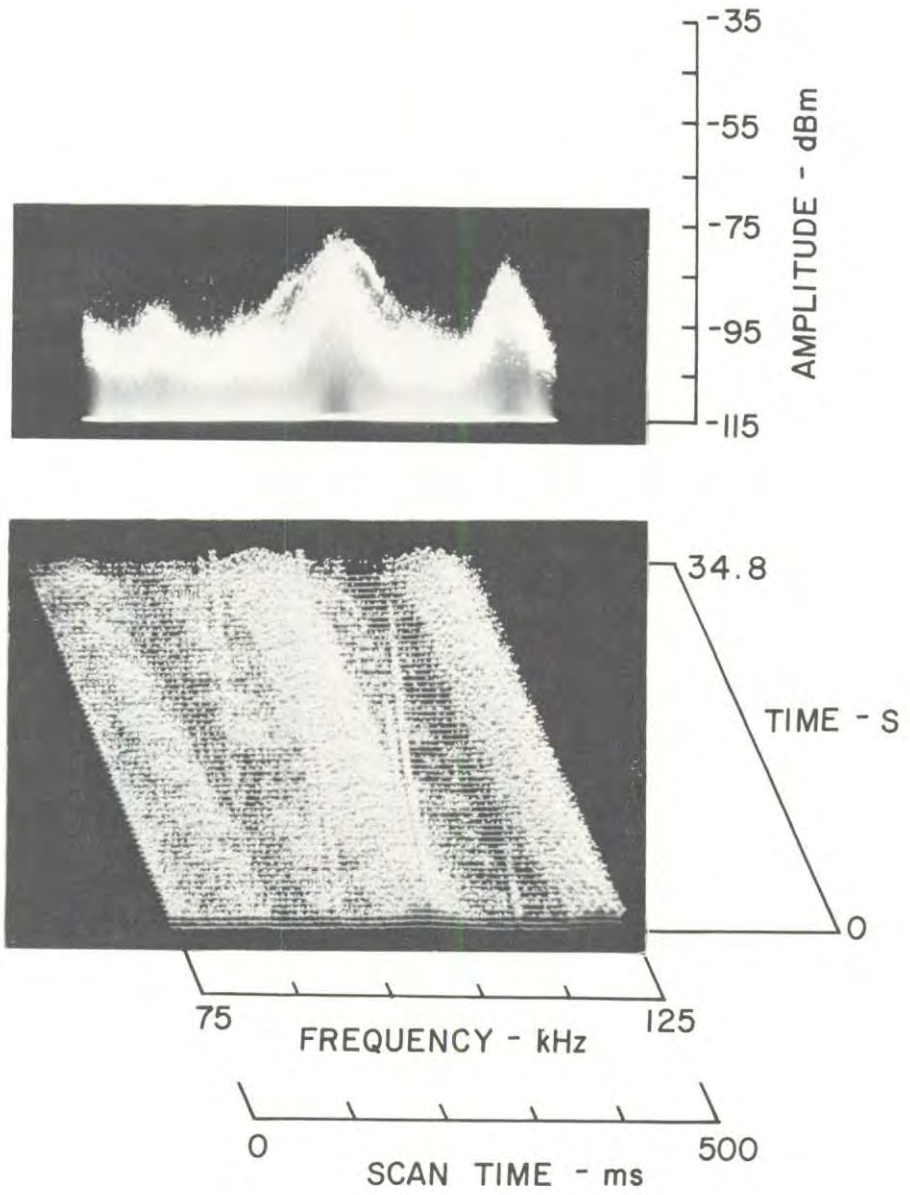

FIGURE 5-3. 3-AXIS VIEW, 1/24/79, 0715, BROADWAY AND PICO

Figure 5-4 illustrates signal reception at 425 Main Street, a site immediately adjacent to a large multiple story building. Neither CW nor Loran-C signals could be detected at the site, and noise levels were the lowest of all sites measured in the Los Angeles area. The nearby building obviously became part of a physical structural arrangement that severely attenuated all LF radio signals.

Loran-C, radio noise, and RFI at the various sites selected for detailed examination are shown in a sequence of fully calibrated 3-axis views in Appendix A. A pair of views were taken at each location with fixed scanning receiver adjustments of F = 100 kHz, W = 50 kHz, IF = 3 kHz, and ST = 500 ms. Where unusual conditions existed, additional views were taken using other receiver adjustments. These additional views follow the standard views, and they contain the same site identification code as the standard view. The time of day and some of the receiver adjustment parameters will be changed. These differences can be seen in the two-line set of parameters on each pair of views.

The reader can scan through the 3-axis views in Appendix A to observe the changes in noise, RFI, and Loran-C signal levels from site to site. The variety of noise and RFI from site to site is impressively diverse. This variety clearly warns against making simplistic conclusions concerning the noise and RFI. Furthermore, the wide variety of conditions suggests that average values of noise and average RFI states by themselves have little meaning.

1/24/79, 1353, 425 Main St.
HP 140, Whip, F 100 kHz, W 50 kHz, IF 3 kHz, ST 500 ms, A -20 dBm/0/+15 dB/NF

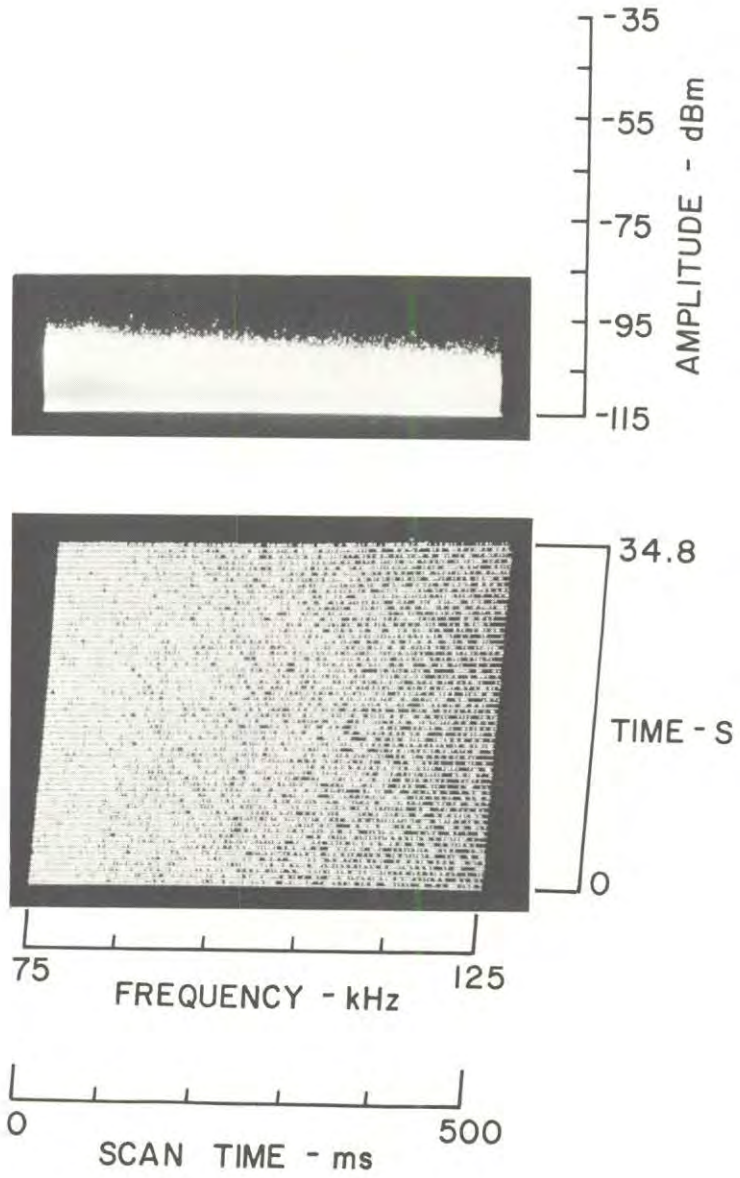

FIGURE 5-4. 3-AXIS VIEW, 1/24/79, 1353, 425 MAIN STREET

5.3 SUPPLEMENTARY MEASUREMENTS

5.3.1 General Description

The Phase I measurements showed that noise and RFI conditions frequently and usually changed over very short distances. Signal and noise levels were shown to vary in peak level by more than 40 dB over distances of less than 100 feet. Such variations would not be evident from the fixed location type of measurements described in Section 5.2 and Appendix A. Thus, as time permitted, additional measurements were made while approaching and leaving the fixed sites and at other sites of special interest. These measurements were made to provide a more complete understanding of the spatial characteristics of the noise and RFI.

5.3.2 Spatial Variations in CW Signal Levels

The 3-axis views in Figures 5-5 through 5-8 show typical variations in CW field strength as the measurement van moved along a street. Figure 5-5 shows four CW signals varying in amplitude as site 106-010 was approached. Amplitude variations of 10 to 30 dB can be seen in the view where the CW frequencies are about 80, 100, 108 and 119 kHz. This view can be compared with the 3-axis view of site 106-010 in Appendix A where the 100 kHz signal is very weak, and the 108 and 119 kHz signals are a few dB higher in strength.

Another example of large variations in CW signal strength is shown in Figure 5-6. The view was taken about 200 feet from site 109-014, and it shows a very sudden decrease in strength of a CW signal at about 88 kHz, while the signal at about 118 or 119 kHz remained constant in amplitude. The 88 kHz signal was not visible in the view for site 109-014 in Appendix A. The view in Appendix A also indicates mild impulsive noise across the entire 50 kHz block of frequencies shown.

Figure 5-7 shows an abrupt change in CW signal levels as the measurement van turned off Sepulveda onto Wilmington. Both 3-axis views shown in Figure 5-7 contain the same data at different viewing aspect angles. Weak CW signals at 80 and 90 kHz did not change in signal level, while the 100 kHz signal decreased in strength and the 119 kHz signal increased in strength. Merely turning around the corner resulted in substantial changes in the CW signal environment.

Figure 5-8 shows a change in CW signal and noise environment noted as the measurement van moved along Wilmington. The two portions of the view were taken at locations about 1/2 mile apart. The 80 and 90 kHz CW signals increased in amplitude by a small amount, and the 119 kHz signal decreased in level. A 100 kHz signal can be seen in the lower portion of the view but not in the upper portion. Impulsive noise was present at the second site, as shown in the lower portion of the view, but not at the first site, as shown in the upper portion.

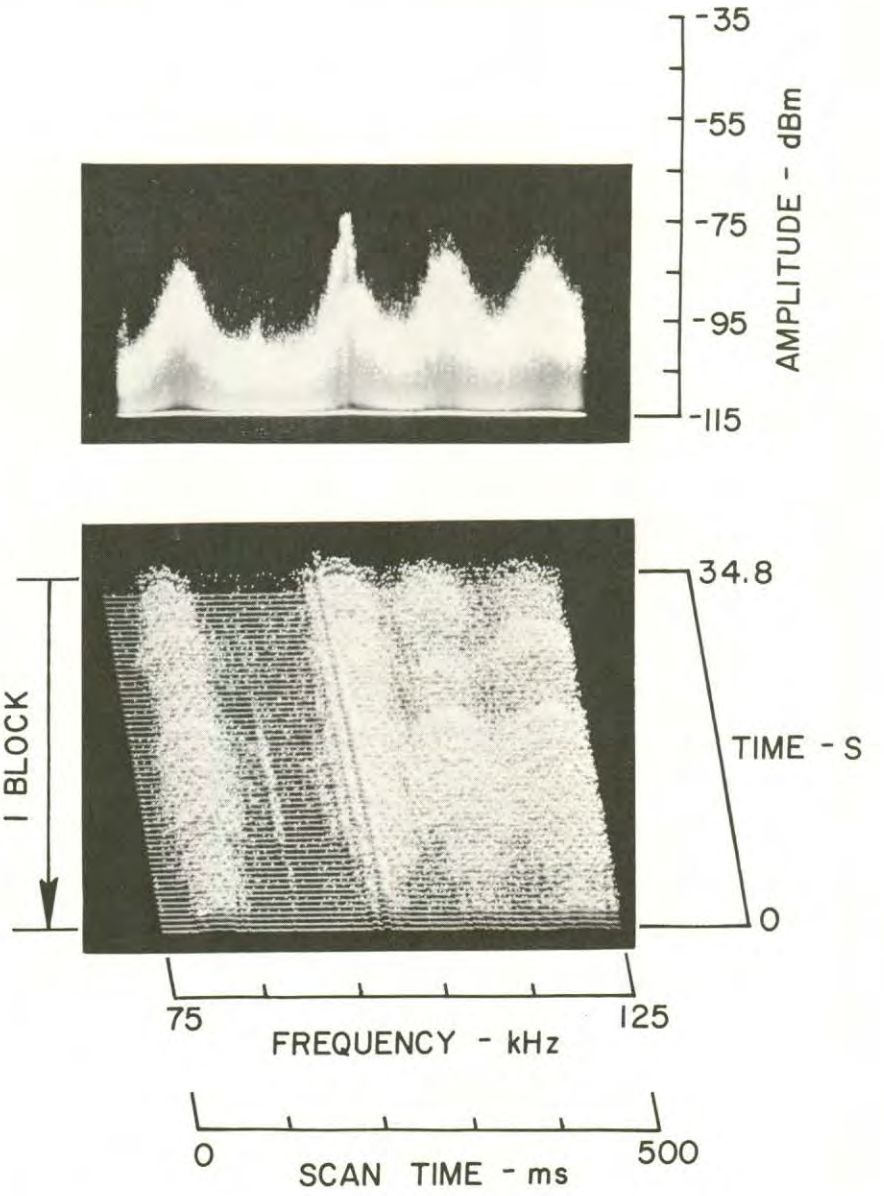

1/22/79, 1220, approaching 106-010
HP 140, Whip, F 100 kHz, W 50 kHz, IF 3 kHz, ST 500 ms, A -20 dBm/0/+15 dB/NF

FIGURE 5-5. 3-AXIS VIEW, 1/22/79, 1220, APPROACHING 106-010

1/23/79, 0827, leaving 109-014
HP 140, Whip, F 100 kHz, W 50 kHz, IF 3 kHz, ST 500 ms, A -20 dBm/0/+15 dB/NF

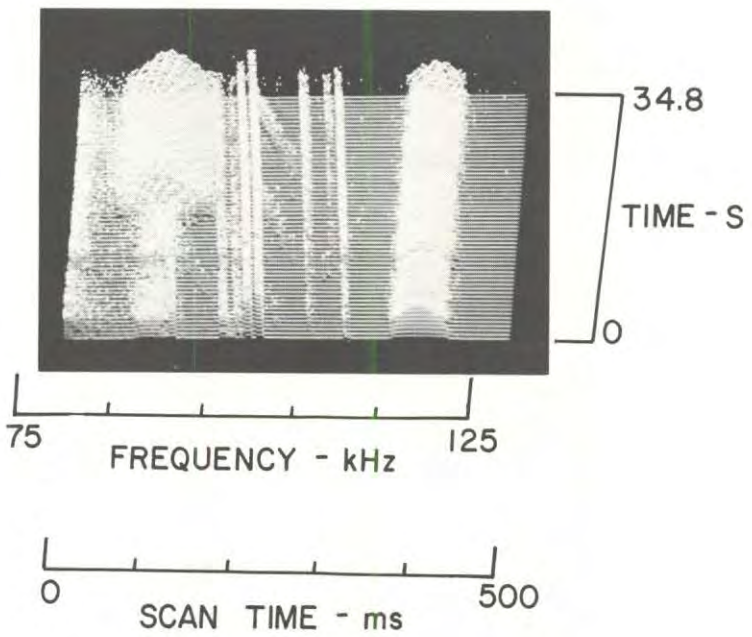

FIGURE 5-6. 3-AXIS VIEW, 1/23/79, 0827, LEAVING 109-014

1/23/79, 0916, from Sepulveda onto Wilmington
HP 140, Whip, F 100 kHz, W 50 kHz, IF 3 kHz, ST 500 ms, A -20 dBm/0/+15 dB/NF

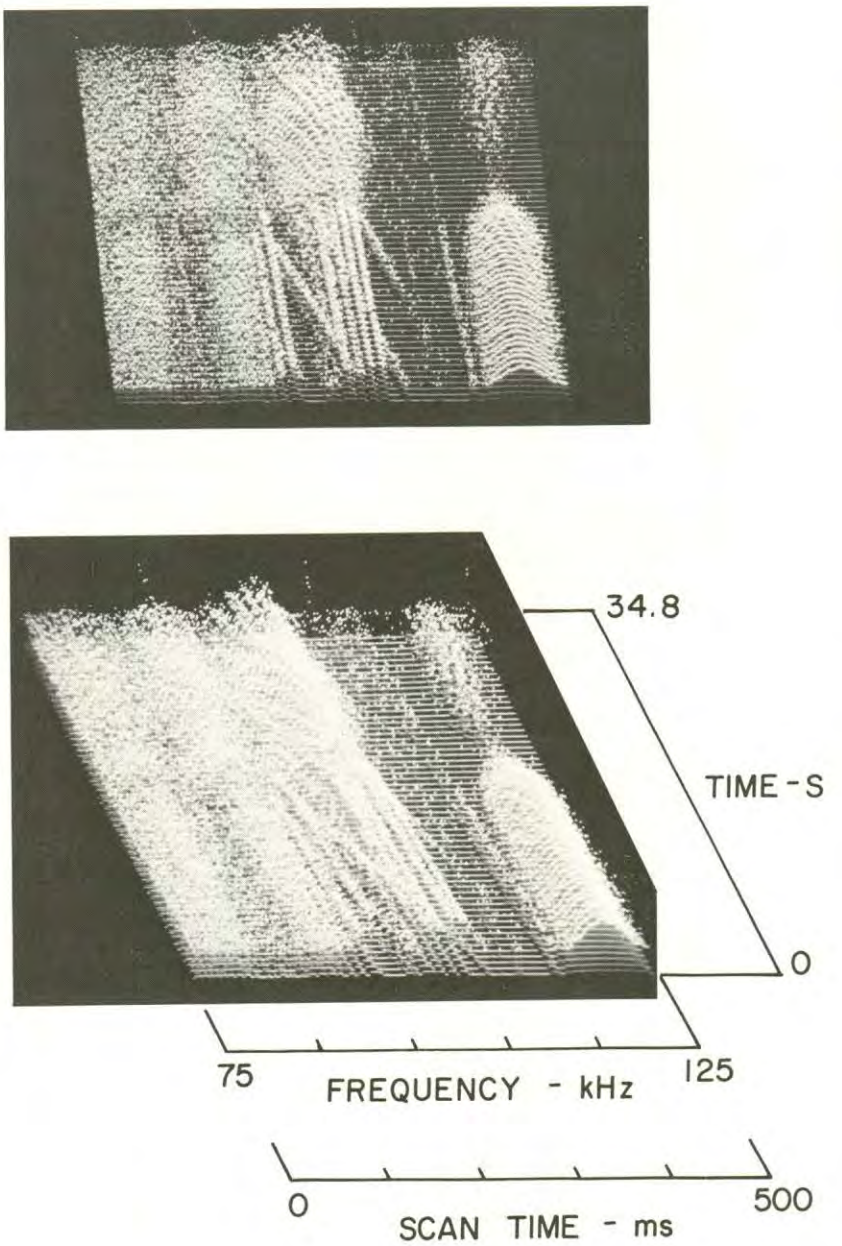

FIGURE 5-7. 3-AXIS VIEW, 1/23/79, 0916, FROM SEPULVEDA ONTO WILMINGTON

1/23/79, 0918, two locations on Wilmington 1/2 mile apart
HP 140, Whip, F 100 kHz, W 50 kHz, IF 3 kHz, ST 500 ms, A -20 dBm/0/+15 dB/NF

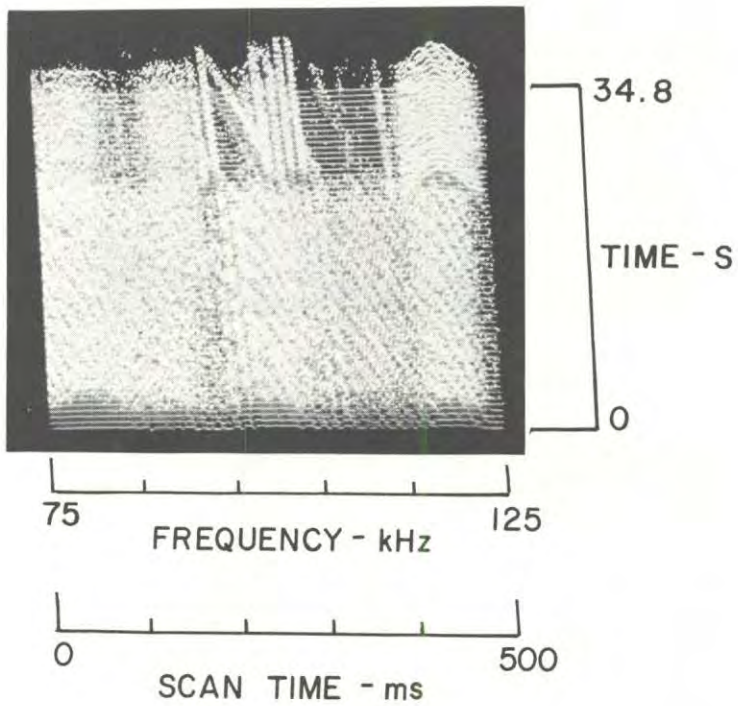

FIGURE 5-8. 3-AXIS VIEW, 1/23/79, 0918, TWO LOCATIONS ON WILMINGTON

5.3.3 Spatial Variations in Impulsive Noise

Results of the Phase I measurements showed that large changes occurred in impulsive noise levels as the measurement van approached and departed from the vicinity of certain electric utility distribution lines. The source of the impulsive noise was believed to be high power control units containing solid state switching devices employed by utility customers. Similar cases of spatial variation were also observed during the Phase II measurements.

A very large and sudden change in impulsive noise levels can be seen in Figure 5-9 where the measurement van turned off Del Amo onto Tillman. The very strong impulsive noise along Del Amo completely disappeared in less than 100 feet of travel on Tillman. The peak amplitude of the noise changed more than 70 dB in strength from Del Amo to Tillman. Another view of the impulsive noise on Del Amo is shown in Figure 5-10 at the corner of Del Amo and Anza. The noise along Del Amo at Anza was about 25 dB below the very high level at Del Amo and Tillman.

Data taken at site 109-018 (see Appendix A) were free of impulsive noise. However, 100 feet further along Watson Center Road strong impulsive noise conditions were observed which were associated with a 12 KV electric utility distribution line that terminated about 100 feet from the fixed measurement site. Figure 5-11 shows the impulsive noise encountered as the measurement van turned into a parking lot at the end of the distribution line, pulled away from the line during a wide turn in the parking lot, and then passed under the same line at a second parking lot entrance about 200 feet from the 109-018 site. The strong dependence of noise level on spatial movements is clearly shown. Additional impulsive noise measurements at a fixed location along Watson Center Road 100 feet from the actual 109-018 site are shown in Figures 5-12 and 5-13. The impulses are evenly spaced at about 2.6 ms intervals. Figure 5-12 shows variations in amplitude of the noise impulses over a 50 kHz wide band of frequencies and Figure 5-13 shows variations in amplitude over a 100 kHz wide band of frequencies.

1/23/79, 0944, from Del Amo onto Tillman
HP 140, Whip, F 100 kHz, W 50 kHz, IF 3 kHz, ST 500 ms, A -20 dBm/0/+15 dB/NF

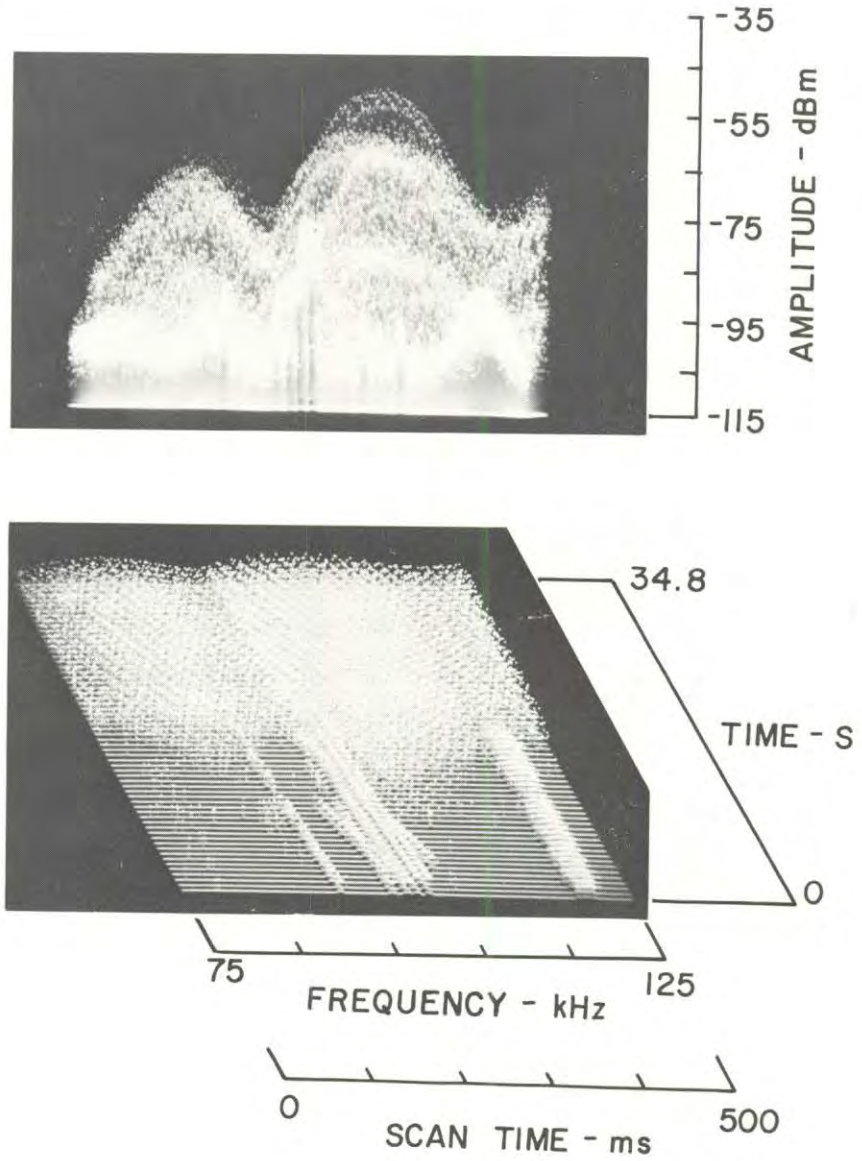

FIGURE 5-9. 3-AXIS VIEW, 1/23/79, 0944, FROM DEL AMO ONTO TILLMAN

1/22/79, 1125, Del Amo and Anza
HP 140, Whip, F 100 kHz, W 50 kHz, IF 3 kHz, ST 500 ms, A -30 dBm/0/+15 dB/NF

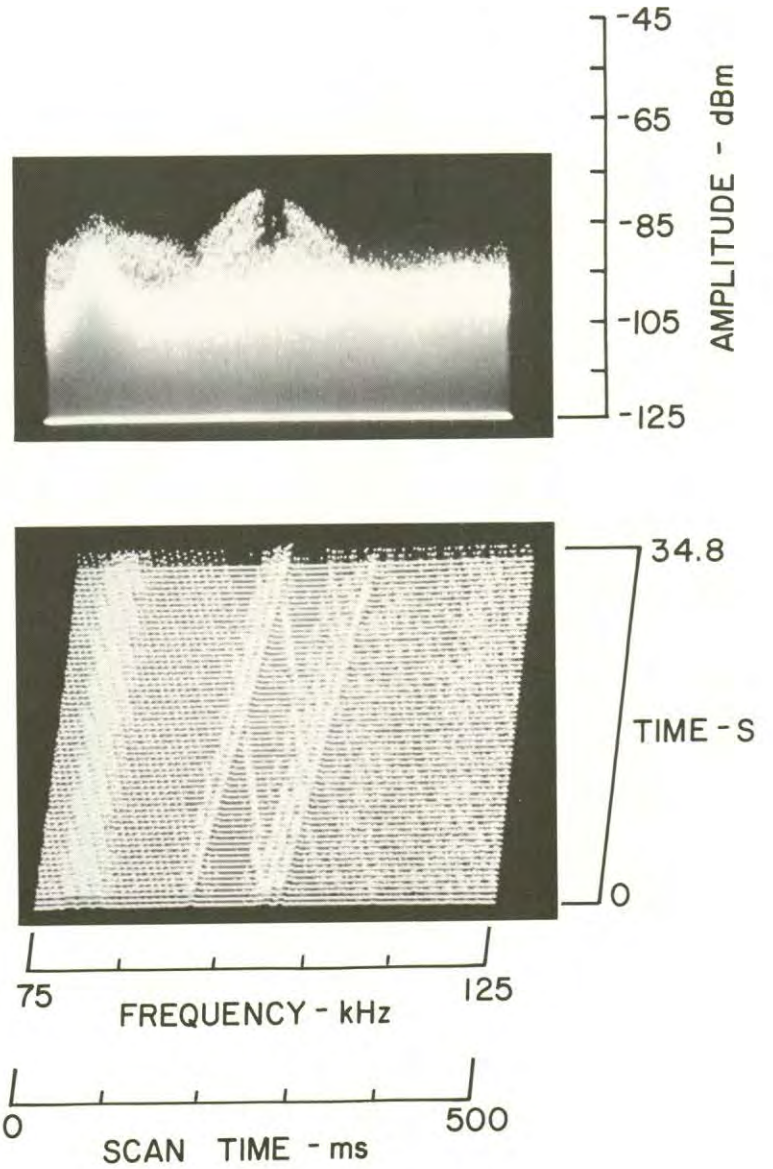

FIGURE 5-10. 3-AXIS VIEW, 1/22/79, 1125, DEL AMO AND ANZA

1/23/79, 0942, leaving 109-018 and u-turn under distribution line
HP 140, Whip, F 100 kHz, W 50 kHz, IF 3 kHz, ST 500 ms, A -20 dBm/0/+15 dB/NF

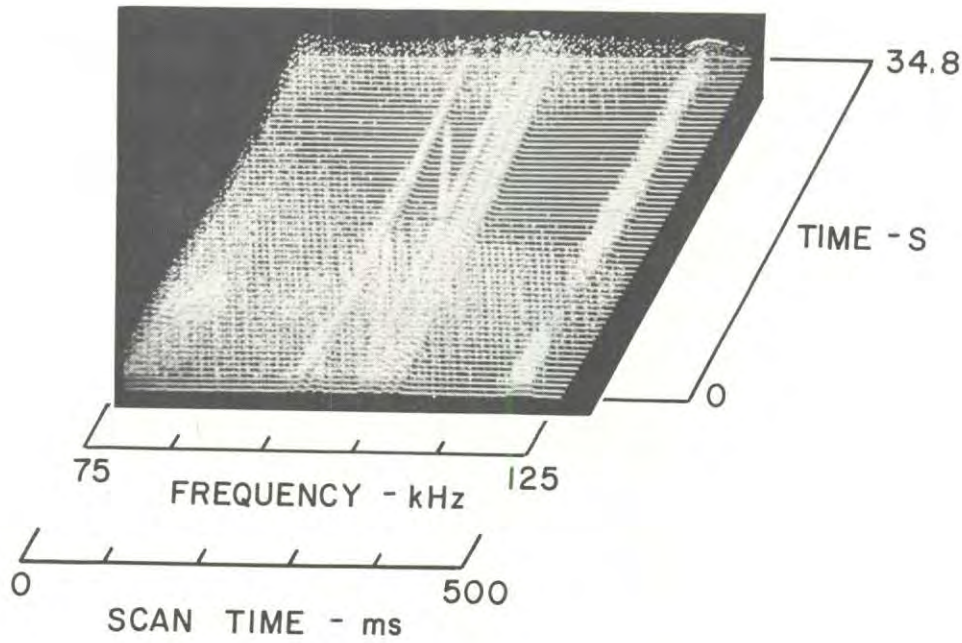

FIGURE 5-11. 3-AXIS VIEW, 1/23/79, 0942, LEAVING 109-018

1/26/79, 0920, 109-018 Site 2
HP 140, Whip, F 100 kHz, W 50 kHz, IF 3 kHz, ST 100 ms, A -20 dBm/0/+15 dB/NF

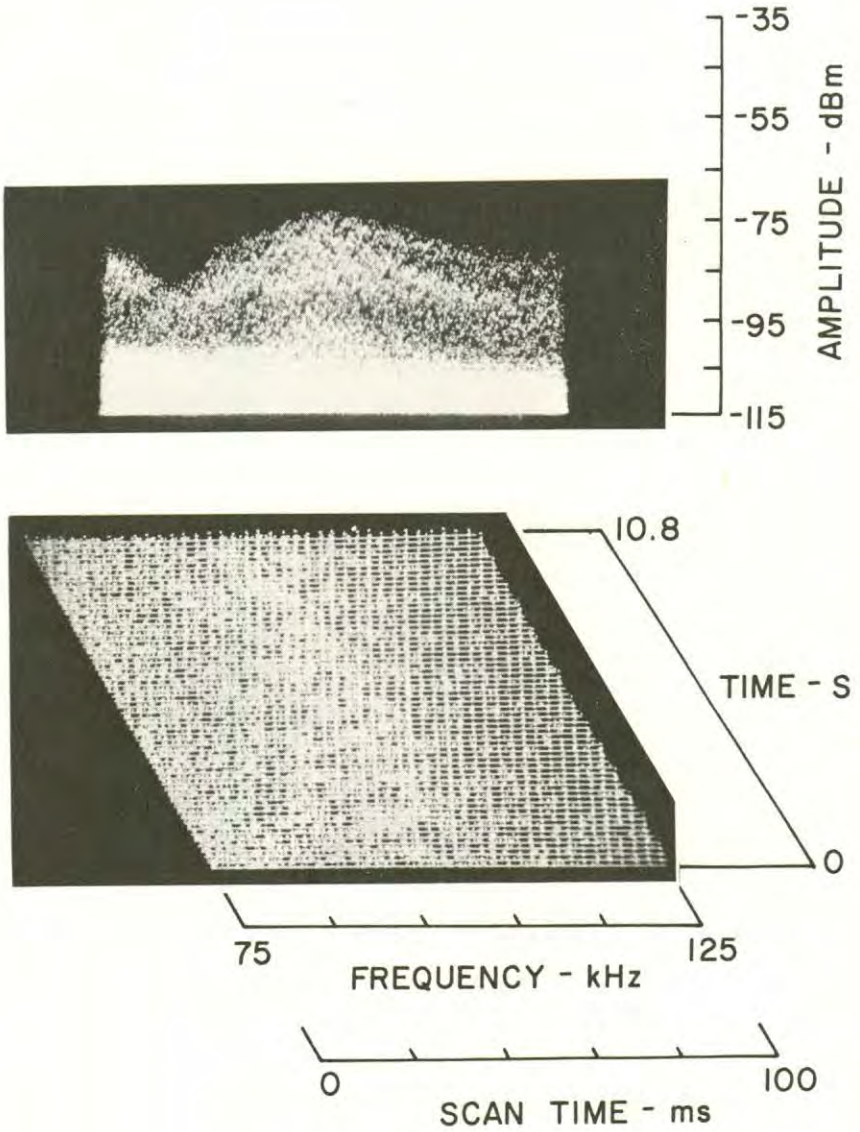

FIGURE 5-12. 3-AXIS VIEW, 1/26/79, 0920, 109-018 SITE 2

1/26/79, 0923, 109-018 Site 2
HP 140, Whip, F 100 kHz, W 100 kHz, IF 3 kHz, ST 100 ms, A -20 dBm/0/+15 dB/NF

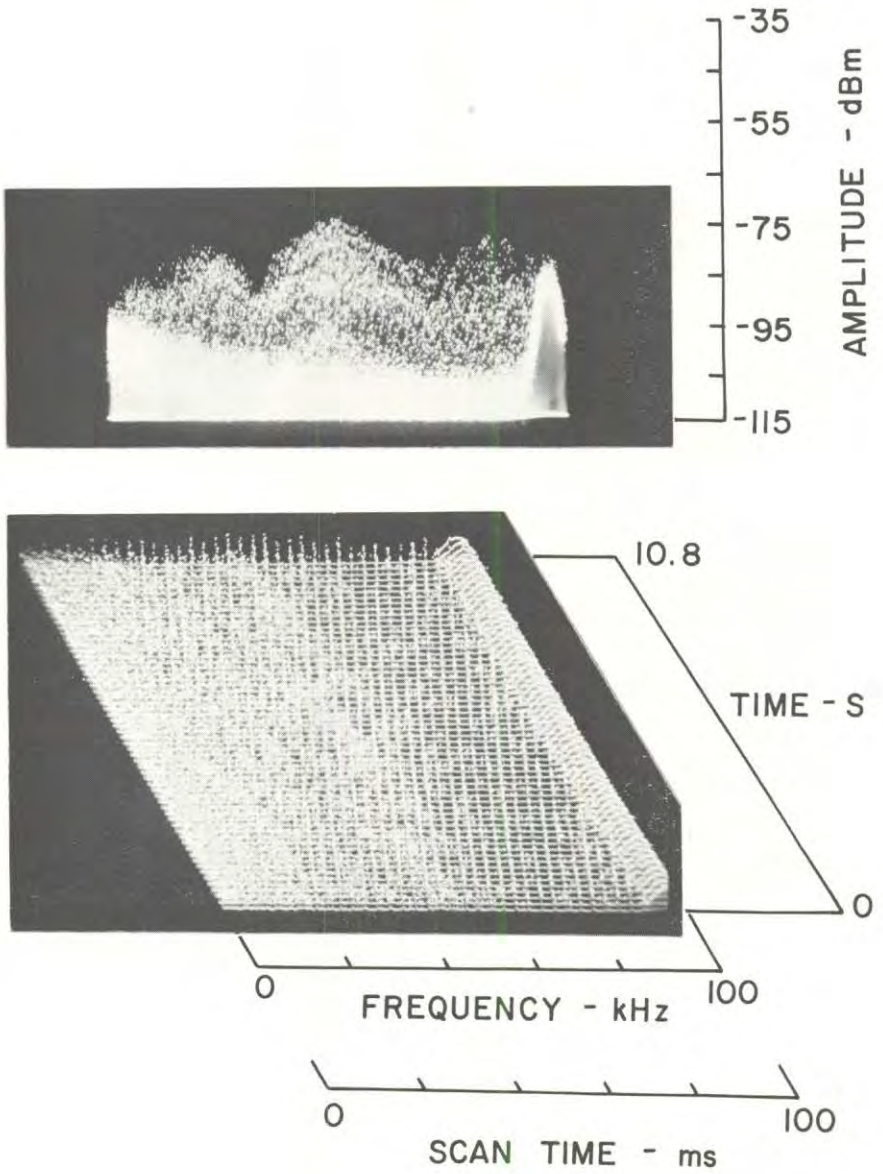

FIGURE 5-13. 3-AXIS VIEW, 1/26/79, 0923, 109-018 SITE 2

The top portion of the view in Figure 5-14 shows the lack of impulsive noise at site 109-018, while the bottom part of the view represents noise at the location used to obtain data in Figures 5-12 and 5-13. Figure 5-14 illustrates the critical aspects of site location and shows that drastically different noise conditions can be encountered only a few feet from a given site.

A nonuniform sequence of pulses emitted from a utility distribution line along Vista Del Mar is shown in Figure 5-15. The groups of two pulses are spaced 8.3 ms apart. The spacing between the two impulses is about 2 ms. Apparently, two separate switching devices were in operation with trigger points separated about 45° apart on the power line waveform.

1/26/79, 0930, Approaching 109-018 Site 2
HP 140, Whip, F 100 kHz, W 100 kHz, IF 3 kHz, ST 100 ms, A -20 dBm/0/+15 dB/NF

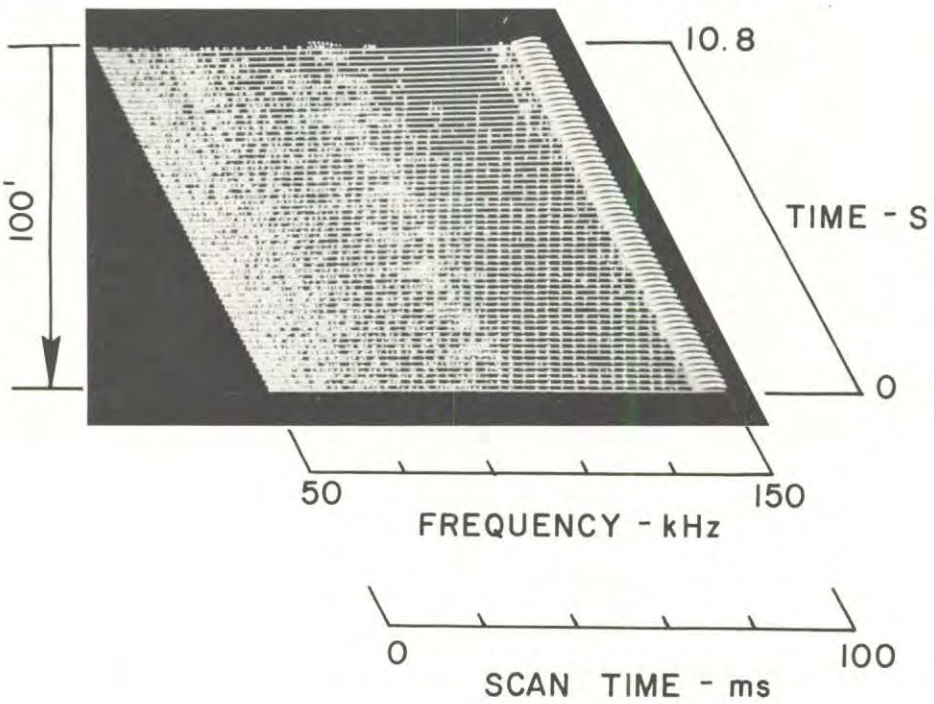

FIGURE 5-14. 3-AXIS VIEW, 1/26/79, 0930, 109-018 SITE 2

1/25/79, 1246, along Vista Del Mar south of El Segundo power plant
HP 140, Whip, F 100 kHz, W 50 kHz, IF 3 kHz, ST 100 ms, A -20 dBm/0/+15 dB/NF

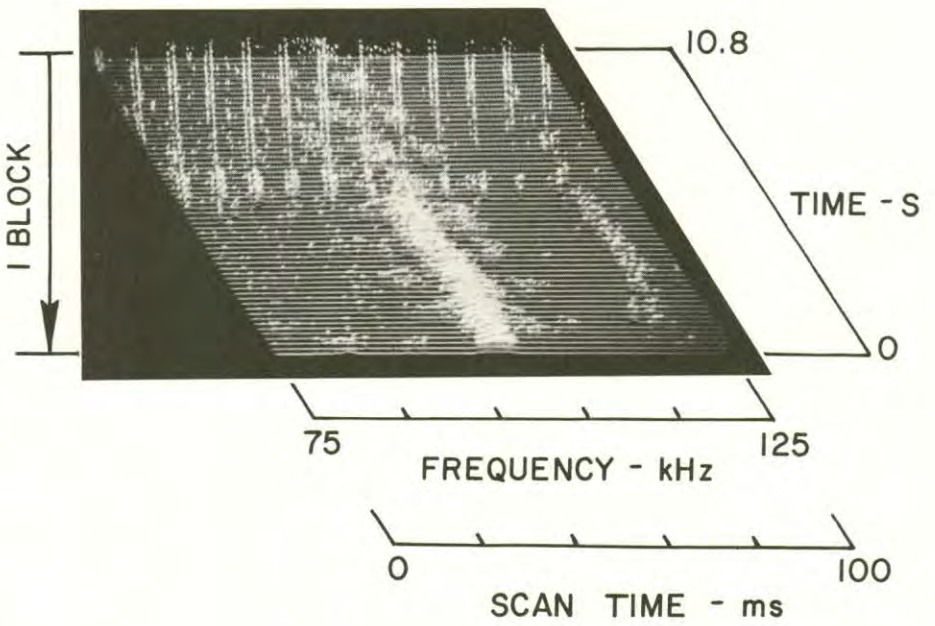

FIGURE 5-15. 3-AXIS VIEW, 1/25/79, 1246, VISTA DEL MAR

5.3.4 Time-Time Presentation of Impulsive Noise

Since the site near 109-018 provided orderly and high levels of impulsive noise with impulses spaced at even intervals of about 2.6 ms, the site was used to obtain time-time views. An example of a time-time view (receiver frequency scanning process stopped) is shown in Figure 5-16, where the top view shows 15 sequential groups of eight pulses from Station Y along with power line-emitted pulses spaced at intervals of about 2.6 ms. The second view from the top shows 16 lines of data taken from the top view. The third view from the top shows the bottom eight lines taken from the view immediately above. The bottom view shows the bottom four lines from the view immediately above. In the bottom view an eight-pulse Loran-C group from Station Y is shown on line 2, along with four power line-associated impulses which are within or near the Loran-C pulse groups. The amplitudes of the Loran-C and power line-associated impulses are nearly the same. Other similar situations can be identified in the other views showing additional scan lines. The views illustrate how power line-associated pulses and Loran-C pulses are mixed together, and how the two appear to a Loran-C receiver.

The time-time views show that the impulsive noise at site 109-018 was definitely not random in amplitude. The lower two views of Figure 5-16 indicate that most pulse amplitudes fell into two main amplitude levels (neglecting some minor variations) which had a very orderly repetitive pattern. Only very minor variations in amplitude were found from one day to the next day. The consistent amplitude pattern, along with the consistent spacing between impulses, indicates that the source mechanism was a very stable and orderly process.

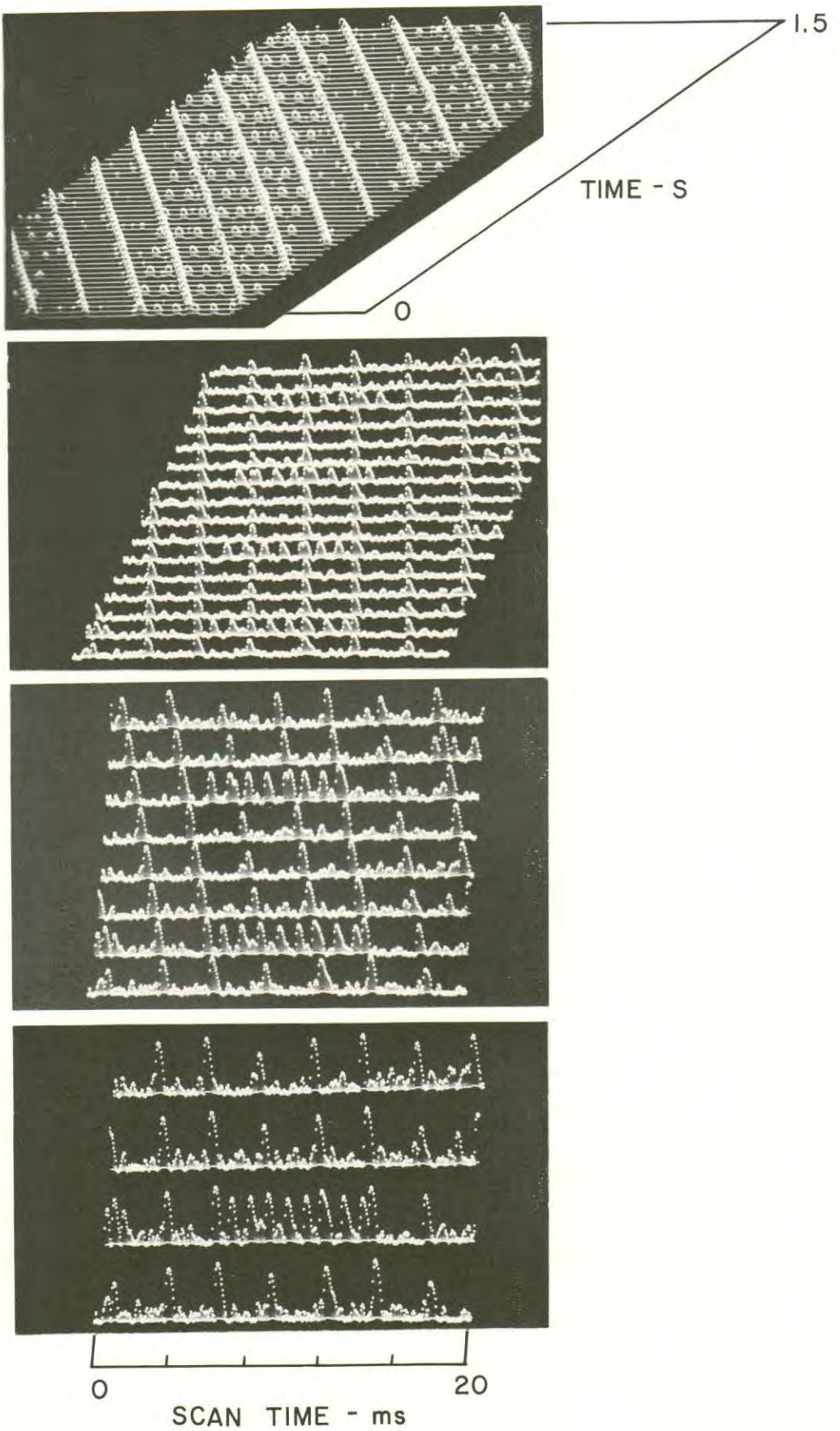

1/26/79, 0855, 109-018 Site 2
HP 140, Whip, F 100 kHz, W T-T, IF 3 kHz, ST 20 ms, A -20 dBm/0/+15 dB/NF

FIGURE 5-16. 3-AXIS VIEW, 1/26/79, 0855, 109-018 SITE 2

5.3.5 Traffic Control and Telephone Line Emissions

The Phase I measurements gave examples of CW signals which briefly appeared as the measurement van moved along a street. These brief bursts of CW signals were tentatively associated with street corners containing traffic control devices and with unshielded overhead telephone lines. Numerous cases of brief CW signals associated with street corners containing traffic control devices were again noted in the Phase II measurements. Examples are shown in Figures 5-17 and 5-18. While many of these signals from the Phase I effort were multiple frequency, the signals observed during the Phase II measurements were of single frequency. The data gave no indication of the reasons for this discrepancy, and there was inadequate time to investigate the sources in sufficient detail to determine why multiple and single frequencies were observed.

An example of a brief CW signal associated with an unshielded telephone line crossing the street in mid-block is shown in Figure 5-19. No other nearby structures were found which might be sources, and the signal peaked in amplitude when the measurement van was directly under the telephone line.

1/23/79, 1100, between 108-023 and 108-024 (traffic control signal)
HP 140, Whip, F 100 kHz, W 50 kHz, IF 3 kHz, ST 500 ms, A -20 dBm/0/+15 dB/NF

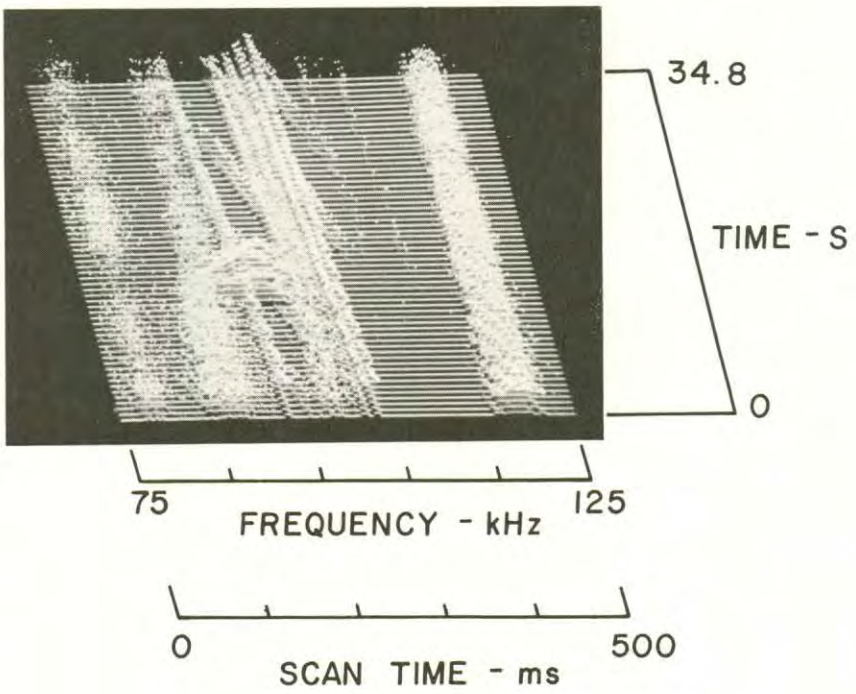

FIGURE 5-17. 3-AXIS VIEW, 1/23/79, 1100, BETWEEN 108-023 AND 108-024

1/26/79, 1211, Rosecrans & Sepulveda
HP 140, Whip, F 100 kHz, W 50 kHz, IF 3 kHz, ST 100 ms, A -20 dBm/0/+18 dB/BPF

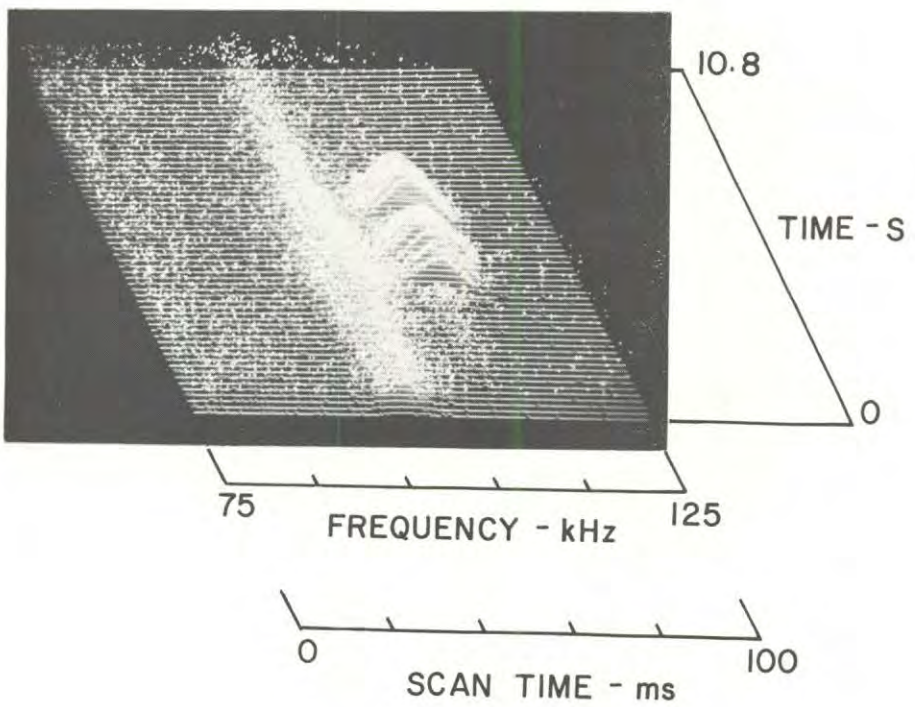

FIGURE 5-18. 3-AXIS VIEW, 1/26/79, 1211, ROSECRANS AND SEPULVEDA

1/26/79, 1156, passing under overhead telephone line, downtown El Segundo
HP 140, Whip, F 100 kHz, W 50 kHz, IF 3 kHz, ST 500 ms, A -20 dBm/0/+15 dB/NF

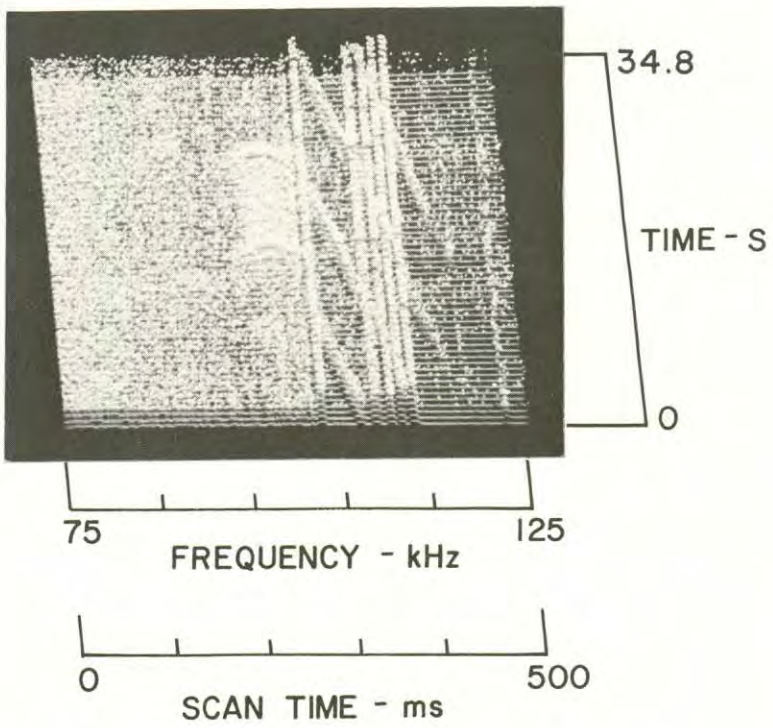

FIGURE 5-19. 3-AXIS VIEW, 1/26/79, 1156, DOWNTOWN EL SEGUNDO

5.3.6 Ignition Noise

Ignition noise from nearby vehicles was noted during the Phase I measurements, but serious effects which might degrade Loran-C reception were not found. Cases of auto and truck ignition noise from nearby vehicles were again observed in the Phase II data, as shown in Appendix A at sites 109-015, 109-016, 108-029, and 104-052. These examples involved automobiles and trucks passing by and near (within about 20 feet) the measurement van. The examples seem to represent minor transitory noise of only minimal importance.

During the Phase II measurements a more noticeable type of ignition interference was present from a truck moving along a street parallel with the measurement van. When the truck was in a parallel lane of traffic and the engine area was in the vicinity of the whip antenna, consistent and longer duration ignition noise was observed, and ignition noise pulses occurred with amplitudes about equal to the Loran-C signals from Station Y. Two examples are shown in Figure 5-20. The curved lines show variations in the interval between ignition pulses as the truck engine RPM varied. At a highway speed of about 45 mph, the spacing from pulse to pulse was about 4 ms.

1/26/79, 0803, Harbor Freeway ignition noise (international truck)
HP 140, Whip, F 100 kHz, W 50 kHz, IF 3 kHz, ST 100 ms, A -20 dBm/0/+15 dB/NF

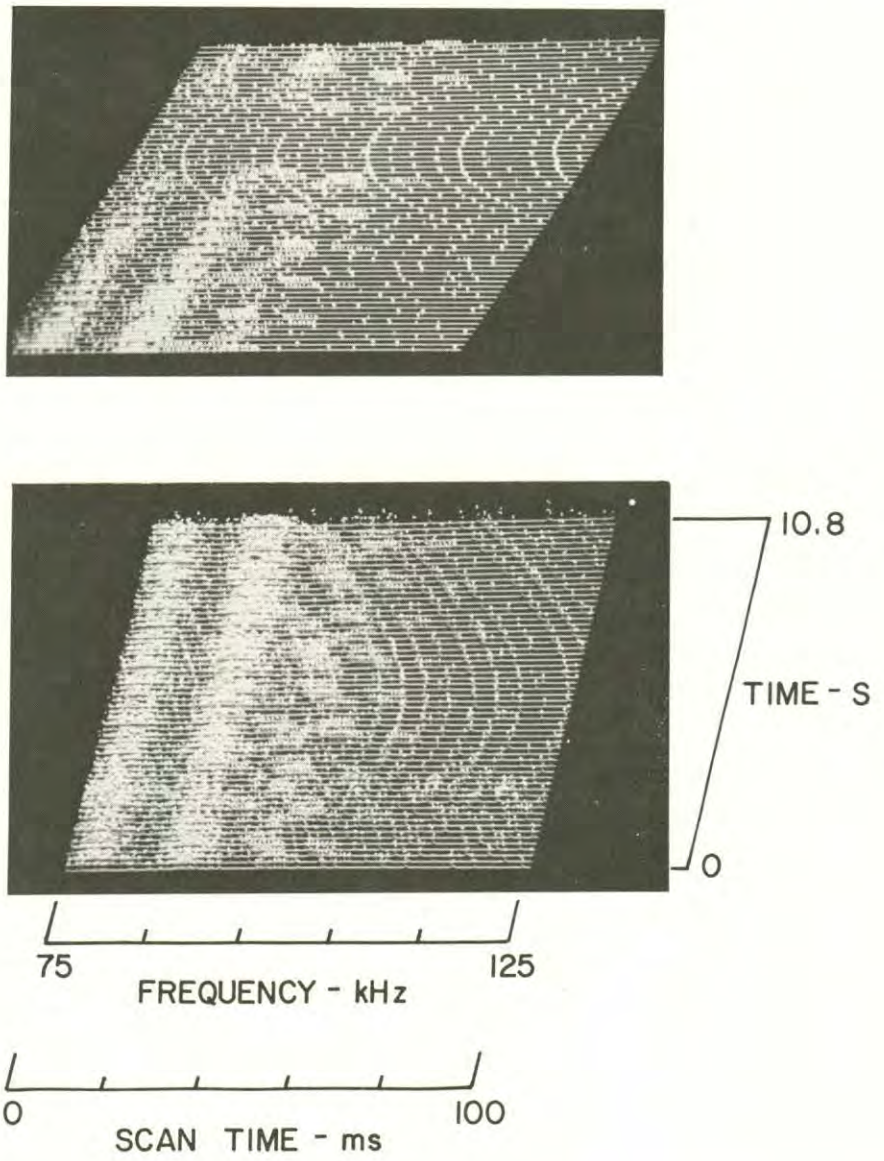

FIGURE 5-20. 3-AXIS VIEW, 1/26/79, 0803, HARBOR FREEWAY IGNITION NOISE

5.3.7 Freeway Effects

Brief decreases in the strength of Loran-C signals and CW signals were observed as the measurement van passed under a cross street and through an underpass. The attenuation of the signals from the underpass structure is shown in Figure 5-21, where the van was traveling on the Harbor Freeway in an area containing occasional overhead street crossings. Also, a brief burst of CW signal at 100 kHz can be seen in Figure 5-21 about 1/4 of the way from the bottom scan line. The CW signal was observed immediately after passing through the underpass, and it probably originated from a traffic control sensor on the overhead street.

Brief periods of impulsive noise were frequently observed when the measurement van proceeded along the freeway and traveled over a cross street on an overpass. An example is shown in Figure 5-22, where a burst of impulsive noise approximately two seconds long occurred. The noise probably originated from utility distribution lines along the cross street.

1/22/79, 1238, Harbor Freeway underpass
HP 140, Whip, F 100 kHz, W 50 kHz, IF 3 kHz, ST 500 ms, A -20 dBm/0/+15 dB/NF

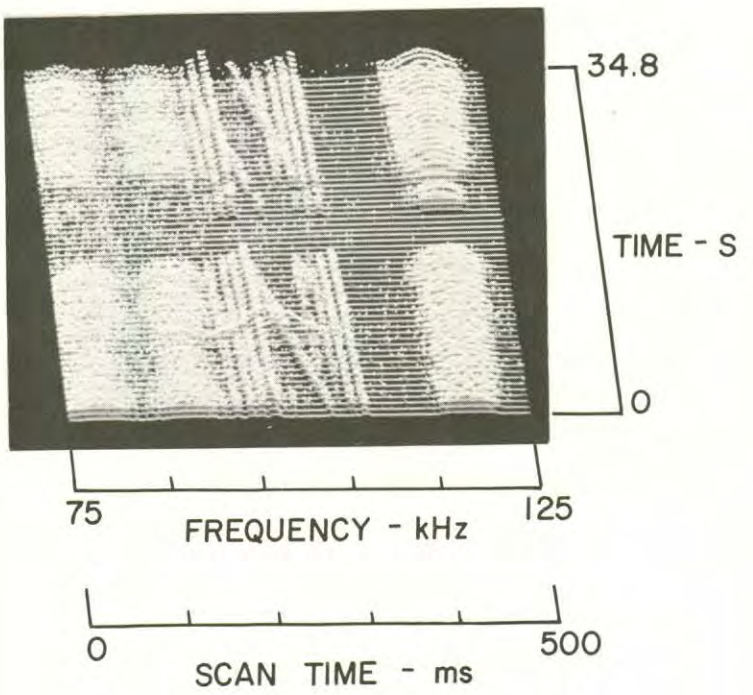

FIGURE 5-21. 3-AXIS VIEW, 1/22/79, 1238, HARBOR FREEWAY UNDERPASS

1/26/79, 0808, Harbor Freeway overpass impulse noise
HP 140, Whip, F 100 kHz, W 50 kHz, IF 3 kHz, ST 100 ms, A -20 dBm/0/+15 dB/NF

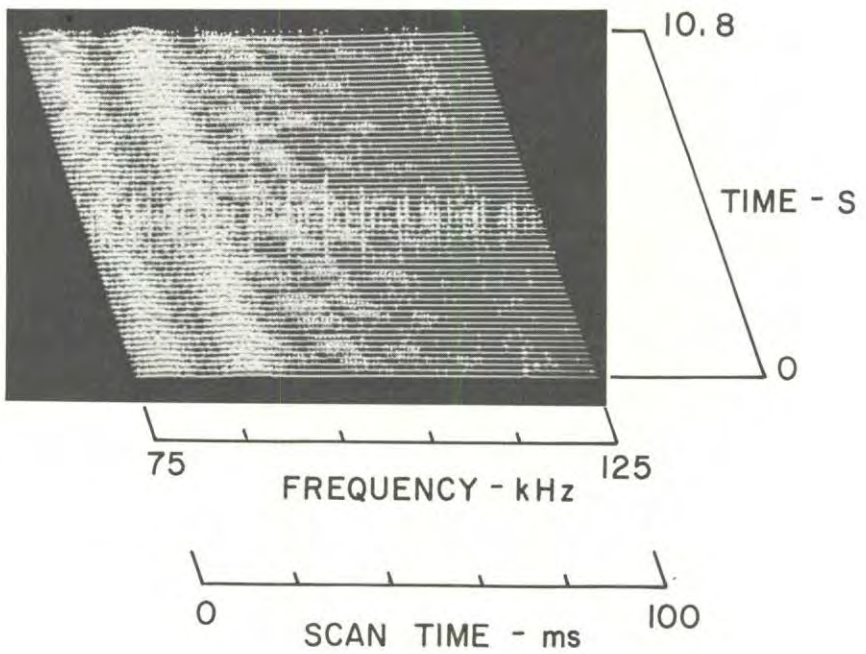

FIGURE 5-22. 3-AXIS VIEW, 1/26/79, 0808, HARBOR FREEWAY OVERPASS

5.3.8 Bursts of Power Line-Associated Noise

Bursts of noise were observed to be emanating from a high voltage utility transmission line crossing Rosecrans between Sepulveda and Vista Del Mar. These bursts are shown in Figure 5-23. Two bursts of noise can be seen in the upper portion of the view, each with a duration of about one second and spaced about 0.2 seconds apart. Downward in the view about 1.5 seconds further, another one-second burst of noise can be seen. About 0.4 seconds further down the view, two closely-spaced, very brief bursts occurred.

Signal structure during each burst had maximum and minimum energy at 8.3 ms intervals as shown by the slanting lines within each noise burst. Also, the maximum overall strength of the bursts peaked as the measurement van passed directly under the overhead transmission line.

Similar bursts of power line-associated noise have been observed in prior measurements at sites in Los Altos Hills, California, and Skaggs Island, California. The noise bursts have been observed to occur for periods up to a few hours and then to disappear for long periods of time. Their origin has not been determined, and possible source mechanisms have been the subject of much speculation. The on-off noise bursts remain a puzzle. While the Rosecrans transmission line provided a case where the source could probably have been tracked down with a small additional measurement effort, the time was not available for additional diagnostic effort.

1/26/79, 1017, Rosecrans
HP 140, Whip, F 27 MHz, W 50 kHz, IF 3 kHz, ST 100 ms, A -10 dBm/0/0/NF

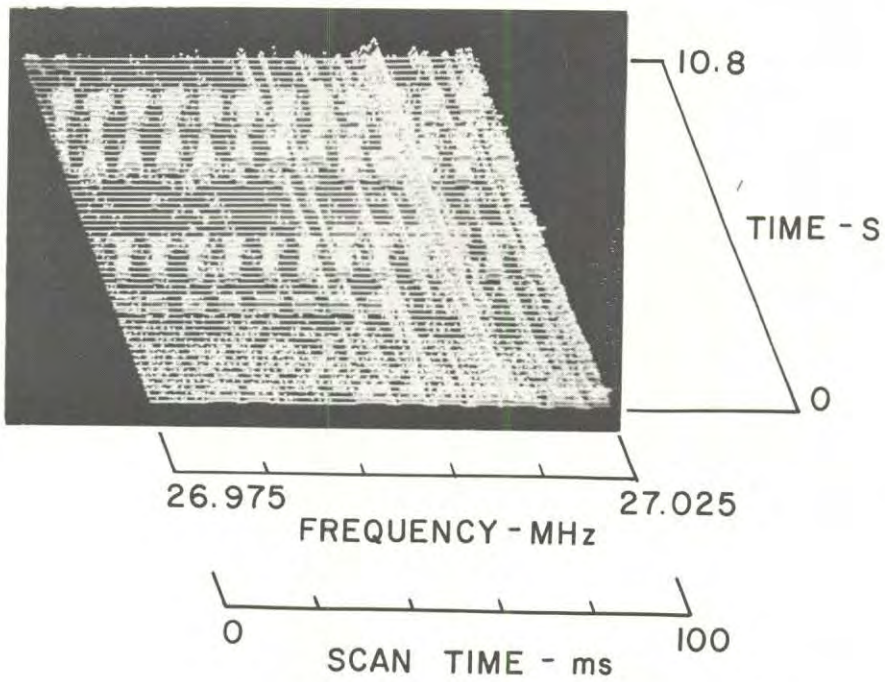

FIGURE 5-23. 3-AXIS VIEW, 1/26/79, 1017, ROSECRANS BETWEEN SEPULVEDA AND VISTA DEL MAR

5.3.9 El Segundo Power Plant

Power line-associated noise was investigated at the output transmission lines for the Southern California Edison El Segundo power plant. The measurement van passed directly under the output lines on Vista Del Mar immediately adjacent to the power plant. Noise was not observed on a typical Loran-C measurement pass directly under the line. On a subsequent measurement pass, the receiver scan width was increased to cover the 0 to 500 kHz band as shown in Figure 5-24. Very weak slanting lines can be seen in portions of the view which were synchronized with the electric power frequency. Also, a brief and weak CW signal was observed at about 380 kHz when the measurement van was directly under the transmission line.

Since very little power line-associated noise was observed at LF frequencies, an additional measurement was made in the 2 MHz region, as shown in Figure 5-25. Low levels of power line-associated noise were observed when directly under the line. This noise could not be detected a few hundred feet from the transmission line.

1/26/79, 1042, on Vista Del Mar passing under El Segundo power plant output lines
HP 140, Whip, F 250 kHz, W 500 kHz, IF 10 kHz, ST 100 ms, A -20 dBm/0/0/NF

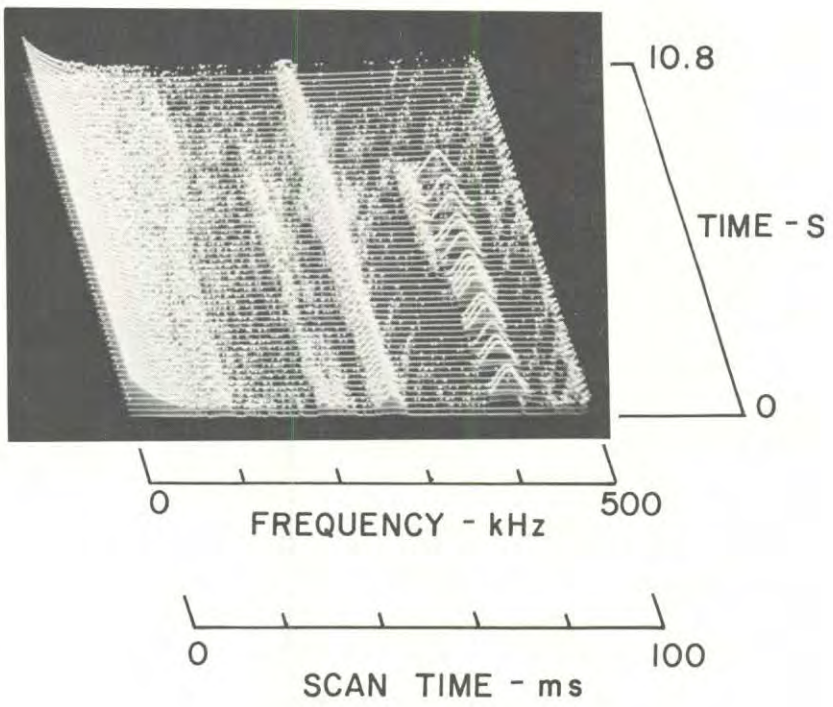

FIGURE 5-24. 3-AXIS VIEW, 1/26/79, 1042, VISTA DEL MAR

1/26/79, 1038, on Vista Del Mar and passing under output lines El Segundo power plant
HP 140, Whip, F 2 MHz, W 50 kHz, IF 3 kHz, ST 100 ms, A -20 dBm/0/0/NF

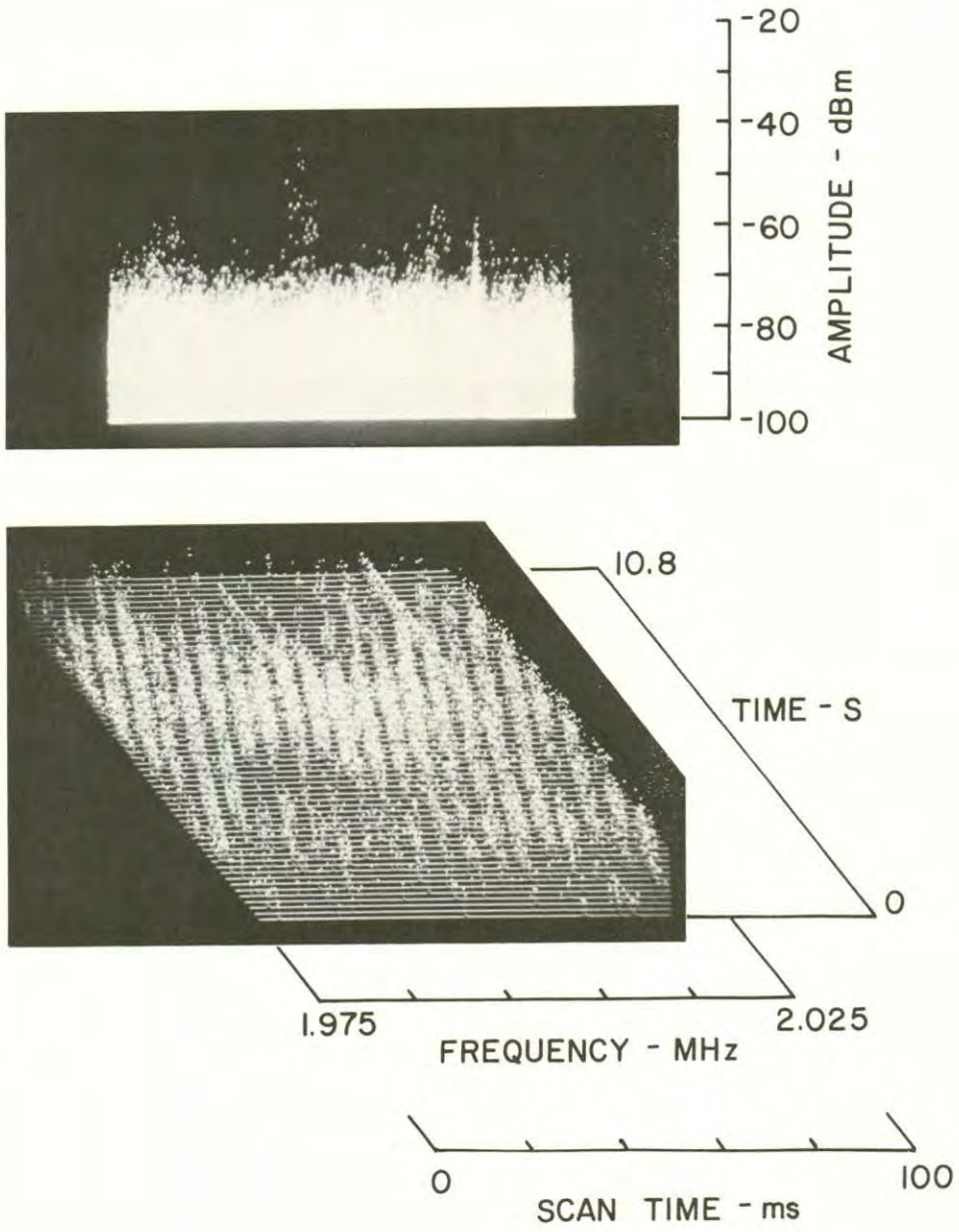

FIGURE 5-25. 3-AXIS VIEW, 1/26/79, 1038, VISTA DEL MAR

6. DISCUSSION

6.1 GENERAL COMMENTS

Results of the Phase II measurement period (January 22 through January 26, 1979) supplement those of the Phase I measurements described in Sections 3 and 4 (December 18 through December 22, 1978). While additional detail and data were collected, the results of this second measurement period were in general agreement with Phase I results. No significant differences in noise and RFI were found.

Slightly different measurement procedures were used in the first and second periods. During the first period the measurement van followed general route patterns for Loran-C receiver performance measurements, but the noise and RFI measurements were made at and around each site, as well as at many other locations where noise was observed. The noise and RFI measurements were of a diagnostic nature, with each measurement tailored to best define the noise being observed. The Phase II measurements were made primarily at specific sites and simultaneously with Loran-C receiver measurements. Supplementary measurements were made as time permitted.

Data from the fixed site measurements described in Section 5.2 and Appendix A have been organized and tabulated in formats convenient for two main objectives, which are:

1. To provide the reader with a valid and easy-to-interpret summary of radio noise and RFI in Los Angeles at and around the Loran-C transmission frequency of 100 kHz.
2. To provide a means to compare noise and RFI results at each site with the performance of Loran-C receivers.

6.2 FIXED SITE RESULTS

Noise and RFI measurements were made at 54 out of the 56 sites scheduled during the measurement period. Data were not obtained at two sites because of time required to clean an oscilloscope camera and to replace a fouled spark plug in the motor generator supplying 115 volt, 60 Hz power to the measurement van. A set of 3-axis views with standard measurement parameters was obtained at each of the 54 sites. The standard views were made with F = 100 kHz, W = 50 kHz, IF = 3 kHz, and ST = 500 ms. Data for sites 106-001 through 106-005 used the 18 dB preamplifier with the bandpass filter. At all remaining sites the 15 dB preamplifier was used without an RF filter.

Occasionally additional measurements were made with a larger scan width (W = 100 kHz) and/or at a faster scan speed (ST = 100 ms). The 3-axis views for these measurements follow the standard views, and their identification codes show the same site identification as the standard view with a different time of day and different measurement parameters.

Data for each site are provided in Appendix A. The 3-axis views in the appendix can be rapidly scanned to examine the variety of noise and CW signal states encountered.

Brief bursts of ignition noise were occasionally observed from vehicles passing the measurement van in an adjacent lane of traffic. Examples are shown in the data for sites 109-015, 109-016, 108-029, and 104-052. Most passing vehicles did not cause ignition impulses to appear in the data, and the examples provided might well represent the occasional super noise vehicle noted by Shepard, et al. (3) in higher frequency measurements.

An examination of the 3-axis views in Appendix A showed that all CW signals in the 75 to 125 kHz band appeared on five frequencies. The CW frequencies were approximately 80, 90, 100, 108, and 119 kHz. Precise frequency measurements were not made, and the accuracy of the above frequencies is about $\pm$ 1 kHz. The finding that all observed CW signals were only on a total of five frequencies considerably simplified data scaling and analysis tasks.

The level of each CW signal, each Loran-C signal, and the maximum peak pulse value of noise at 100 $\pm$ 10 kHz were scaled from the 3-axis views in Appendix A. The values of amplitude at the preamplifier input with all calibration factors incorporated are shown in Table 6-1. The columns of Table 6-1, from left to right, are:

Column 1	Site identification number (see Table 5-2)
2	Signal level in dBm of Loran-C Master Station located at
3	Signal level in dBm of Loran-C Station W located at
4	Signal level in dBm of Loran-C Station X located at
5	Signal level in dBm of Loran-C Station Y located at
6	Peak impulse level of noise in dBm in the 100 $\pm$ 10 kHz band
7	Signal level in dBm of CW signal at 80 kHz
8	Signal level in dBm of CW signal at 90 kHz
9	Signal level in dBm of CW signal at 100 kHz
10	Signal level in dBm of CW signal at 108 kHz
11	Signal level in dBm of CW signal at 119 kHz

The symbol < appears in columns 2 through 5 and it was used whenever the Loran-C signal was below the receiver noise level. The symbol - also appears in columns 2 through 5 and indicates times when signal level values could not be scaled from the 3-axis views because other signals prevented

scaling. A 0 was used in columns 6 through 11 whenever noise or a CW signal was entirely absent from the 3-axis views.

The mean value of the peak measurements, $\bar{x}$, standard deviation, σ, and number of samples, N, are listed at the bottom of Table 6-1. The mean values and their standard deviations are provided because of the high interest in overall Loran-C receiving conditions. However, these values must be used with caution. The following listed factors must be considered when using the mean and standard deviation values.

1. The CW signals (except for 119 kHz) are location-dependent. For example, the 108 kHz signal only appears at sites 041 through 050. The 80, 90, 100, and 108 kHz signals are missing from sites 104-051 through 104-056. The 100 kHz signal does not appear at many blocks of sites. The 80 and 90 kHz signal does not appear at sites 106-001 through 106-005.

   These site-dependent factors suggest that a different set of sites probably would yield different signal levels.

2. Low levels of Loran-C signal indicated by the symbol < and implied by some cases where the symbol - was used, are not included in the mean and standard deviations. Thus, the mean levels of Loran-C signals are artificially high and the standard deviations are artificially low.

3. The impulsive noise levels are extremely dependent upon locations. Sometimes the peak amplitude of impulsive noise varied more than 50 dB over distances as short as 100 feet. Thus the levels shown represent only that at the precise measurement location.

4. The CW signal at 119 kHz appeared in all 3-axis views except at site 106-005. The source of the 119 kHz signal is believed to be a USN transmitter in central California. The mean value of this signal is probably reasonable.

TABLE 6-1. SIGNAL AND NOISE LEVELS

SITE NO.	LORAN-C SIGNALS				NOISE	CW SIGNALS				
	M	W	X	Y	N	80	90	100	108	119
106-001	-86	-88	-86	-76	0	0	0	-98	0	-100
106-002	-83	-83	-79	-76	0	0	0	-98	0	-96
106-003	-81	-85	-81	-78	-71	0	0	-86	0	-98
106-004	-76	-78	-76	-73	-84	0	0	-92	0	-99
106-005	-91	-88	-80	-76	0	0	0	0	0	0
106-006	<	-90	-83	-75	0	-96	0	0	-94	-96
106-007	-83	-81	-73	-66	0	-85	0	0	-86	-84
106-008	-76	-73	-68	-61	0	-83	0	0	-77	-81
106-009	<	-71	-69	-66	0	0	-87	-86	0	-87
106-010	<	-75	-73	-66	-83	-85	0	0	-76	-75
109-011	<	-83	-79	-70	0	-95	-95	0	0	-87
109-012	-80	-75	-68	-63	0	-90	-88	0	0	-84
109-013	-85	-83	-73	-63	0	-95	-93	0	0	-85
109-014	-78	<	-73	-63	0	0	0	0	0	-85
109-015	-78	<	-73	-63	0	-96	-93	-87	0	-87
109-016	-73	-74	-69	-64	0	-94	-95	-90	0	-86
109-017	--	--	--	-70	0	0	0	-71	0	-92
109-018	-85	-83	-73	-63	0	0	0	0	0	-86
109-019	-70	-70	-65	-63	0	-95	-95	0	0	-91
109-020	-78	-76	-66	-66	0	-95	-96	0	0	-95
108-021	-77	-77	-68	-67	0	-96	-96	0	0	-96
108-022	-76	-75	-68	-66	0	-95	-93	0	0	-90
108-023	-74	-72	-66	-62	0	-94	-85	0	-92	-83
108-024	--	--	--	-78	0	-87	-87	-86	0	-87
108-025	--	--	--	--	-90	0	0	-67	0	-85
108-026	-75	-75	-65	-65	0	0	-95	0	0	-90
108-027	-72	-73	-69	-64	0	-95	-94	0	0	-87
108-028	-76	-78	-73	-65	0	-94	-90	0	0	-91
108-029	<	<	-78	-73	0	0	0	-87	0	-95
108-030	-77	-78	-70	-66	0	-92	-90	0	0	-87

TABLE 6-1. SIGNAL AND NOISE LEVELS (CONTINUED)

SITE NO.	LORAN-C SIGNALS				NOISE	CW SIGNALS				
	M	W	X	Y	N	80	90	100	108	119
107-031	--	--	-72	-63	-75	-86	-89	0	0	-87
107-032	-83	-83	-71	-67	0	-96	-93	0	0	-88
107-033	-77	-78	-78	-66	-78	0	0	0	0	-92
107-034	--	-74	-71	-66	0	-87	-93	0	0	-92
107-035				NO MEASUREMENT						
107-036	--	--	-79	-80	-88	0	0	0	0	-93
107-037	-71	-73	-65	-63	0	0	-85	0	0	-86
107-038	-73	-73	-63	-63	0	0	-85	0	0	-86
107-039	-73	-73	-66	-63	0	0	-85	0	0	-89
107-040	-75	-73	-66	-63	0	-90	-81	0	0	-87
110-041	-78	-83	-71	-66	0	-86	-86	0	-78	-86
110-042	-76	<	-75	-69	0	-81	-84	0	-84	-87
110-043				NO MEASUREMENT						
110-044	-85	<	-75	-75	0	-90	0	0	-85	-92
110-045	-94	-95	-74	-70	0	-92	-85	0	-79	-94
110-046	--	--	--	--	--	-75	-70	-79	-66	-70
110-047	--	--	--	--	0	-77	-72	-85	-70	-79
110-048	-67	-69	-66	-66	0	-76	-78	0	-67	-85
110-049	-70	-94	-64	-64	0	-85	-77	0	-79	-85
110-050	-76	-76	-78	-78	0	-90	-87	0	-94	-85
104-051	<	<	-70	-68	-75	0	0	0	0	-90
104-052	-85	-85	-73	-73	0	0	0	0	0	-95
104-053	-74	-74	-66	-62	0	0	0	0	0	-87
104-054	-78	-78	-66	-64	0	0	0	0	0	-90
104-055	-80	-80	-70	-68	-80	0	-95	0	0	-95
104-056	-78	-78	-72	-72	0	0	0	0	0	-95
N	35.0	35.0	43.0	45.0	9.0	30.0	32.0	9.0	14.0	47.0
$\bar{x}$	-77.31	-77.46	-70.47	-66.71	-80.44	-89.23	-88.03	-82.00	-80.50	-87.57
σ	5.36	5.93	4.37	4.57	6.27	6.29	6.86	7.98	9.22	5.06

The data in Table 6-1 can be used to compare measured noise and RFI with receiver performance. Such a comparison must take into consideration the complex combination of impulsive noise intervals and amplitudes, the non-flat properties of the noise impulses, the CW signals at various frequencies and various levels, the amplitudes of the Loran-C signals, and the signal processing techniques employed by each model of Loran-C receiver tested.

The non-flat properties of impulsive noise across the relatively narrow band of frequencies generally considered necessary for successful Loran-C receiver performance are of special interest (assumed to be about 20 kHz wide centered at 100 kHz). Usually noise is assumed to be flat across the receiver bandwidth; however, most measured examples of impulsive noise were non-flat as shown in the 3-axis views for sites 108-025, 107-031, 107-033, 107-034, 107-036, 110-047, 104-051, and 104-055 in Appendix A.

Intermittent impulsive noise conditions were observed at sites 107-034 and 110-046.

Table 6-2 provides an overall summary of noise and CW signals at each site and allows the reader to compare general noise and CW signal conditions to site descriptors. The site identification numbers employed in Tables 5-2 and 6-1 are used as well as the site descriptors contained in Table 5-2. A T was added to the power line status whenever a nearby utility high voltage transmission line was noted. The remaining columns are as follows:

Column Heading

Noise	0 indicates no noise. 1 indicates the presence of impulsive noise in the 100 $\pm$ 10 kHz band.
CW = 80 CW = 90 CW = 100 CW = 108 CW = 118	0 indicates no CW signals. 1 indicates a weak CW signal (< 10 dB above receiver noise). 2 indicates a strong CW signal ($\geq$ 10 dB above receiver noise).

TABLE 6-2. COMPARISON OF SITE PARAMETERS WITH MEASURED RESULTS

SITE PARAMETERS			MEASURED RESULTS					
SITE NO.	SITE CAT.*	POWER LINE CAT.†	NOISE	CW = 80	CW = 90	CW = 100	CW = 108	CW = 119
106-001	C	1	0	0	0	1	0	1
106-002	R	0 T	0	0	0	1	0	1
106-003	C	1 T	1	0	0	2	0	1
106-004	I	2	1	0	0	1	0	1
106-005	R	0	0	0	0	0	0	0
106-006	R	0 T	0	1	0	0	1	1
106-007	C	1	0	2	0	0	2	2
106-008	O	0	0	2	0	0	2	2
106-009	I	1	0	0	1	2	0	2
106-010	I	2 T	1	2	0	0	2	2
109-011	R	0	0	1	1	0	0	2
109-012	O	0	0	1	2	0	0	2
109-013	C	0	0	1	1	0	0	2
109-014	C	1	0	0	0	0	0	2
109-015	C	1	0	1	1	2	0	2
109-016	I	1 T	0	1	1	1	0	2
109-017	I	2 T	0	0	0	2	0	1
109-018	I	0	0	0	0	0	0	2
109-019	R	0	0	1	1	0	0	1
109-020	R	0	0	1	1	0	0	1

* Site category: C - commercial, R - residential, I - industrial, O - open.

† Power lines show number of lines present (one side or both sides of street): 1 - one side, 2 - both sides, underline of number - van directly under lines, T - nearby utility transmission line.

TABLE 6-2. COMPARISON OF SITE PARAMETERS WITH MEASURED RESULTS (CONTINUED)

SITE PARAMETERS			MEASURED RESULTS					
SITE NO.	SITE CAT.*	POWER LINE CAT.†	NOISE	CW = 80	CW = 90	CW = 100	CW = 108	CW = 119
108-021	I	1 T	0	1	1	0	0	1
108-022	I	0	0	1	1	0	0	1
108-023	O	0	0	1	2	0	1	2
108-024	I	$\underline{1}$	1	2	2	2	0	2
108-025	R	1	1	0	0	2	0	2
108-026	R	0	0	0	1	0	0	1
108-027	R	1	0	1	1	0	0	2
108-028	C	0	0	1	1	0	0	1
108-029	C	$\underline{1}$	0	0	0	2	0	1
108-030	C	1	0	1	1	0	0	2
107-031	I	1	1	2	2	0	0	2
107-032	C	1	0	1	1	0	0	2
107-033	I	1	1	0	0	0	0	1
107-034	I	$\underline{2}$	0	1	1	0	0	1
107-035	C	0	-	-	-	-	-	-
107-036	C	0	1	0	0	0	0	1
107-037	R	0	0	0	1	0	0	2
107-038	R	0	0	0	1	0	0	2
107-039	R	0 T	0	0	1	0	0	2
107-040	O	0 T	0	1	1	0	0	2

* Site category: C - commercial, R - residential, I - industrial, O - open.

† Power lines show number of lines present (one side or both sides of street): 1 - one side, 2 - both sides, underline of number - van directly under lines, T - nearby utility transmission line.

TABLE 6-2. COMPARISON OF SITE PARAMETERS WITH MEASURED RESULTS (CONTINUED)

SITE PARAMETERS			MEASURED RESULTS					
SITE NO.	SITE CAT.*	POWER LINE CAT.†	NOISE	CW = 80	CW = 90	CW = 100	CW = 108	CW = 119
110-041	R	0	0	2	1	0	2	2
110-042	C	1	0	2	1	0	2	2
110-043	O	0	-	-	-	-	-	-
110-044	R	1	0	1	0	0	2	1
110-045	C	1	0	1	2	0	2	1
110-046	I	1 T	1	2	2	2	2	2
110-047	C	2 T	1	2	2	1	2	2
110-048	I	1 T	0	2	2	0	2	2
110-049	I	0	0	2	2	0	2	2
110-050	R	1	0	1	2	0	1	2
104-051	R	1	1	0	0	0	0	1
104-052	C	1 T	0	0	0	0	0	1
104-053	O	0	0	0	0	0	0	2
104-054	R	1	0	0	0	0	0	1
104-055	R	0	1	0	1	0	0	1
104-056	C	1	0	0	0	0	0	1
CW or Noise 0			42	23	22	41	40	1
CW or Noise 2			12	20	22	5	3	23
CW 2			0	11	10	8	11	30

* Site category: C - commercial, R - residential, I - industrial, O - open.

† Power lines show number of lines present (one side or both sides of street): 1 - one side, 2 - both sides, underline of number - van directly under lines, T - nearby utility transmission line.

Impulsive noise was observed in the standard 3-axis views or in the additional 3-axis views at 12 out of the 54 sites. Ten of these 12 sites had nearby utility distribution lines as shown in the Gould site survey. The two sites that had impulsive noise conditions, but did not have a distribution line indicated in the Gould site categorization (sites 107-036 and 104-055) were close to a nearby distribution line that did not fit the Gould categorization. Thus, whenever impulsive noise was observed, a utility distribution line was nearby.

Seven distribution lines directly overhead the measurement vehicles did not emanate impulsive or other noise at levels sufficient to exceed the 3-axis threshold level setting ($\approx$ -100 dBm). In addition, fourteen distribution lines located across the street from the measurement vans did not emanate sufficient impulsive or other noise to exceed the threshold level of the 3-axis views.

CW signals were observed at many of the Phase II sites. A total of 13 of the 54 sites had CW signals at or very close to 100 kHz. The signal strength was less than 10 dB above the measurement system receiver noise level at five sites and equal to or greater than 10 dB above the receiver noise at eight sites.

At 90 kHz CW signals were observed at 32 of the 54 sites. Twenty-two of these cases resulted in signals less than 10 dB above the receiver noise, and ten cases gave signals equal to or exceeding 10 dB above the receiver noise.

At 80 kHz CW signals were found at 31 of the 54 sites. Twenty of these cases resulted in signals less than 10 dB above receiver noise, and eleven cases gave signal levels equal to or greater than 10 dB above receiver noise.

At 108 kHz CW signals were found at 14 of the 54 sites. Three of these cases resulted in signals less than 10 dB above the receiver noise level, and eleven gave signal levels equal to or greater than 10 dB above receiver noise.

The 119 kHz CW communications signal appeared at 53 of the 54 sites. Twenty-three cases gave signal levels less than 10 dB above receiver noise, while 30 cases gave signal levels equal to or greater than 10 dB above receiver noise.

A Loran-C receiver experienced CW RFI at 100 kHz at five sites and excessive CW RFI at eight sites. The impact of the CW signals at 80, 90, 108, and 118 kHz on Loran-C performance would depend upon the RF filter employed in the receiver and upon signal detection processes employed by each individual receiver. The significance of the CW signals at or beyond Loran-C band limits must be examined for each individual receiver.

While the sources of the CW signals were not specifically identified (except for traffic control and telephone line CW signals), the 80, 90, 100, and 108 kHz signals appeared at distinct sequences of sites. Also, strong CW signals tended to cluster at sequences of sites. These patterns are typical of near-field reception of power line carrier signals. Also, the 100 kHz CW signal was associated with the power carrier signal at 100 kHz which was identified in Sections 3 and 4.

6.3 SUPPLEMENTARY MEASUREMENTS

The supplementary measurements described in Section 3.3 must be considered when evaluating results of the fixed site measurements. The supplementary measurements show very strong spatial variations in both noise and CW signals as the measurement van moved over very short distances. Furthermore, the supplementary measurements show that all cases of impulsive noise and most CW signals emanate from nearby metallic devices (power lines, traffic control devices, telephone lines, etc.). Near-field radiation characteristics are evident from the data and from the observed physical relationships involved. The actual impulsive noise sources themselves may have been blocks or miles from the measurement site, but the radiation mechanism and coupling into the Loran-C whip antenna was primarily a near-field process.

6.4 NOISE AND CW SIGNAL MAPPING

Previous measurements of urban and suburban area radio noise suggested that impulsive noise and CW signals might be combined by some convenient method which could be used to generate noise/RFI contour maps for the portions of Los Angeles examined in the Phase I and Phase II measurements. However, the near-field properties of the noise and most CW signals resulted in small isolated areas of noise/RFI where large changes in level occurred over distances as small as 10 feet to 30 feet. These active areas were separated by low noise areas where conventional atmospheric noise levels were observed. Thus, any realistic noise mapping program would require the very fine scale mapping of a very large area where significant contours would often be spaced about 10 feet to 20 feet apart. The measurement task to support the mapping of noise and RFI for Los Angeles would be formidible. Obviously, the conventional contour mapping of noise and RFI is not recommended.

A more productive approach would be to better understand the near-field radiation models of each significant source and then ascertain the noise or CW activity associated with each possible source. Such data could be used as the basis for regionally-oriented fine scale contour maps.

Each relatively small area of high noise was usually associated with a single radiator of noise. Also, each area of high CW signal level (except for the 119 kHz communications signal) appeared to be associated with a single radiator or a very few radiators. Noise or CW signals from multiple sources were only rarely identified. Thus, the conventional techniques of composite mapping of various kinds of noise from multiple sources could not be used to describe the noise and RFI environment encountered by vehicular Loran-C receivers operated in Los Angeles.

Noise and CW signals were generally lower in level in the main downtown area of Los Angeles than in the urban and suburban areas surrounding downtown. The low levels of downtown noise and CW signals were associated with the lack of overhead utility distribution lines (most downtown power distribution was underground), the absence of utility transmission lines, and the attenuation of all signals near 100 kHz when near multistory structures.

Sufficient measurements were taken at and around site 109-018 (Watson Center/Wilmington) to establish approximate fine scale contours of peak impulsive noise levels for the immediate area. Figure 28 shows the main physical features of the site including the location of a nearby utility distribution line which radiated significant impulsive noise. The distribution line ended about 100 feet from the 109-018 site. Ten dB contours of noise (see Figures 5-13, 5-14, 5-15, and A-29 for noise detail) are superimposed on the physical map. The contours of peak impulsive noise level show very low noise levels at site 109-018 itself and high noise levels when closer to the distribution line. The noise level decreased somewhat with distance along the distribution line along Watson Center, causing the contours to pinch inward near the top of the area shown. The distance scale on the map shows the relatively small area with significant levels of impulsive noise. A vehicle with a Loran-C receiver turning off Wilmington onto Watson Center would abruptly encounter impulsive noise shortly after the turn. The noise would gradually decrease in level as the vehicle proceeded along Watson Center.

The noise contours in Figure 6-1 show the relationship between the impulsive noise encountered by a Loran-C receiver installed in a vehicle and the noise radiator (a 13.6 KV distribution line). Similar contour maps can be established for all other noise and CW signals found in the Phase I and Phase II effort with a few additional measurements and a description of the physical properties of the noise radiator.

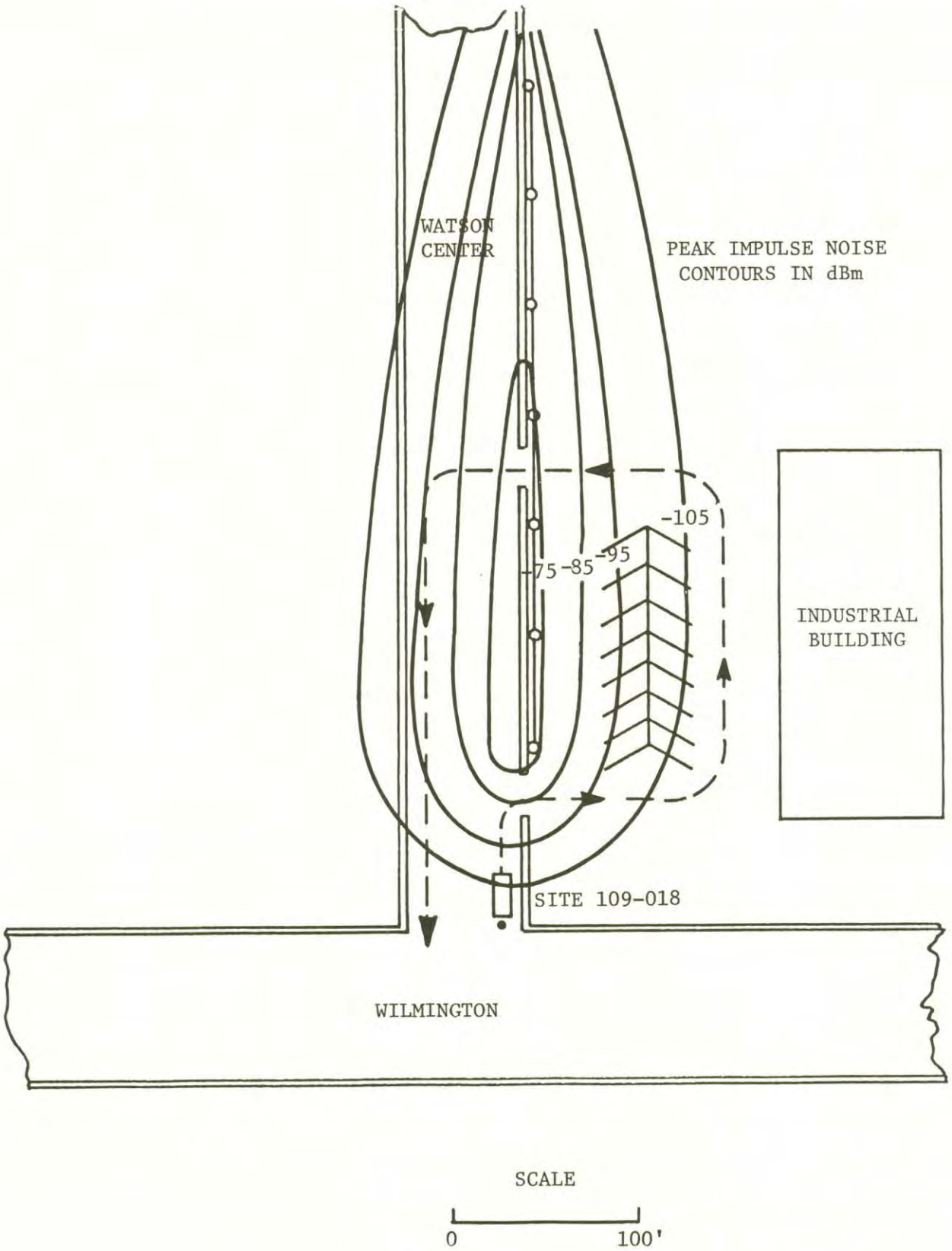

FIGURE 6-1. PHYSICAL LAYOUT OF SITE 109-018

6.5 NOISE DESCRIPTORS AND OTHER MEASUREMENTS

A number of descriptors of radio noise have appeared in the literature including peak, quasi-peak, rms, and average values, as well as various distributions of amplitudes, zero crossing rates, intervals, and widths. Hagn has reviewed and summarized the various definitions and fundamental parameters of noise and RFI (4). The government has recommended that noise power be used as the basic noise parameter (5); however, other additional measurements of noise are acknowledged as necessary for specific analysis tasks. The most widely used reference for received noise levels is the CCIR Report 322 (6), which is based upon noise power. Spaulding and his associates have published convenient noise definitions which are consistent with CCIR and government recommendations (7-9), and they have presented a number of excellent measurements of noise affecting various communications systems. A recent book by Skomal (10) summarizes much of the available information and data on man-made noise. Feldman has presented data on radio noise levels in a study specifically directed toward the rural area noise environment encountered by low frequency navigation systems such as Loran-C (11).

Most of the above referenced descriptors and definitions of radio noise can be related to the 3-axis views presented in this report, and the basic information to obtain noise values in accordance with the various descriptors is contained in the digital data stream which forms the views. These digital data are available at the digital interface on the EMTEL display. Also, the 3-axis views can be hand-scaled to derive sufficient information for approximate values of peak noise, noise power, interval times, and other factors.

The author prefers to relate the 3-axis views to the terminology and definitions used by Spaulding (9) and many others, where mean noise power is:

$$p_n = f_a(k\,T_o\,b)$$

where p_n = mean noise power in watts

f_a = effective antenna noise factor

k = Boltzman's constant τ $1.38 \cdot 10^{-23}$ Joules/°K

T_o = reference temperature (288°K)

b = receiver noise power bandwidth in Hz

T_a = effective antenna temperature in the presence of external noise.

The above expression for p_n can be reduced to:

$$P_n = F_a + B - 204 \quad \text{dBw}$$

which is the power available from the terminals of an equivalent lossless antenna where

P_n = available noise power in dBw

F_a = 10 log f_a, the effective antenna noise figure

B = 10 log b.

The corresponding rms field strength measured by the 108 inch whip antenna (length << λ) is given by:

$$E_n = F_a + 20 \log f + B - 95.5 \quad \text{dB}(1\mu\text{V/m})$$

where E_n = rms field strength for the bandwidth b

f = frequency in MHz

B = 10 log b.

The amplitude scales for the 3-axis views in this report can be recalibrated in terms of either P_n or E_n from the above relationships and from data contained the the two-line code on each 3-axis view.

The dB difference between average noise voltage and rms noise voltage, called V_d, is a convenient indicator of the degree of impulsiveness where:

$$V_d = -20 \log \frac{V_{av}}{V_{rms}} .$$

An excellent indicator of the amplitude properties of a given sample of noise is the amplitude probability distribution (APD), which is the fraction of total time, T, for which the noise envelope is above level V_i.

$$APD = Prob[V \geq V_i] = 1 - P(V).$$

The 3-axis views shown in this report also permit the viewer to very rapidly scale impulse intervals due to the unique time synchronization of most impulses to the power line frequency. Distributions of pulse spacing intervals can be simply established for most cases in that only a few sub-multiples of 16.6 ms are involved in the impulse spacings.

Data on the mean power level of noise at and near 100 kHz are given by CCIR (6) and Feldman (11). These sources and all other available published sources indicate that atmospheric radio noise should be the predominant noise limiting the performance of Loran-C receivers. However, the measurements described in this report showed that man-made radio noise was the predominant noise limiting the performance of Loran-C

receivers installed in vehicles and operated in the Los Angeles area. The sources of data for CCIR Report 322 and Feldman were from isolated and remote radio noise measurement sites which did not include the near-field coupling to noise and CW sources found to be of major concern in the Los Angeles area. Loran-C systems designed for use in city areas must take into account the properties of the noise environment of the urban and suburban area.

7. CONCLUSIONS

The measurements of man-made noise and RFI in the urban and suburban areas of Los Angeles provided data useful in assessing the performance of Loran-C receivers operated in and around the region. Vehicular Loran-C receivers moving along the streets and highways of Los Angeles would be subjected to a wide variety of radio environments. At times low natural noise levels would result in excellent Loran-C receiver performance. The extremely rapid transition from low level natural noise conditions to very high levels of impulsive noise, or very high levels of CW RFI, or combinations of the two states, must be carefully considered by the designers of vehiclular Loran-C receivers.

Early in the measuerment program the possibility of the construction of noise maps showing portions of Los Angeles containing high noise levels was discussed among the measurement participants. The data show that any effective contour mapping of noise levels must be based upon contour intervals of a few tens of feet rather than the larger intervals implied by other available noise maps. Obviously, a realistic contour map of noise cannot be generated for the Los Angeles area with conventional radio noise measurement and mapping techniques.

The very rapid amplitude change with distance for radio noise associated with utility power lines suggests that cities confining most overhead distribution lines to alleys in mid-block would have lower street noise levels than cities with overhead distribution lines running along street edges. Underground power lines would also result in low street radio noise levels. Of special interest was the general observation that radio noise levels in the downtown area of Los Angeles (where power lines were largely underground) were generally much lower than in the area surrounding downtown. This null in noise level in the center of the large urban area of Los Angeles was not consistent with the generalized urban area noise model of Skomal (12 which gave a maximum for noise levels in the center of the urban area. Skomal's model also suggests that urban and suburban area radio noise can be adequately described with conventional contour maps. This is not consistent with the "hot-spot" areas of man-made noise found in Los Angeles.

The inductive or near-field coupling between most noise and RFI radiators and a vehicular Loran-C antenna was obvious, once encountered. This aspect of a noise source-to-sink model has not been emphasized in the recent literature on man-made radio noise, but it was of primary importance in understanding the noise environment encountered by vehicular Loran-C receivers.

The various primary sources of RFI (traffic control sensors, unshielded overhead telephone lines, and power line carrier communications) also coupled into the vehicular Loran-C antenna with inductive or near-field modes. Very low power and physically small sources produced very large input signals into the antenna whenever the measurement van was physically close to a source.

A single noise or RFI source was often the major contributor to the undesired radio environment. At most only a few sources were involved at any specific measurement location. Complex mixtures of noise and RFI from a large number of sources were not found. This suggests that a program to rapidly locate and identify each primary source of noise and RFI would be technically feasible. However, the next obvious step, noise and RFI suppression at each source would involve complex issues of radio spectrum management, adequacy of incidental radiation rules, inductive or near-field radiation considerations in noise and RFI models, cost of control measures versus cost of benefits, and other related factors.

APPENDIX A

3-AXIS VIEWS FOR FIXED SITES

LIST OF 3-AXIS VIEWS

LIST OF 3-AXIS VIEWS (Continued)

LIST OF 3-AXIS VIEWS (Continued)

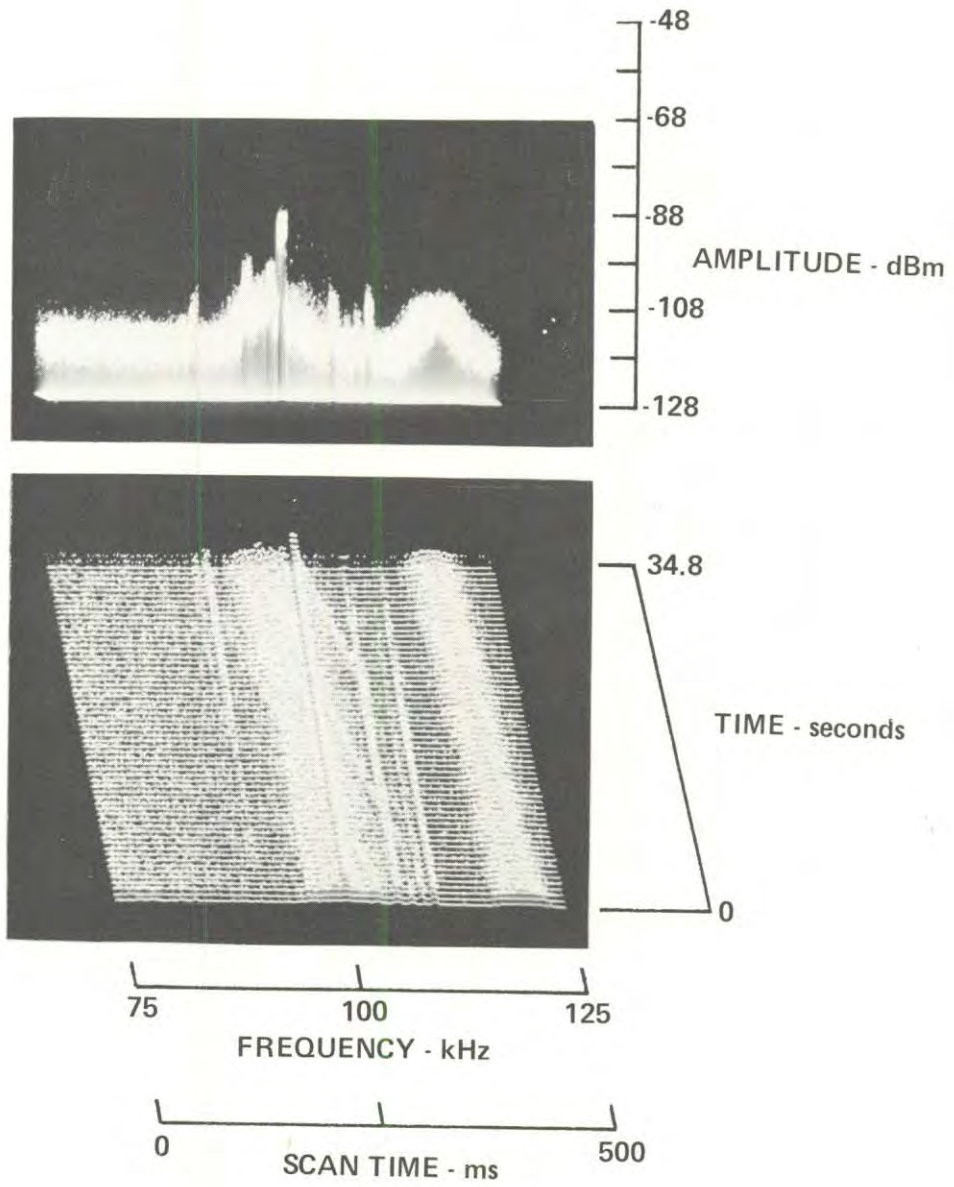

1-22-79, 0831, 106-001
HP140, Whip, F100, W50, IF3, ST 500, A -30/0/+18/BPF

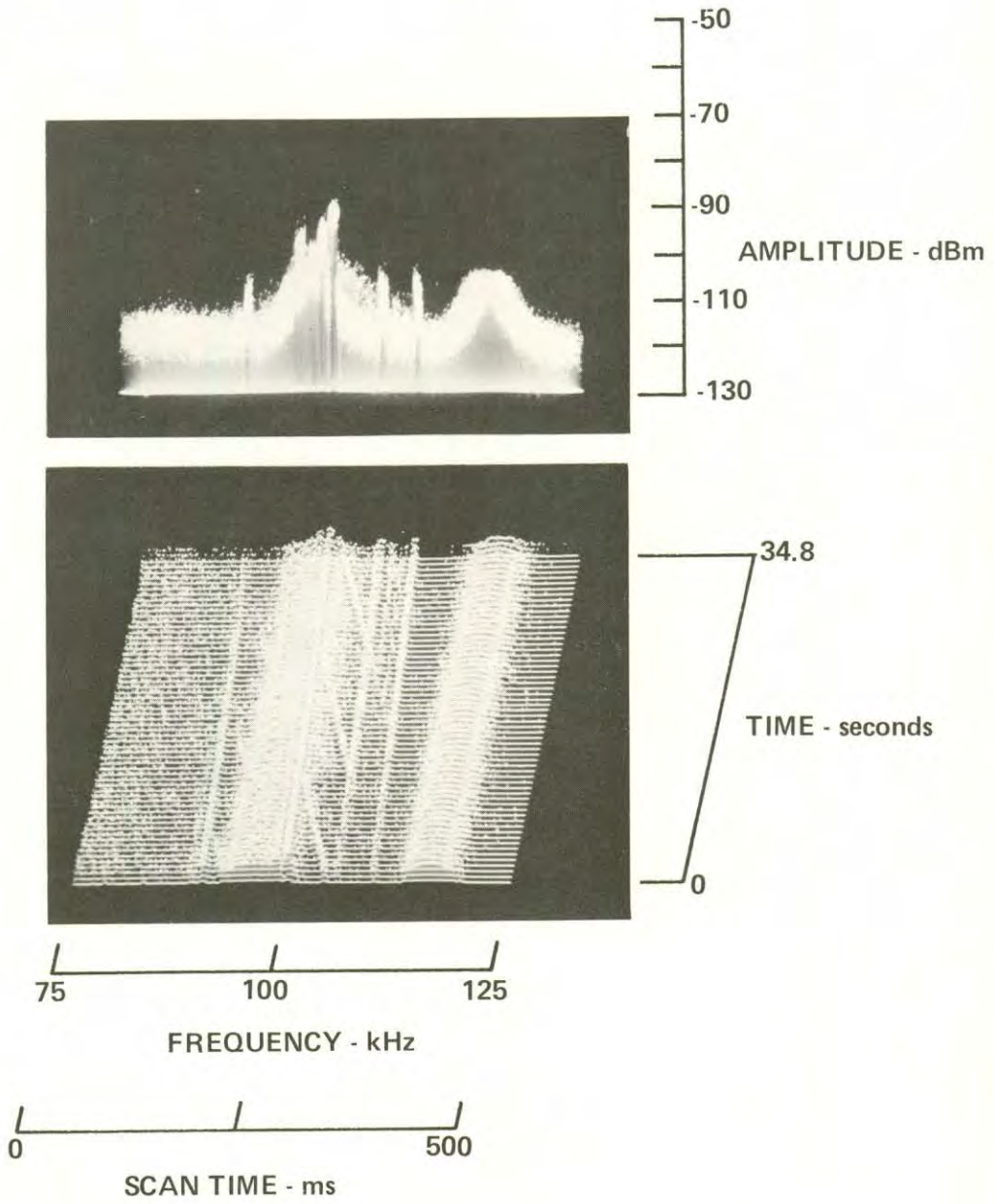

1-22-79, 0845, 106-002
HP140, Whip, F100, W50, IF3, ST 500,A -32/0/+18/BPF

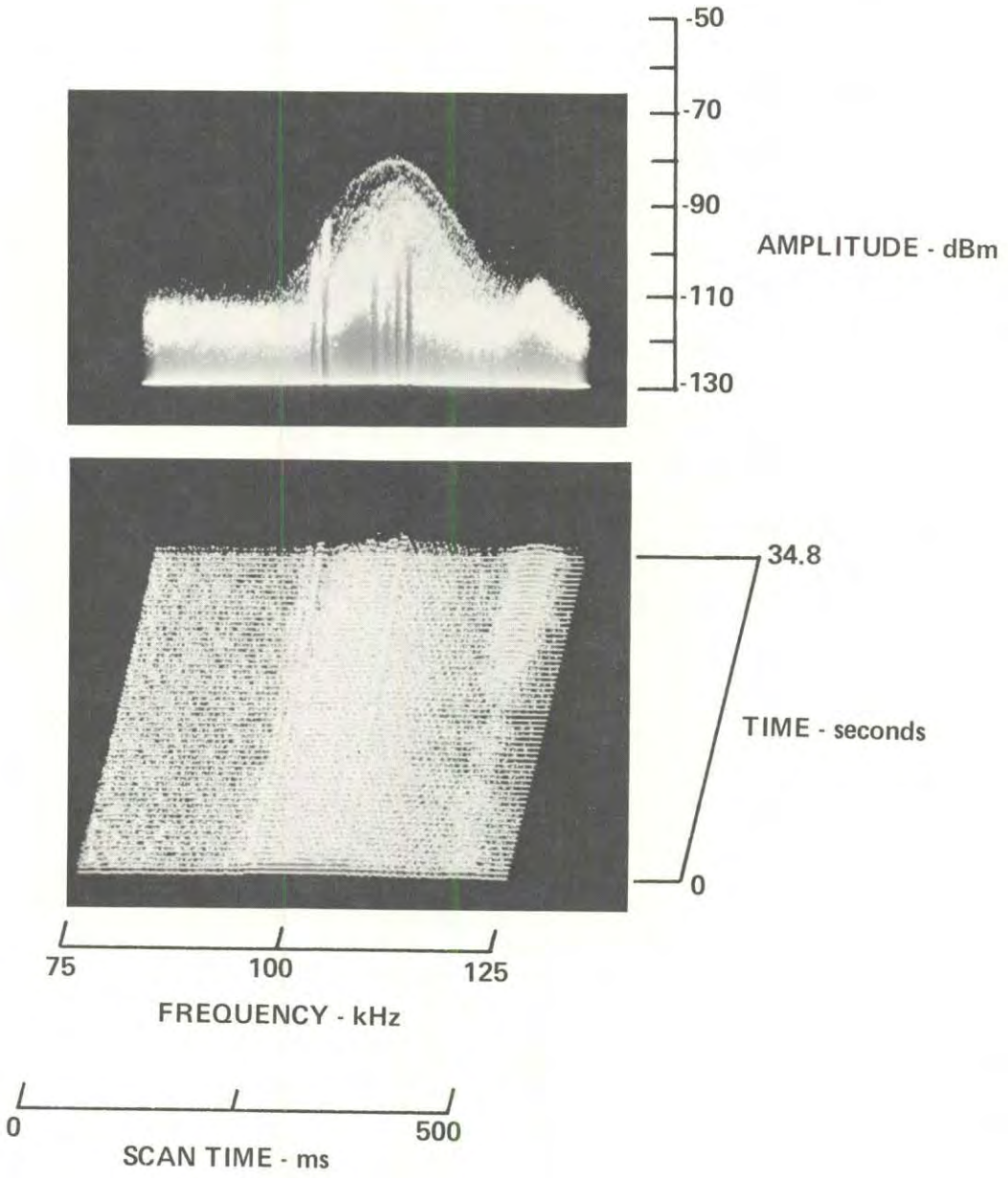

1-22-79, 0905, 106-003 (under 12 kV line)
HP140, Whip, F100, W50, IF3, ST 500, A -32/0/+18/BPF

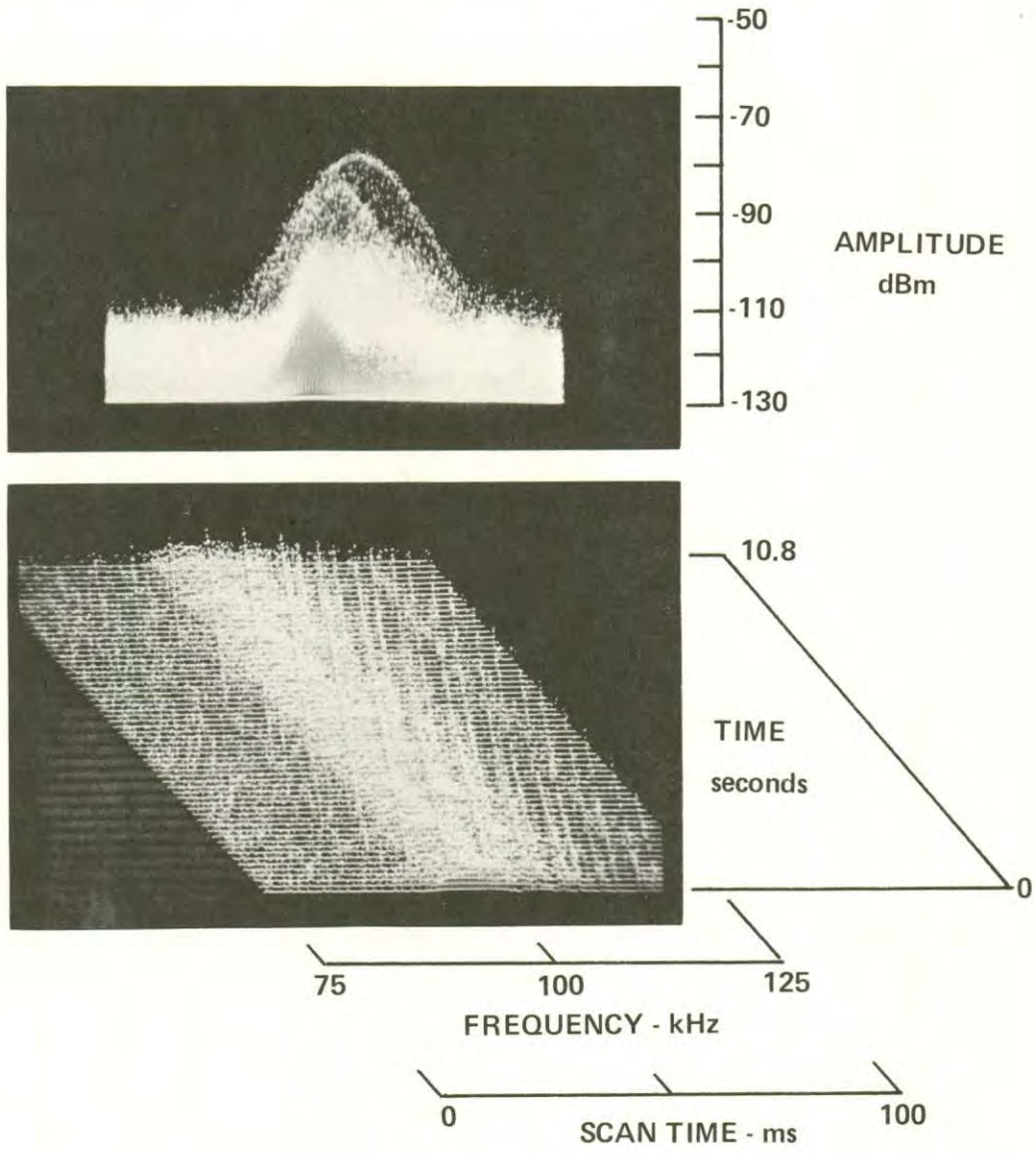

1-22-79, 0928, 106-003 (under 12 kV line)
HP140, Whip, F100, W50, IF3, ST 100, A -32/0/+18/BPF

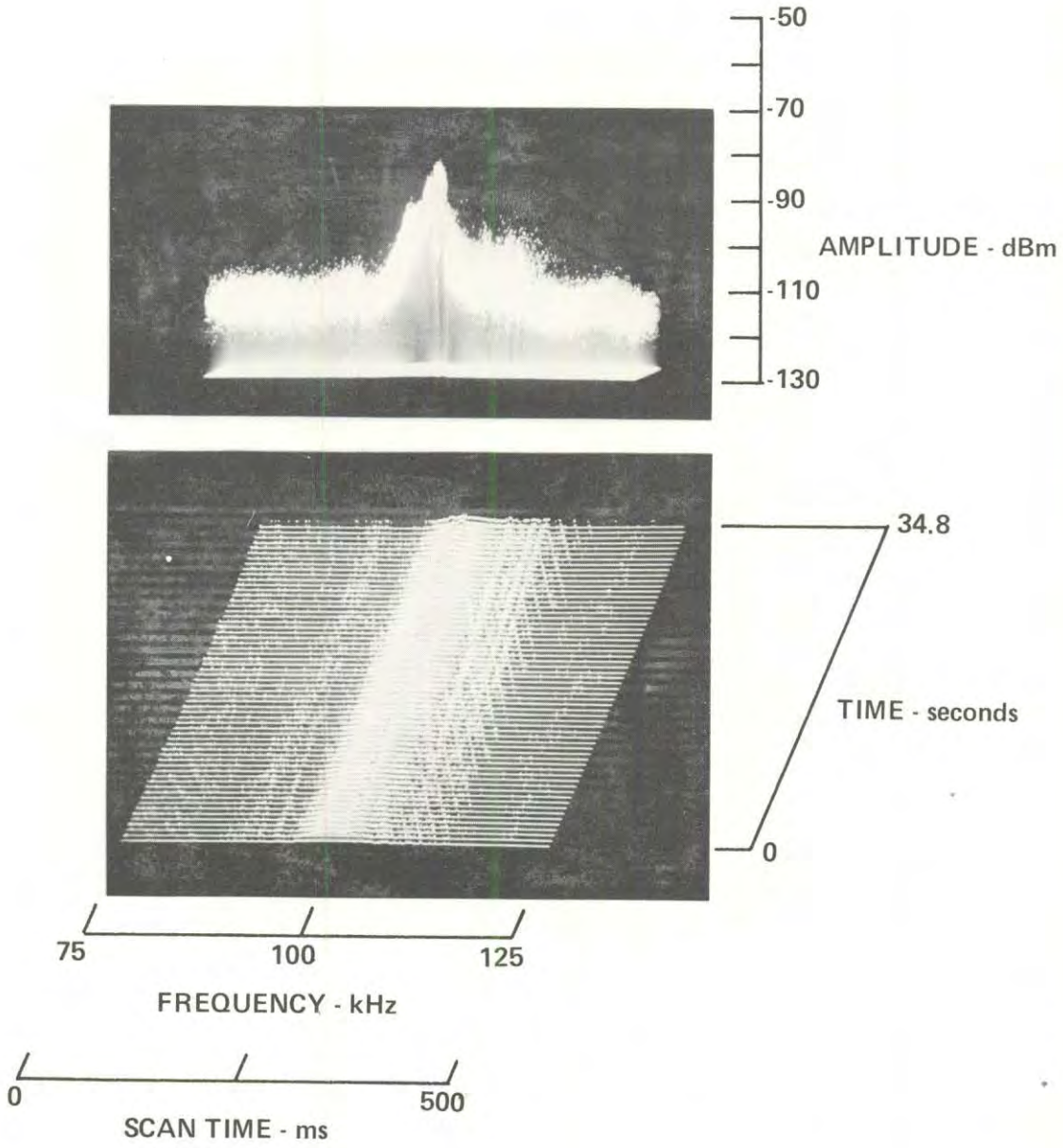

1-22-79, 0946, 106-004
HP140, Whip, F100, W50, IF3, ST 500, A -32/0/+18/BPF

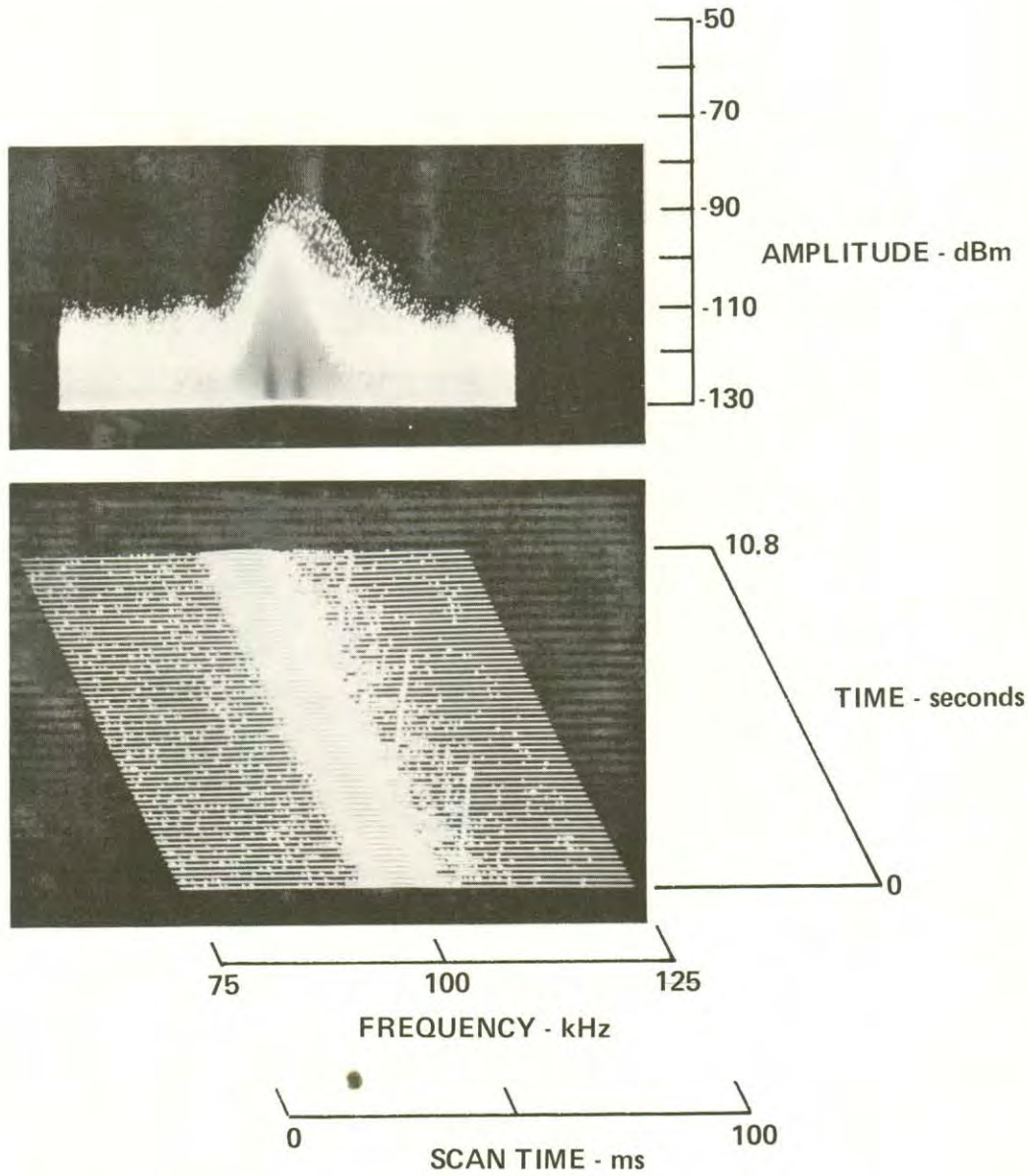

1-22-79, 0948, 106-004
HP140, Whip, F100, W50, IF3, ST 100, A -32/0/+18/BPF

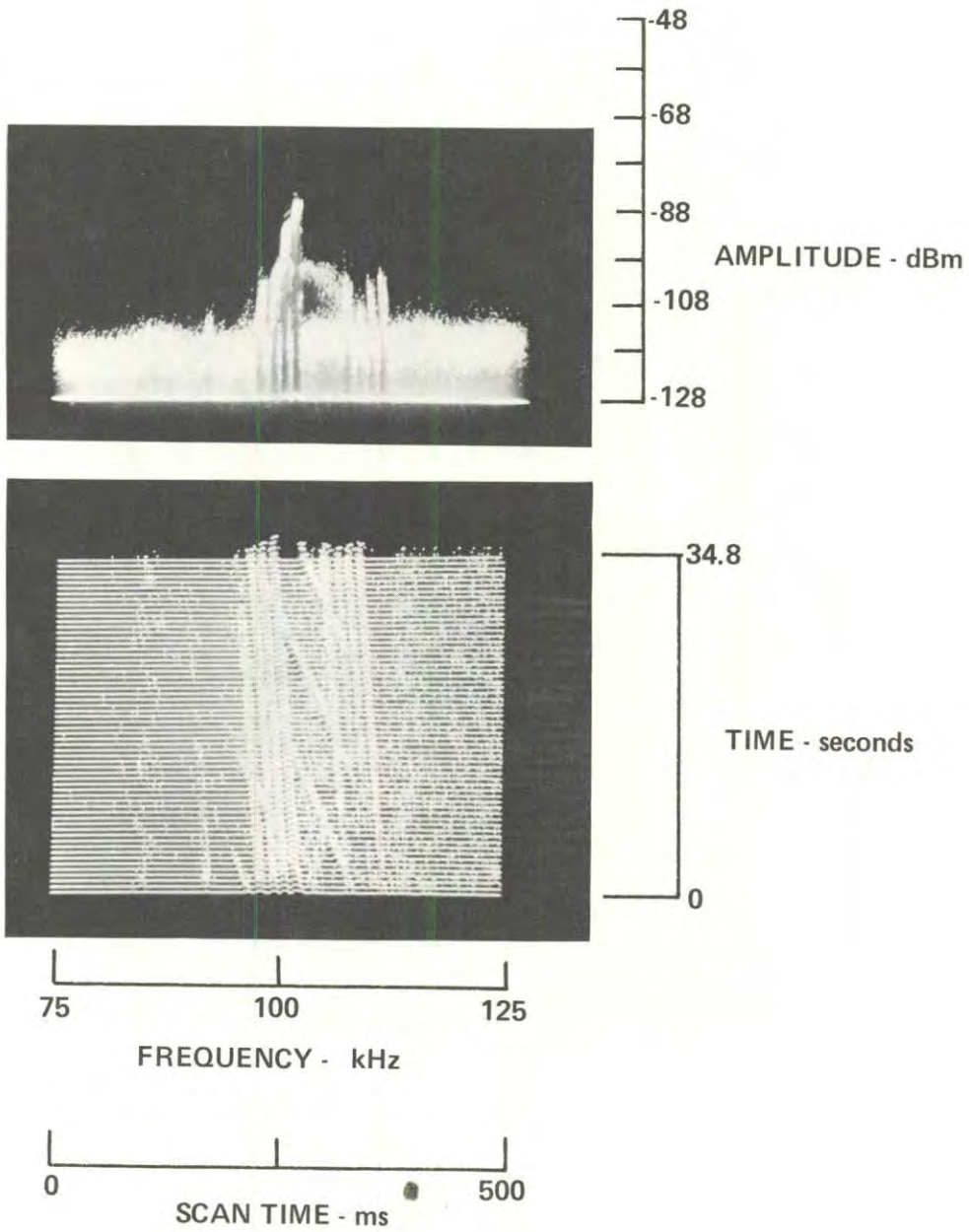

1-22-78, 1017, 106-005
HP140, Whip, F100, W50, IF3, ST 500, A -30/0/+18/BPF

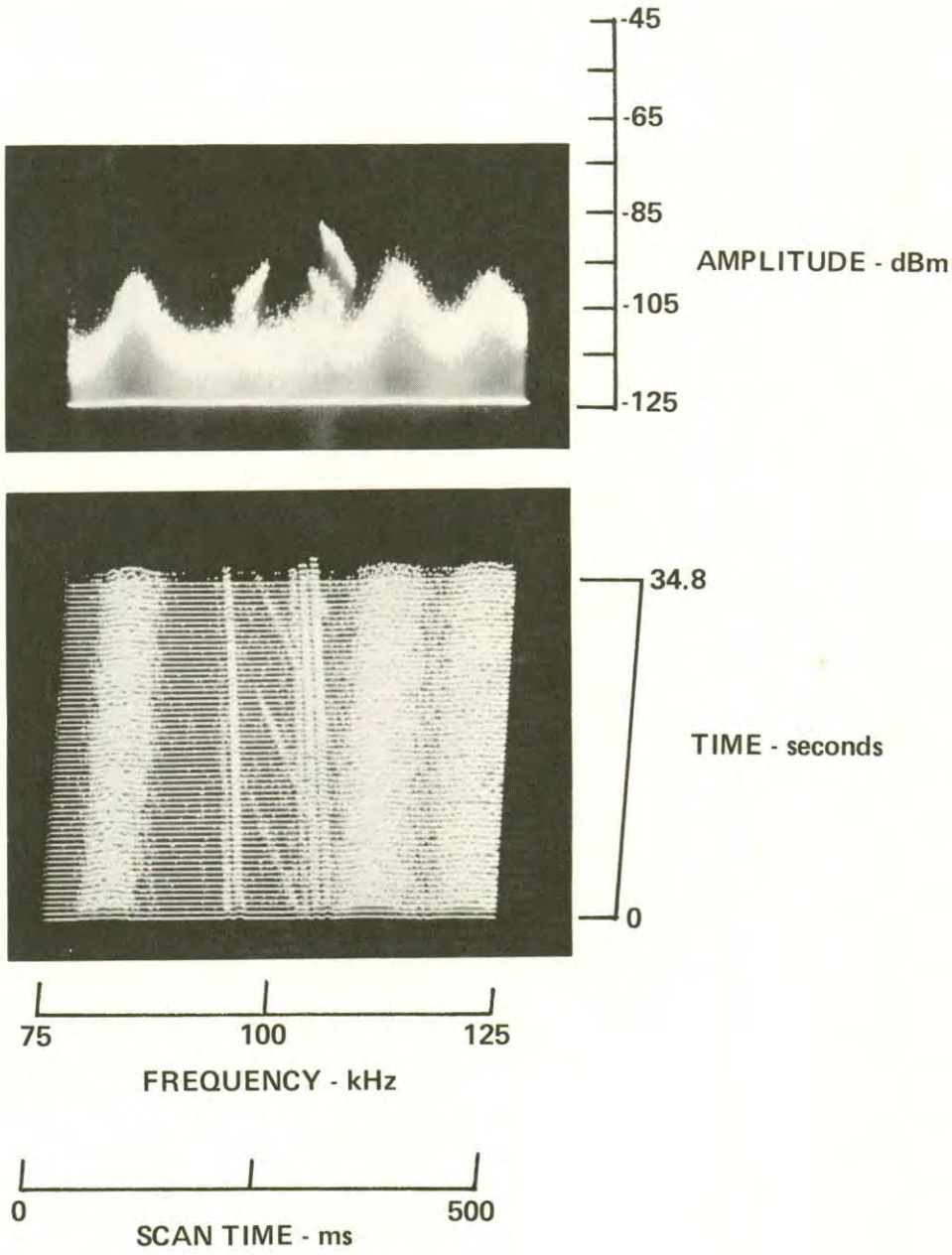

1-22-79, 1334, 106-006
HP140, Whip, F100, W50, IF3, ST 500, A -30/0/+15/NF

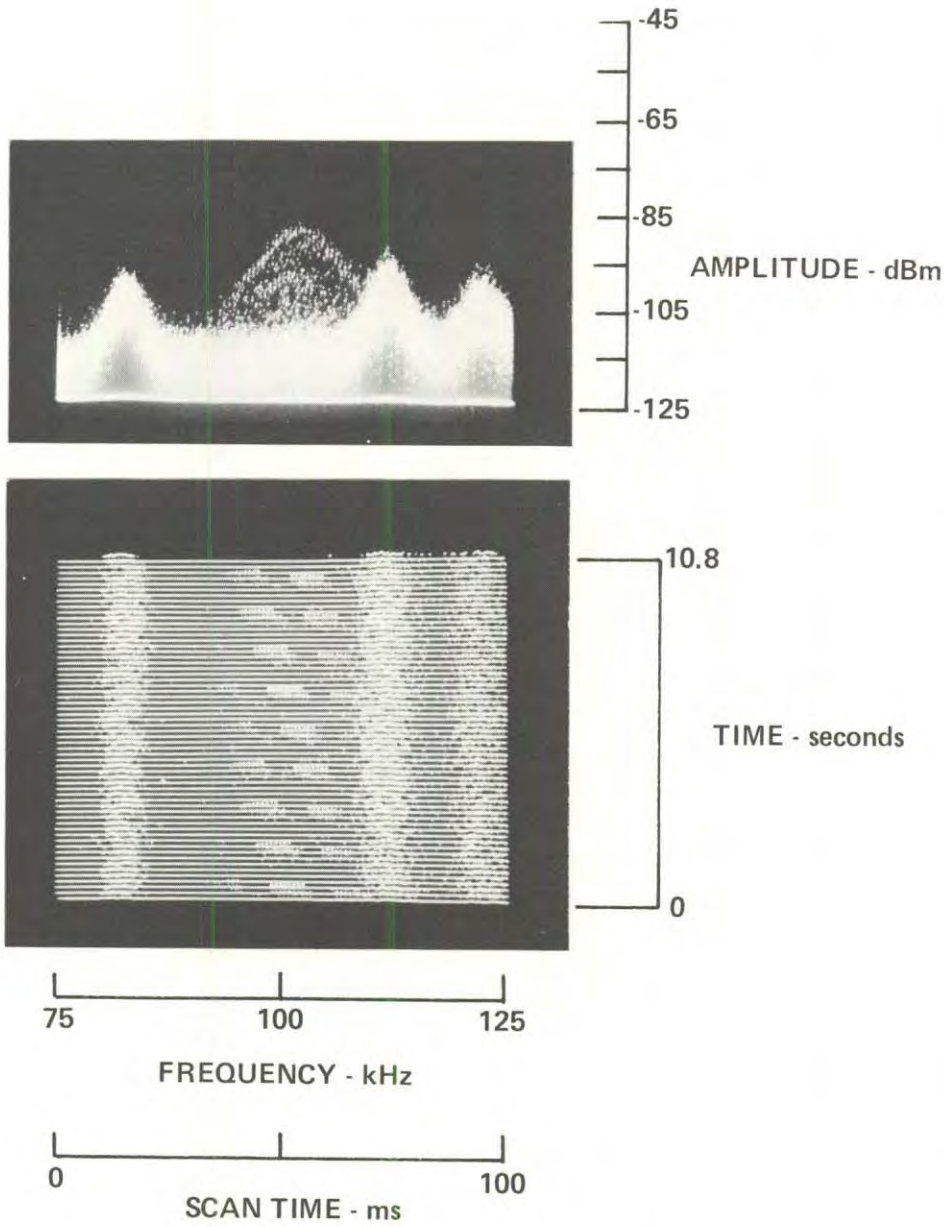

1-22-79, 1036, 106-006
HP140, Whip, F100, W50, IF3, ST 100, A -30/0/+15/NF

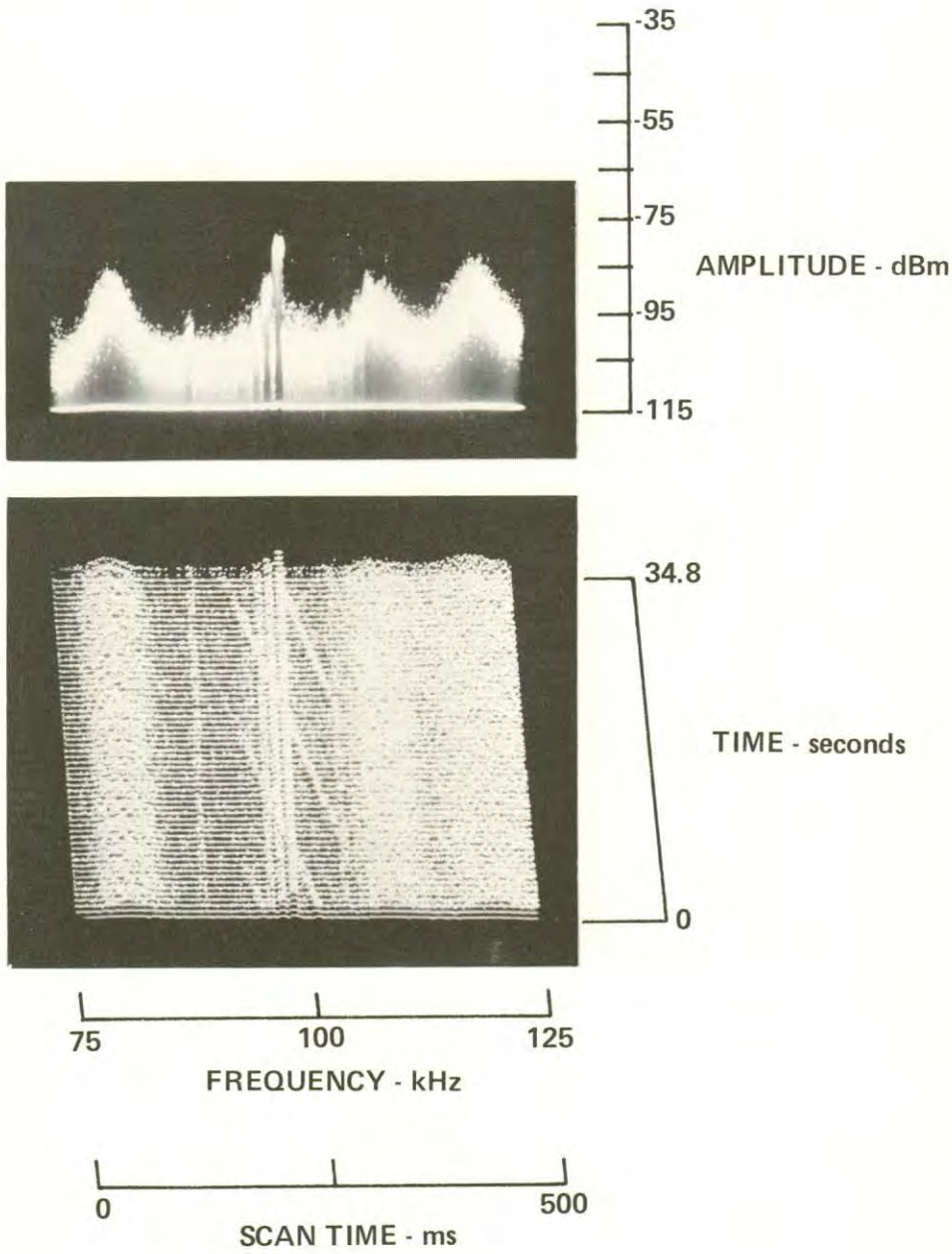

1-22-79, 1131, 106-007
HP140, Whip, F100, W50, IF3, ST 500, A -20/0/+15/NF

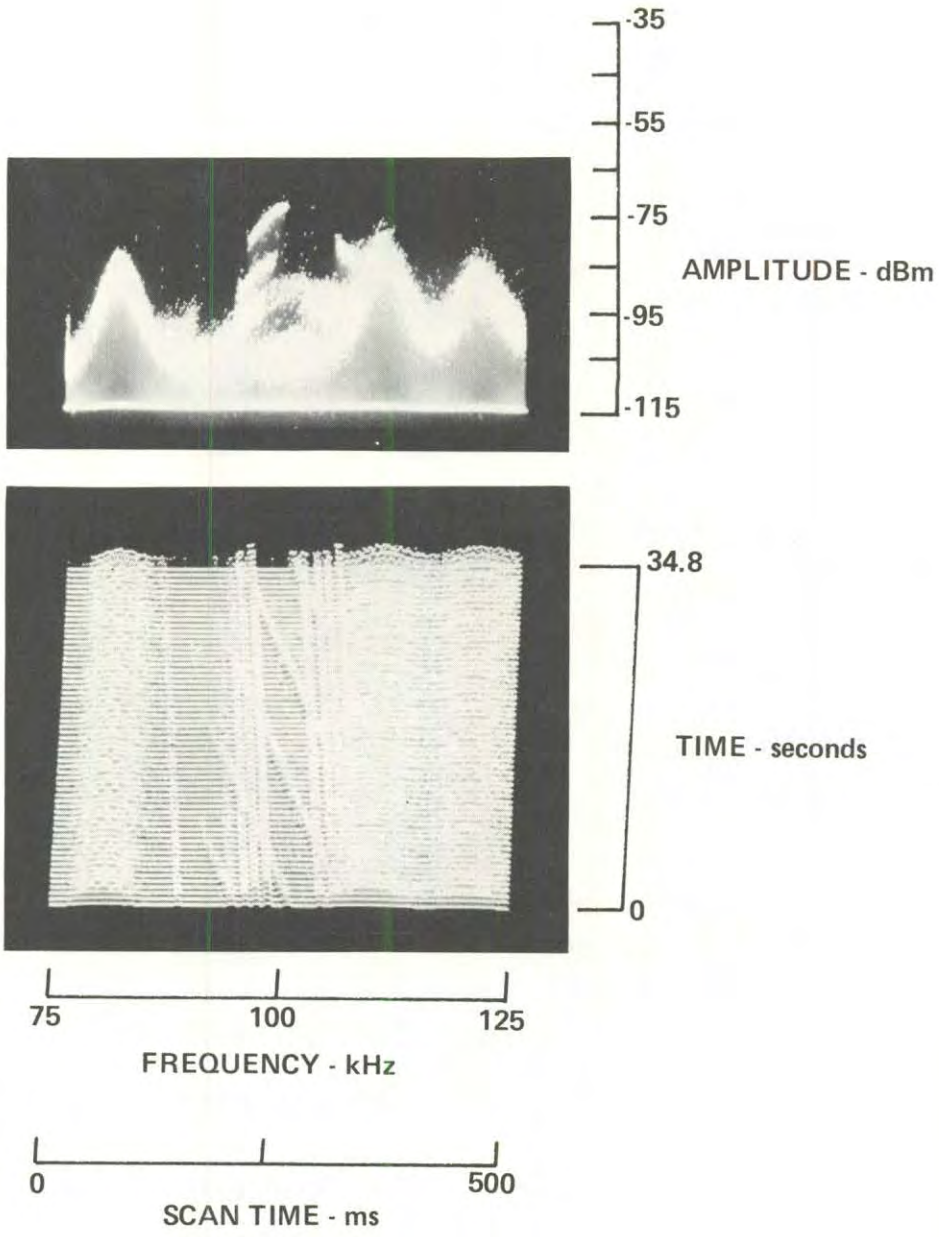

1-22-79, 1142, 106-008
HP140, Whip, F100, W50, IF3, ST 500, A -20/0/+15/NF

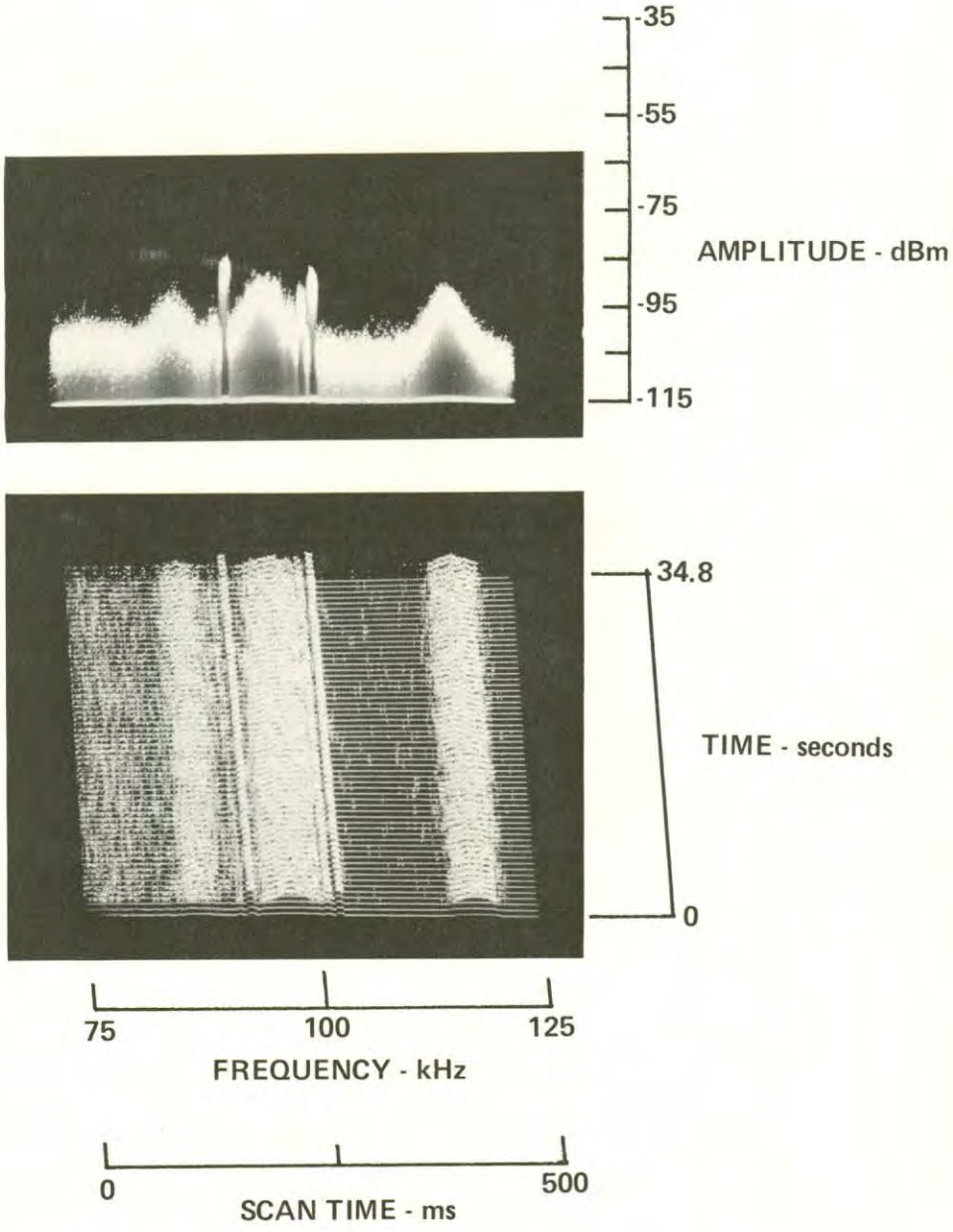

1-22-79, 1159, 106-009
HP140, Whip, F100, W50, IF3, ST 500, A -20/0/+15/NF

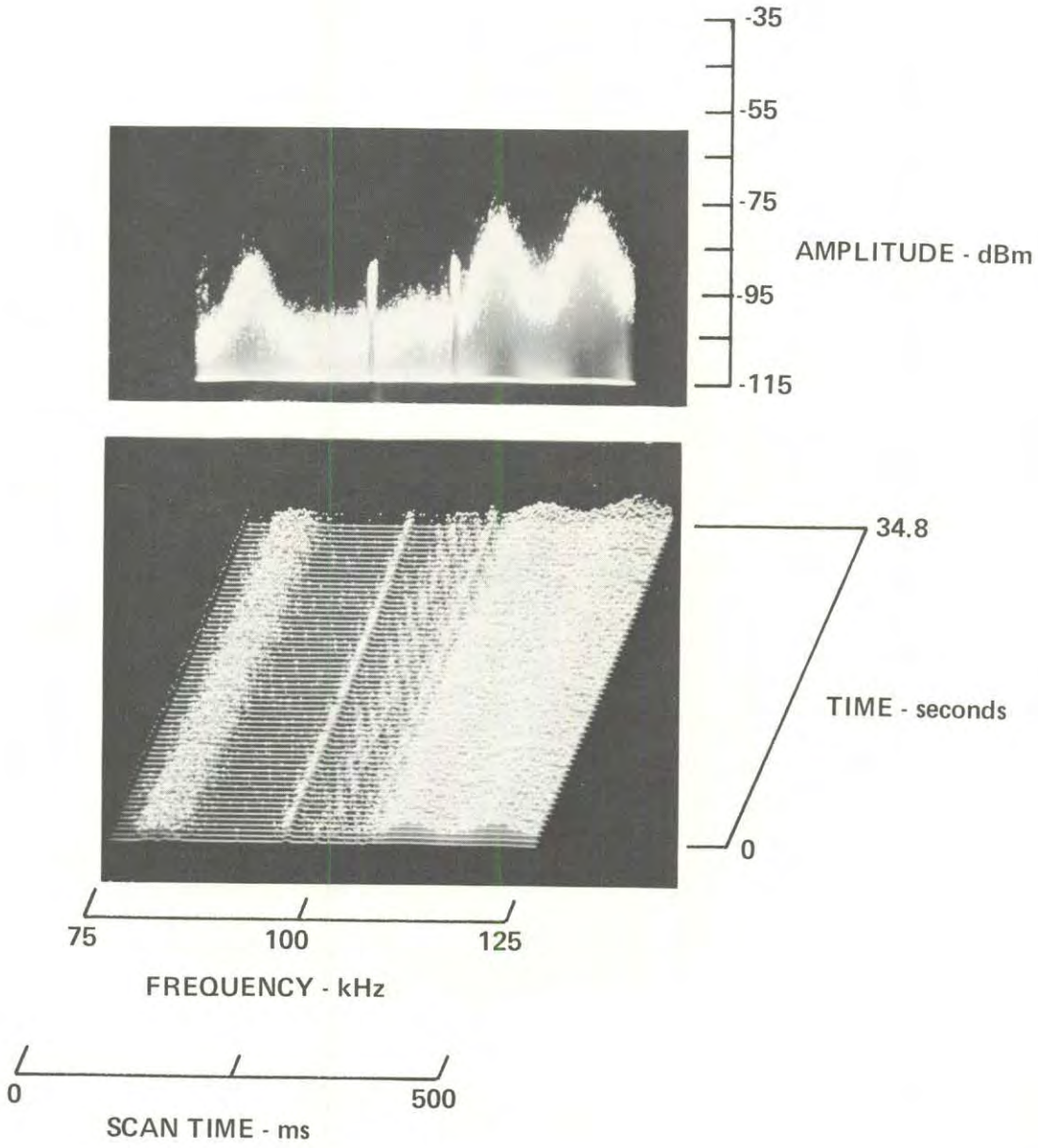

1-22-79, 1222, 106-010
HP140, Whip, F100, W50, IF3, ST 500, A -20/0/+15/NF

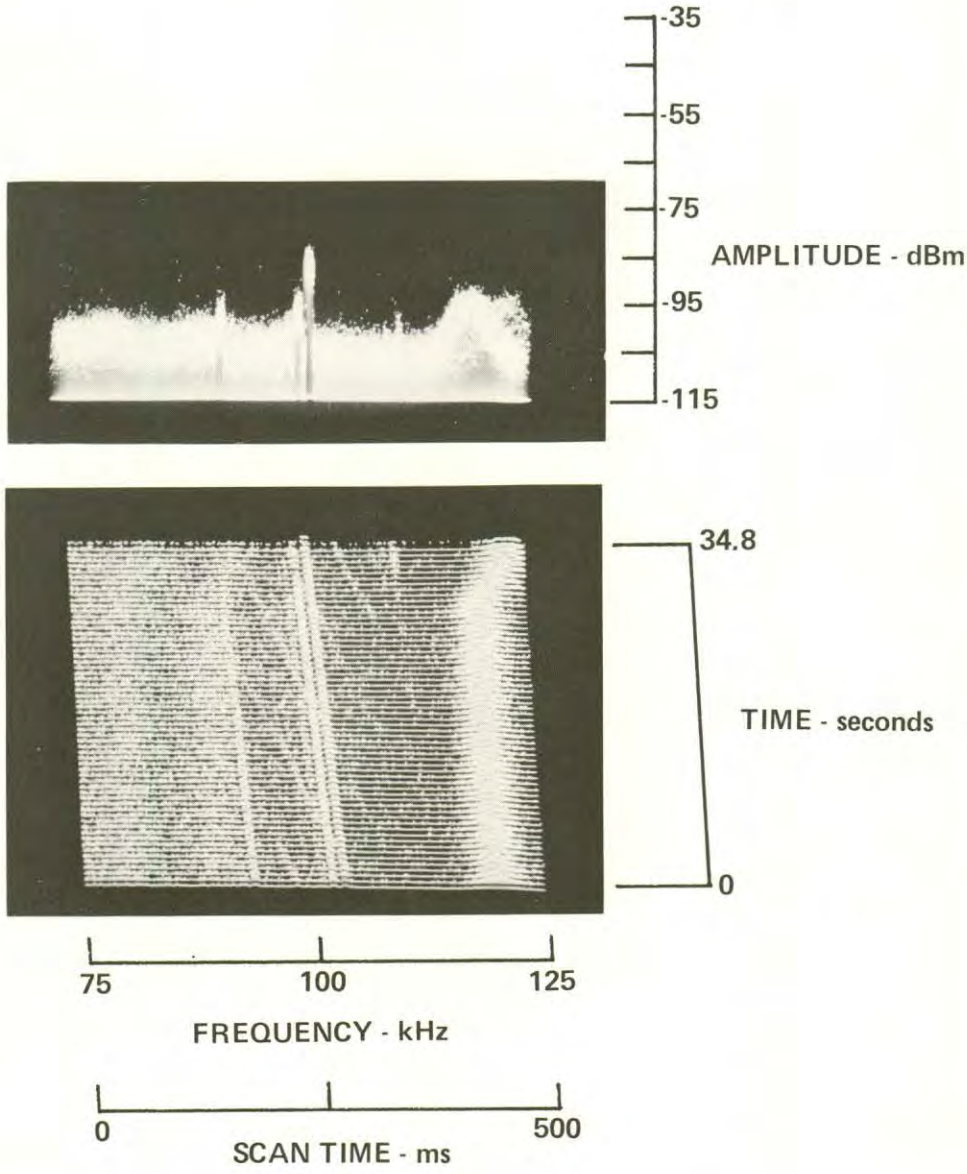

1-22-79, 1251, 109-011
HP140, Whip, F100, W50, IF3, ST 500, A -20/0/+15/NF

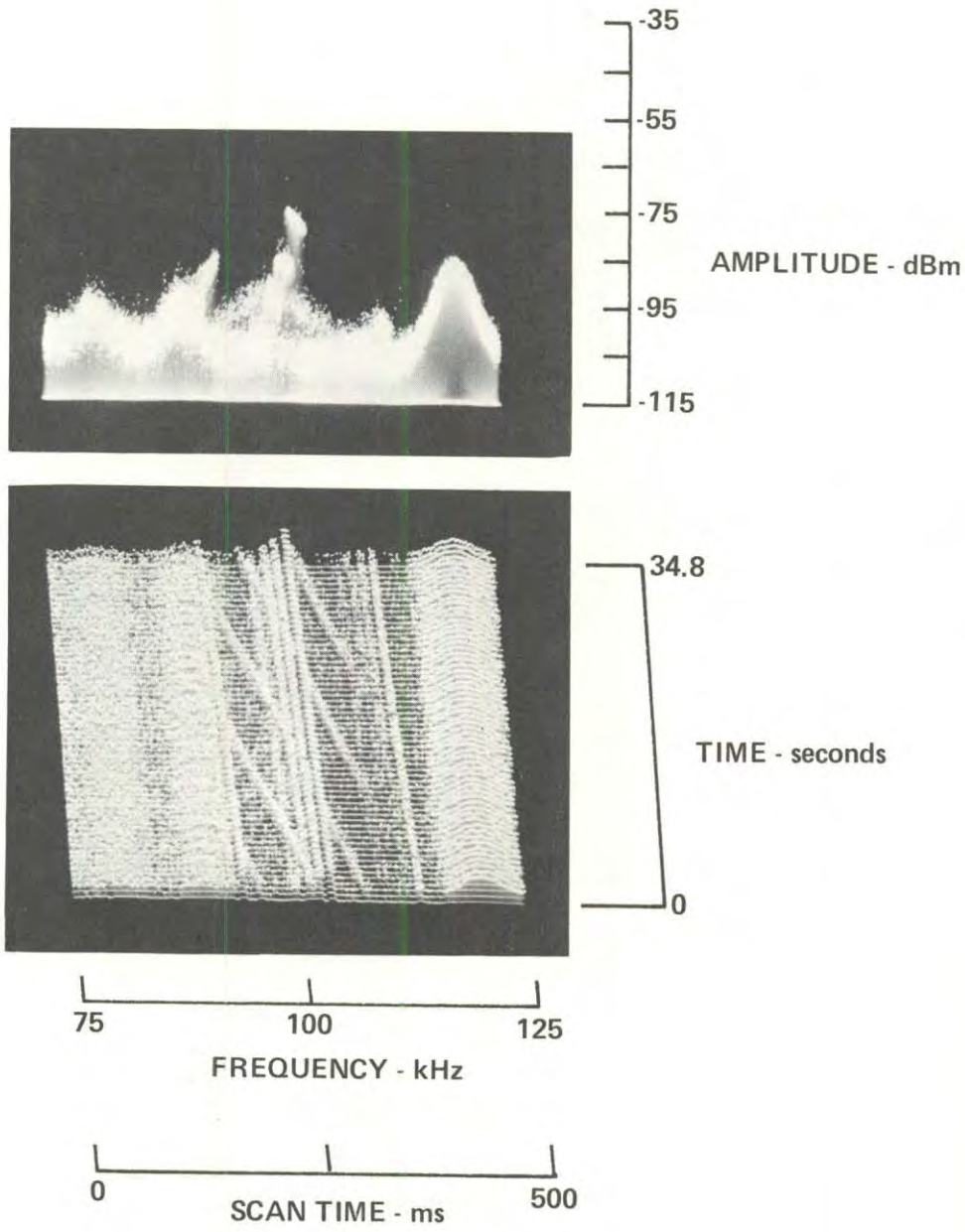

1-22-79, 1304, 109-012
HP140, Whip, F100, W50, IF3, ST 500, A -20/0/+15/NF

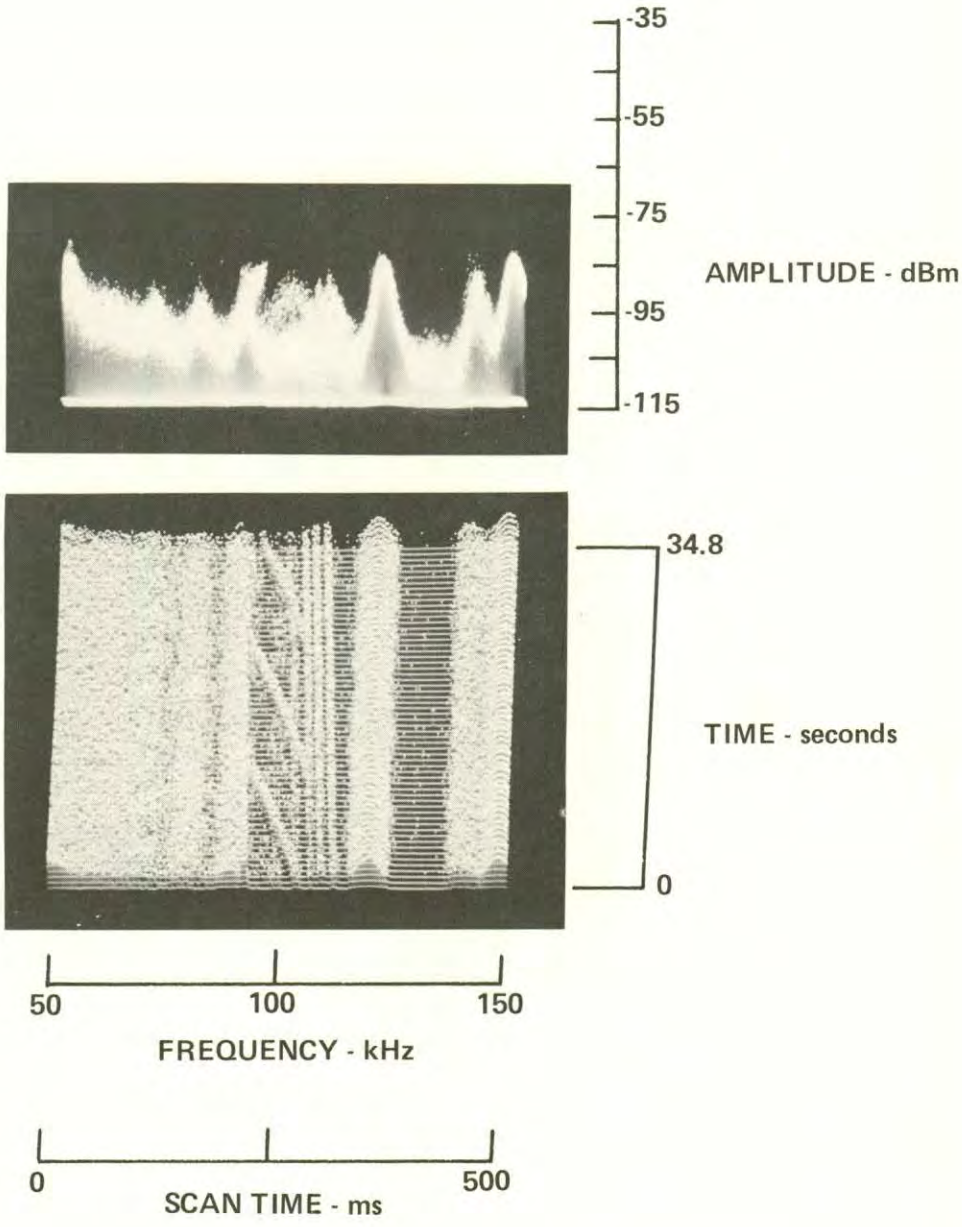

1-22-79, 1307, 109-012
HP140, Whip, F100, W100, IF3, ST 500, A -20/0/+15

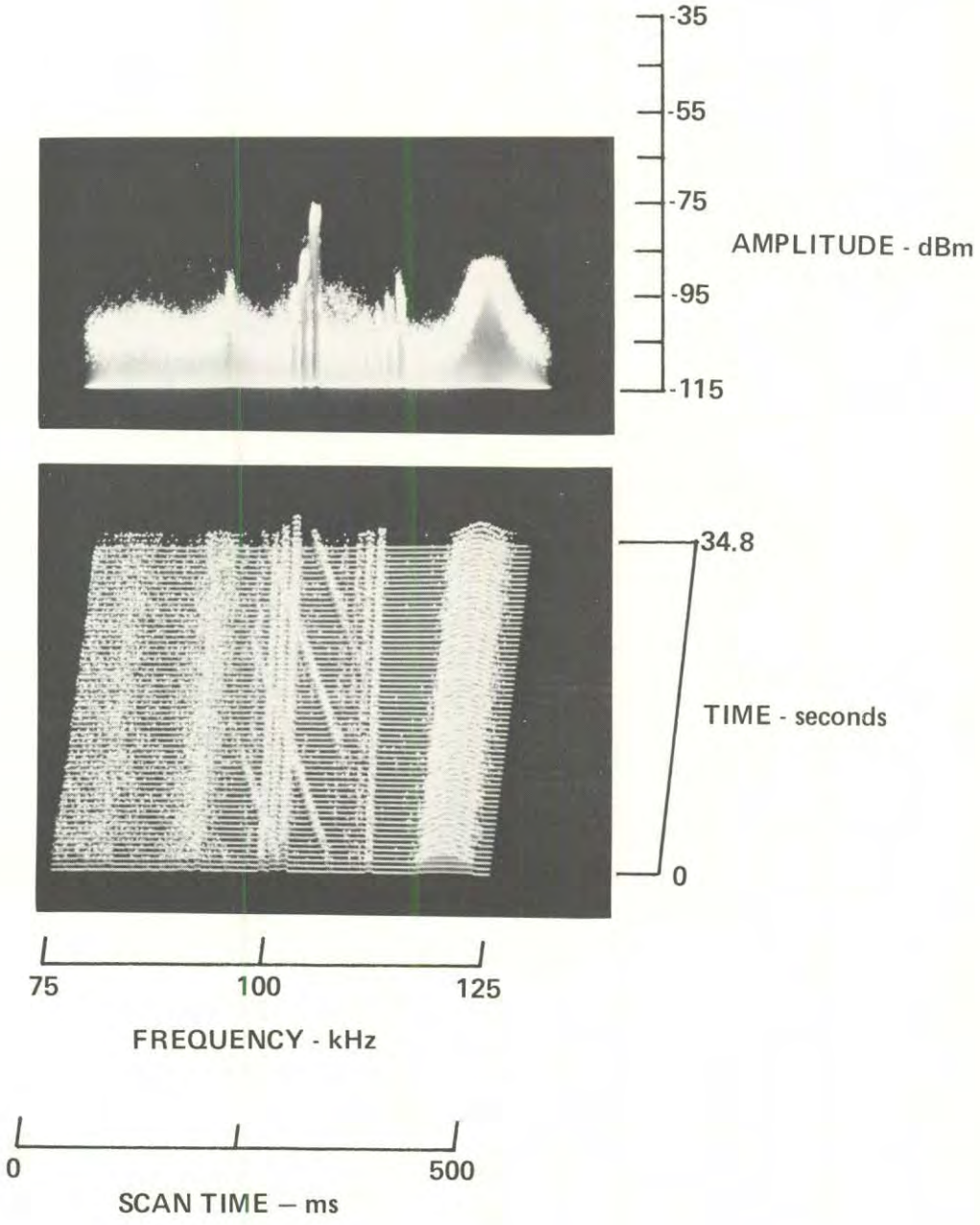

1-22-79, 1320, 109-013
HP 140, Whip, F100, W50, IF3, ST500, A -20/0/+15/NF

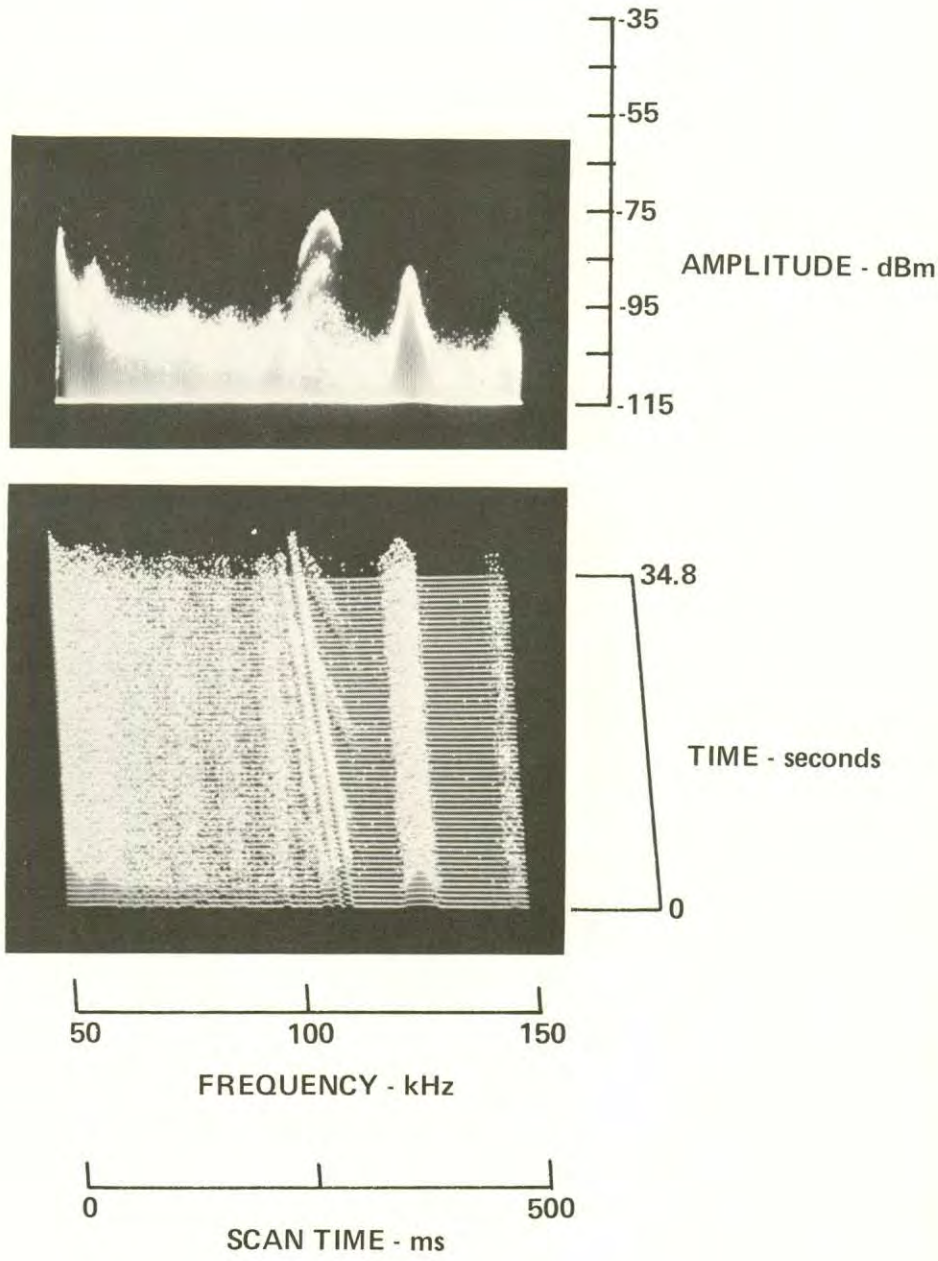

1-22-79, 1327, 109-013
HP140, Whip, F100, W100, IF3, ST 500, A -20/0/+15/NF

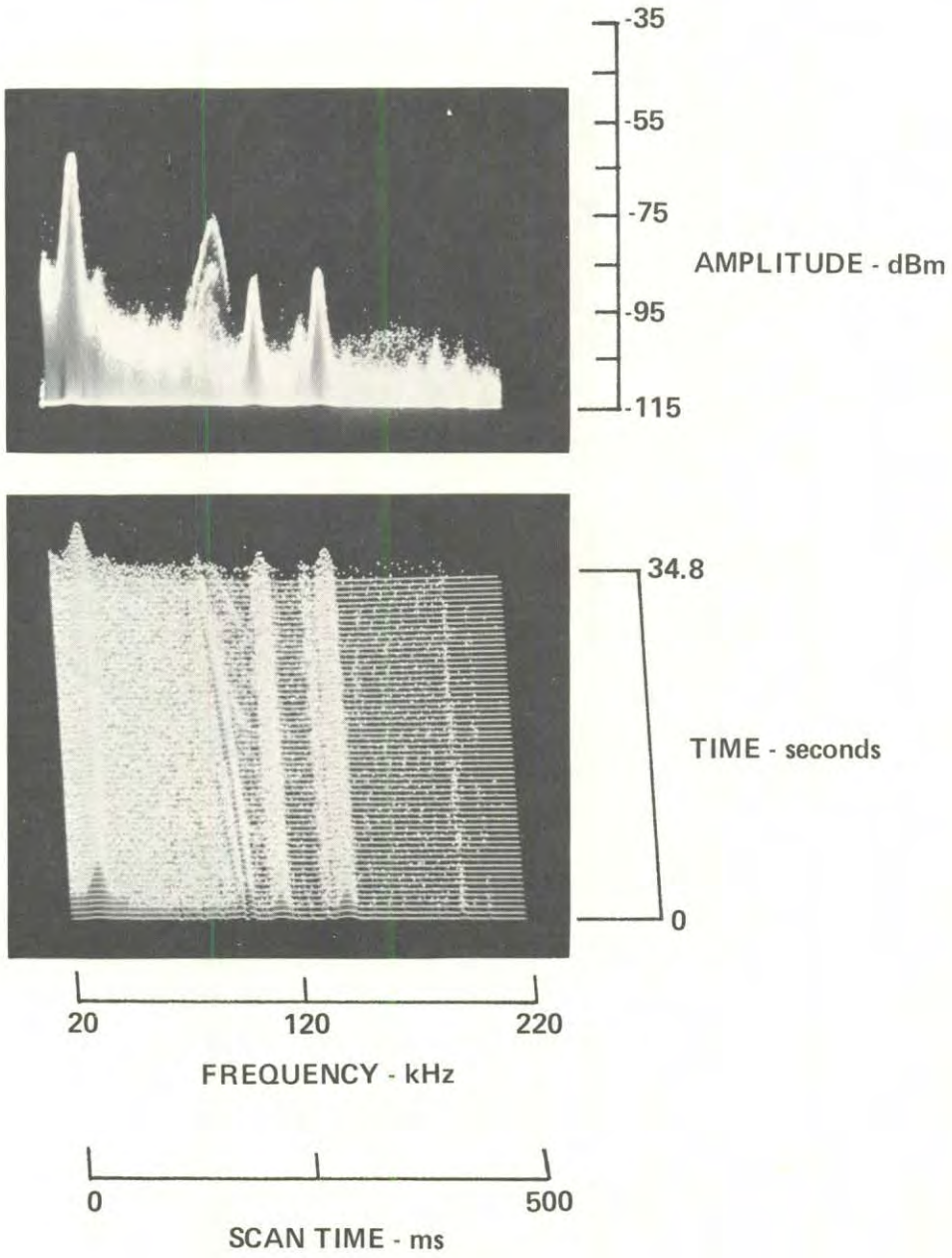

1-22-79, 1332, 109-013
HP140, Whip, F120, W200, IF3, ST 500, A -20/0/+15/NF

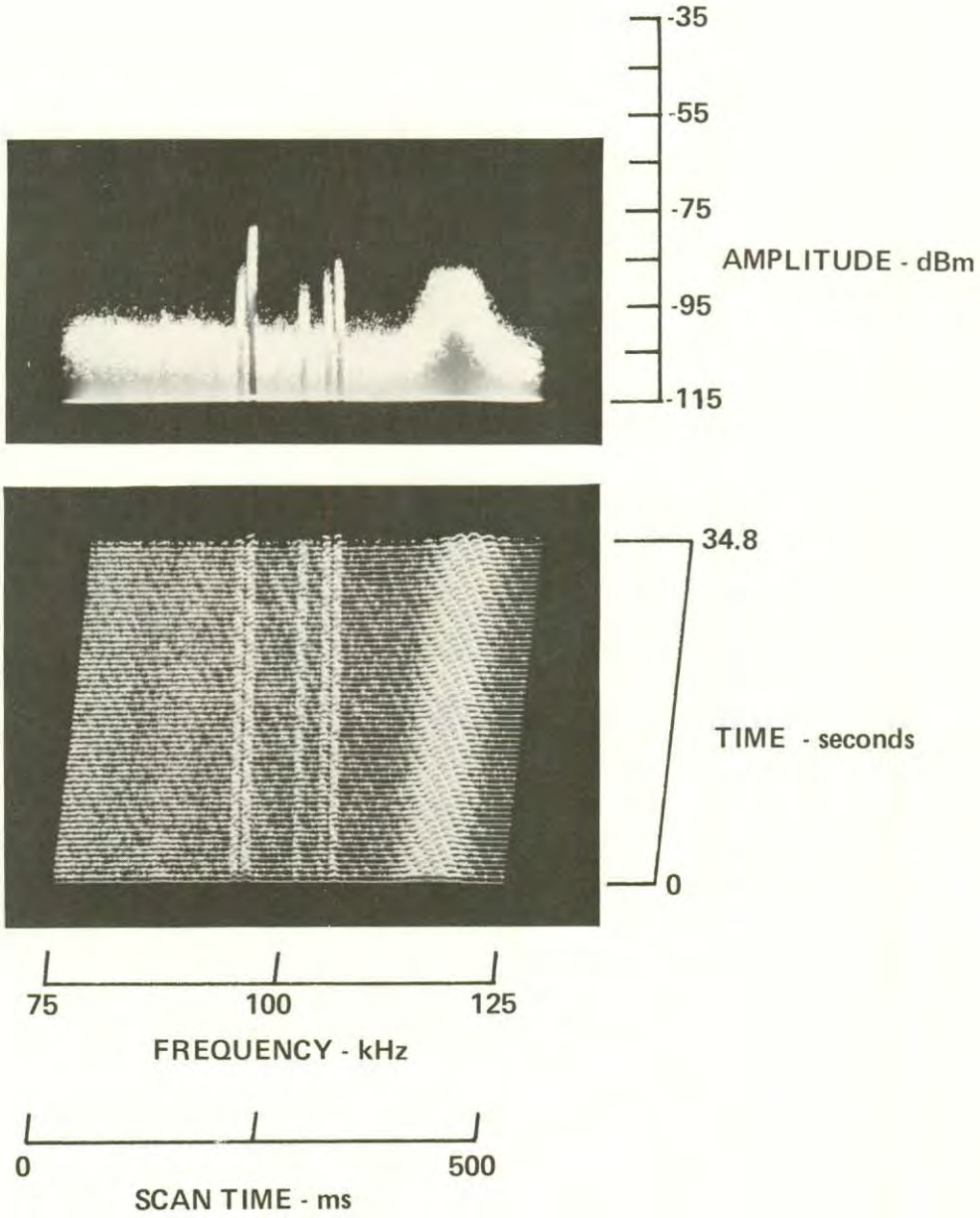

1-23-79, 0756, 109-014
HP140, Whip, F100, W50, IF3, ST 500, A -20/0/+15/NF

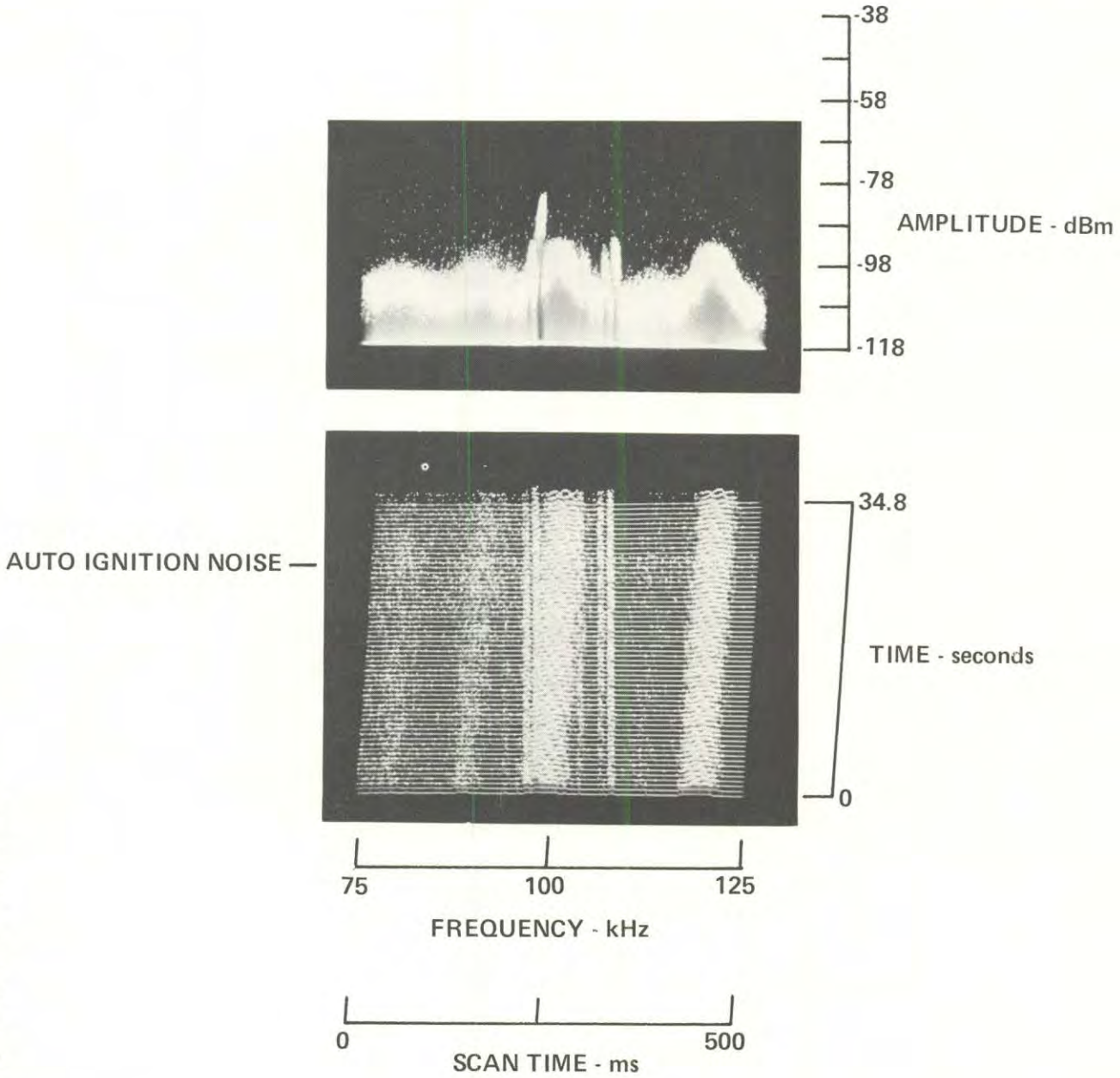

1-23-79, 0808, 109-015
HP140, Whip, F100, W50, IF3, ST 500, A -20/0/+18/with Filter

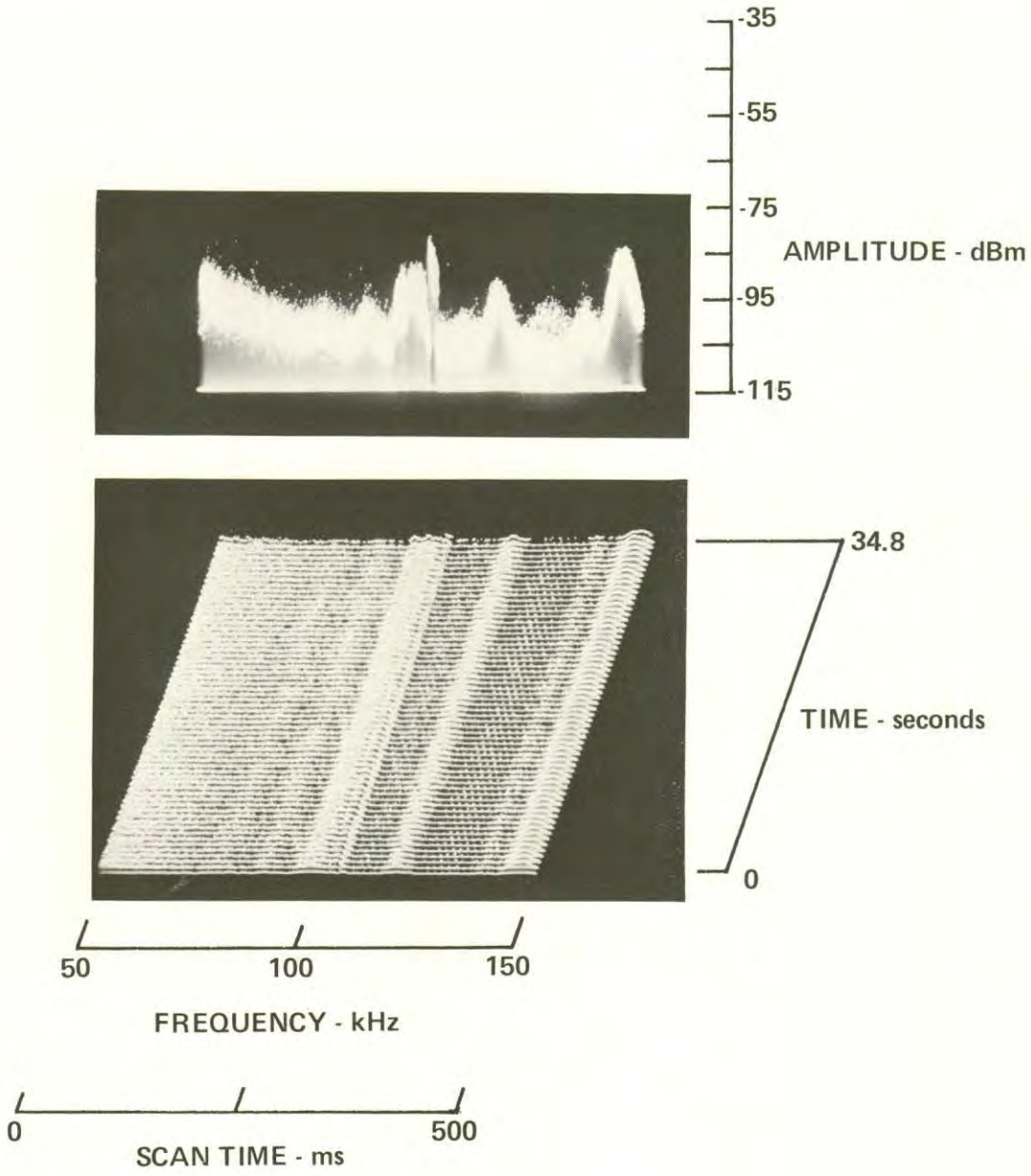

1-23-79, 0822, 109-015
HP140, Whip, F100, W100, IF3, ST 500, A -10/0/+15/NF

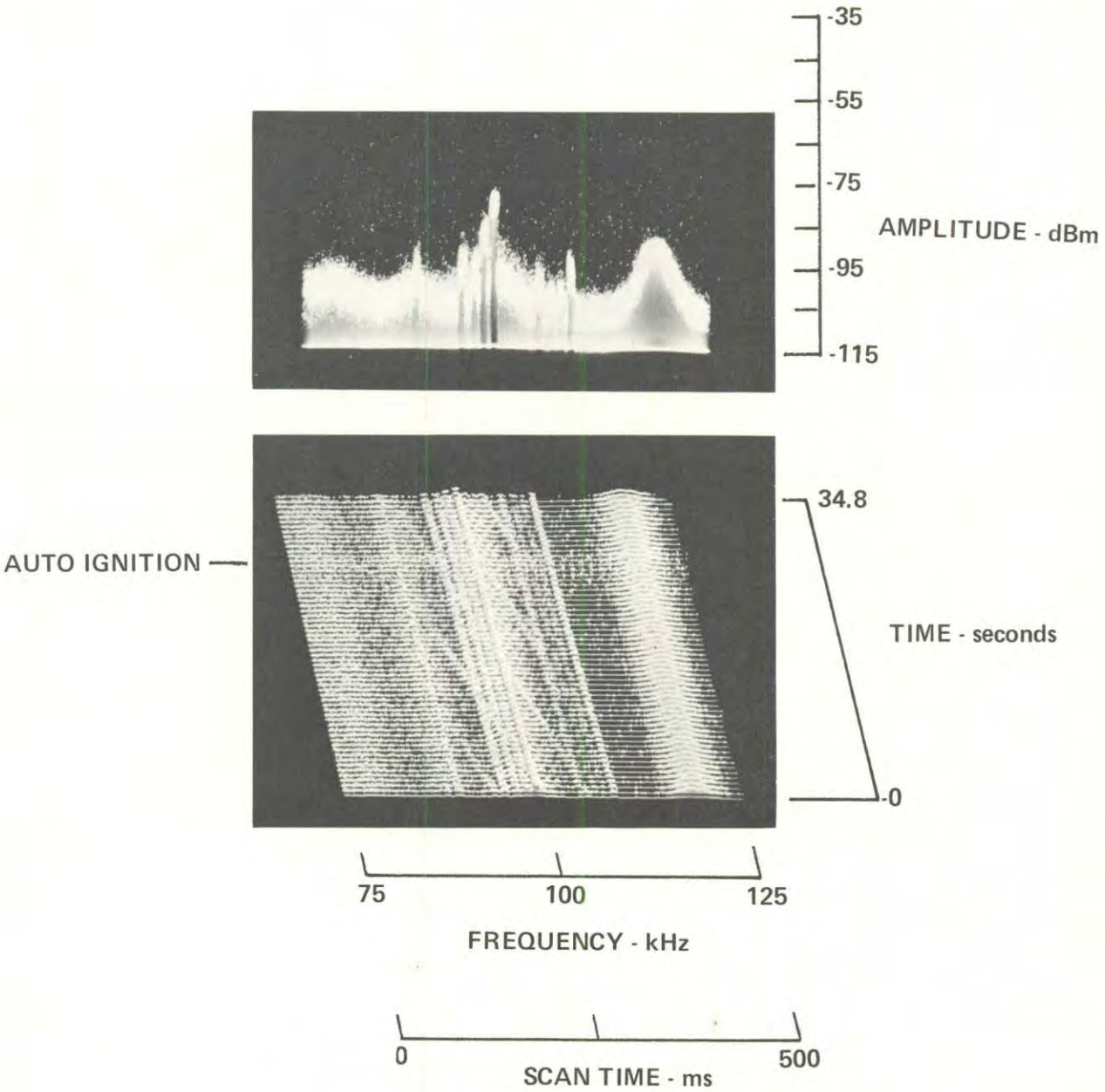

1-23-79, 0831, 109-016
HP140, Whip, F100, W50, IF3, ST 500, A -20/0/+15/NF

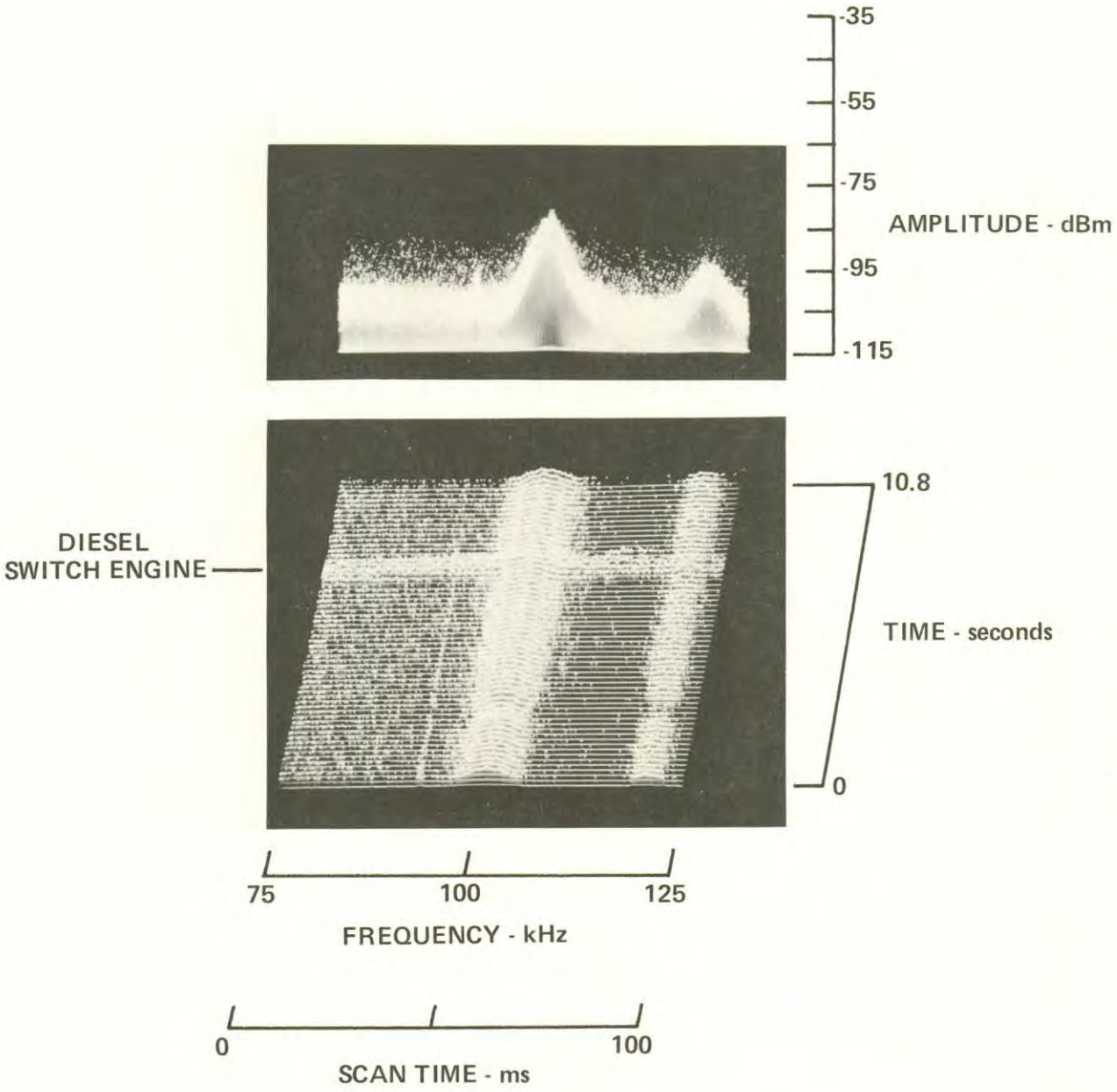

1-23-79, 0844, 109-017
HP140, Whip, F100, W50, IF3, ST 100, A -20/0/+15/NF

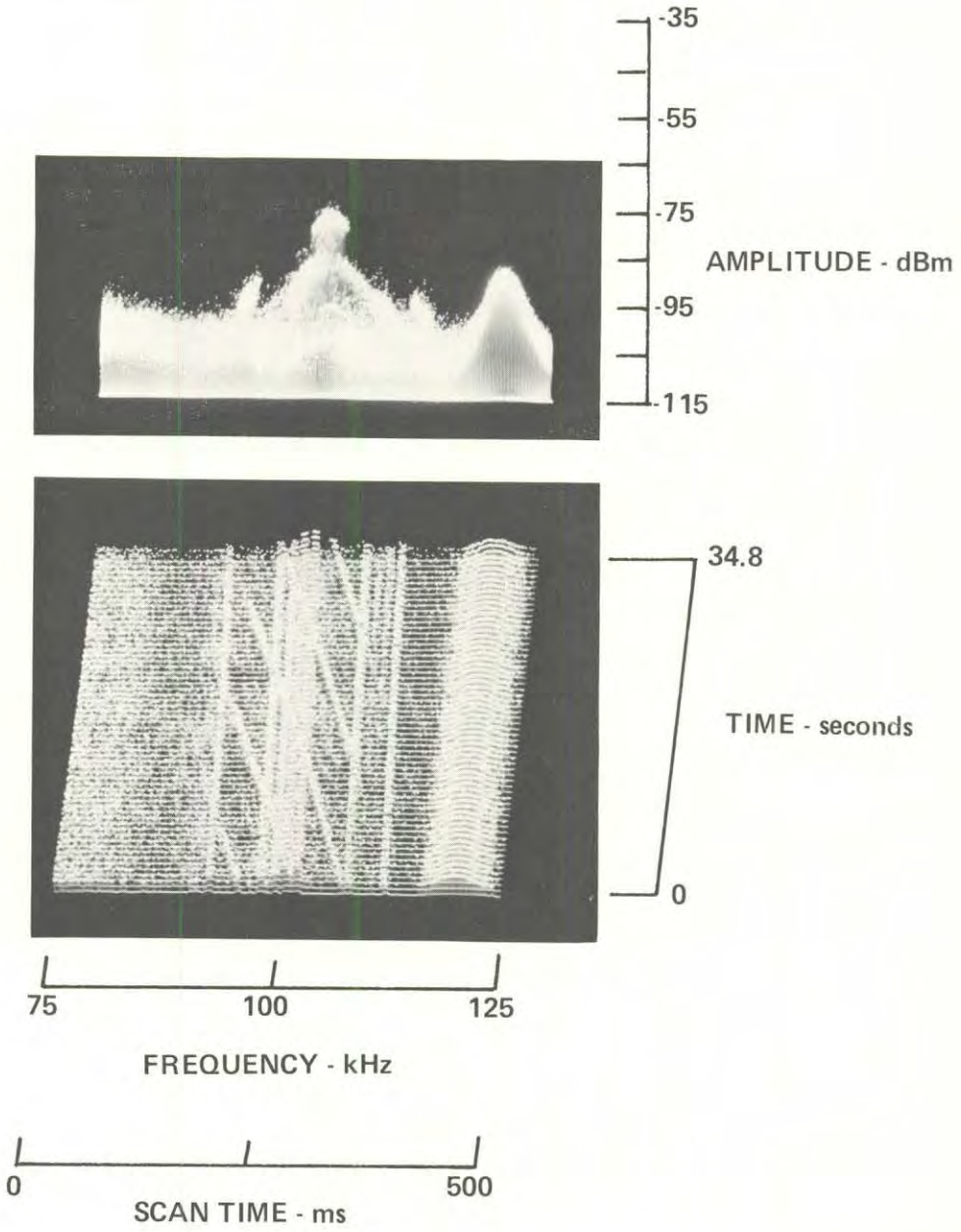

1-23-79, 0933, 109-018
HP140, Whip, F100, W50, IF3, ST 500, A -20/0/+15/NF

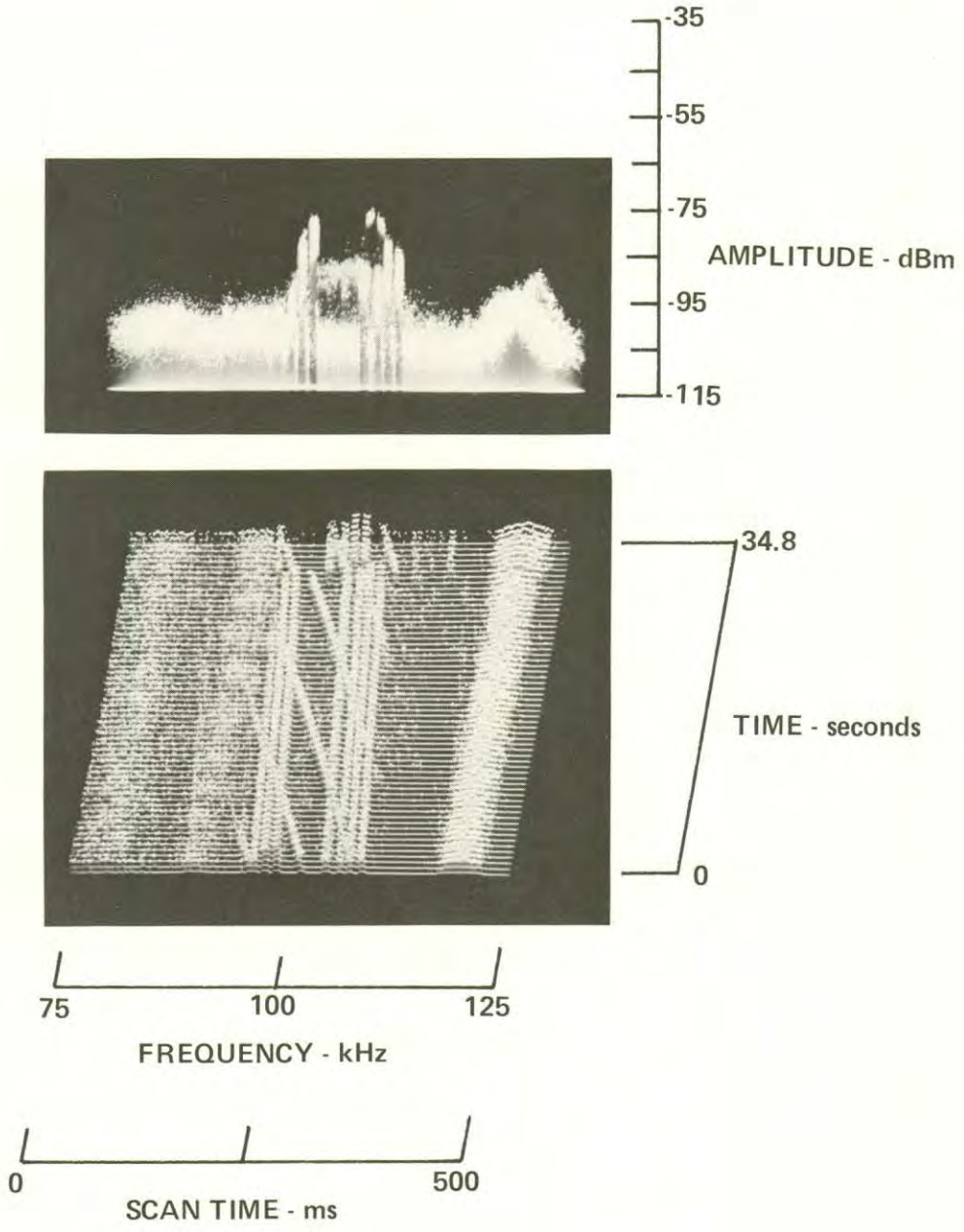

1-23-79, 0947, 109-019
HP140, Whip, F100, W50, IF3, ST 500, A -20/0/+15/NF

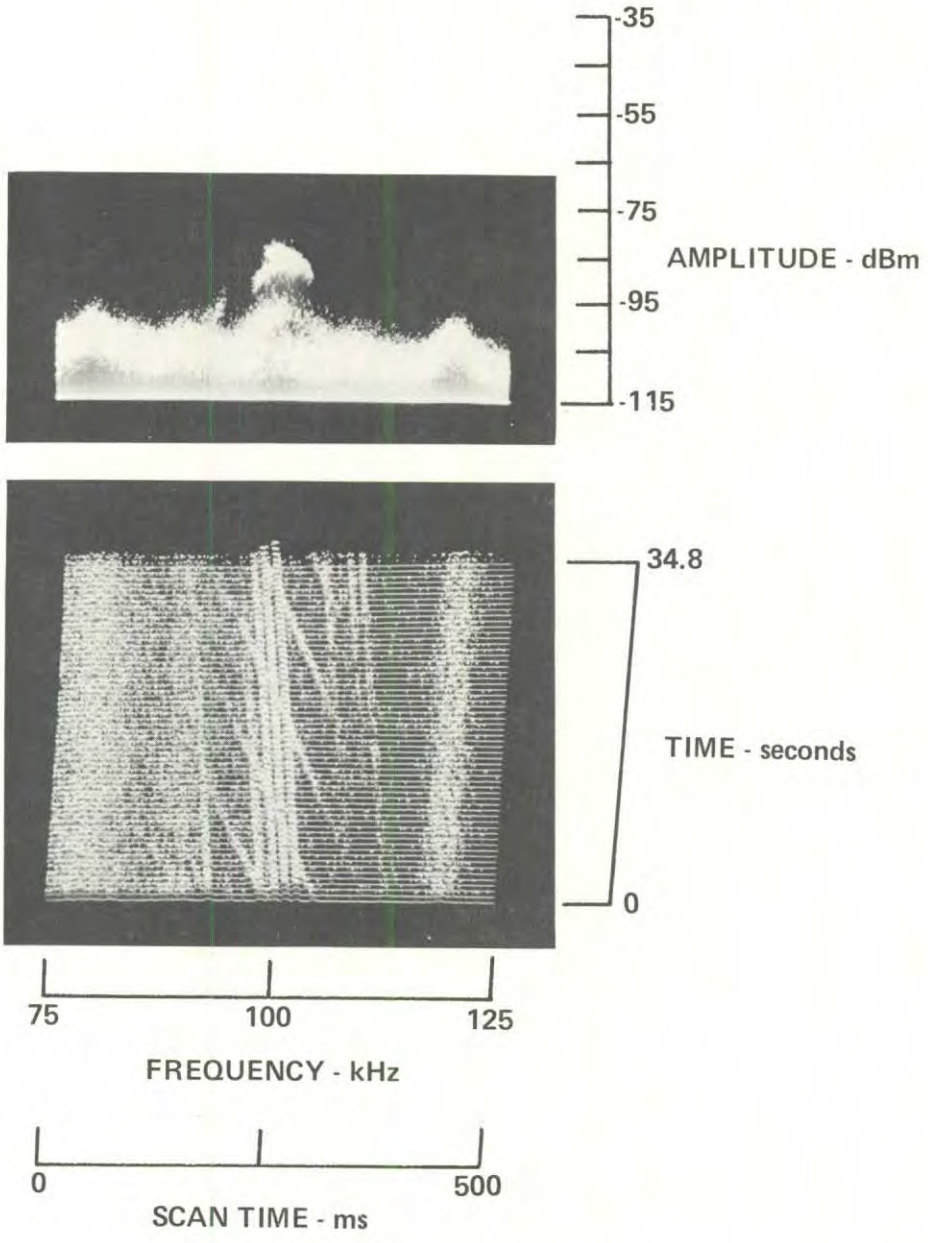

1-23-79, 1005, 109-020
HP140, Whip, F100 W50, IF3, ST 500, A -20/0/+15/NF

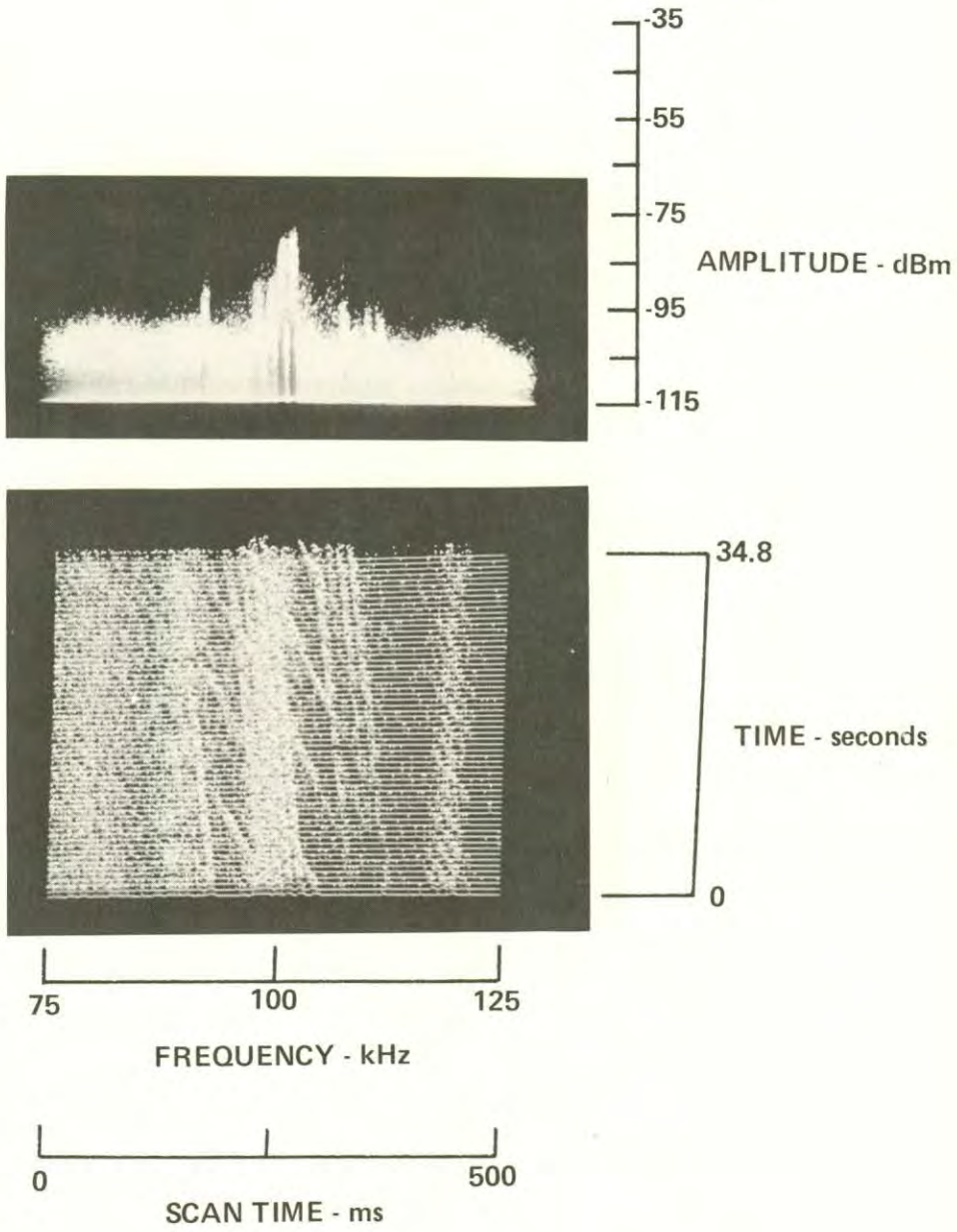

1-23-79, 1017, 108-021
HP140, Whip, F100, W50, IF3, ST 500, A -20/0/+15/NF

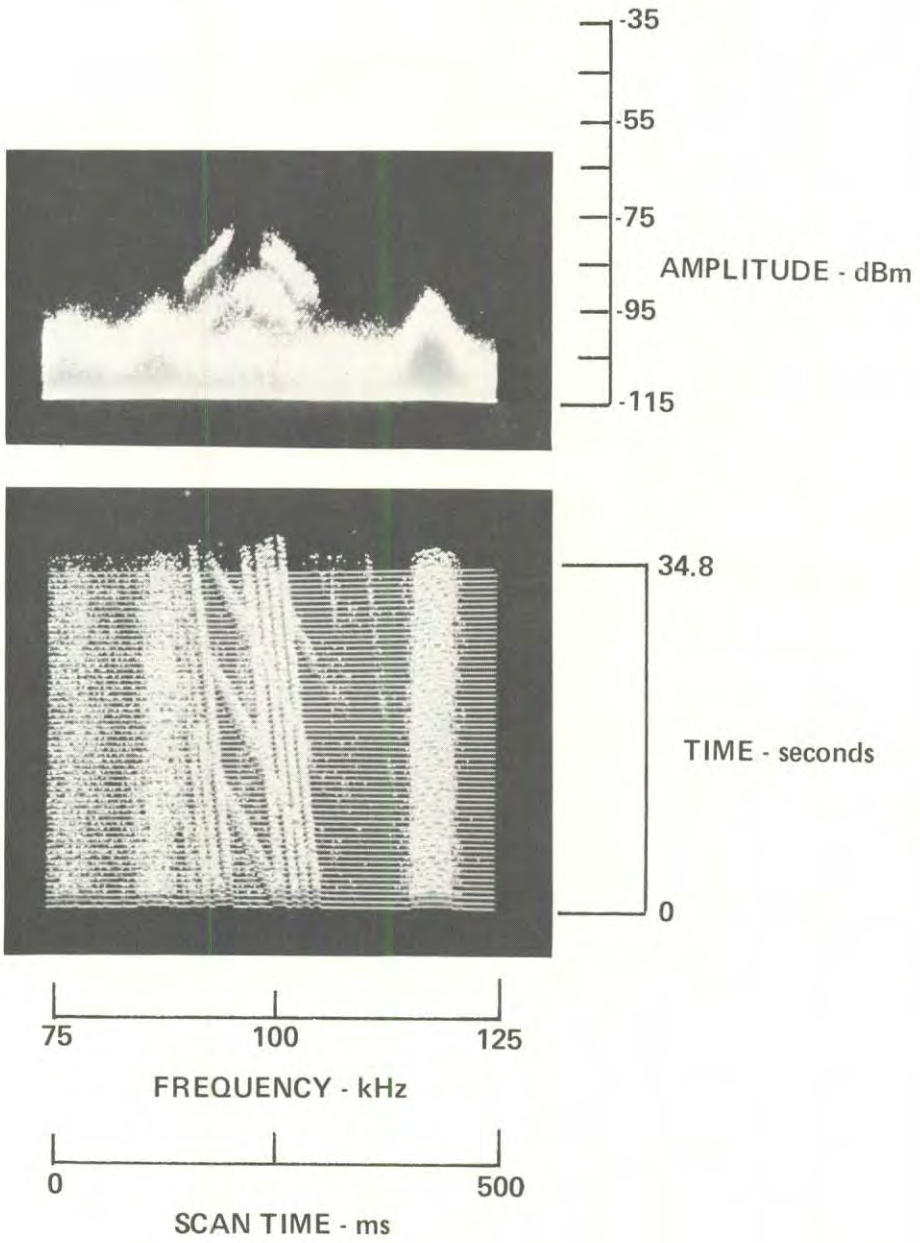

1-23-79, 1026, 108-022
HP140, Whip, F100, W50, IF3, ST500, A -20/0/+15/NF

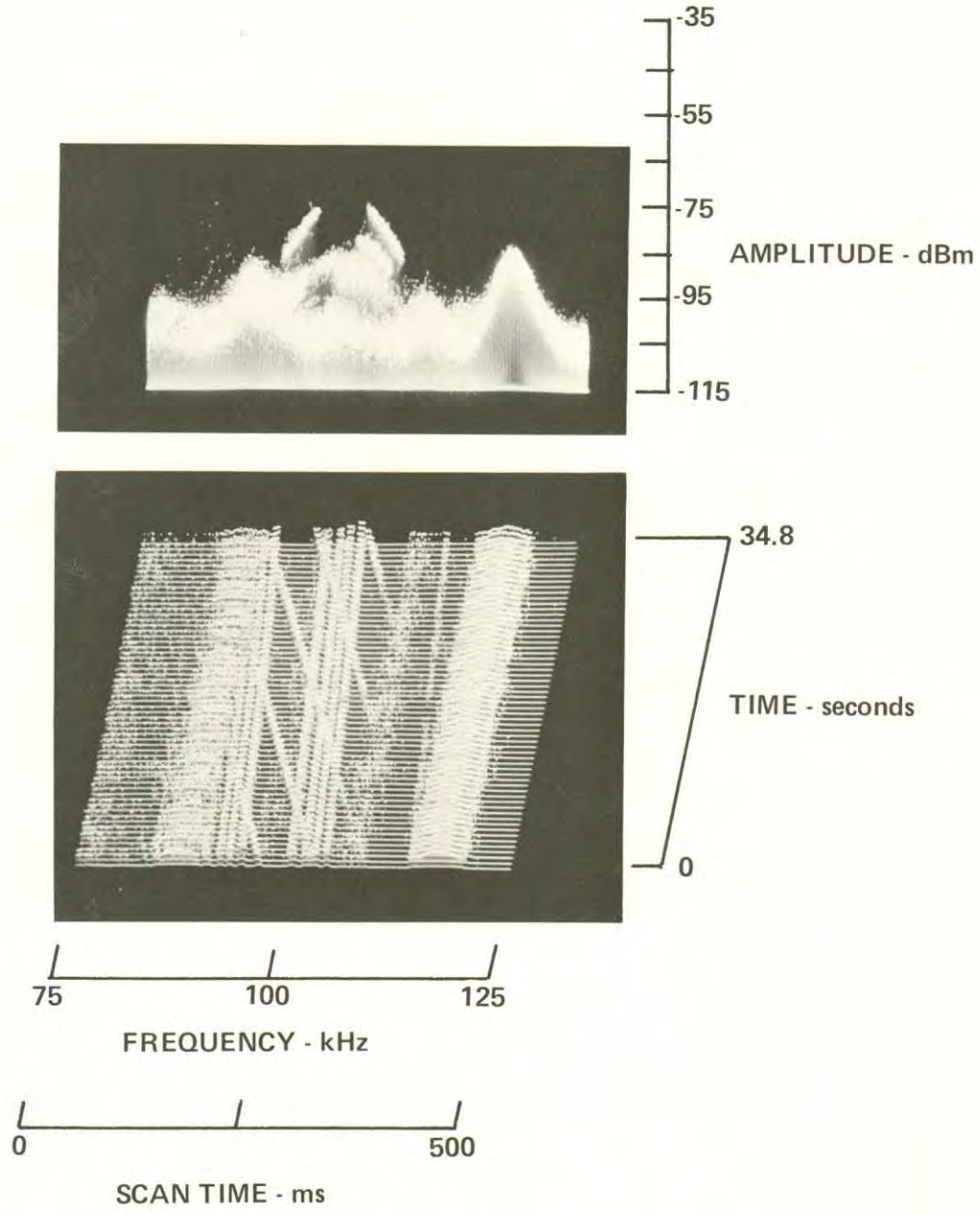

1-23-79, 1138, 108-023
HP140, Whip, F100, W50, IF3, ST 500, A -20/0/+15/NF

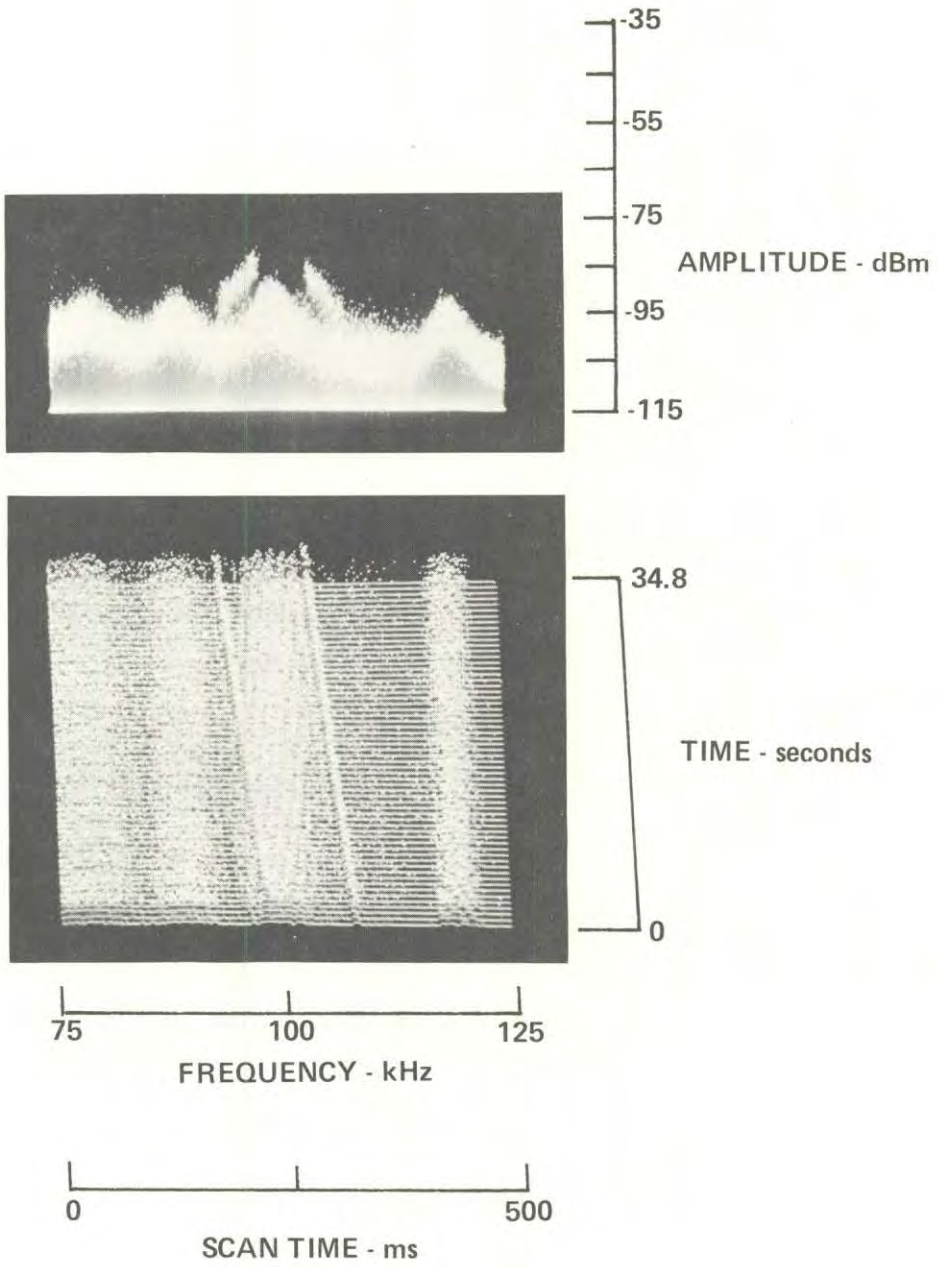

1-23-79, 1146, 108-024
HP140, Whip, F100, W50, IF3, ST 500, A -20/0/+15/NF

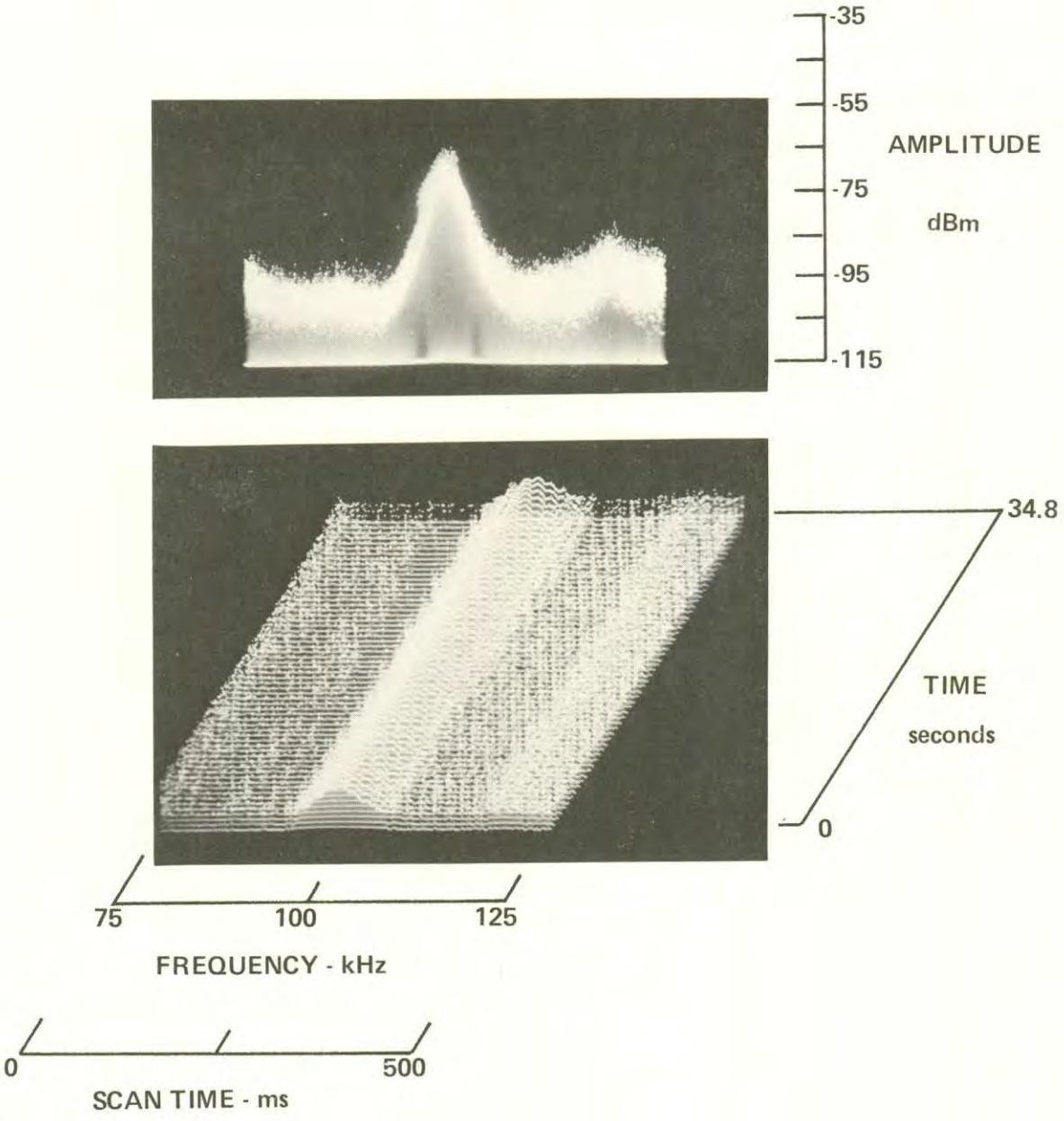

1-23-79, 1203, 108-025
HP140, Whip, F100, W50, IF3, ST 500, A -20/0/+15/NF

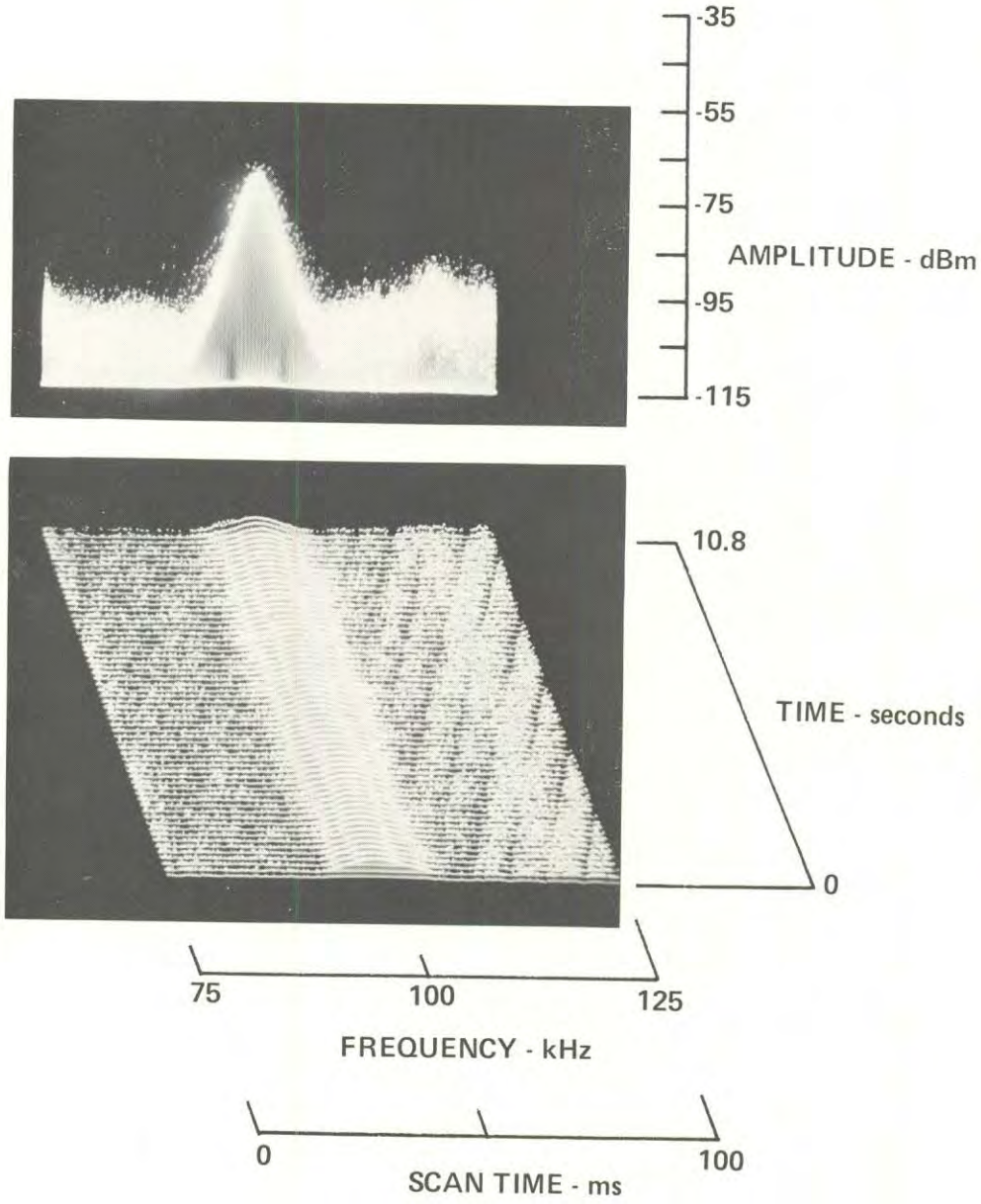

1-23-79, 1218, 108-025
HP140, Whip, F100, W50, IF3, ST 100 , A-20/0/+15/NF

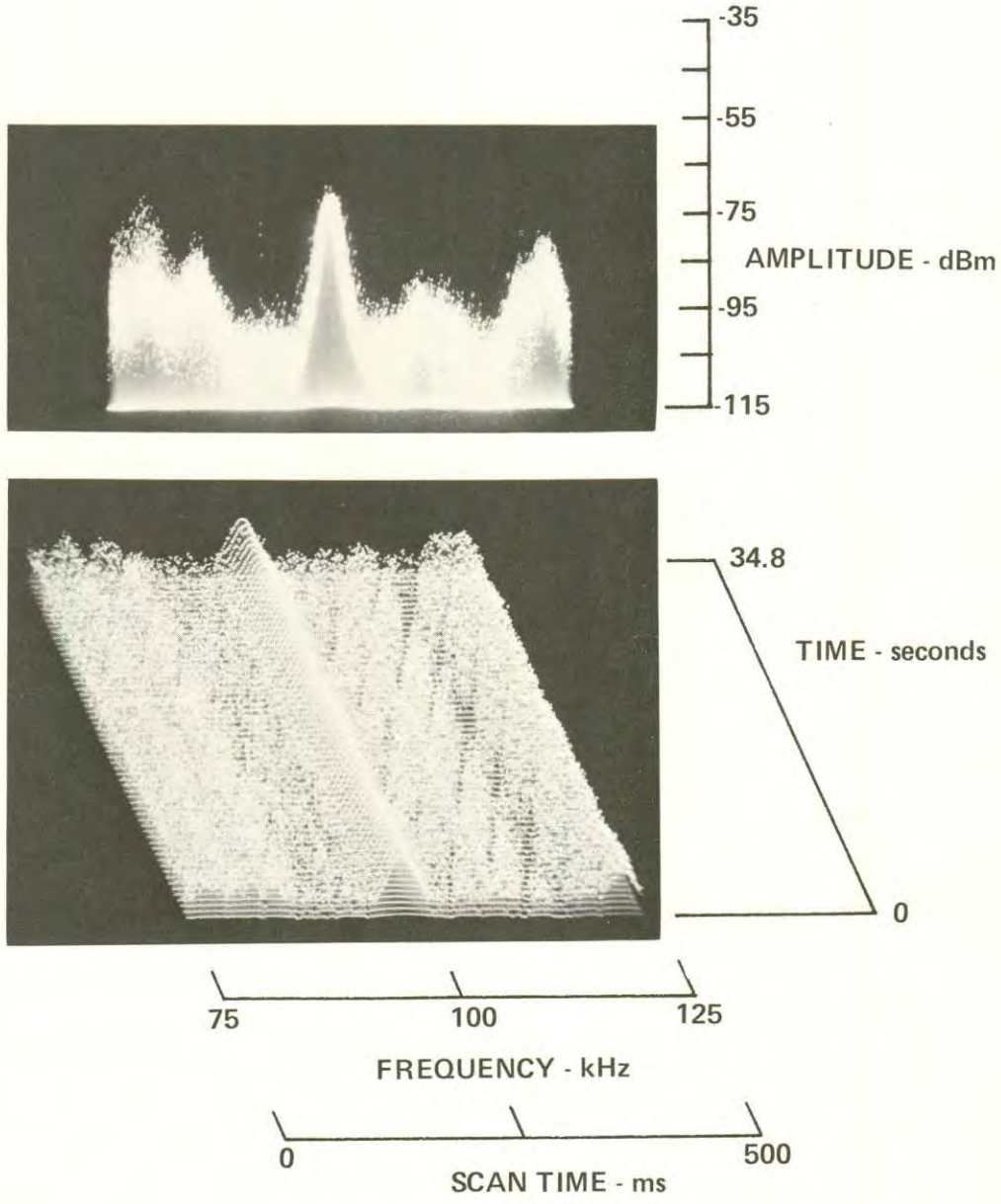

1-23-79, 1221, 108-025
HP140, Whip, F100, W50, IF3, ST 500, A -20/0/+15/NF

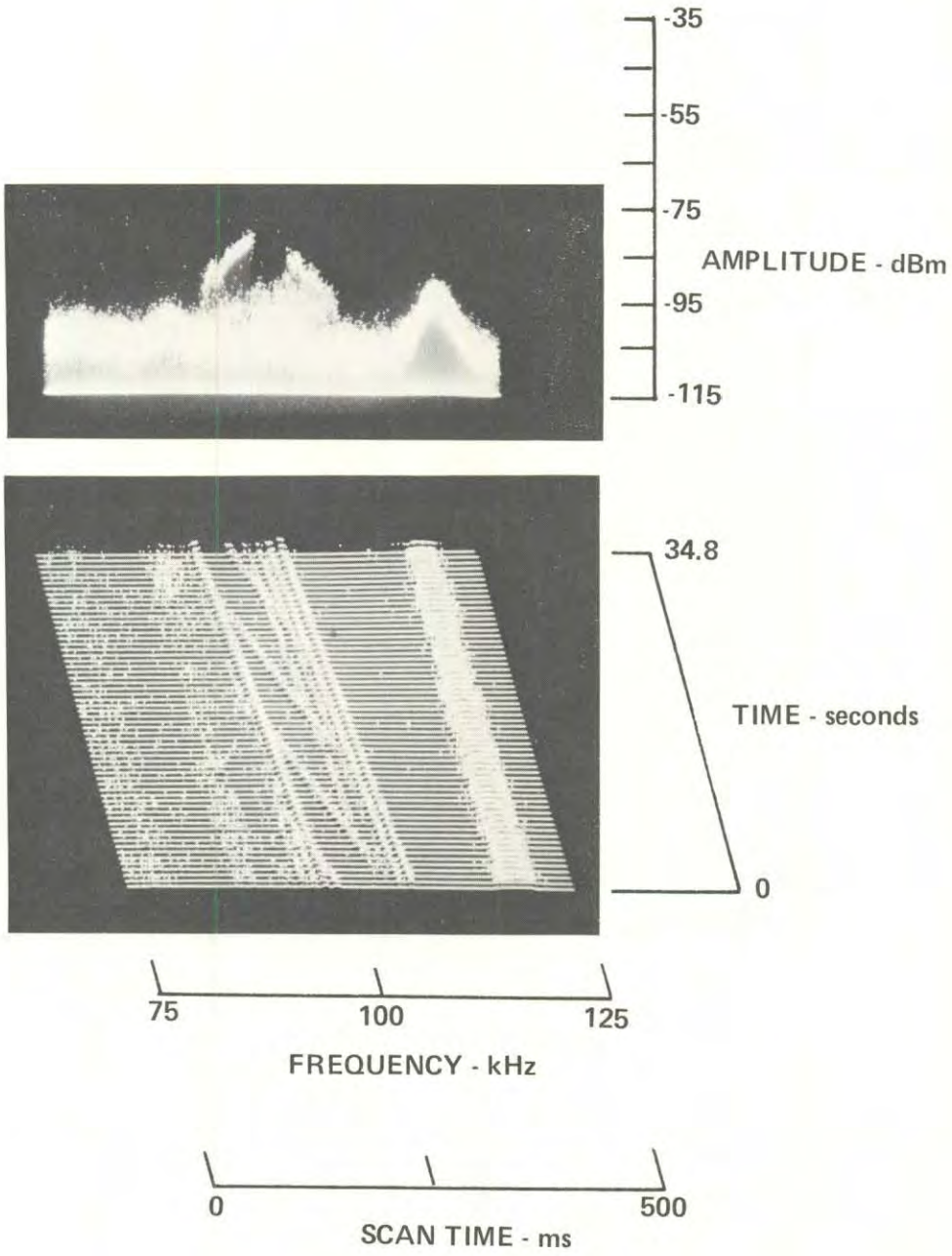

1-23-79, 1242, 108-026
HP140, Whip, F100, W50, IF3, ST 500, A-20/0/+15/NF

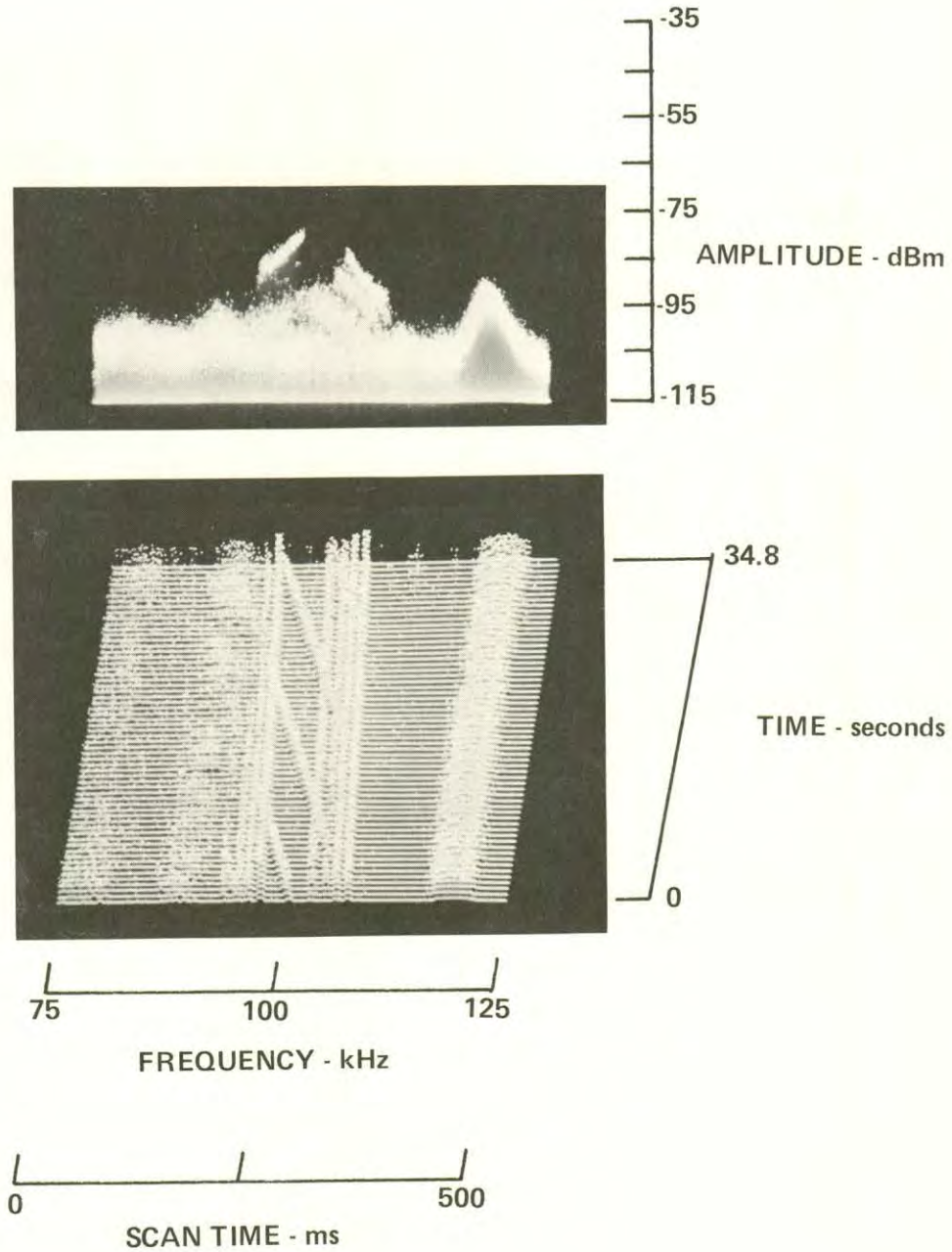

1-23-79, 1252, 108-027
HP140, Whip, F100, W50, IF3, ST 500, A -20/0/+15/NF

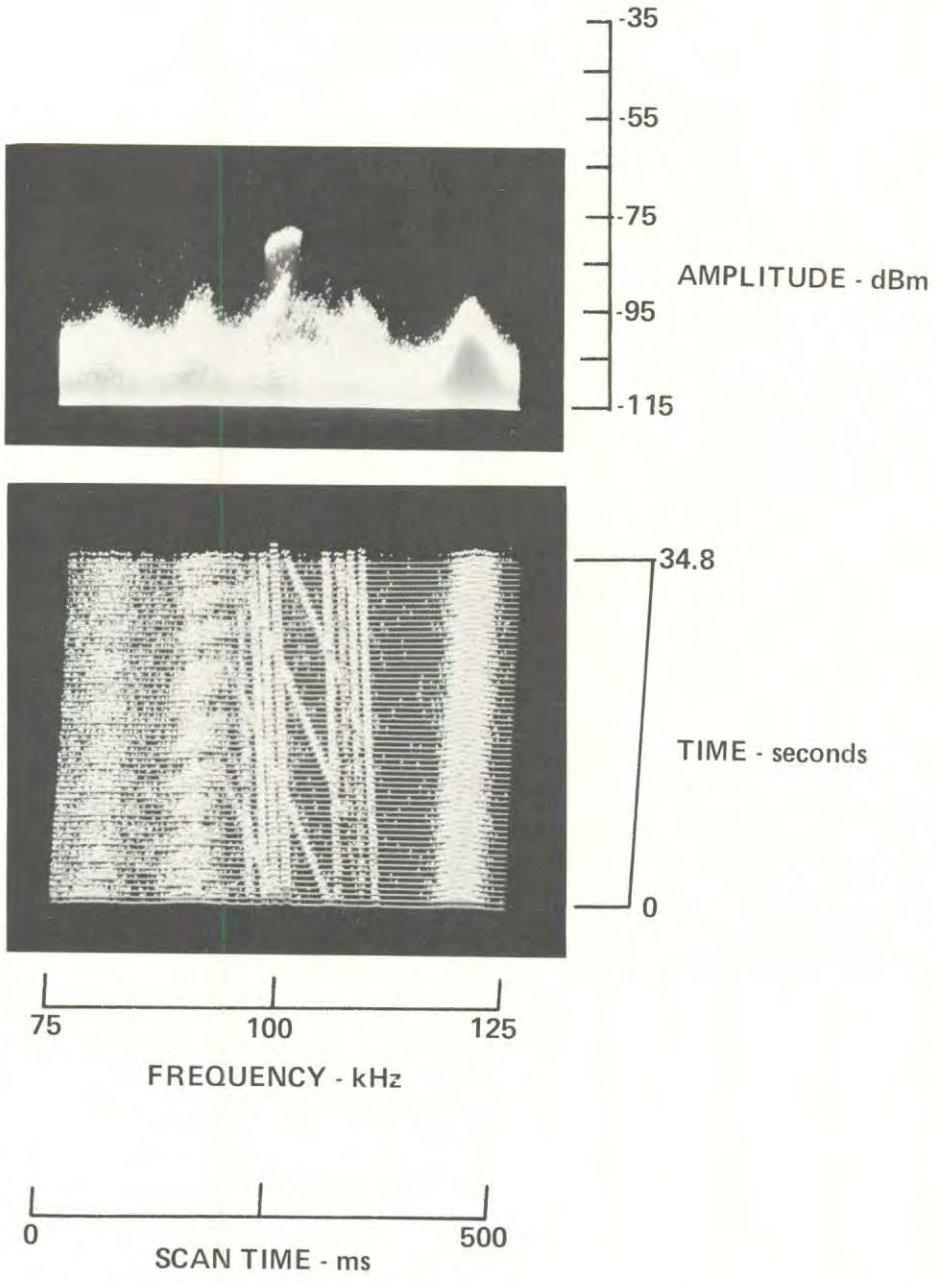

1-23-79, 1323, 108-028
HP140, Whip, F100, W50, IF3, ST 500, A -20/0/+15/NF

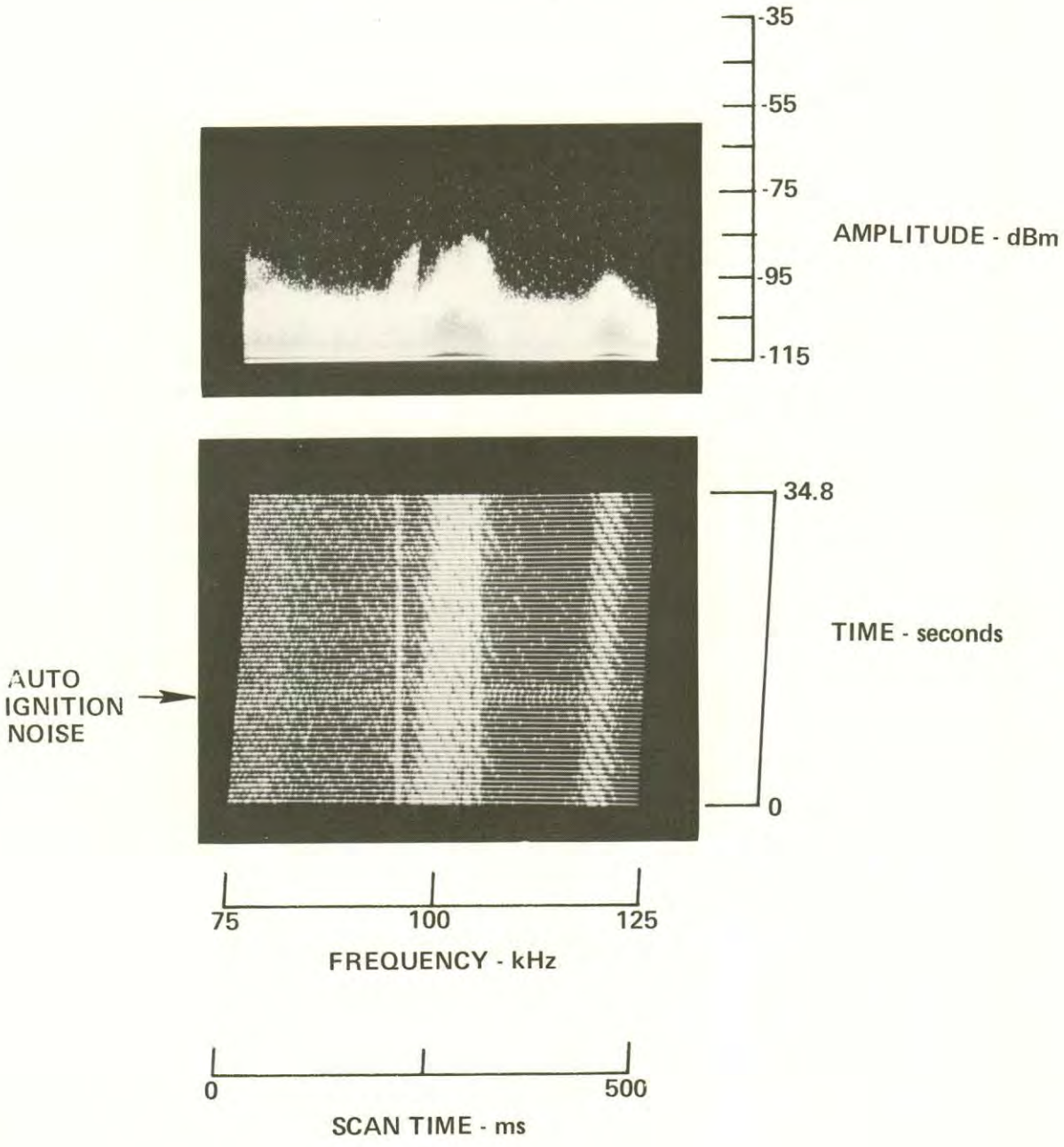

1-23-79, 1308, 108-029
HP140, Whip, F100, W50, IF3, ST 500, A -20/0/+15/NF

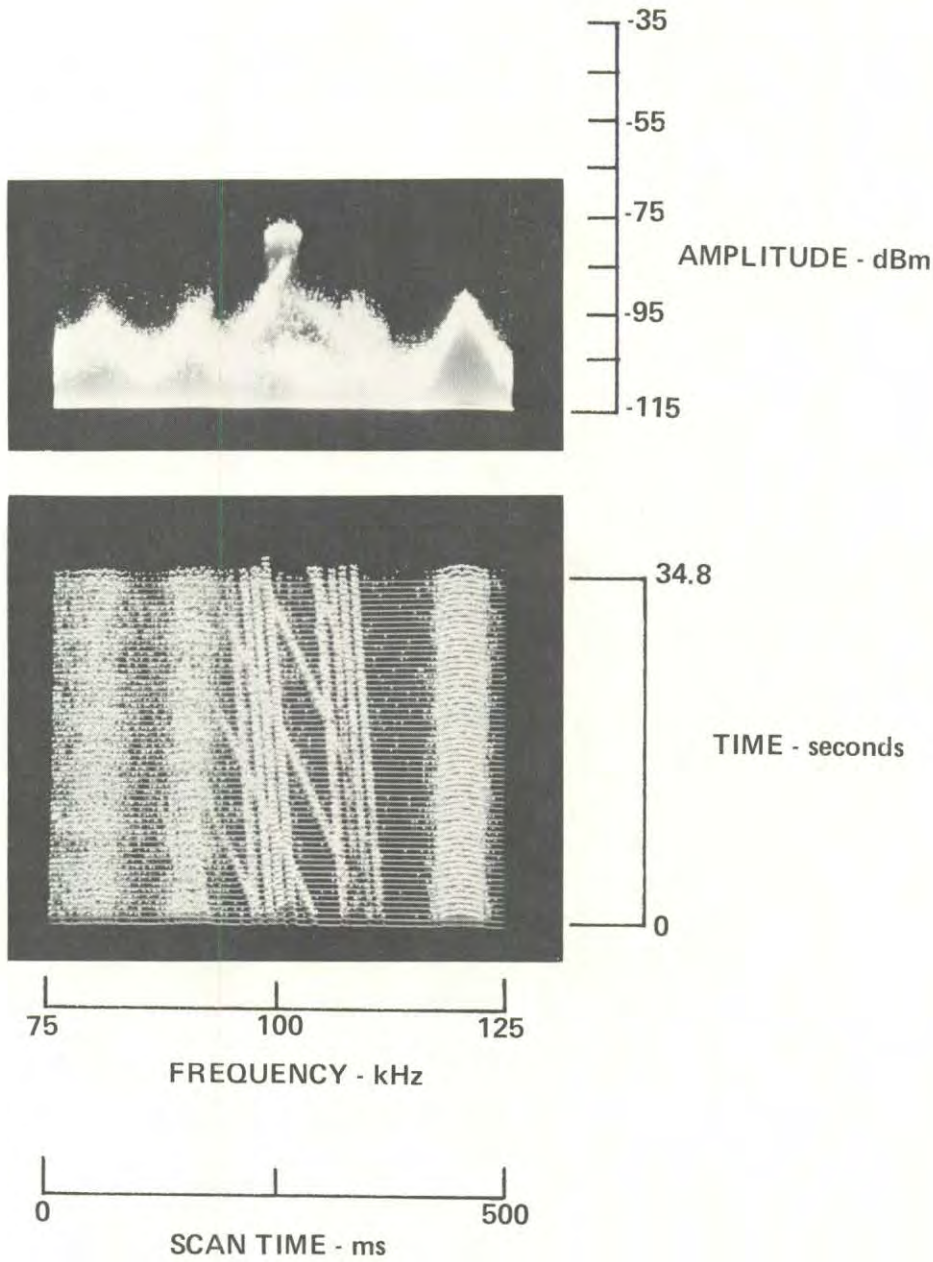

1-23-79, 1333, 108-030
HP140, Whip, F100, W50, IF3, ST 500, A -20/0/+15/NF

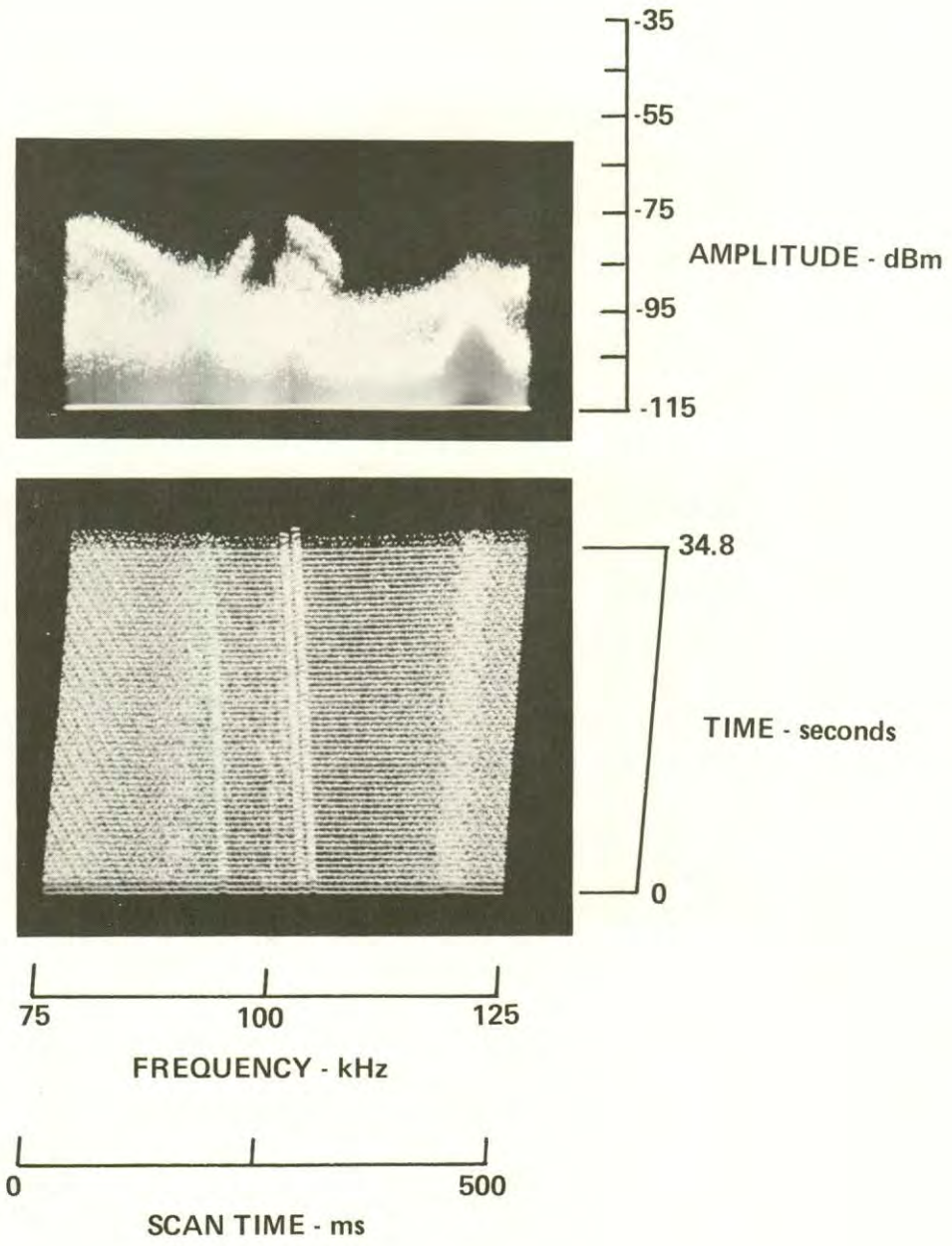

1-24-79, 0814, 107-031
HP140, Whip, F100, W50, IF3, ST500, A -20/0/+15/NF

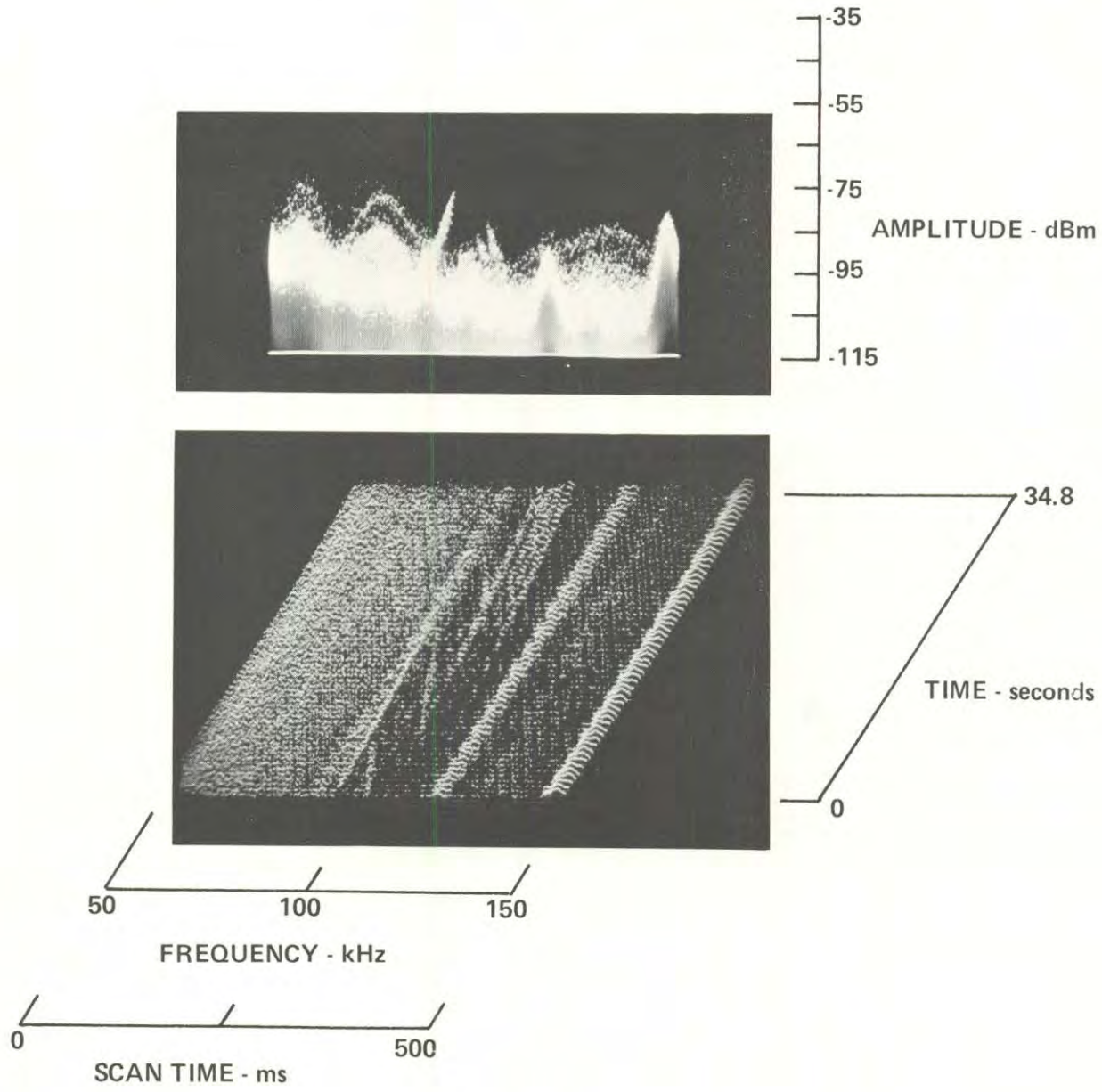

1-24-79, 0816, 107-031
HP140, Whip, F100, W100, IF3, ST 500, A-20/0/+15/NF

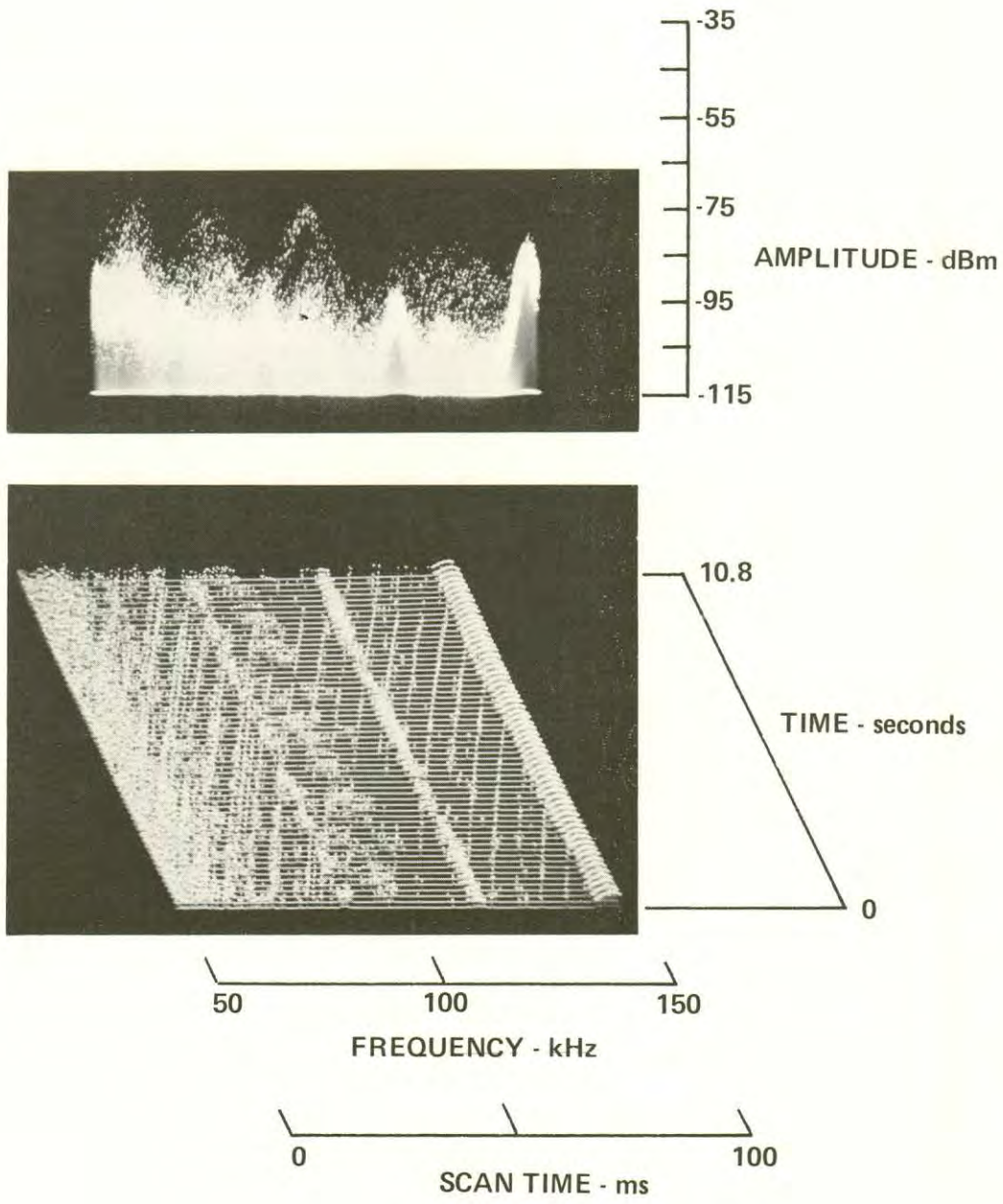

1-24-79, 0819, 107-031
HP140, Whip, F100, W100, IF3, ST 100, A -20/0/+15/NF

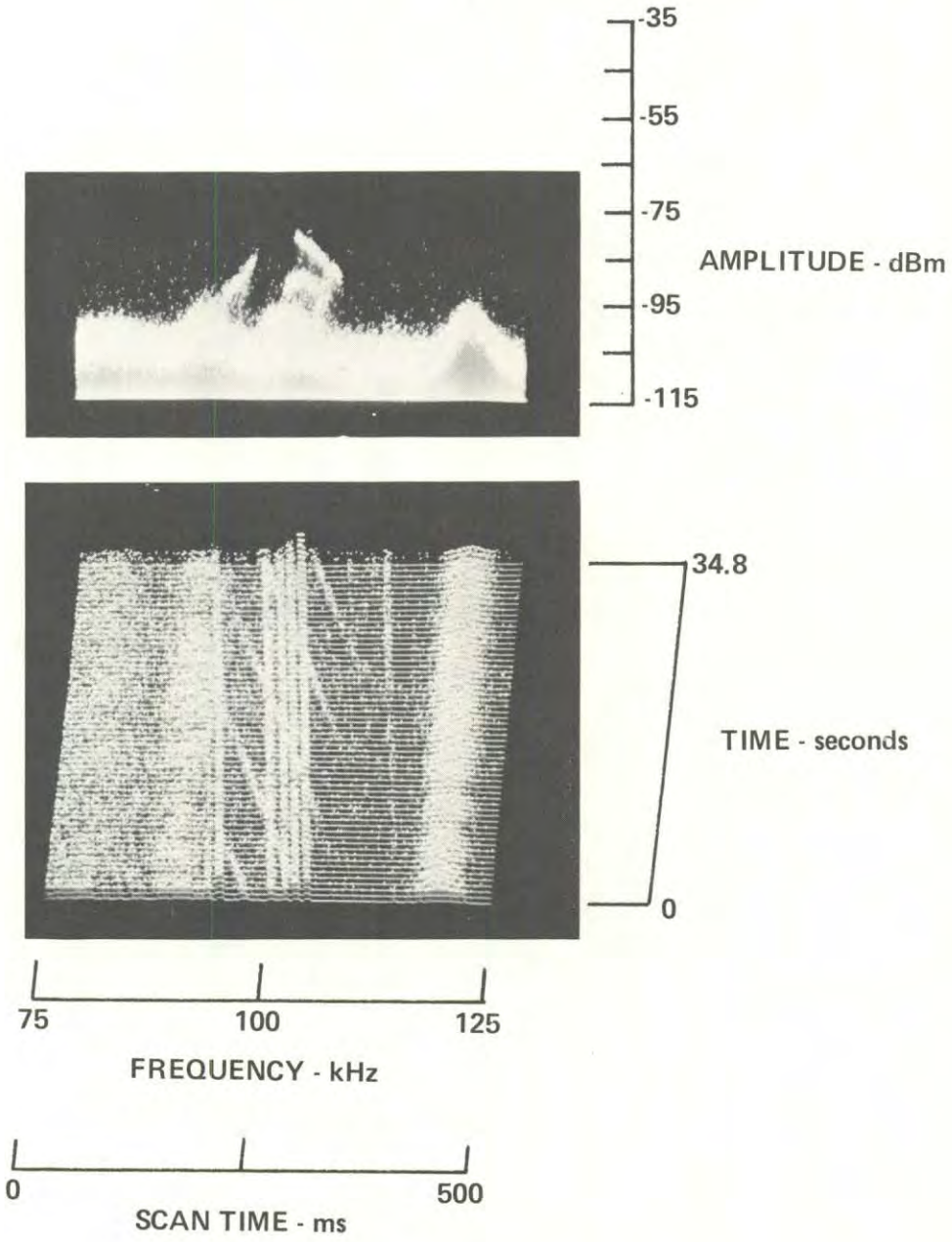

1-24-79, 0833, 107-032
HP140, Whip, F100, W50, IF3, ST 500, A -20/0/+15/NF

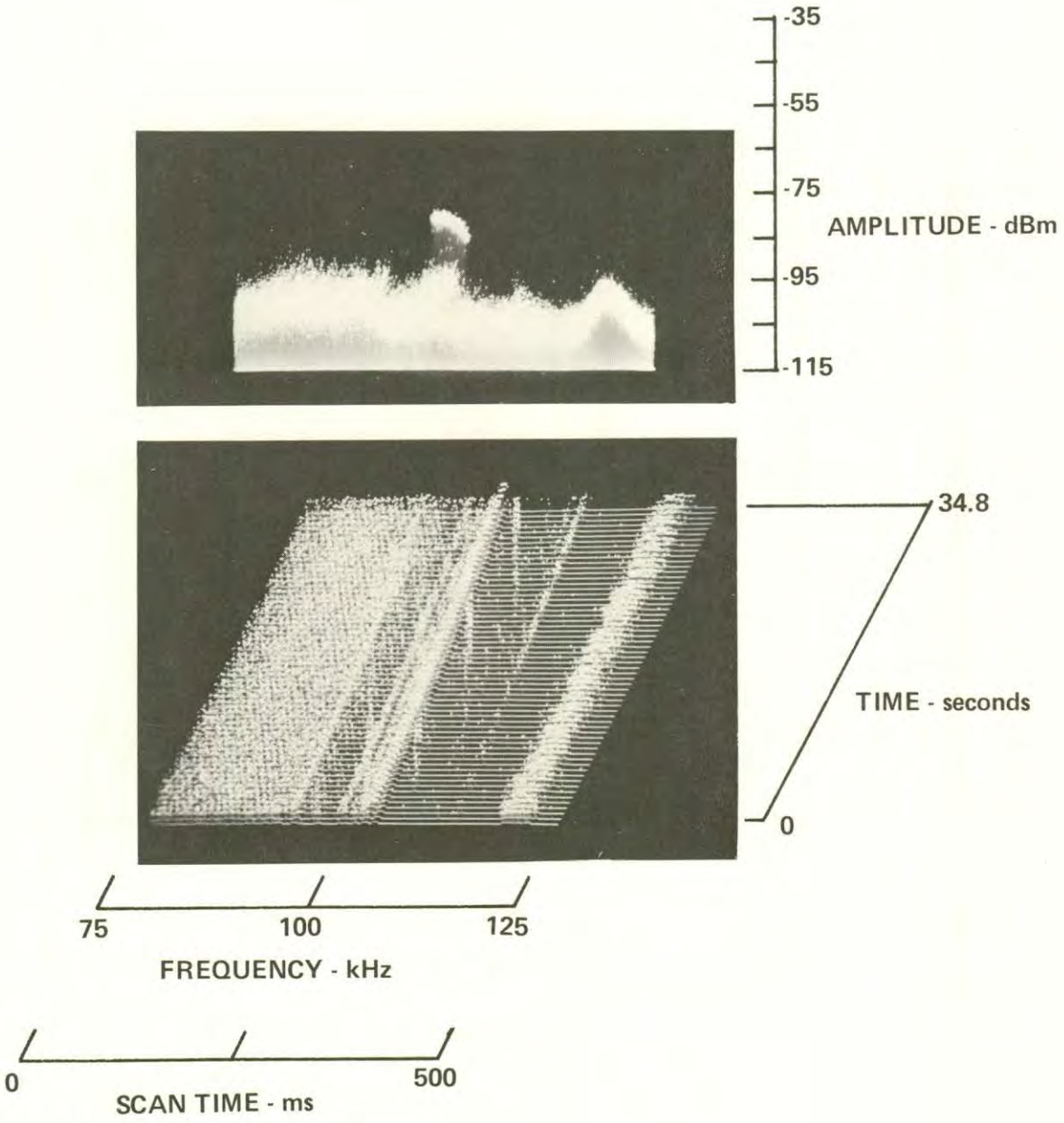

1-24-79, 0834, 107-033, Location 1
HP140, Whip, F100, W50, IF3, ST 500, A -20/0/+15/NF

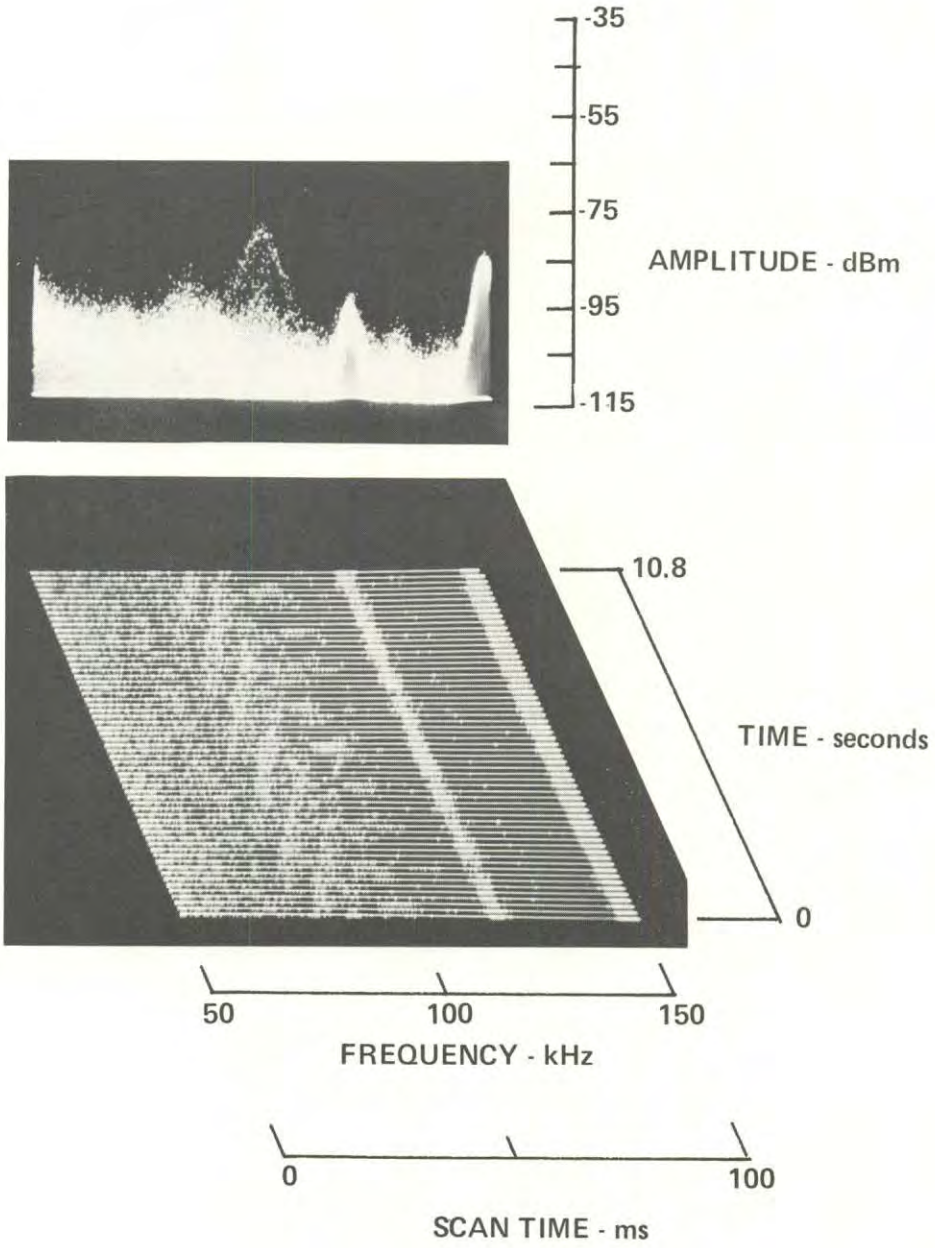

1-24-79, 0838, 107-033, Location 1
HP140, Whip, F100, W100, IF3, ST 100, A -20/0/+15/NF

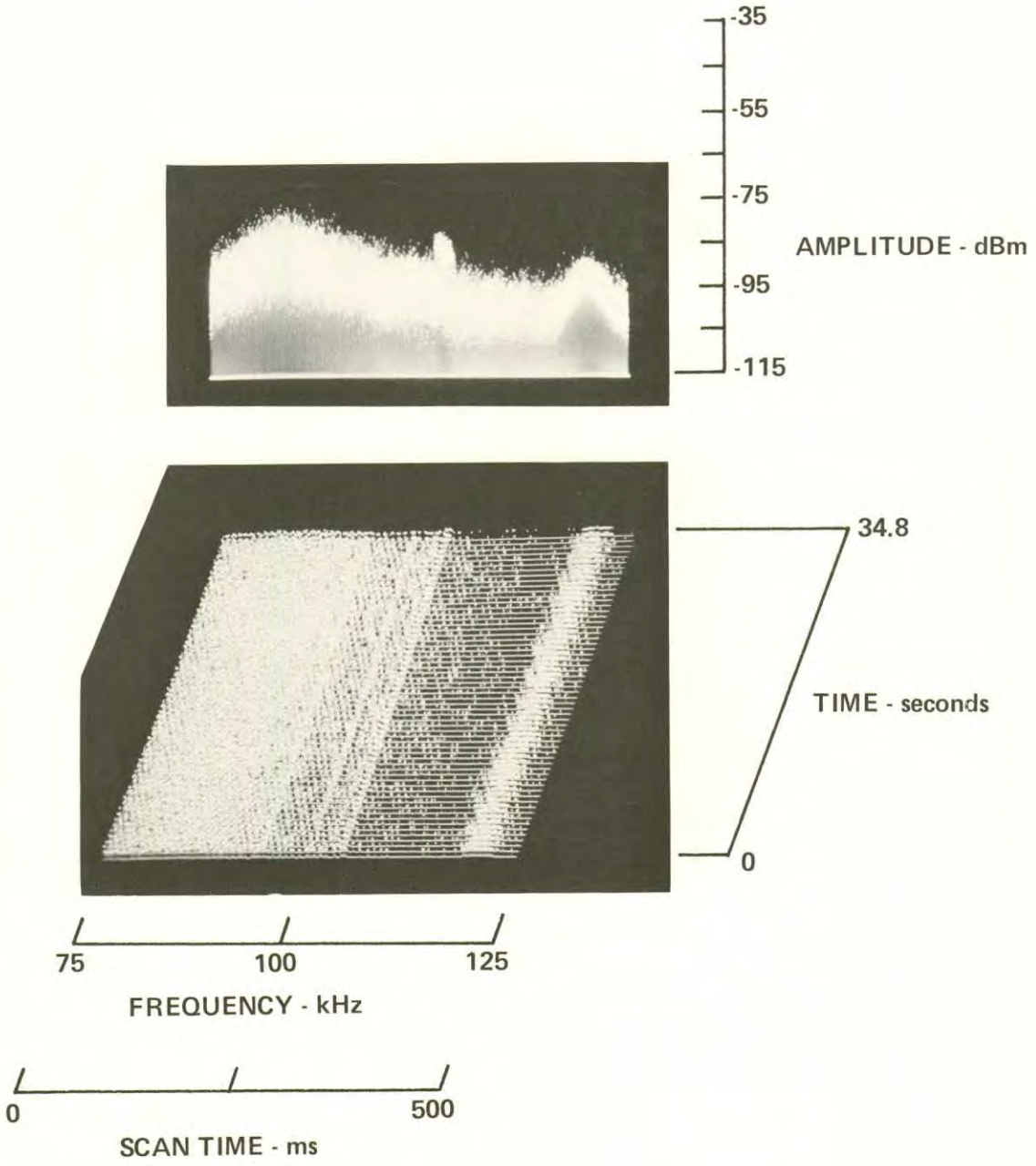

1-24-79, 0901, 107-033, Location 2
HP140, Whip, F100, W50, IF3, ST 500, A -20/0/+15/NF

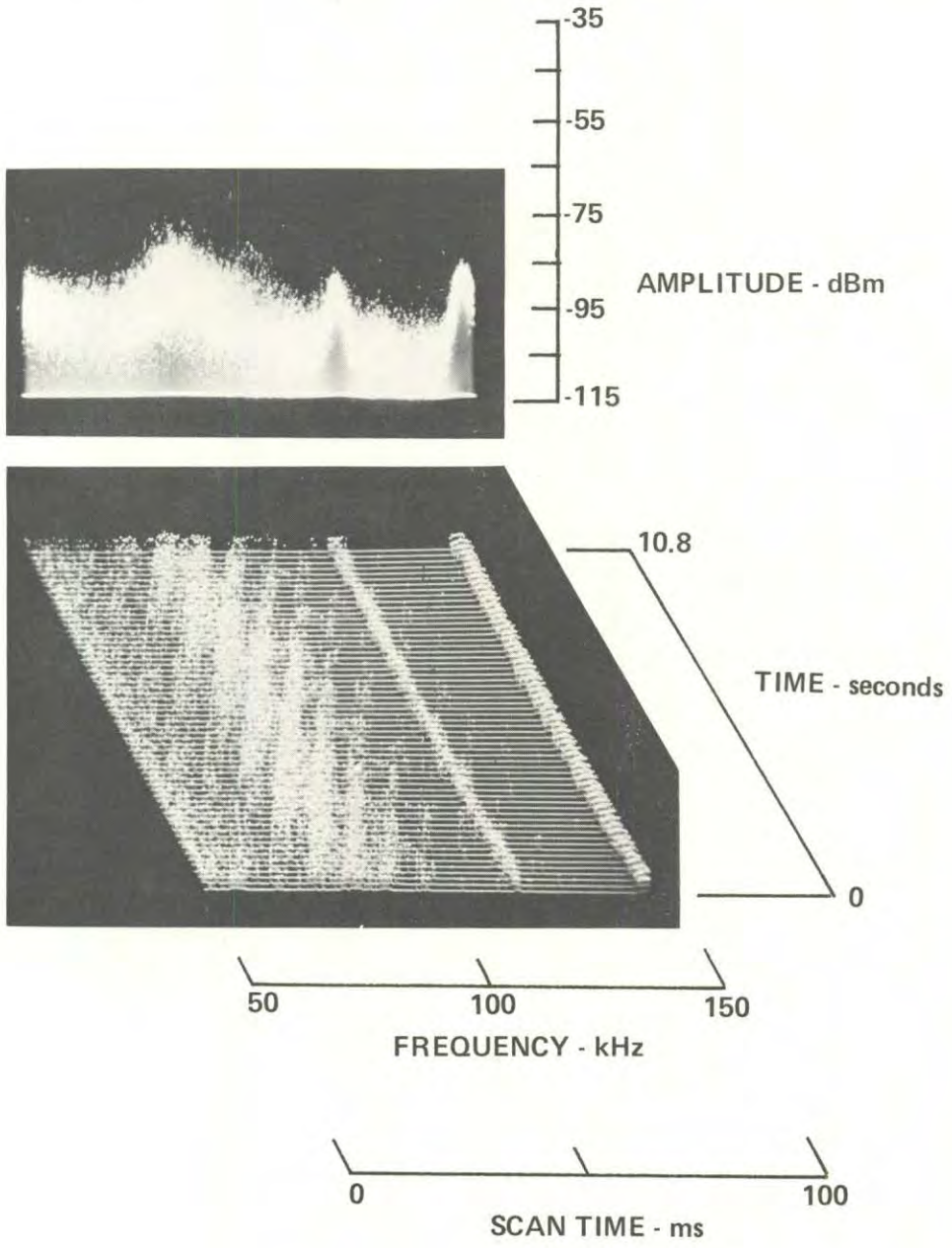

1-24-79, 0902, 107-033, Location 2
HP140, Whip, F100, W100, IF3, ST 100, A -20/0/+15/NF

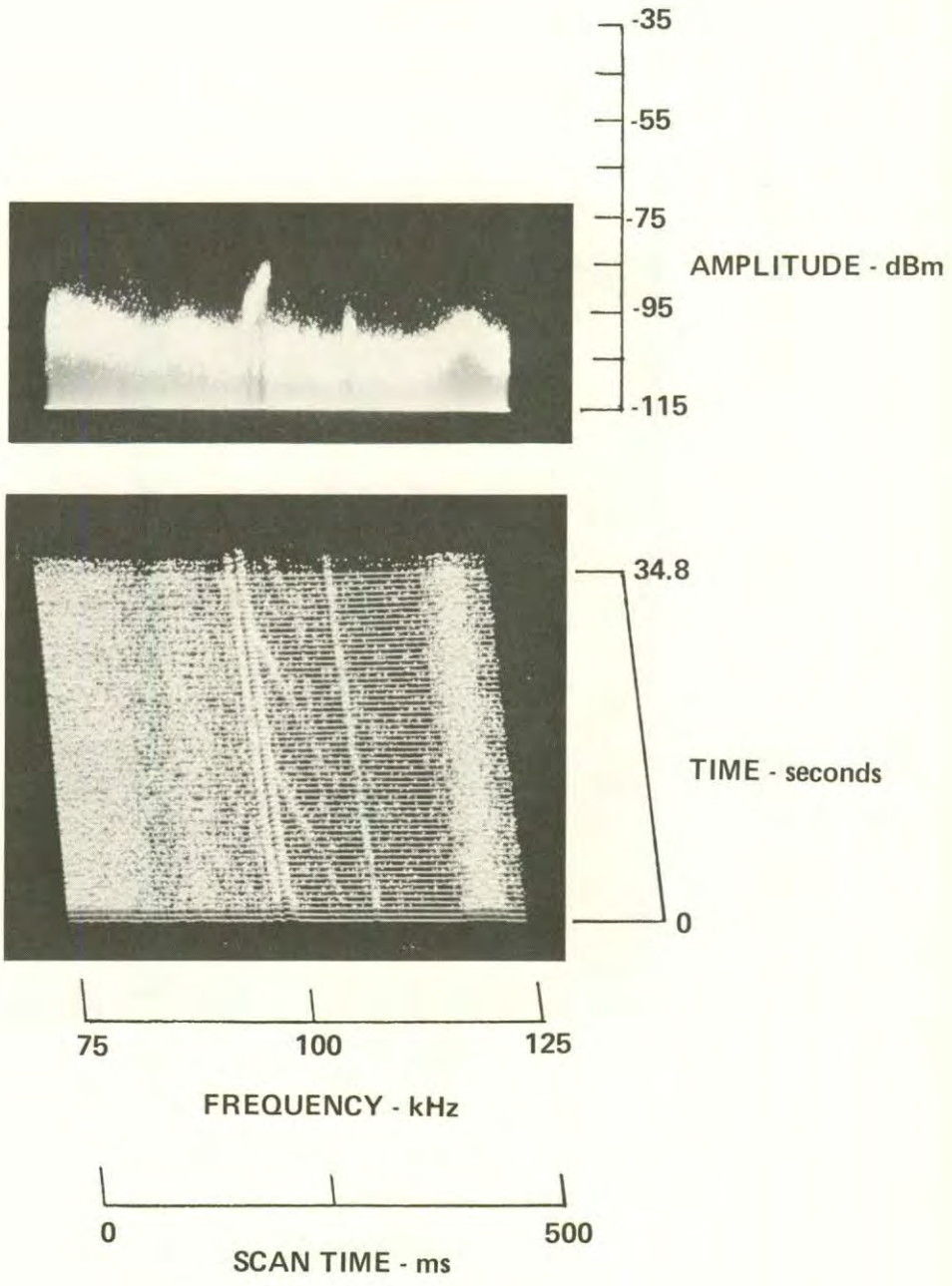

1-24-79, 0905, 107-034
HP140, Whip, F100, W50, IF3, ST 500, A -20/0/+15/NF

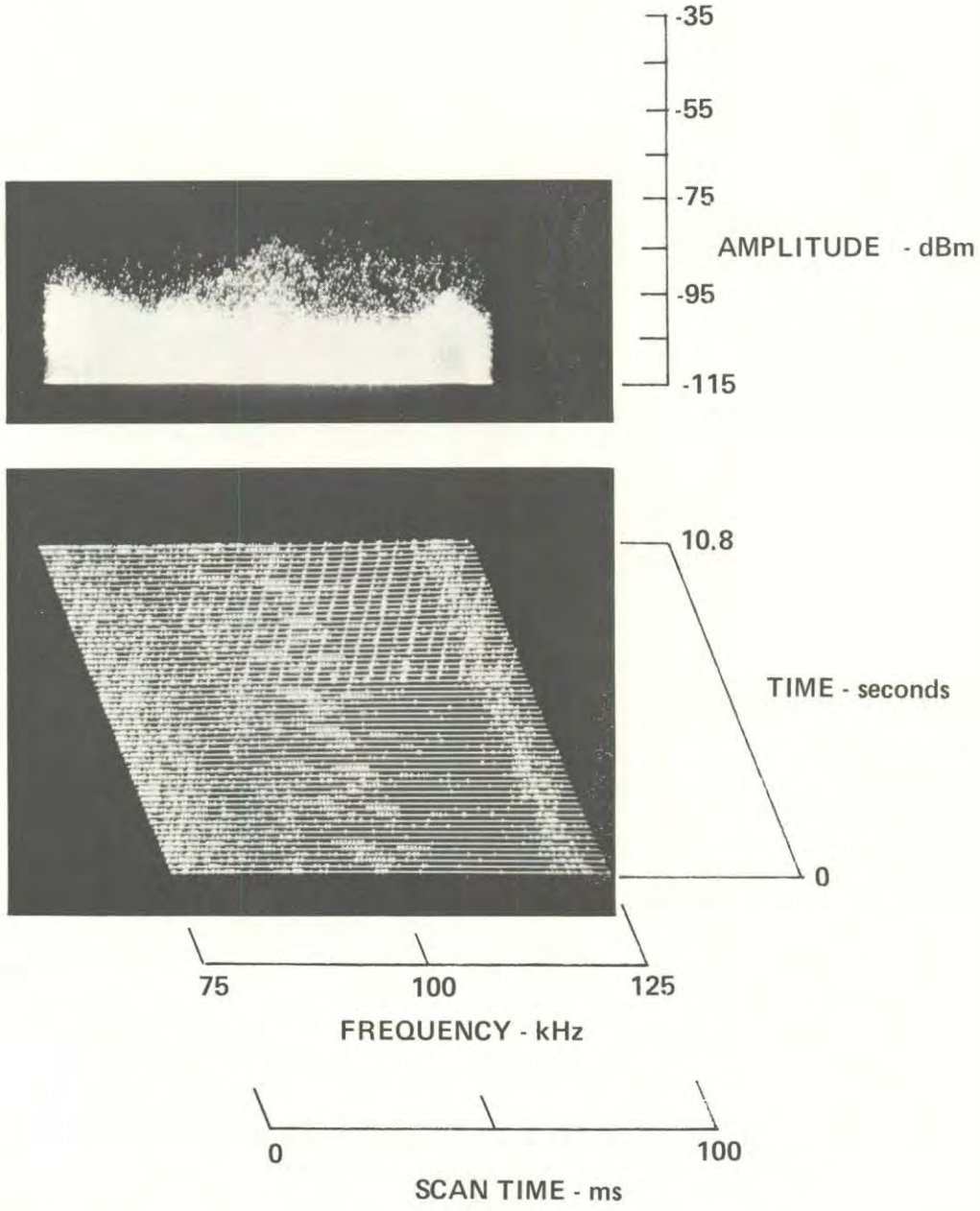
-35
-55
-75
AMPLITUDE - dBm
-95
-115
10.8
TIME - seconds
0
75
100
125
FREQUENCY - kHz
0
100
SCAN TIME - ms

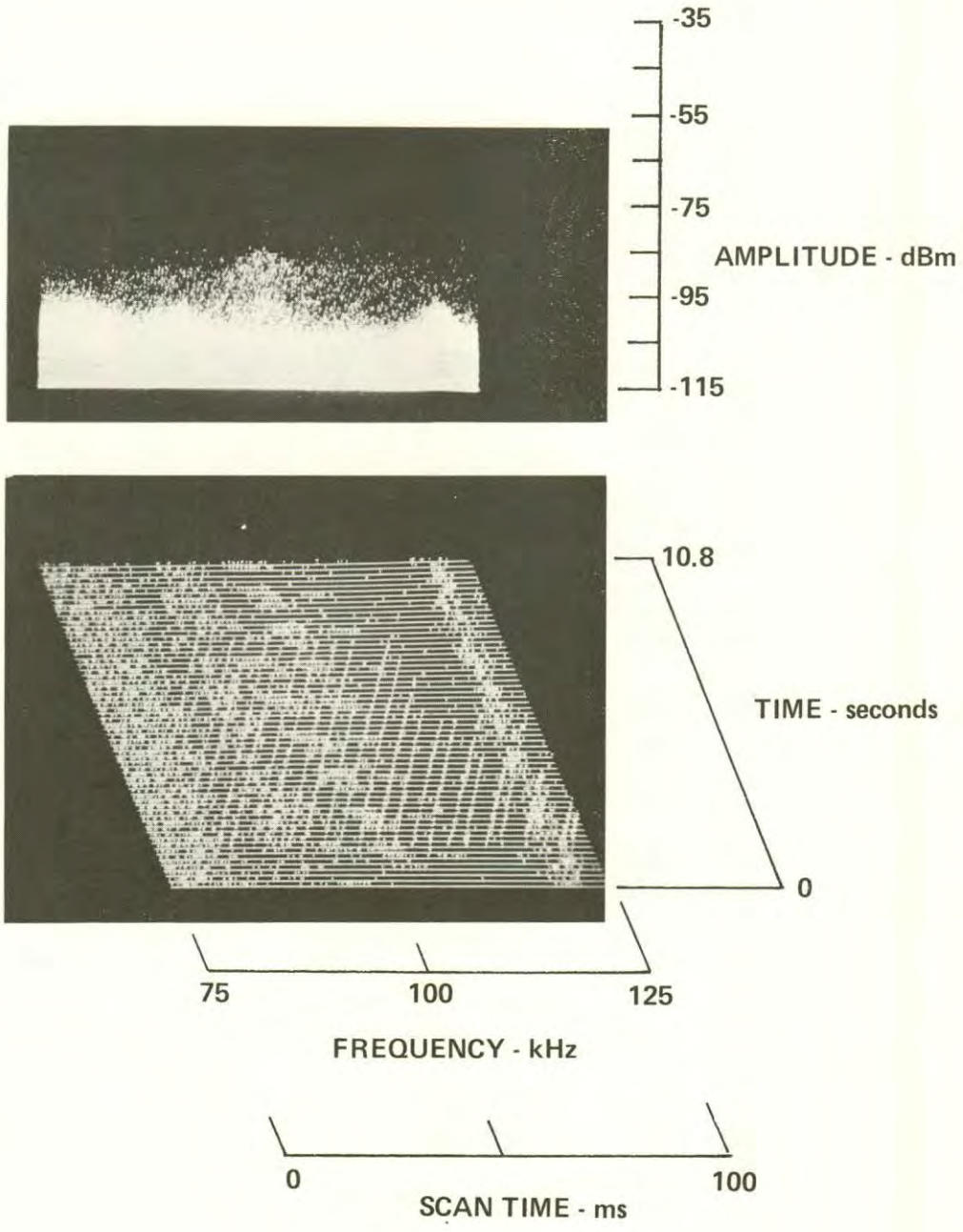

1-24-79, 0923, 107-034
HP140, Whip, F100, W50, IF3, ST 100, A -20/0/+15/NF

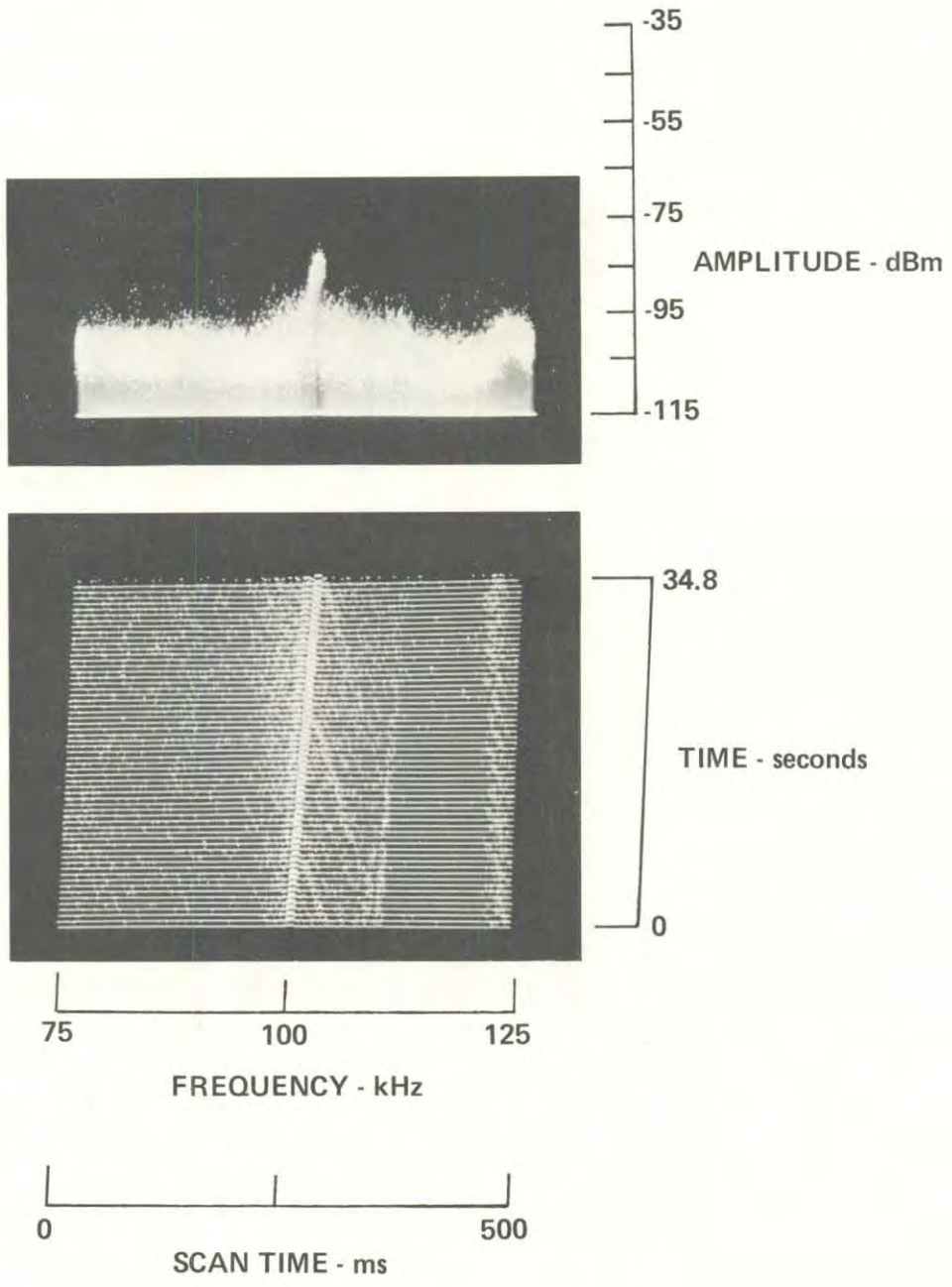

1-24-79, 1001, 107-036
HP140, Whip, F100, W50, IF3, ST 500, A -20/0/+15/NF

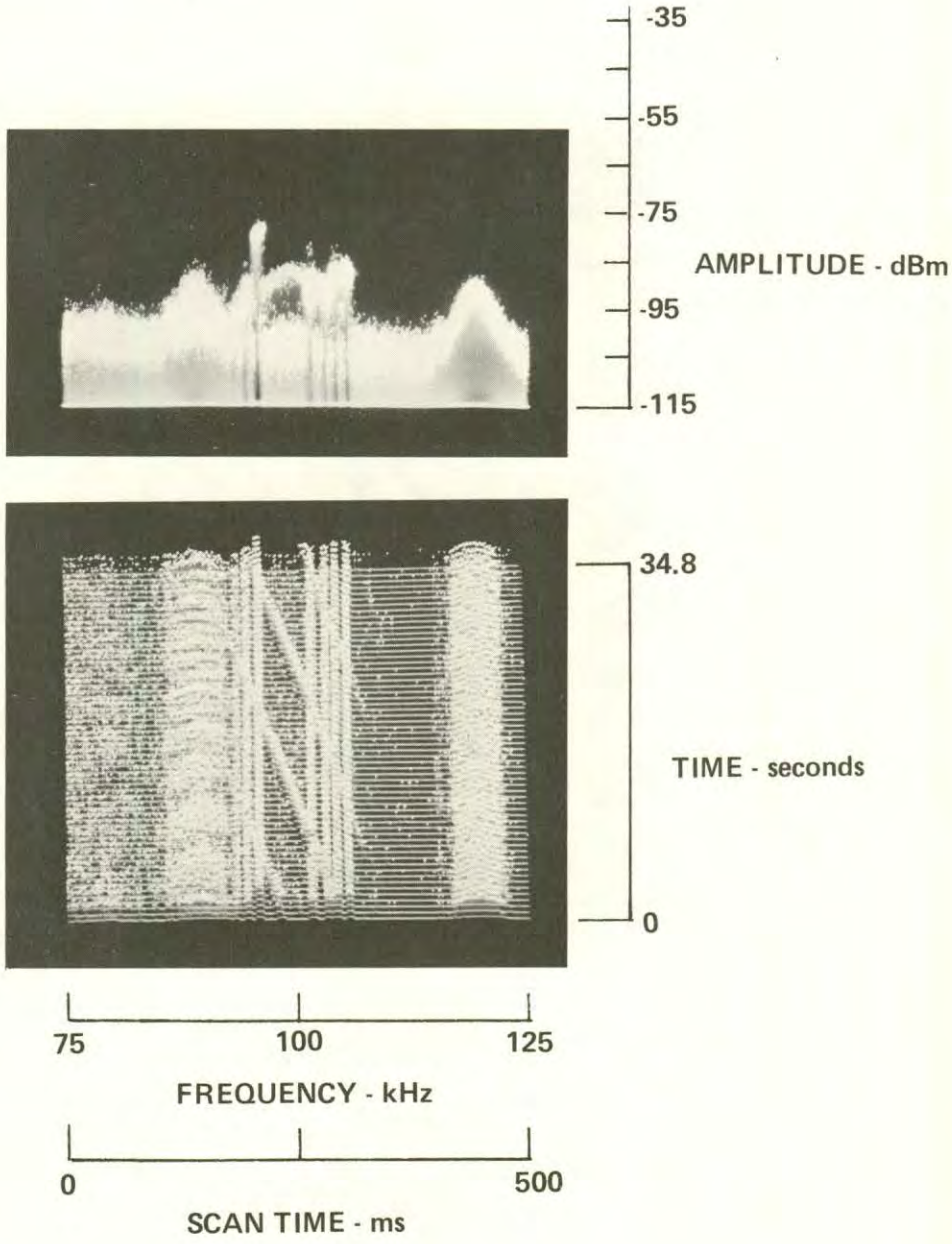

1-24-79, 1006, 107-037
HP140, Whip, F100, W50, IF3, ST 500, A -20/0/+15/NF

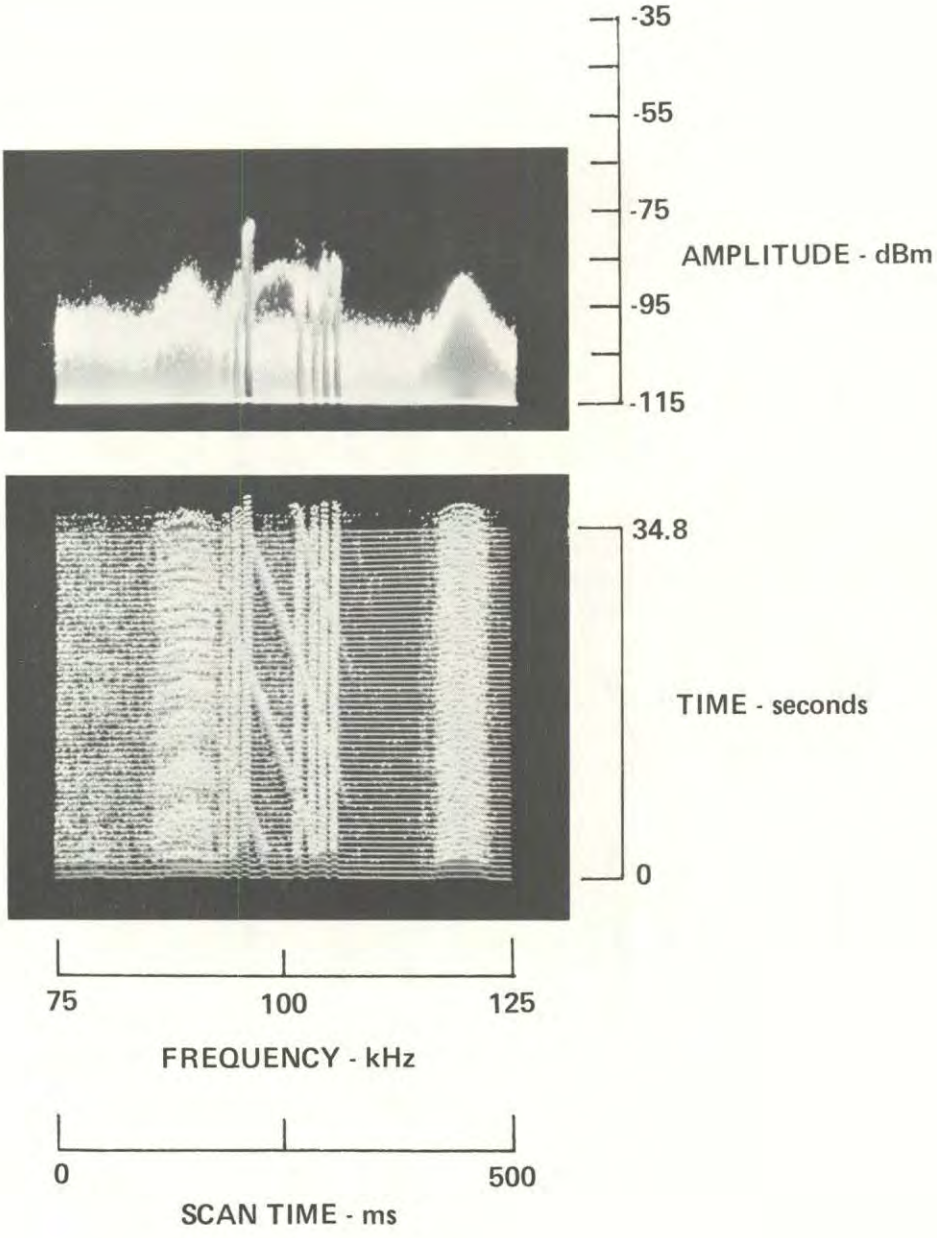

1-24-79, 1011, 107-038
HP140, Whip, F100, W50, IF3, ST 500, A -20/0/+15/NF

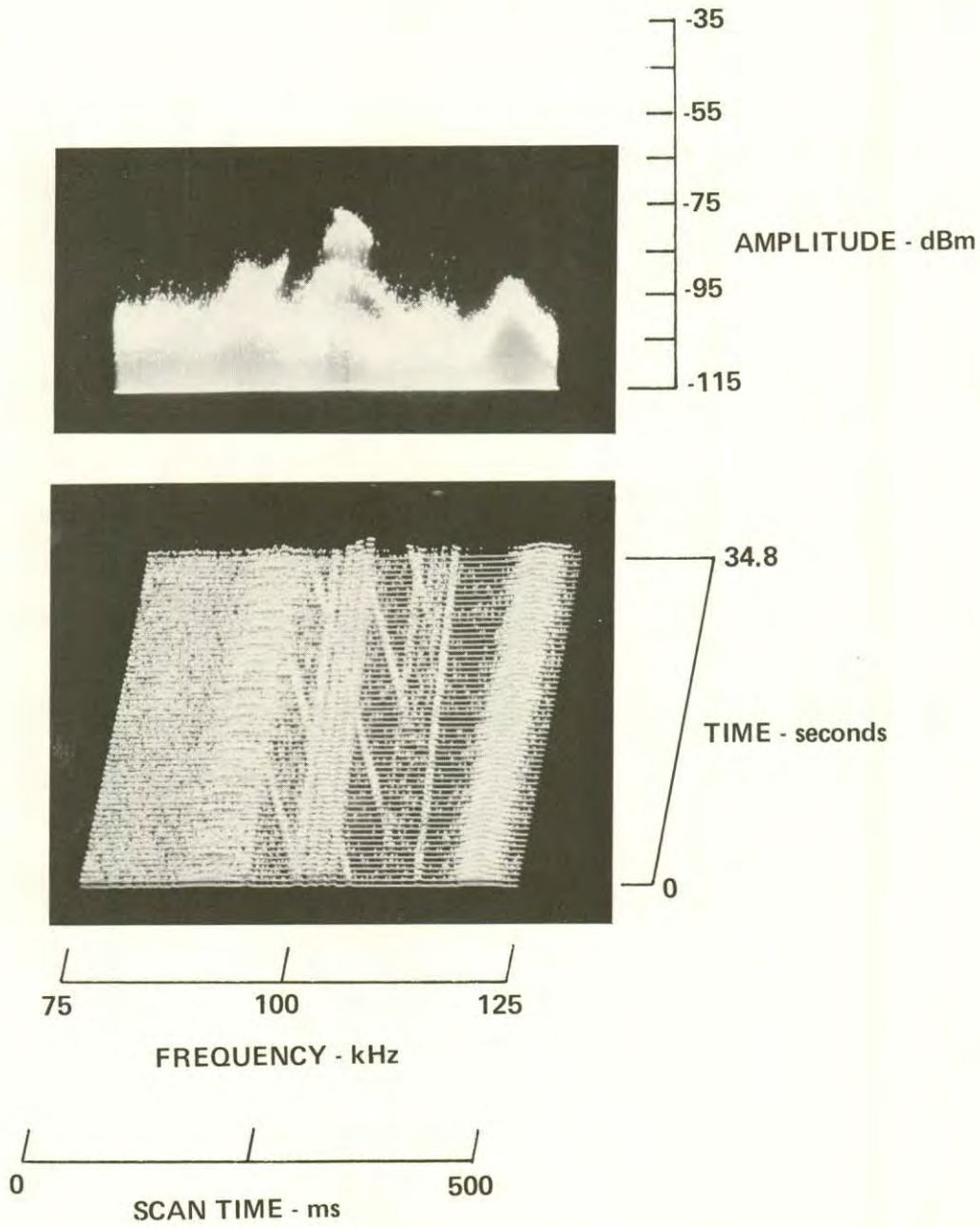
-35
-55
-75
AMPLITUDE - dBm
-95
-115
34.8
TIME - seconds
0
75
100
125
FREQUENCY - kHz
0
500
SCAN TIME - ms

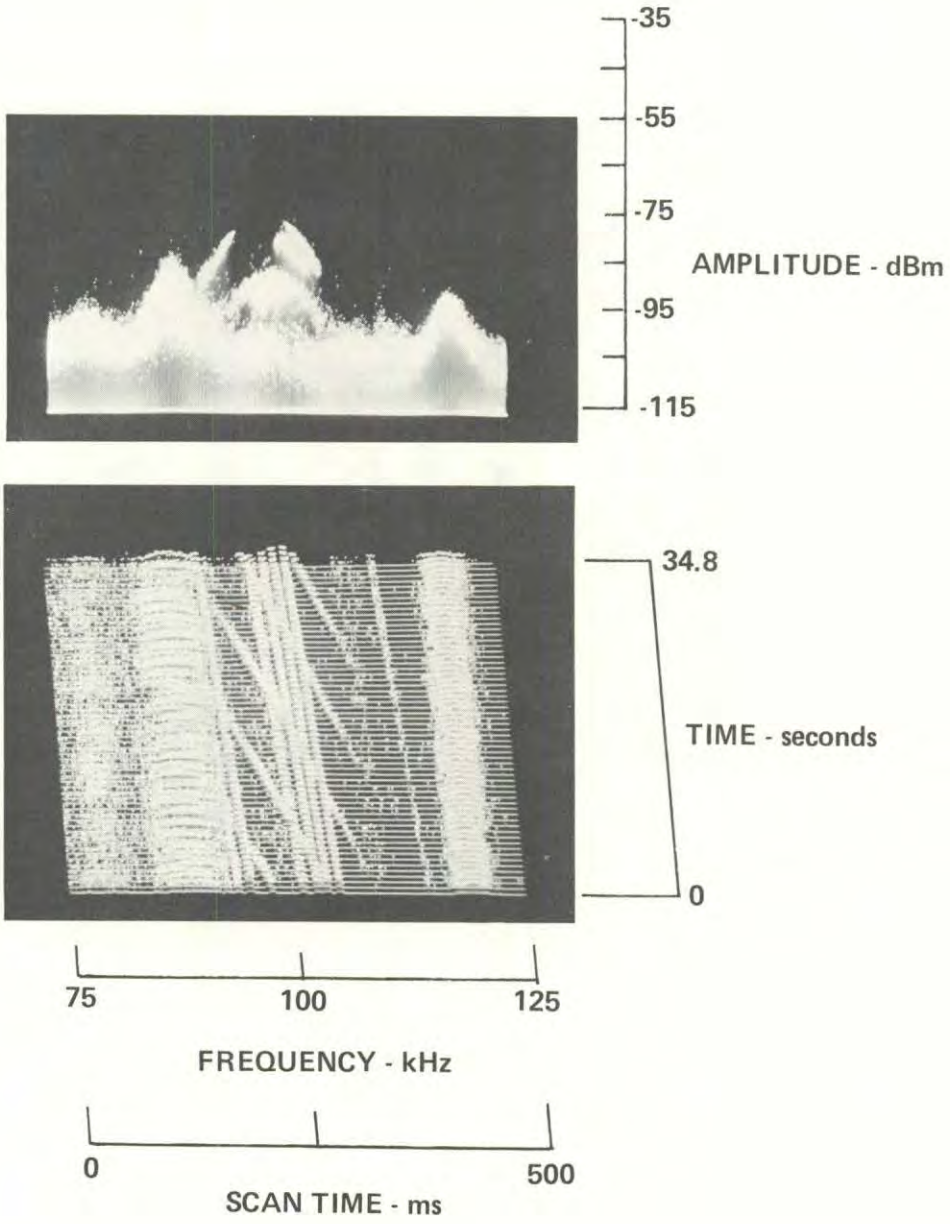

1-24-79, 1040, 107-040
HP140, Whip, F100,W50, IF3, ST 500, A -20/0/+15/NF

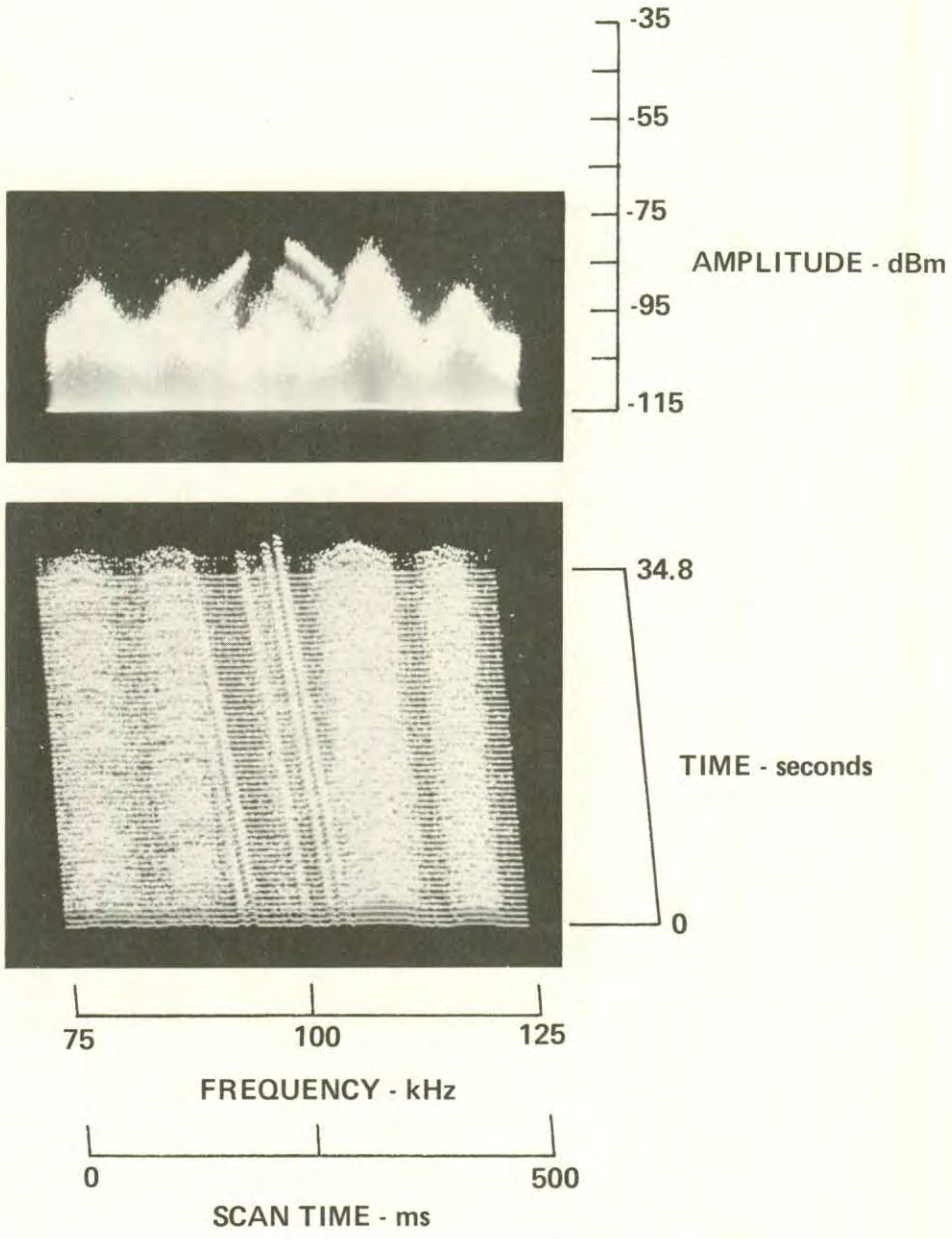

1-25-79, 0752, 110-041
HP140, Whip, F100, W50, IF3, ST 500, A -20/0/+15/NF

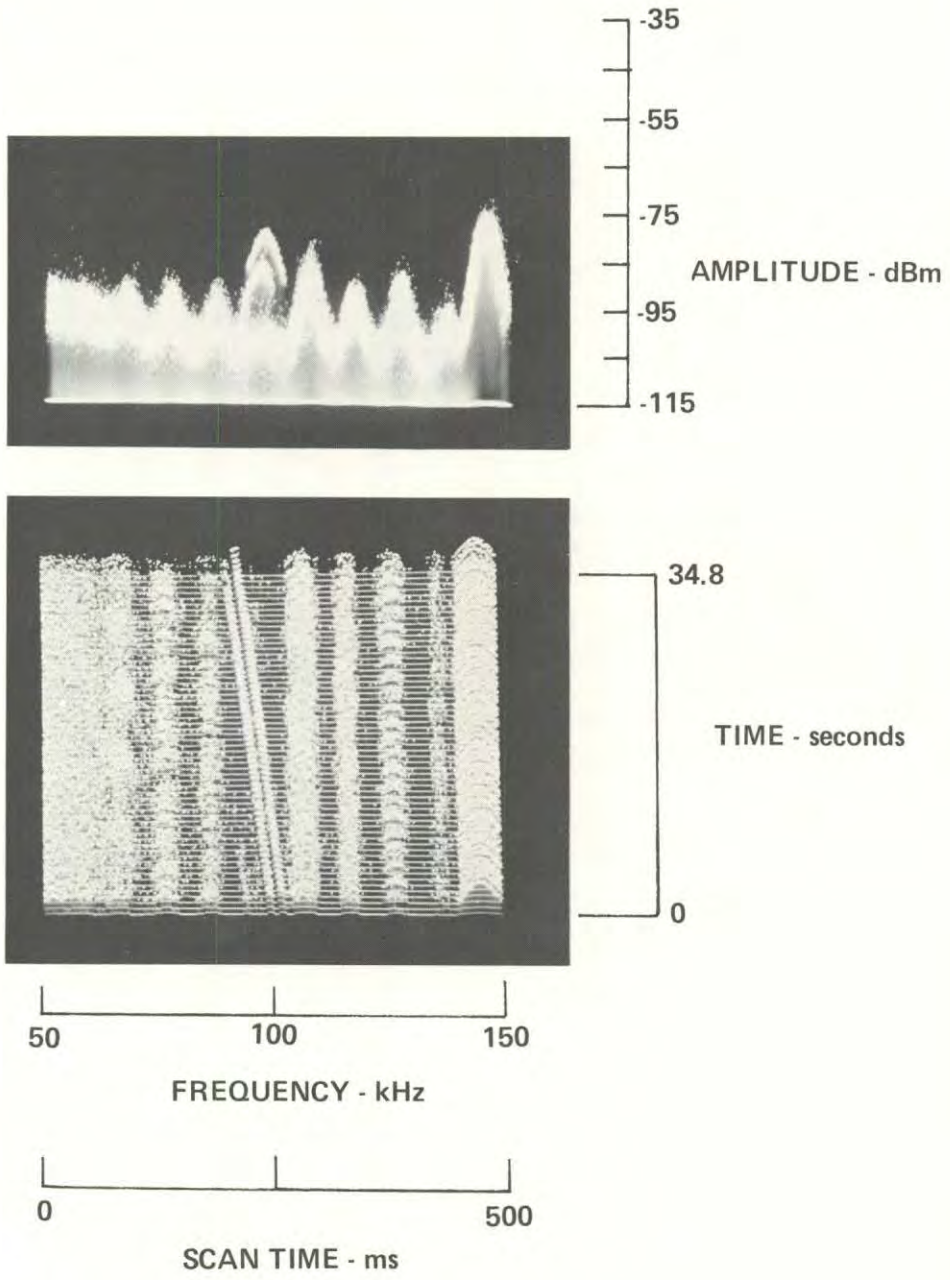

1-25-79, 0757, 110-041
HP140, Whip, F100, W100, IF3, ST 500, A -20/0/+15/NF

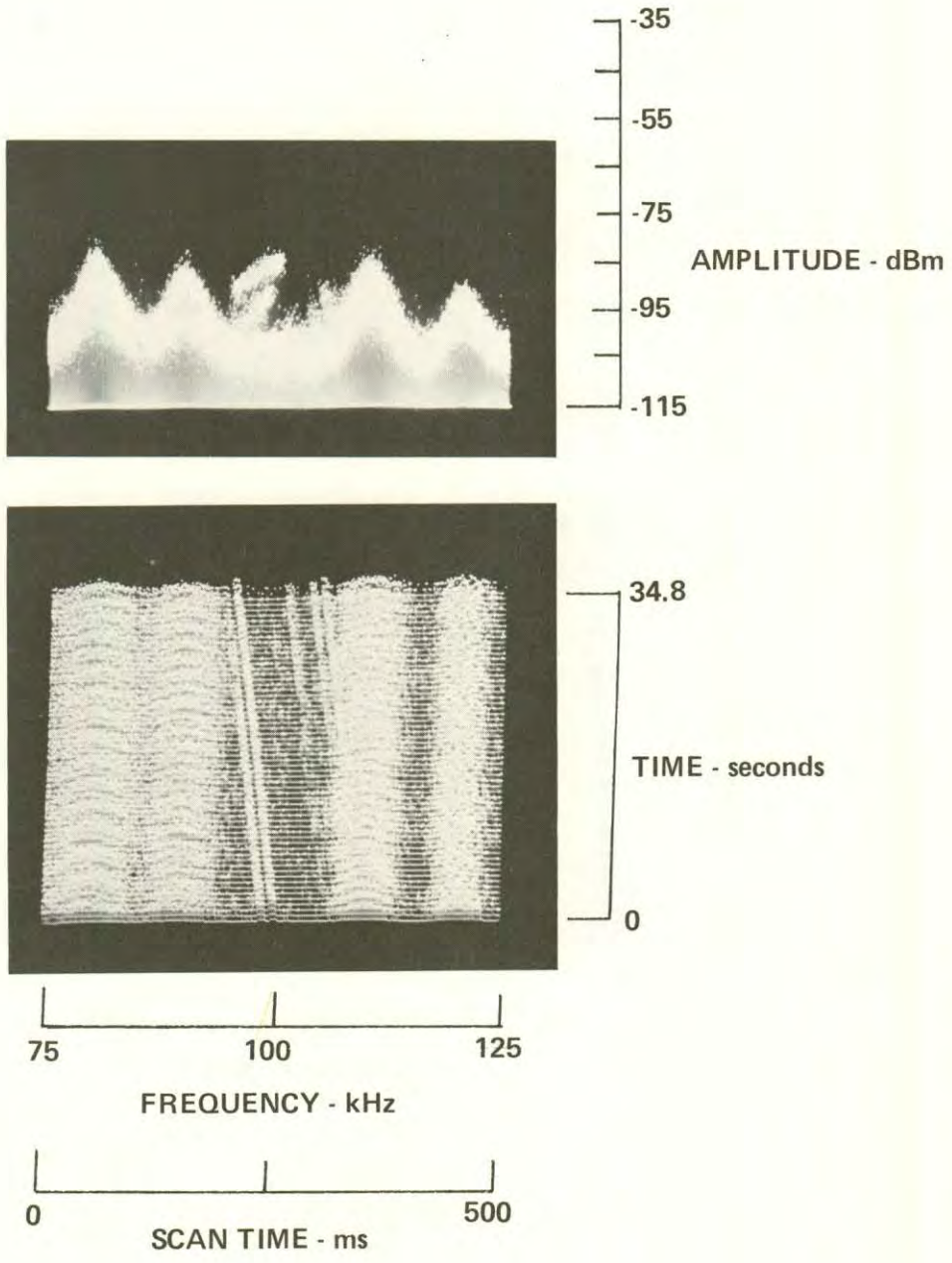

1-25-79, 0803, 110-042
HP140, Whip, F100, W50, IF3, ST 500, A -20/0/+15/NF

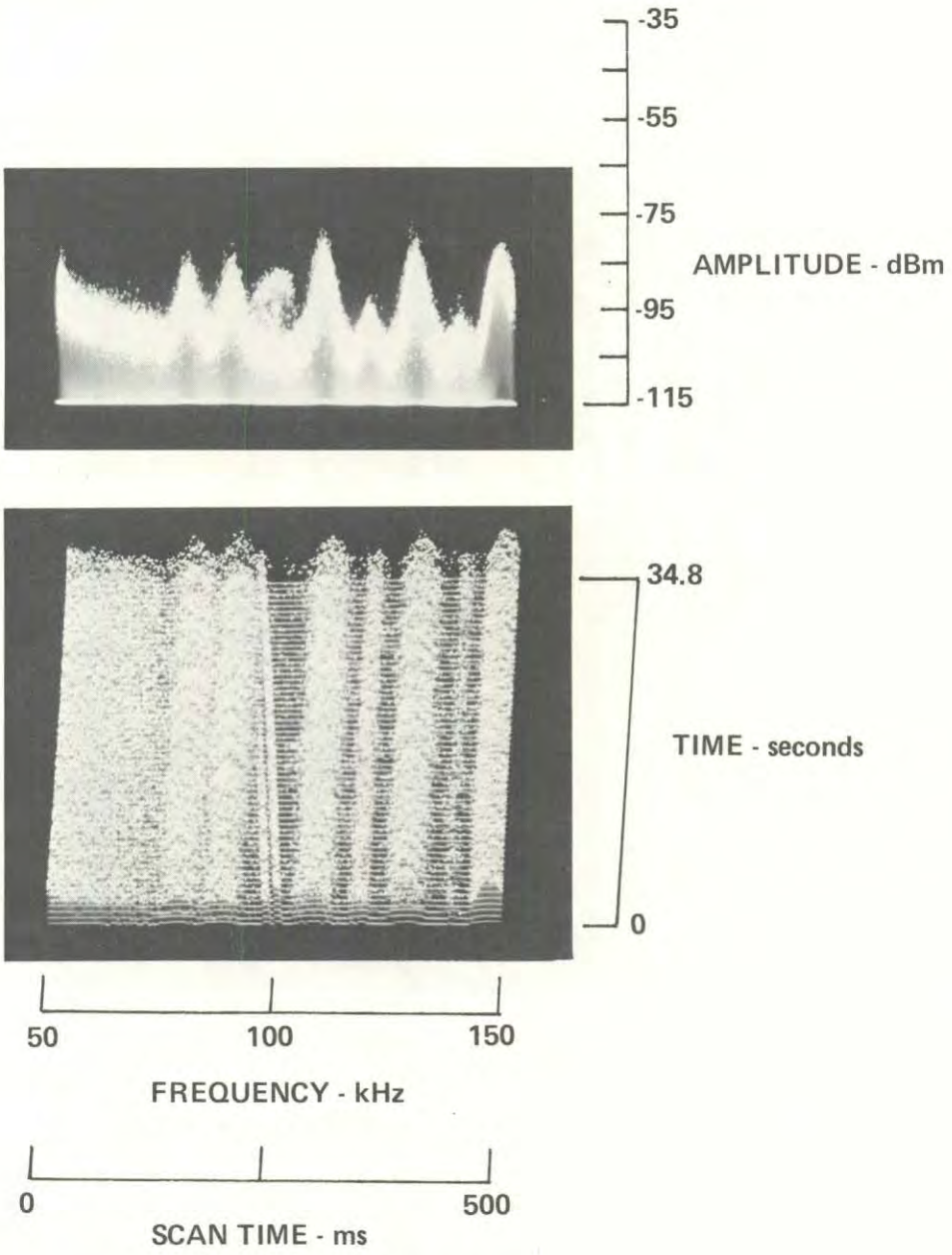

1-25-79, 0810, 110-042
HP140, Whip, F100, W100, IF3, ST 500, A -20/0/+15

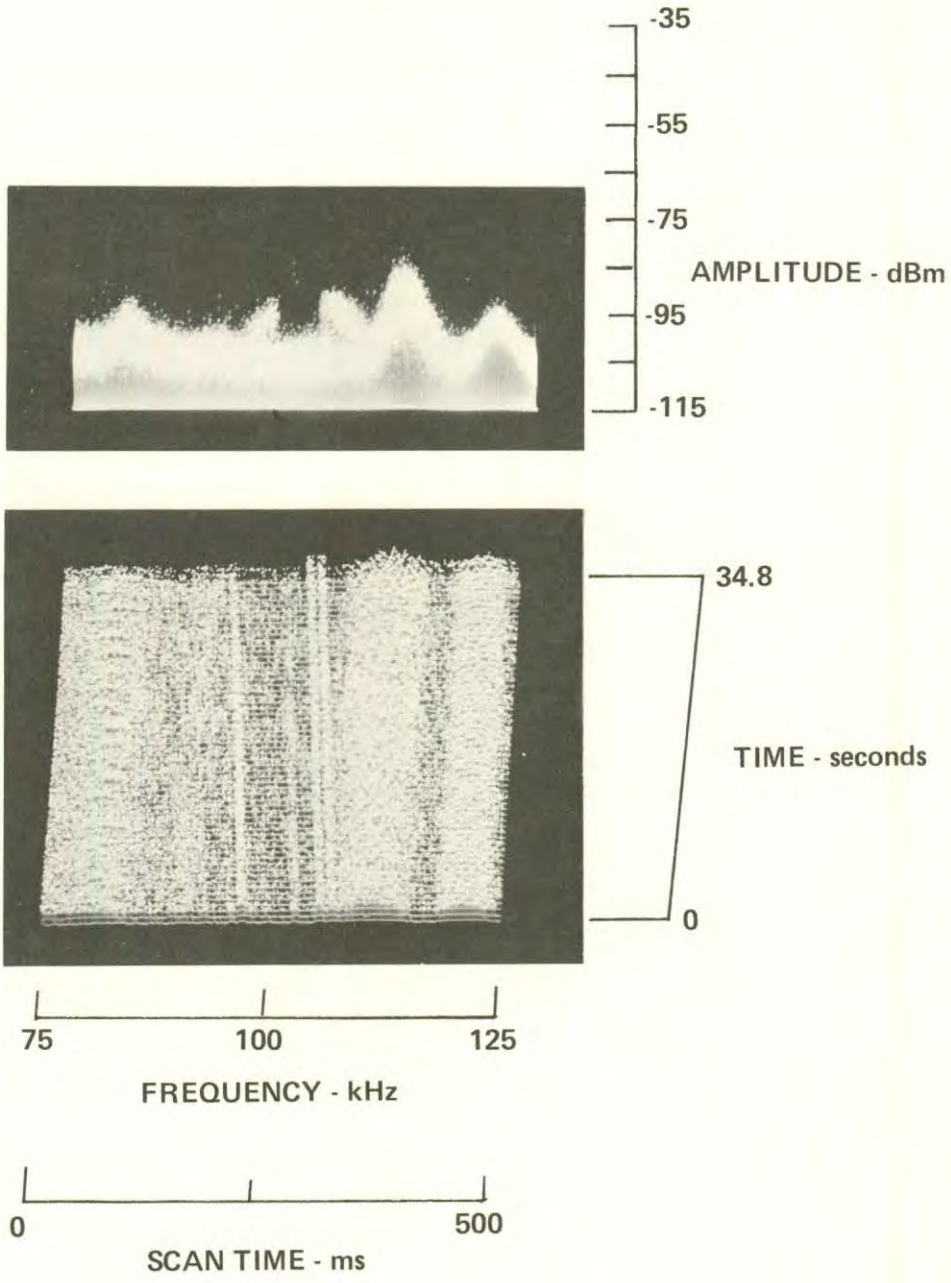

1-25-79, 0817, 110-044
HP140, Whip, F100, W50, IF3, ST 500, A -20/0/+15/NF

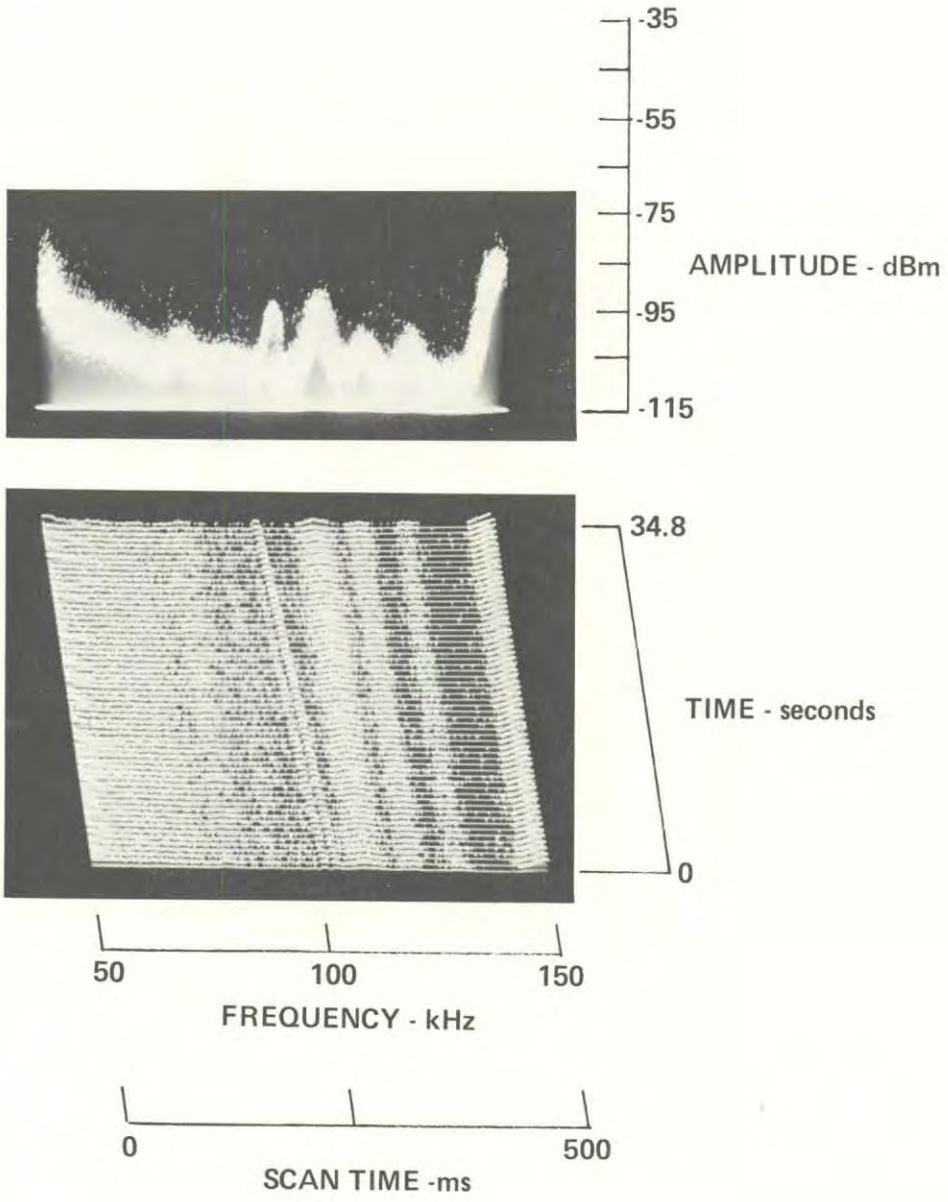

1-25-79, 0823, 110-044
HP140, Whip, F100, W100, IF3, ST 500, A -20/0/+15/NF

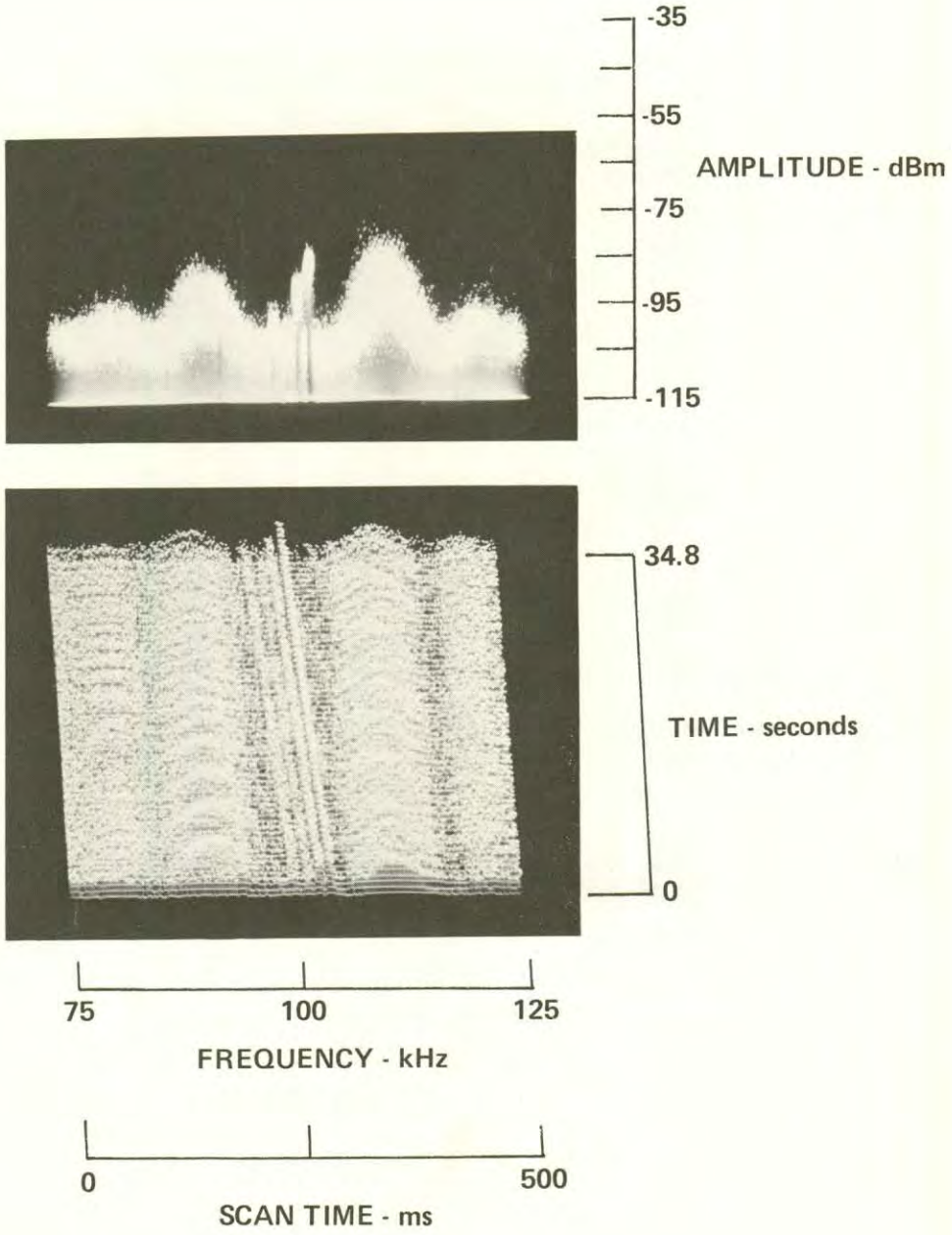

1-25-79, 0833, 110-045
HP140, Whip, F100, W50, IF3, ST 500, A -20/0/+15/NF

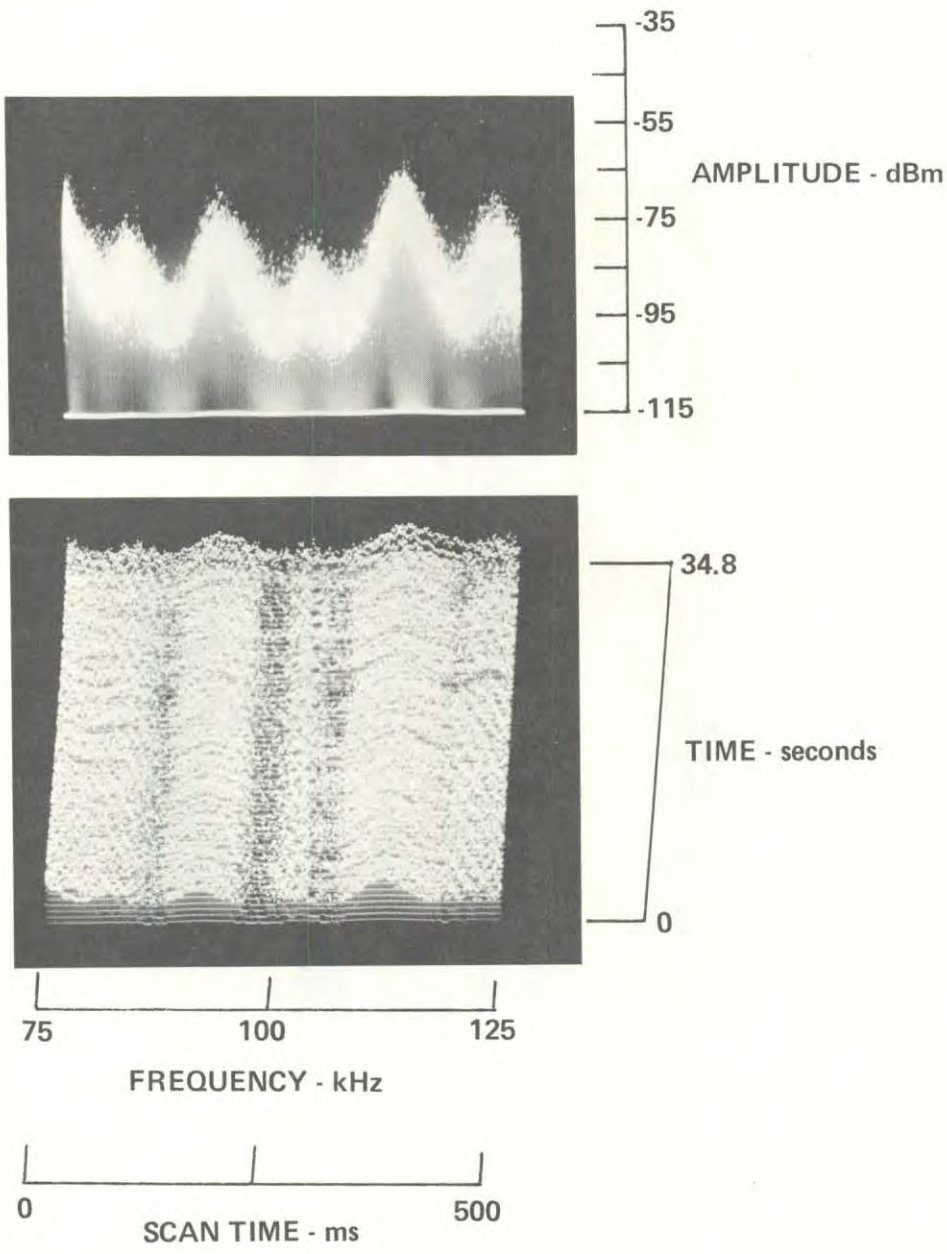

1-25-79, 0846, 110-046
HP140, Whip, F100, W50, IF3, ST500, A -20/0/+15/NF

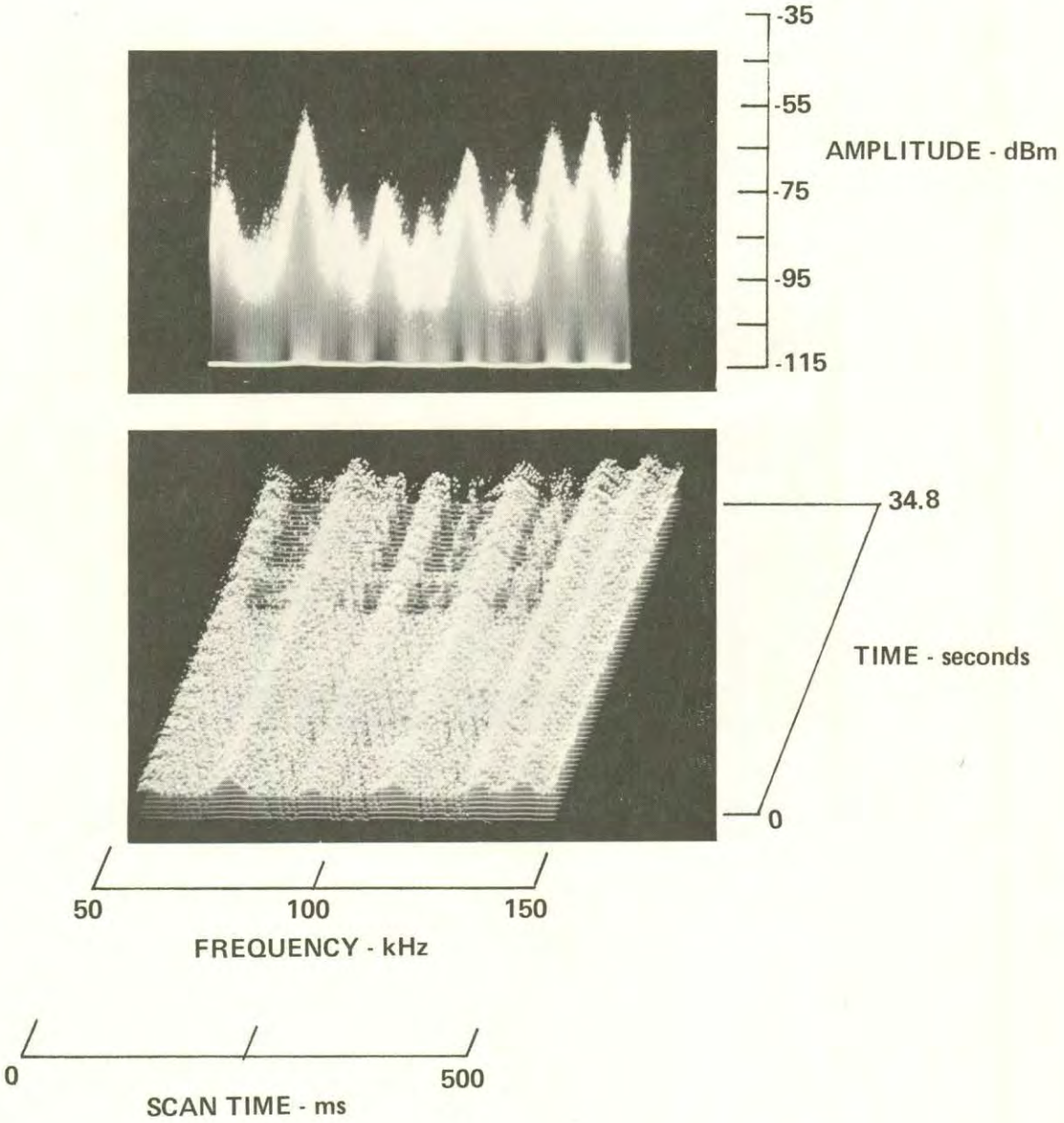

1-25-79, 0853, 110-046,
HP140, Whip, F100, W100, IF3, ST 500, A -20/0/+15/NF

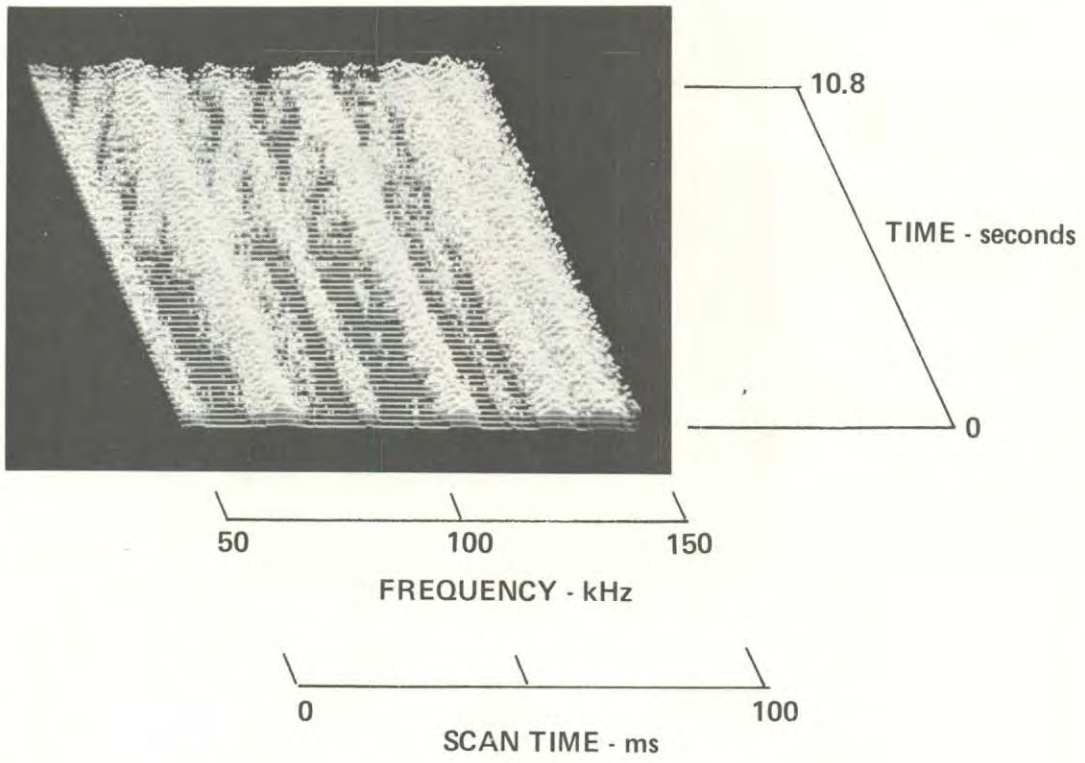

1-25-79, 0851, 110-046
HP140, Whip, F100, W100, IF3, ST 100, A -20/0/+15/NF

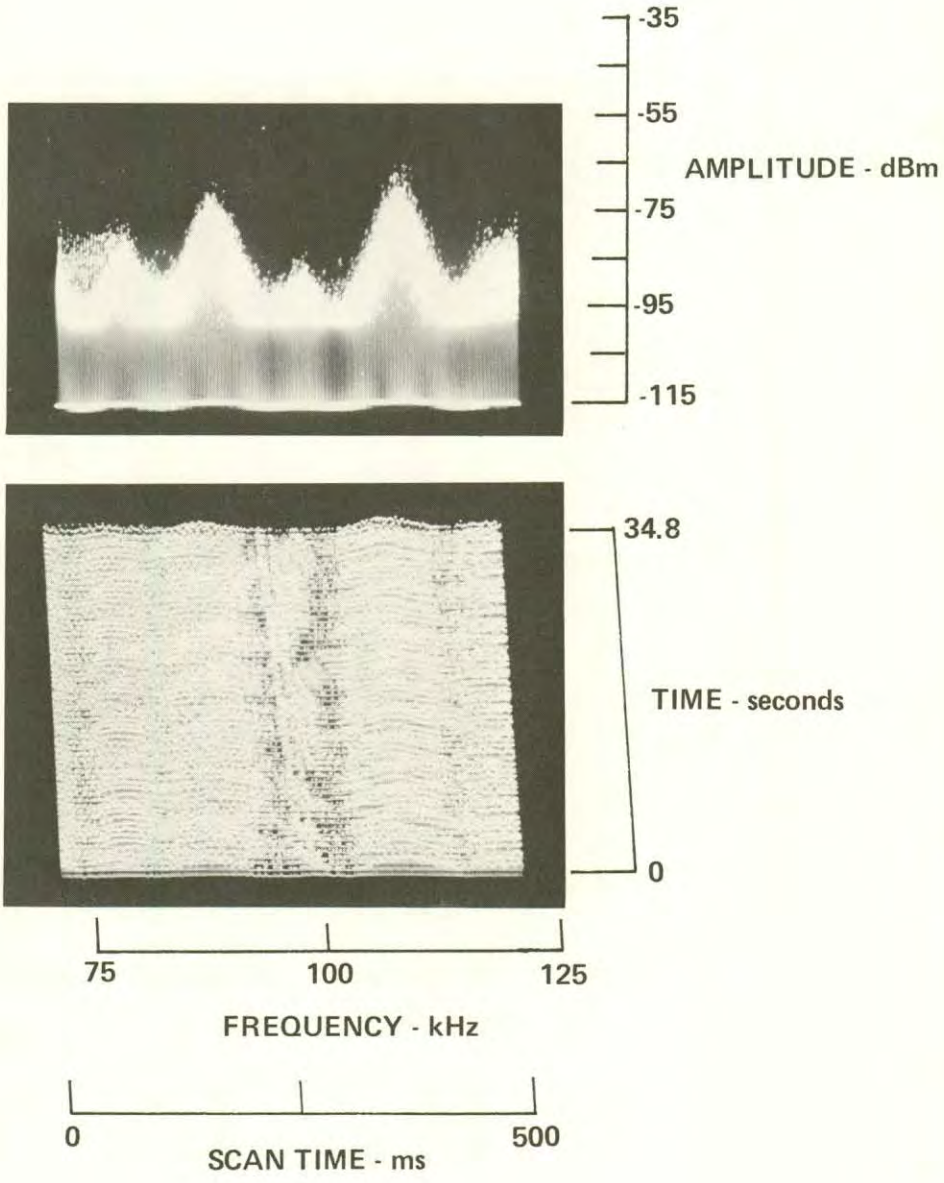

1-25-79, 0904, 110-047
HP140, Whip, F100, W50, IF3, ST 500, A -20/0/+15/NF

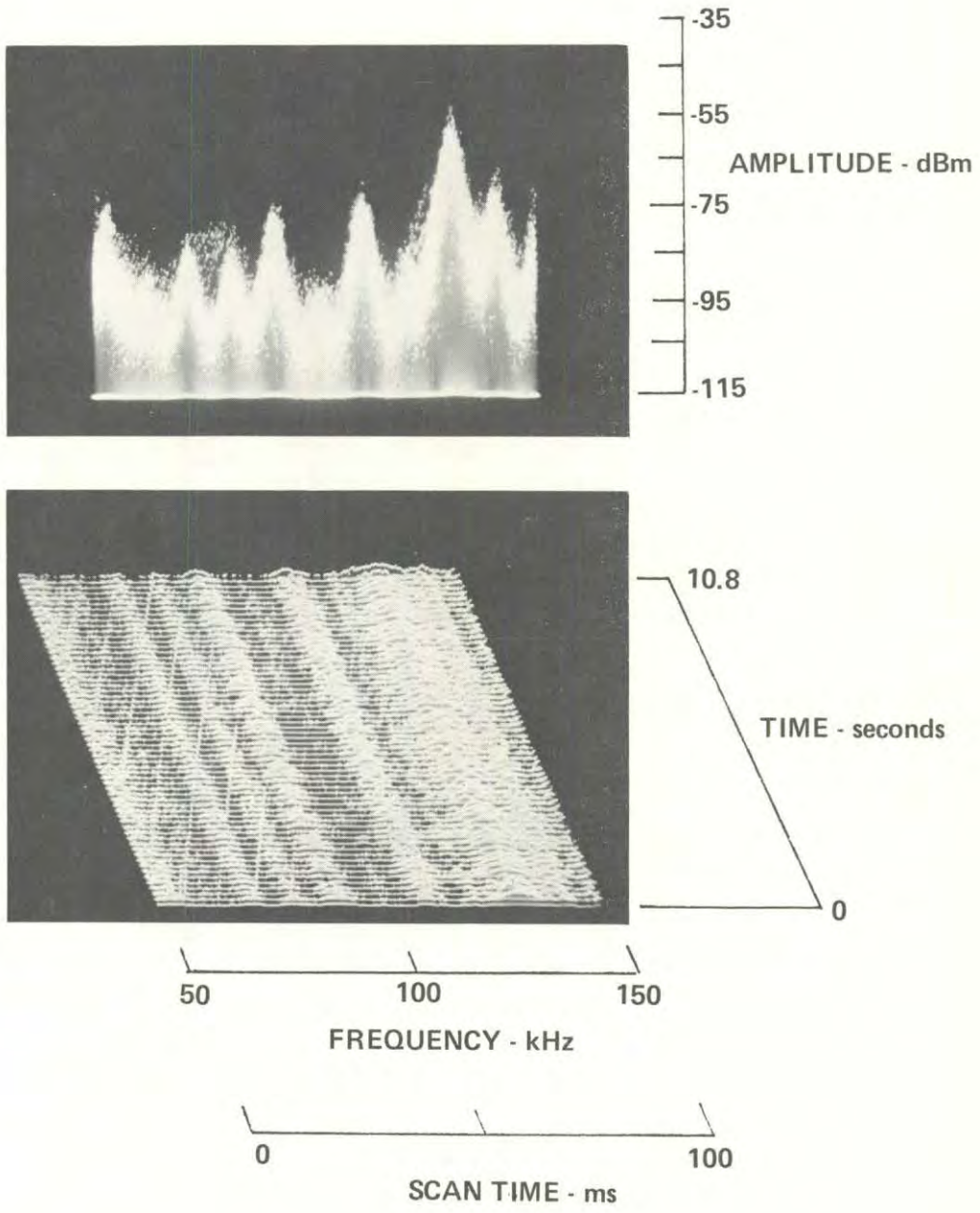

1-25-79, 0914, 110-047
HP140, Whip, F100, W100, IF3, ST 100, A -20/0/+15/NF

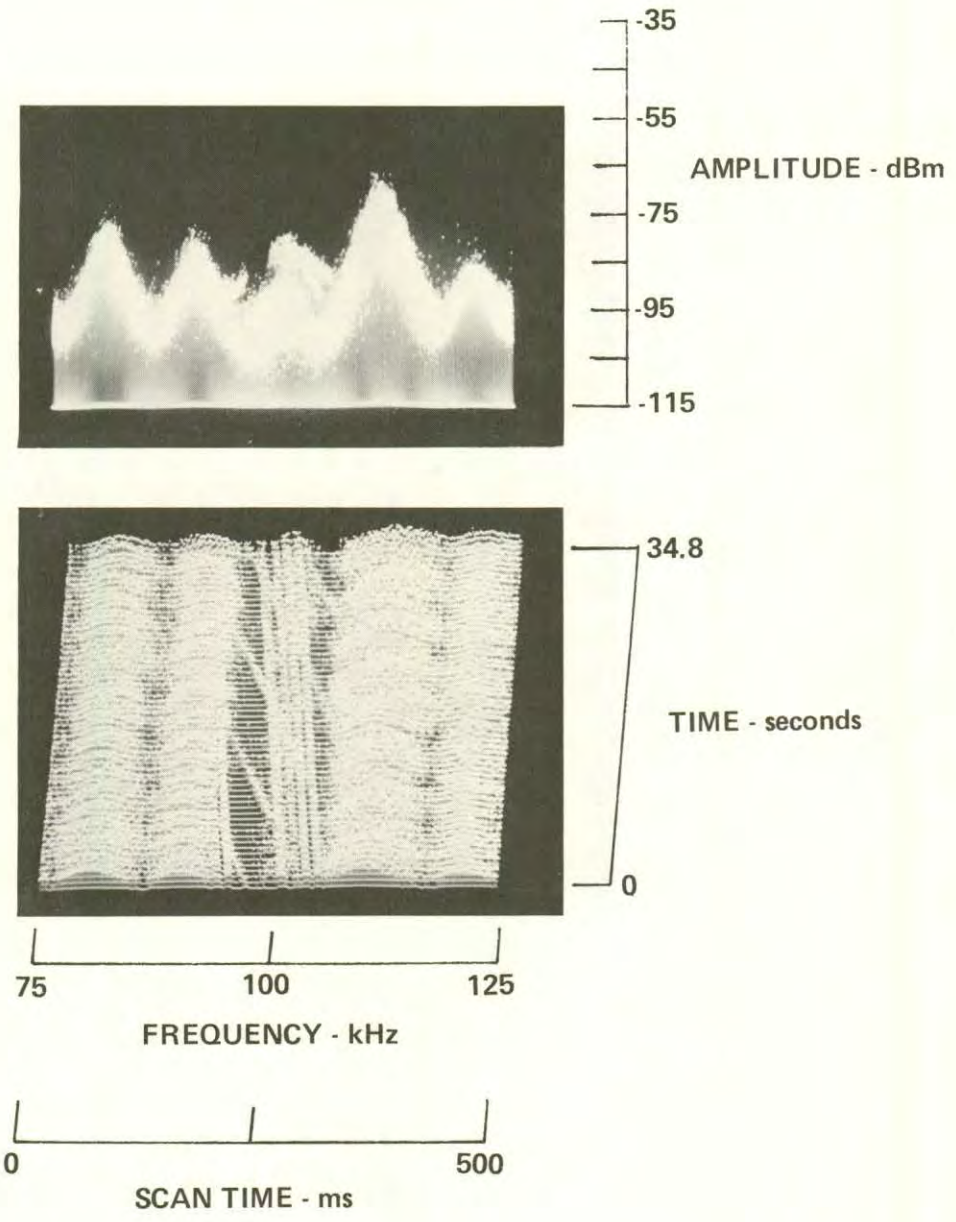

1-25-79, 0932, 110-048
HP140, Whip, F100, W50, IF3, ST 500, A -20/0/+15

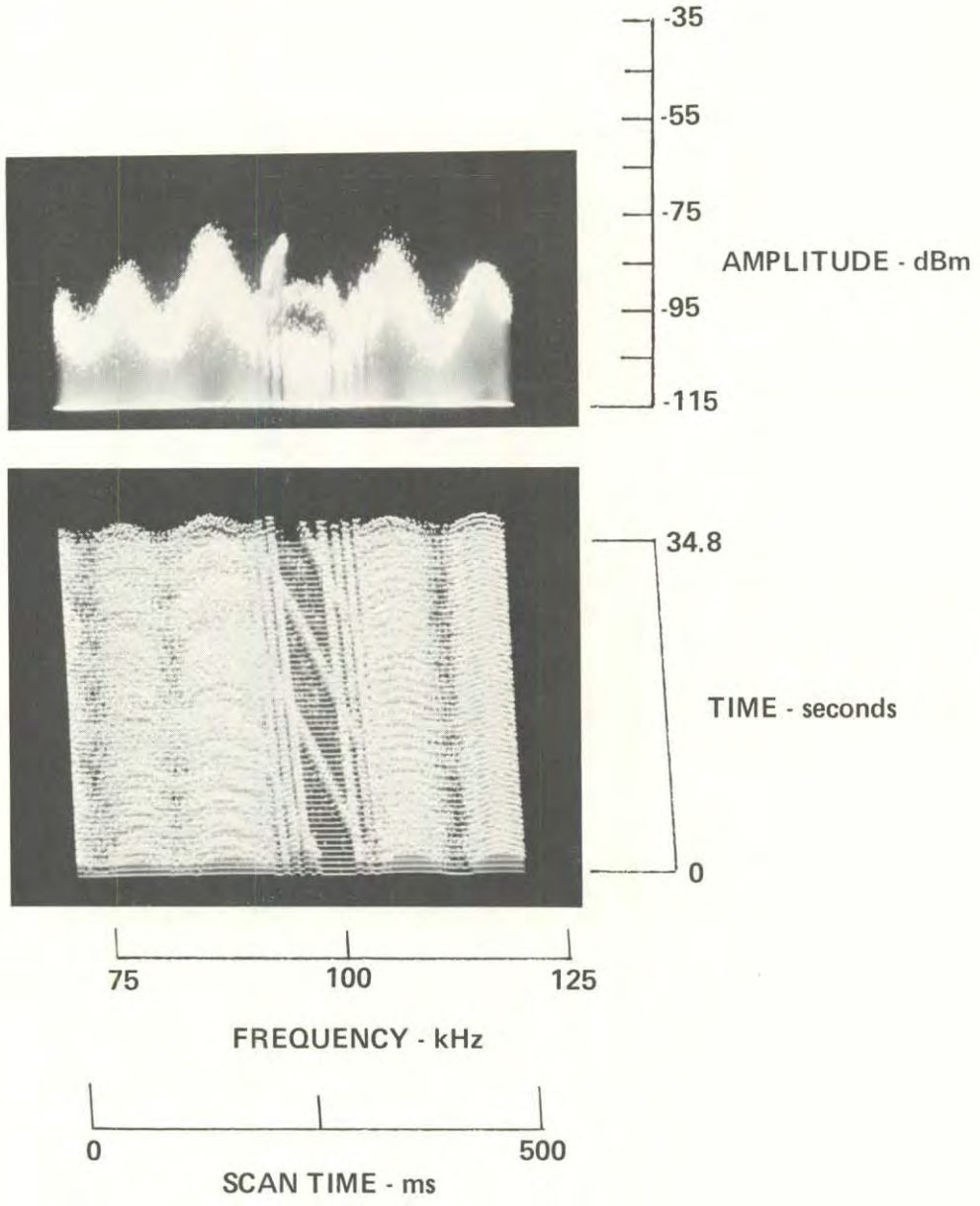

1-25-79, 0948, 110-049
HP140, Whip, F100, W50, IF3, ST 500, A -20/0/+15/NF

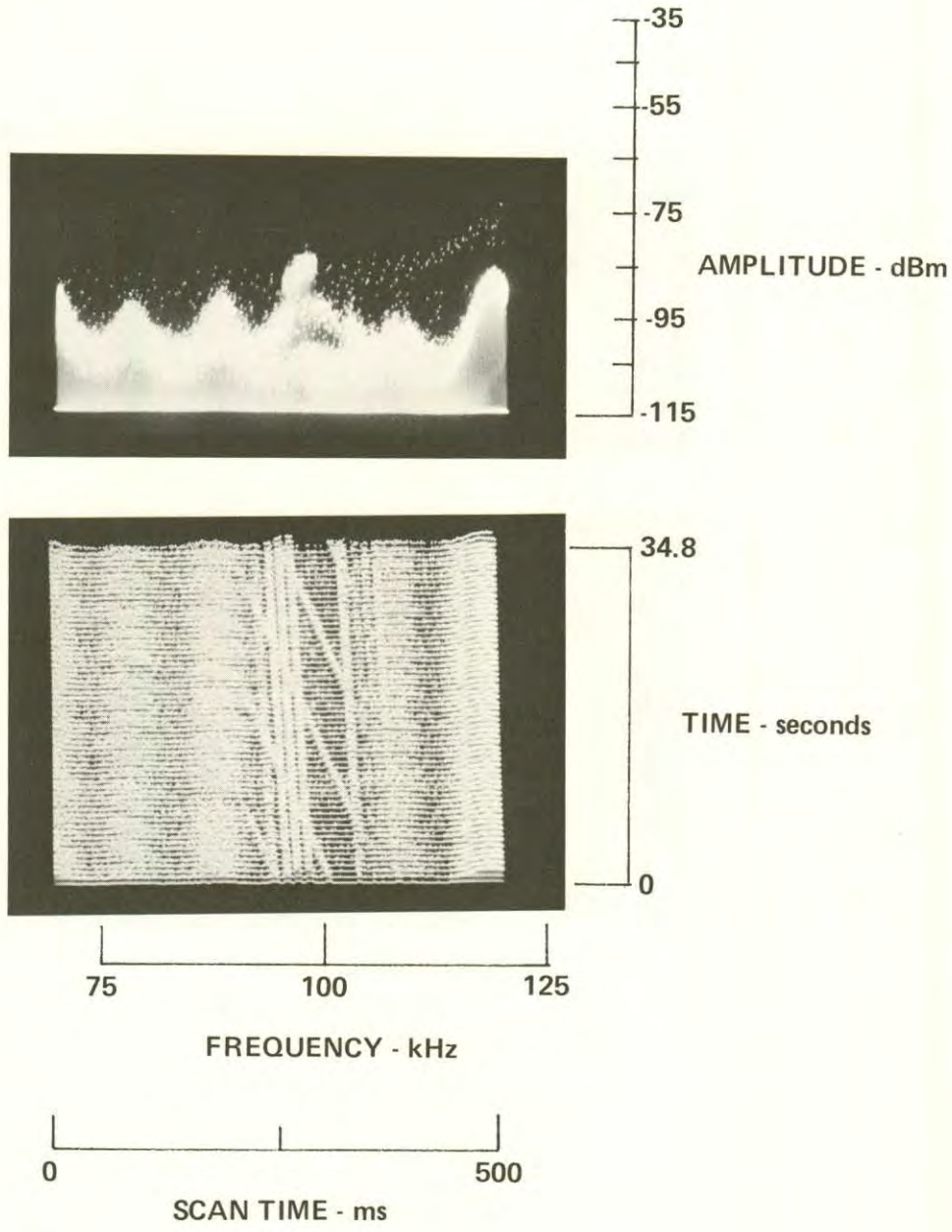

1-25-79, 0958, 110-050
HP140, Whip, F100, W50, IF3, ST 500, A -20/0/+15/NF

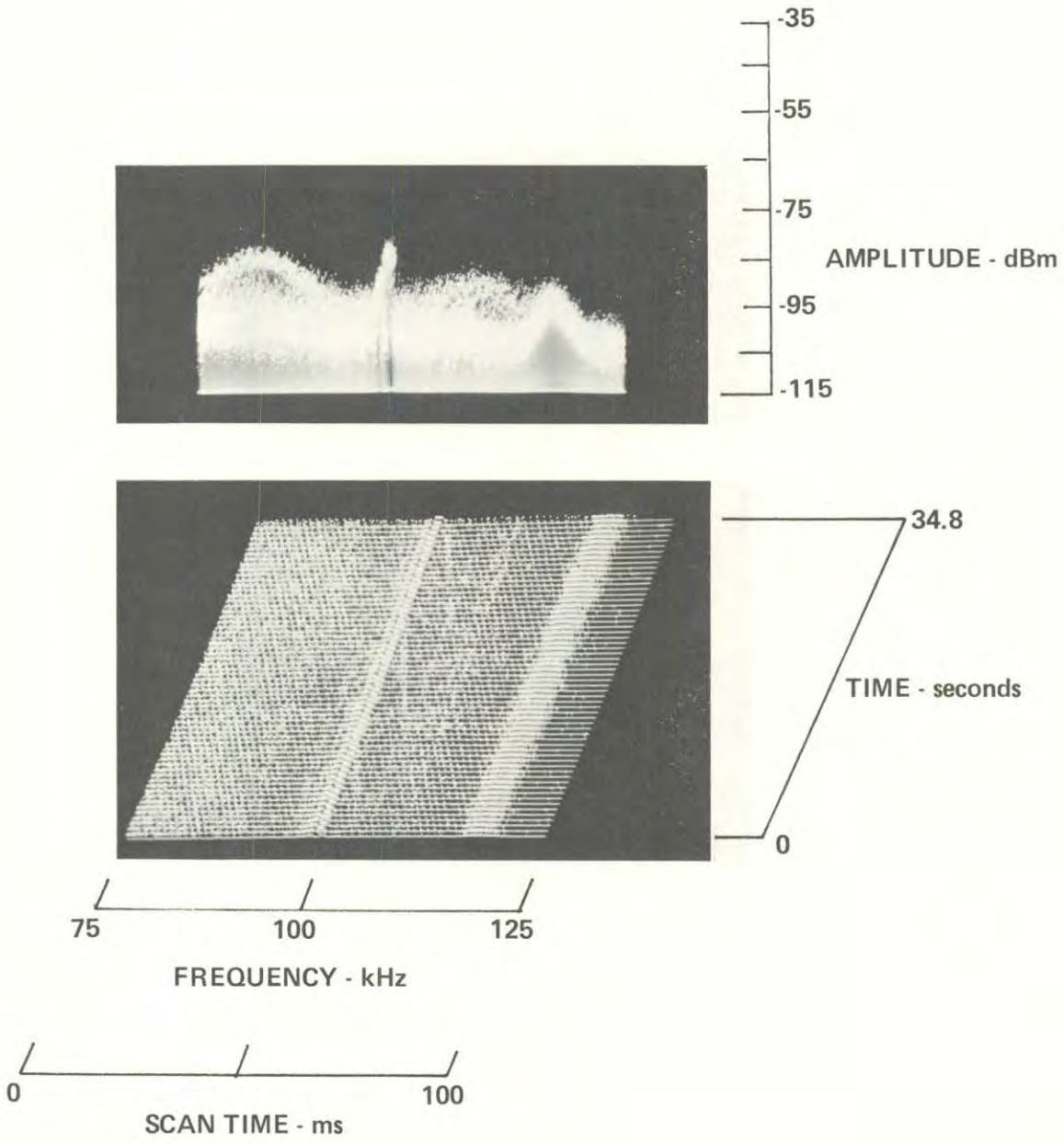

1-25-79, 1228, 104-051
HP140, Whip, F100, W50, IF3, ST 100, A -20/0/+15/NF

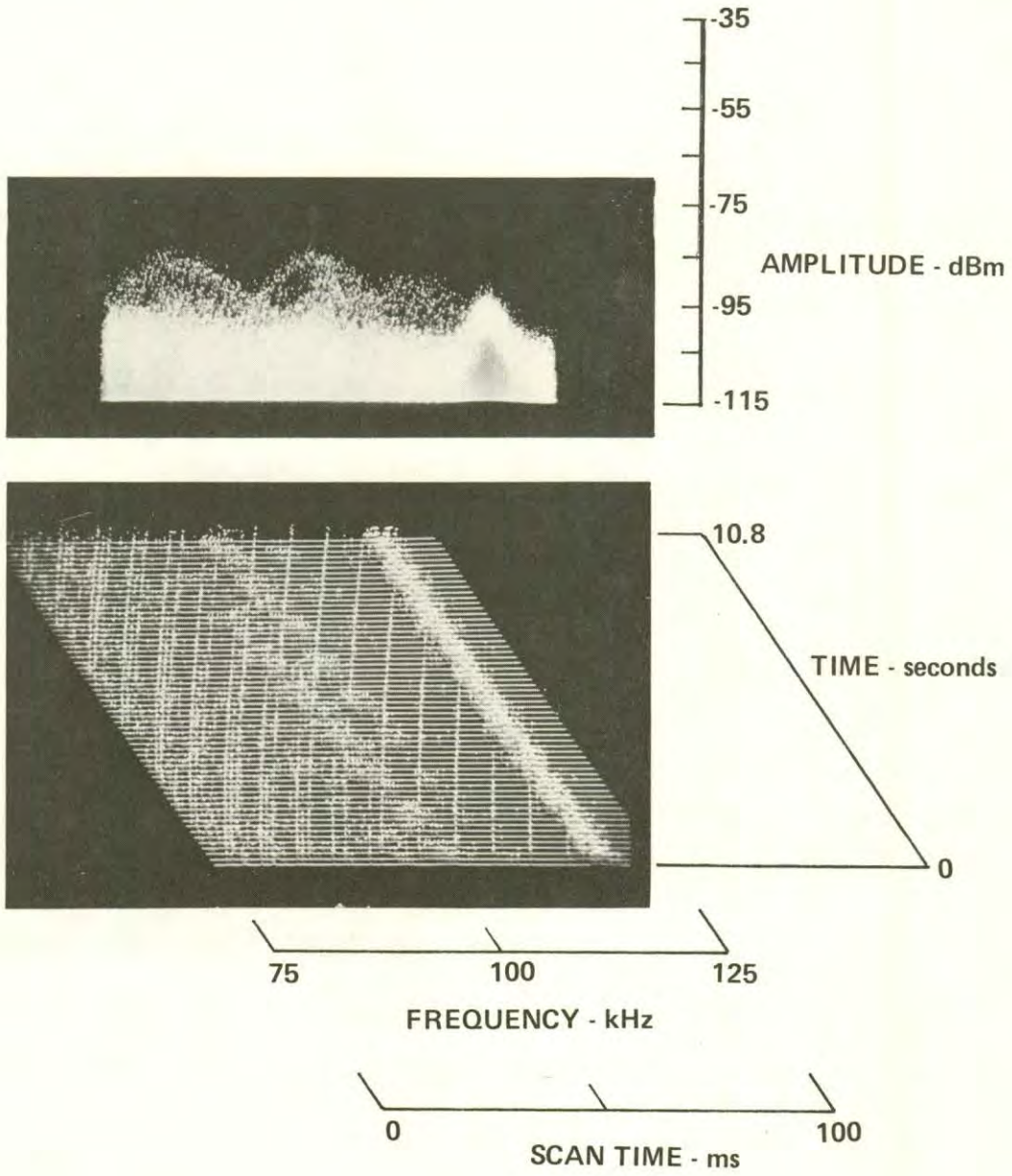

1-25-79, 1227, 104-051
HP140, Whip, F100, W50, IF3, ST 100, A -20/0/+15

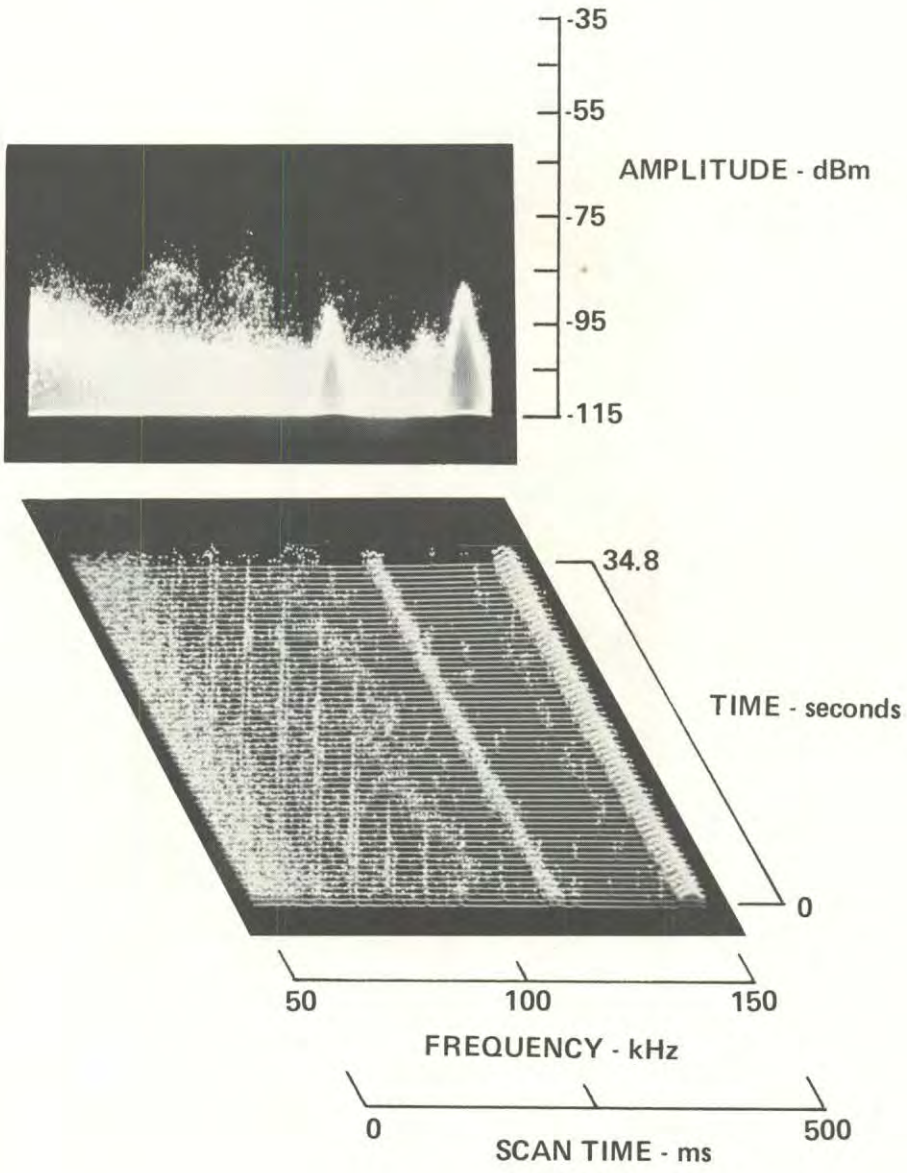

1-25-79, 1230, 104-051
HP140, Whip, F100, W100, IF3, ST 500, A -20/0/+15/NF

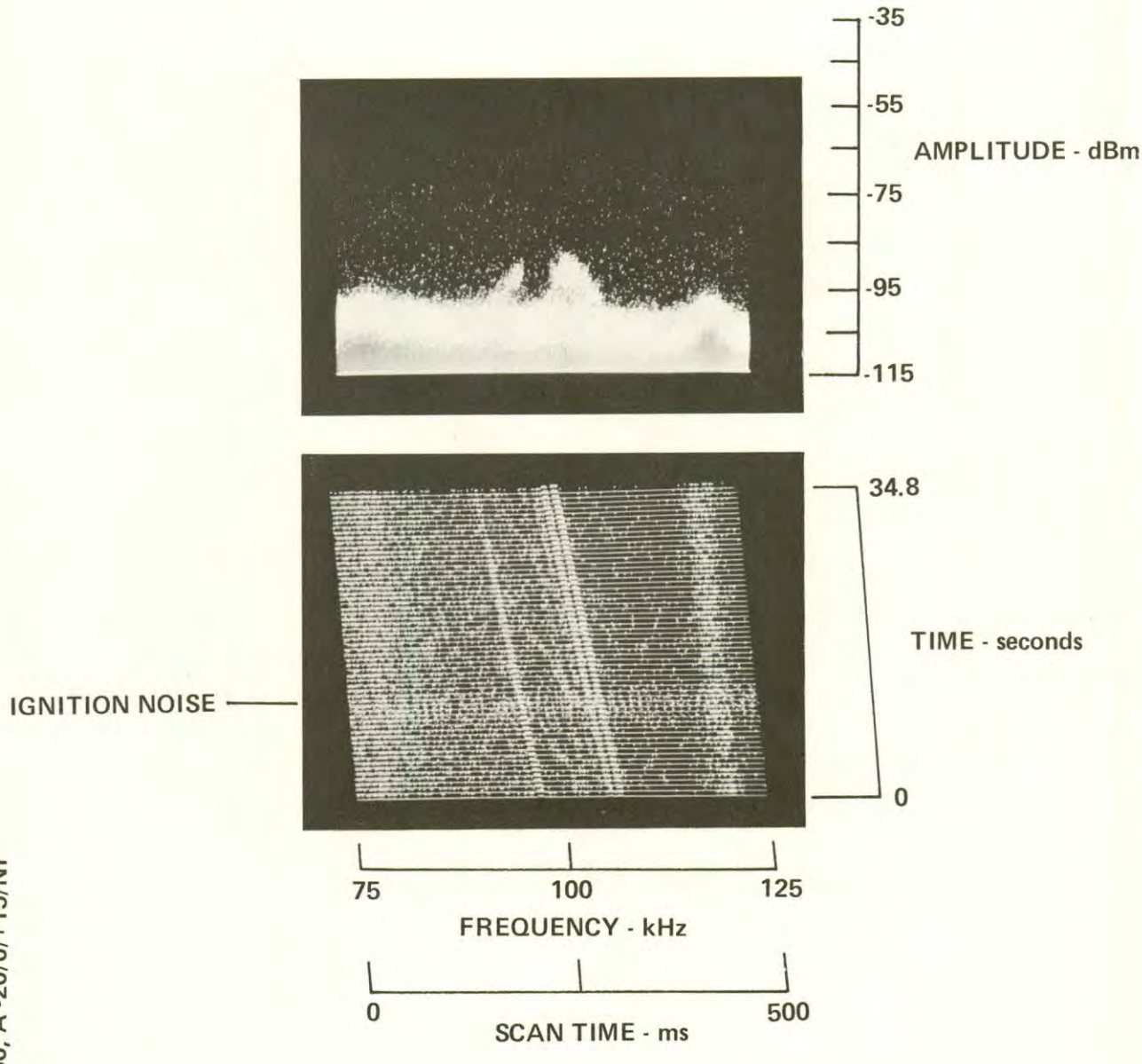

1-25-79, 1238, 104-052
HP140, Whip, F100, W50, IF3, ST 500, A -20/0/+15/NF

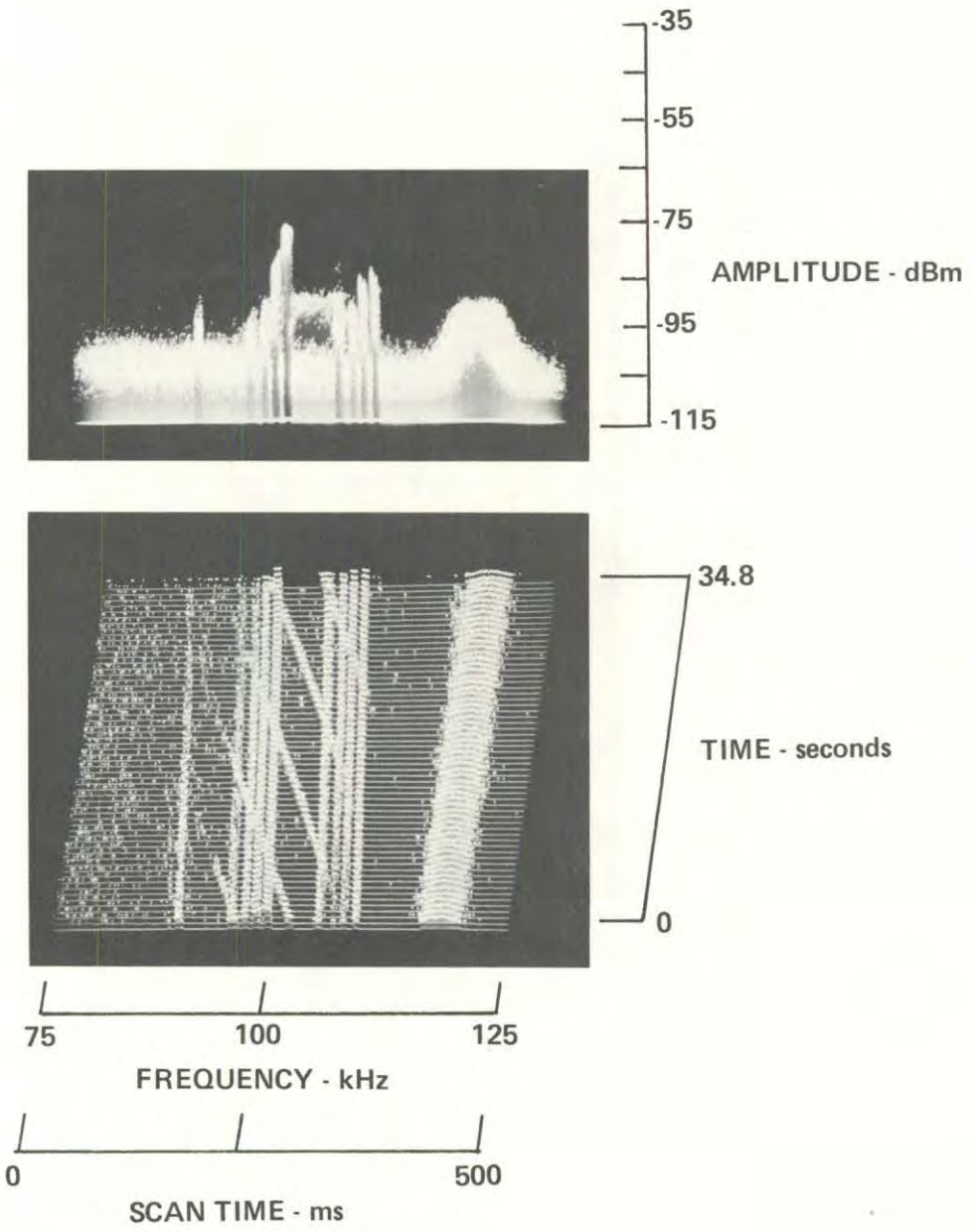

1-25-79, 1253, 104-053
HP140, Whip, F100, W50, IF3, ST 500, A -20/0/+15/NF

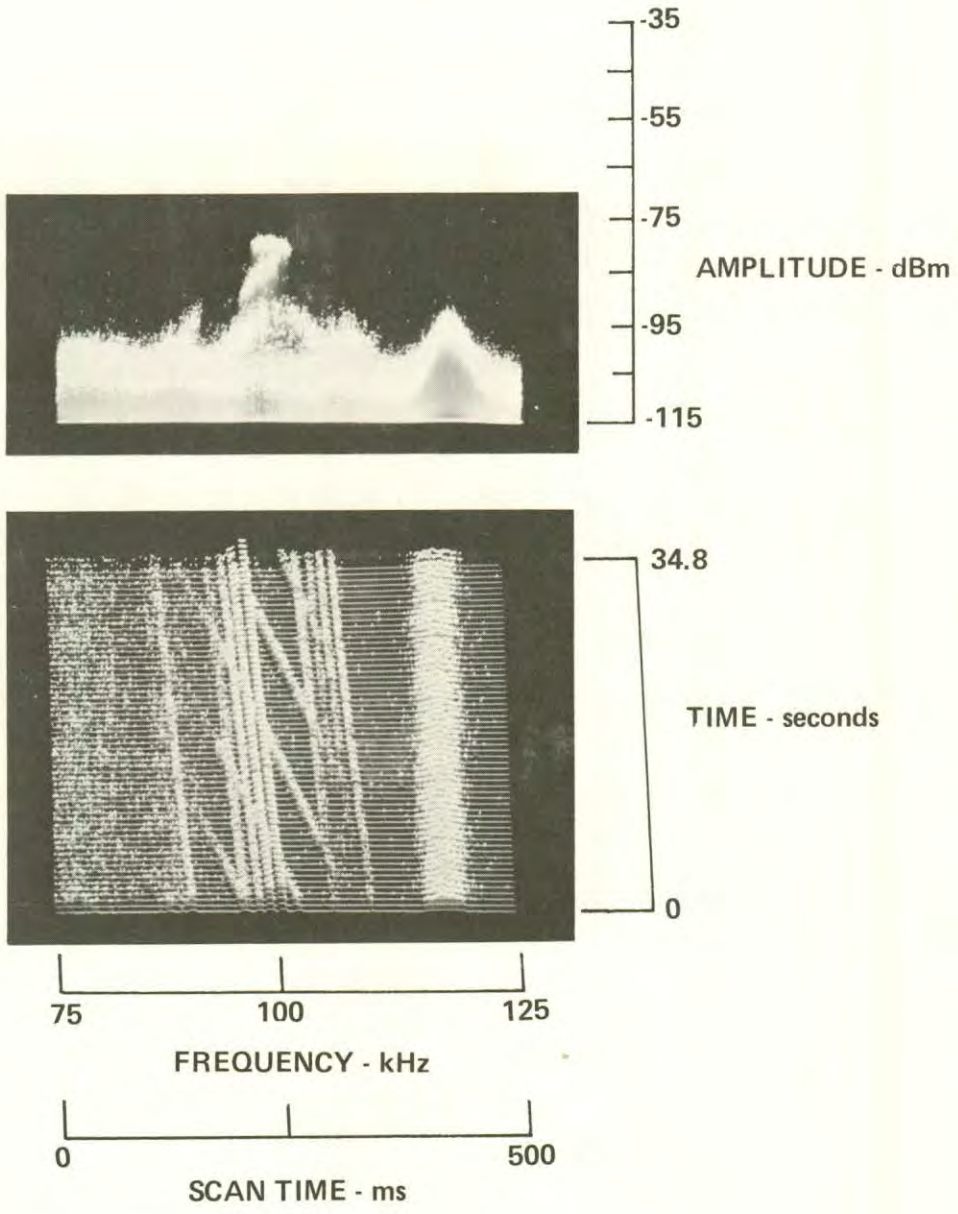

1-25-79, 1306, 104-054
HP140, Whip, F100, W50, IF3, ST 500, A -20/0/+15/NF

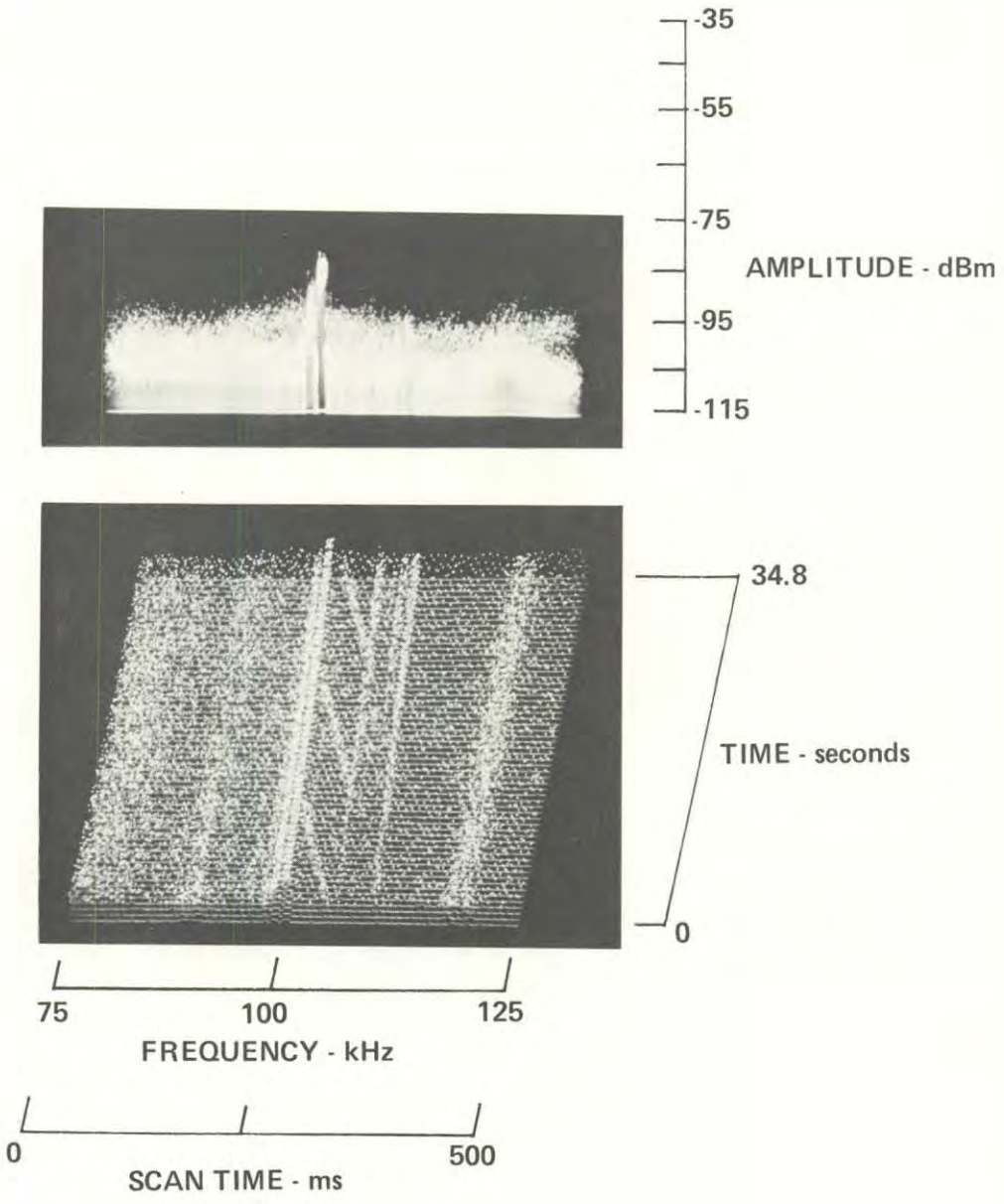

1-25-79, 1322, 104-055
HP140, Whip, F100, W50, IF3, ST 500, A -20/0/+15/NF

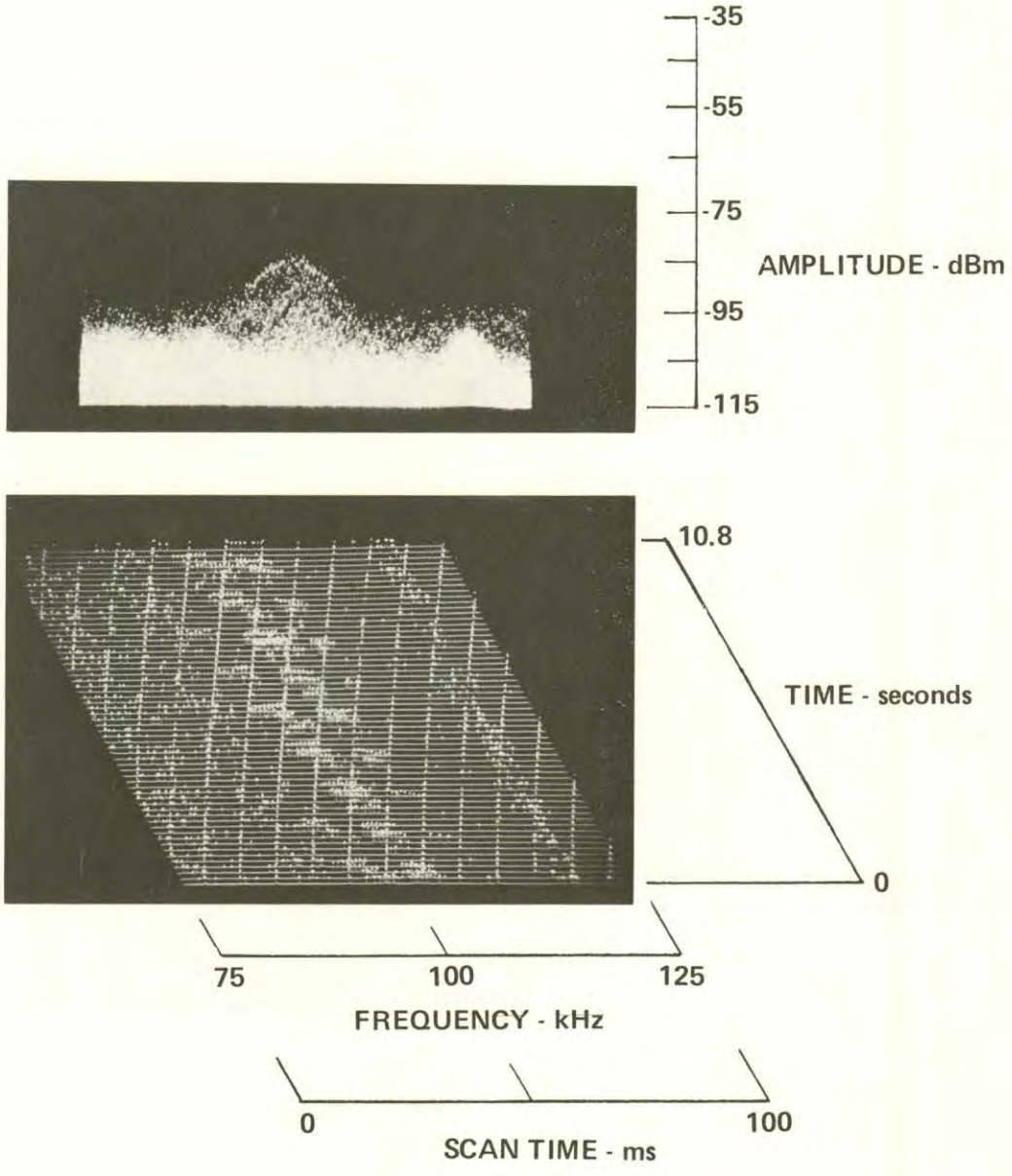

1-25-79, 1321, 104-055
HP140, Whip, F100, W50, IF3, ST 100, A -20/0/+15/NF

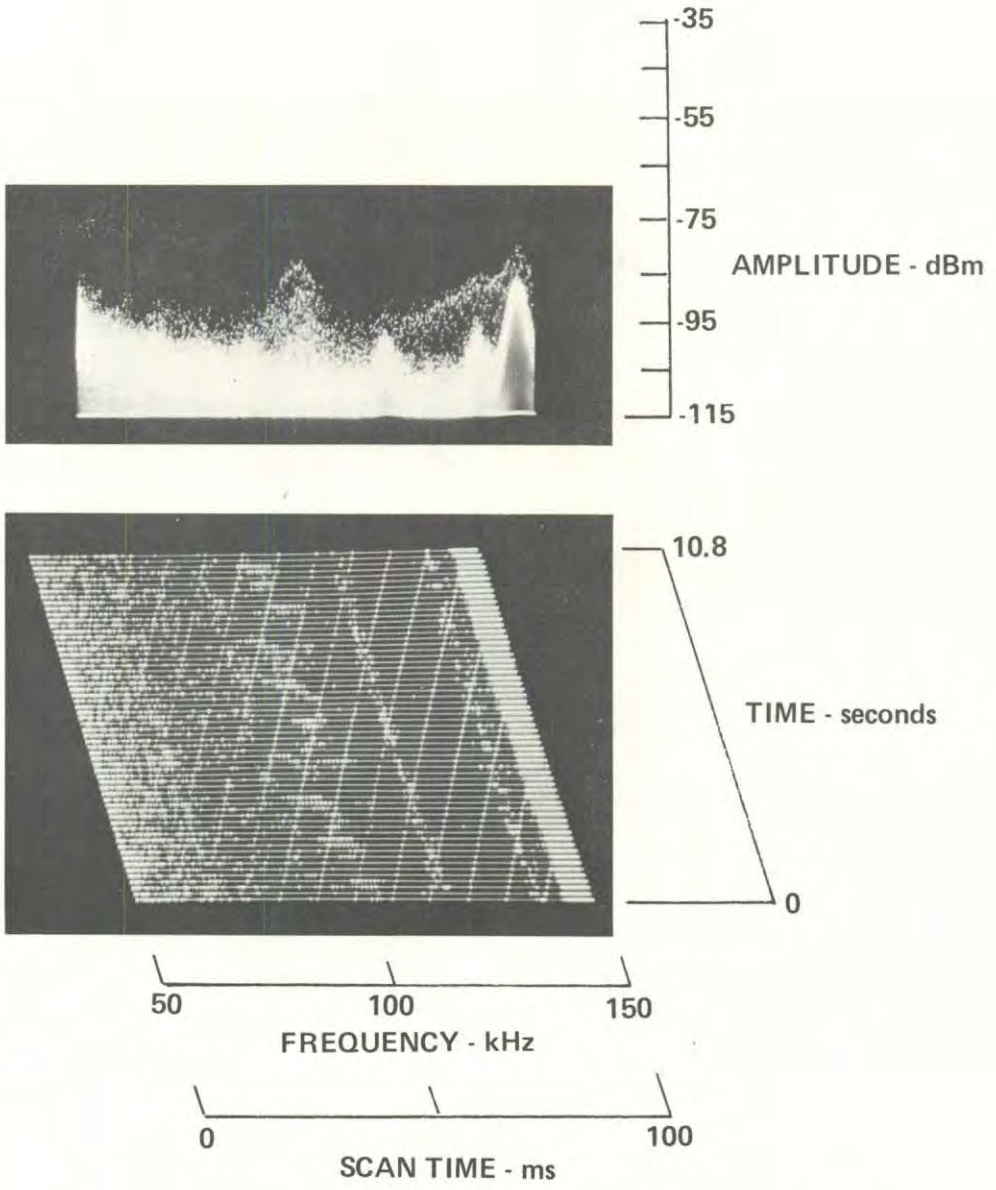

1-25-79, 1325, 104-055
HP140, Whip, F100, W100, IF3, ST100, A-20/0/+15/NF

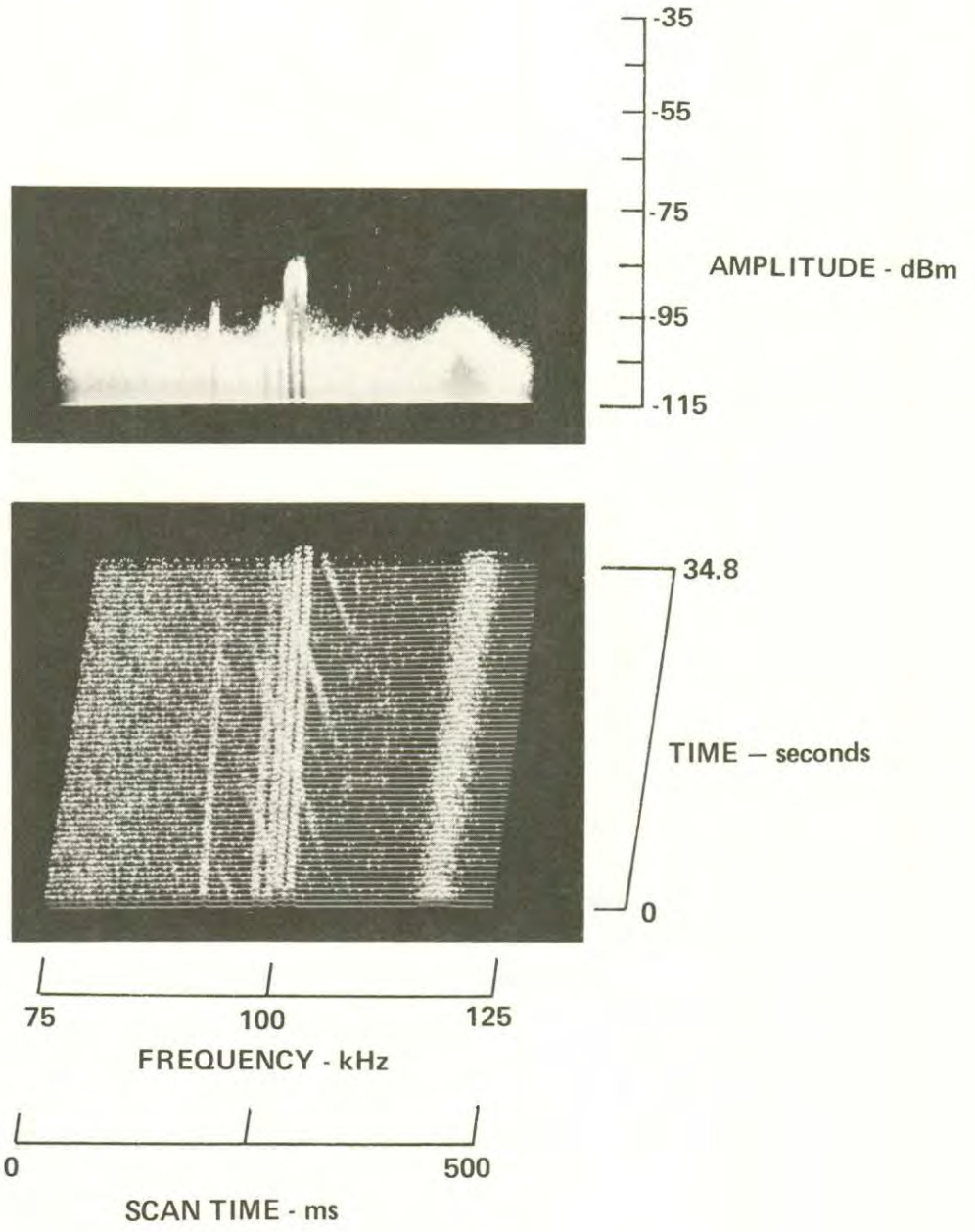

1-25-79, 1332, 104-056
HP140, Whip, F100, W50, IF3, ST 500, A -20/0/+15/NF

APPENDIX B

REPORT OF NEW TECHNOLOGY

The work performed under this contract during the collection and analysis of noise and interference data as reported herein has led to data on the types of interference expected to be encountered in the Loran-C band for the urban environment. This is the first quantified data of this type for the urban environment.

REFERENCES

1. D.A. Feldman, "An Atmospheric Noise Model with Application to Low Frequency Navigation Systems," Ph.D. Thesis, Massachusetts Institute of Technology, June 1972.

2. P.G. Mauro and J.D. Gakis, "The Effects of Primary Power Transmission Lines on the Performance of Loran-C Receivers in Experimental Terrestrial Applications," Report No. DOT-TSC-RSPA-79-8, July 1979.

3. R.A. Shepard, J.W. Engles, and G.H. Hagn, "Automobile Ignition Noise and the Super Noisy Vehicle," EMC Symposium Record, IEEE 76-CH-1104-9-EMC, pp. 403-412, 1976.

4. G.H. Hagn, "Definitions and Fundamentals of Electromagnetic Noise, Interference, and Compatibility," NATO/AGARD Meeting on Electromagnetic Noise, Interference, and Compatibility, October 21-25, 1974, Paris, France.

5. "Manual of Regulations and Procedures for Radio Frequency Management," Office of Telecommunications Policy, Executive Office of the President.

6. "World Distribution and Characteristics of Atmospheric Radio Noise," CCIR Report 332, ITU, Geneva, Switzerland, 1964.

7. R.J. Matheson, "Instrumentation Problems Encountered Making Man-Made Electromagnetic Noise Measurements for Predicting Communications Performance," IEEE Trans. on Electromagnetic Compatibility, Vol. EMC-12, No. 4, November 1970.

8. A.D. Spaulding and R.T. Disney, "Man-Made Radio Noise, Part I: Estimates for Business, Residential, and Rural Areas," OT REport 74-38, Office of Telecommunications, U.S. Department of Commerce, June 1974.

9. A.D. Spaulding, "Man-Made Radio Noise: The Problem and Recommended Steps Toward Solution," OT Report 76-85, Office of Telecommunications, U.S. Department of Commerce, April 1976.

10. E.N. Skomal, Man-Made Radio Noise, Van Nostrand Reinhold Co., 1978.

11. D.A. Feldman, "An Atmospheric Noise Model with Application to Low Frequency Navigation Systems," Ph.D. Thesis, Massachusetts Institute of Technology, June 1972.

12. E.N. Skomal, "Results of an AM Broadcast AVL Experiment," IEEE Transactions on Vehicular Technology, Vol. VT-26, No. 1, February 1977.

BIBLIOGRAPHY

L.O. Barthold, et al., "Transmission Line Reference Book, 115-138 KV Compact Line Design," Electric Power Research Institute, Palo Alto, California, 1978.

R.B. Churchill, "Modeling the Relative Amplitude Probability Distribution of Power Line Noise," ESD-TR-75-019, DOD Electromagnetic Compatibility Analysis Center, Annapolis, Maryland, October 1975.

R.A. Shepard and J.C. Gaddie, "Measurement of the APD and the Degradation Caused by Power Line Noise at HF," Final Report, Contract N00039-74-C-0077, Stanford Research Institute, Menlo Park, California, April 1976.

Course Text, IEEE Tutorial Course, "The Location, Correction, and Prevention of RI and TVI Sources from Overhead Power Lines," IEEE, New York, New York, 1975.

M.S. Gupta, Electrical Noise Fundamentals and Sources, IEEE Press, New York, New York, 1977.

R. Caldicott, et al., "Model Study of Electric Field Effects in Sub-Stations," EPRI EL-632, prepared by Ohio State University for the Electric Power Research Institute, Palo Alto, California, January 1978.

L.E. Zaffanella and D.W. Deno, "Electrostatic and Electromagnetic Effects of Ultrahigh-Voltage Transmission Lines," EPRI EL-802, prepared by General Electric Company for the Electric Power Research Institute, Palo Alto, California, June 1978.

H.N. Shaver, V.E. Hatfield, and G.H. Hagn, "Man-Made Radio Noise Parameter Identification Task," Final Report, Contract N00039-71-A0223, Stanford Research Institute, Menlo Park, California, May 1972.

R.A. Shepard, J.C. Gaddie, V.E. Hatfield, and G.H. Hagn, "Measurements of Automobile Ingition Noise at HF," Final Report, Contract N00039-71-A-0223, Stanford Research Institute, Menlo Park, California, February 1973.

Special Issue on Spectrum Management, IEEE Trans. on Electromagnetic Compatibility, Vol. EMC-19, No. 19, August 1977.

W.R. Lauber, "Amplitude Probability Distribution Measurements of the Apple Grove 775 KV Project, " IEEE Trans. on Power Apparatus and Systems, Vol. PAS-95, No. 4, July/August 1976.

A.D. Watt and E.L. Maxwell, "Measured Statistical Characteristics of VLF Atmospheric Radio Noise," Proc. IRE, Vol. 45, pp. 55-62, January 1957.

R.A. Shepard, "Measurements of Amplitude Probability Distributions and Power of Automobile Ignition Noise at HF," IEEE Trans. on Vehicular Technology, Vol. VT-23, No. 3, August 1974.

B26
14